FINAL TECHNICAL DOCUMENTARY REPORT

For

ADVANCED STUDY ON OPTICAL COMMUNICATIONS FROM DEEP SPACE (Extension)

Prepared Under Modification No. 4, Contract No. NAS 9-3650

For

NATIONAL AERONAUTICS AND SPACE ADMINISTRATION
Manned Spacecraft Center
Houston, Texas

By

WESTINGHOUSE ELECTRIC CORPORATION
Defense and Space Center
Surface Division

P. O. Box 1897 Baltimore, Maryland 21203

ABSTRACT

Plans for testing optical components of various types of laser communication systems are presented. Materials are selected for testing, and the requirements for both simulated and space flight testing of these materials are presented. A series of communication theory and communication system performance tests are recommended. Details of these tests, required special test equipment, test procedures, and data reduction techniques are explained. Standard test equipment, and ways of implementing these tests are recommended. Predicted results of tests are presented. A computer model to calculate power requirements for deep space optical communications is presented and explained. Sample test results for PPM, PL, and coherent modulation are given. A range tracking system that is compatible with digital television, and has an unambiguous range of 100×10^6 miles, is developed. Predictions of its performance during deep space missions are calculated.

TABLE OF CONTENTS

LIST OF FIGURES

LIST OF COMPUTER FLOW CHARTS

Section I

INTRODUCTION

This report presents the results of a continuation of Westinghouse's study of optical communications for deep space applications. Most of the theoretical bases for this work are contained in the Interim Reports[2,3,4] and the Final Report[1] on Phase I of Contract NAS 9-3650, performed by Westinghouse for NASA from 1 October 1964 to 25 October 1965. Applicable data from these reports are in Sections III through VI of this report. Tests of optical materials and laser communication theory are recommended. A computer program for calculating the optical power requirements for deep space laser communications is presented and discussed. A ranging system that is compatible with the proposed data format, and system constraints and has a range in excess of 100 million miles, is presented. The laser requirements for proper performance of this system during midcourse tracking and at maximum range are calculated. A complete bibliography of the references used in this work is in Section VII.

A. Purpose

This is the Final Technical Documentary Report on work performed under a supplemental agreement to contract NAS 9-3650, performed under the sponsorship of the National Aeronautics and Space Administration's Manned Spacecraft Center. The period of work covered by this report is from 12 August 1966 to 12 March 1967.

The study provides a program for material testing and testing the theory of laser communications that should be implemented in order to prove the space worthiness and effectiveness of optical communications

for deep space flight. It recommends a ranging system that can be used in conjunction with deep space probes that use data formats similar to the one proposed for laser communications in the final report[1] on NAS 9-3650. Finally, this study has developed a highly flexible computer program for determining the power requirements for effective laser communications under a variety of system and environmental conditions.

B. Program

The study program consisted of four, nearly independent, studies of specific problems in testing laser communications systems, proving their space worthiness, adding a ranging sub-system to the laser communication system, and computerizing the results of the modulation theory studies performed under NAS 9-3650.

Task 1 of the program, which was the development of plans for recommended tests of optical materials when exposed to the space environment, began with a study of available literature on laser communication systems to determine the optical materials that would be needed in a deep space system. Based on this, a preliminary list of materials to be tested was evolved. A study of these materials, when exposed to the space environment, determined those parameters of the materials which were subject to variation. Using this data, test parameters were selected. A set of test objectives were defined, and materials test plans for achieving these objectives were developed. Recommended tests are to be conducted in a simulated environment

when possible, but, in cases where adequate simulation facilities are not available, spaceborne tests of optical components and materials are recommended.

Task II of the program, which was the development of test plans for correlating laboratory results of laser communication studies with the theoretical results obtained from studies of modulation theory, began with a review of existing test systems. Then, the optical and electronic configurations for testing a low data rate laser communication system in NASA's optical tunnel were developed. Since tests were to be performed near the quantum limit, it was also necessary to develop plans for monitoring equipment capable of measuring extremely low signal levels. Methods of varying the optical noise background, and the effects of noise on the monitors performance were investigated.

Electronic and optical configurations for testing both laser communication theory and system performance in the NASA optical tunnel was postulated. Wherever possible, specific types of "off the shelf" test equipment were recommended for use during these tests. If the specific requirements for a piece of electronic test equipment could not be met with existing equipment, performance requirements were specified. Also, when existing laser communication equipment must be modified before tests can be conducted using this test system, recommendations for modification were determined.

Then, the problem of testing a laser communication system over an 11 mile range was investigated. On the basis of this work, recommendations as to the types of testing, the electronic configuration of the

test equipment, the types of test equipment required, and a means of keeping to stations in synchronism were prepared. Test procedures were outlined, and a means of reducing the test data to more useful formats was suggested.

Task III, which was the mechanication of the power model for laser communicators presented in the Final Report[1] on NAS 9-3650, began with a review of the power model presented in that report. An improved model was developed, which took into account system and environmental parameters not included in the original model. This model was then programmed, and run for cases corresponding to those shown in the Final Report.[1] After debugging, it was used to predict results for cases of interest defined during Task II and Task IV of the contract.

Task IV, which was the development of a ranging system which could be used with the proposed digital communication format, began with a review of existing and proposed range tracking systems. Laser radar systems, continuous range code generators in the spacecraft, and active transponders were considered. Then, based on the restriction placed on a laser range tracking system that was to operate in conjunction with the communication system, several alternate range trackers were postulated. After reviewing the effects of doppler shifts, instabilities in the spcecraft oscillator, and other factors, a single range tracking system was selected for further study. Its accuracy in range and range rate were determined, as were the modifications required in the spacecraft transmitter/receiver. A block

diagram for this ranging system, when incorporated in the spacecraft, was developed. Calculations, and computer runs, were made to determine its performance at 50 and 100 million miles from Earth. Finally, an attempt was made to compare this range tracking system with those used for DSIF and APOLLO.

C. Status

This report concludes the effort on this contract.

D. Personnel

Personnel who contributed to this program are: C. D. Hedges, T. R. Hughes (Project Manager), C. E. Wernlein (Project Engineer), R. M. Baker, G. Wend, A. Fox, A. L. Avant, H. S. Fitzhugh, G. S. Ley, I. T. Basil, and Z. L. Collins.

Section II

CONCLUSIONS AND RECOMMENDATIONS

The conclusions and recommendations presented here summarize the conclusions and recommendations contained in the Monthly Progress Reports issued under this contract and contain the major conclusions reached during the study phases of this program. Each major task of the program is discussed separately, following the sequence of task numbers contained in the statement of work,[5] as follows:

Task I - Materials Test Plans

Task II - Communication Theory Test Plans

Task III - Power Model

Task IV - Ranging Analysis

A. Task I - Materials Test Plans

The majority of optical material tests should be carried out in a simulated space environment. This allows control of conditions, monitoring of temporary changes in materials, and minimizes test costs. However, actual space tests of materials during orbital tests should also be included as part of this program. These tests will use a minimum of real time instrumentation, but they will allow correlation of the results of simulation testing with the results of actual testing in space.

It is believed that the primary lens, electro-optic modulating materials, and laser materials are more sensitive to the space environment than any other portions of a laser communication system. This is based on either their required exposure to the space environment or their known susceptibility to radiation. For these reasons, it is recommended that tests of these materials be given precedence in the materials testing program.

B. Task II - Communication Theory Test Plans

It has been concluded that because of noise in signal problems, and the cost of developing the necessary test equipment, tests of laser communication theory at 30 megabits/second are not practical. This is true both for tunnel testing and over an outdoor range. Therefore, the following tests of laser communication theory are recommended:

1) Using a simple analog system in the tunnel
2) Using a modified PCM/PL system, including a separate modulator driver at 1 megabit/second, in the tunnel.

Only one test of the PCM/PL system at maximum bit rate is recommended. This will be done in the optical tunnel, where the noise environment is controlled. This test should determine the performance characteristics of the Hughes system, and will not be a test of laser communication theory. It is recommended that tests of theory be given precedence over this test.

Outdoor tests that are described in this report fall into three categories. Two of these are recommended for performance during the test program, and the third might be attempted under ideal atmospheric conditions. These categories are as follows:

1. Measurement of the analog characteristics of the test link.
2. Measurement of the effect of the propagation mechanism on the error rate and error distribution over a 1 megabit/second PCM/PL system (Modified Hughes).
3. Measurement of the performance of the Hughes system at 30 megabits/second over the test range. This test is not recommended because of instrumentation problems.

In addition to the test programs, this section of the report describes optical and electronic monitoring equipment that is needed. Ways of implementing this equipment are discussed. It is recommended that this equipment be developed before any test of laser communication theory or of laser system performance is attempted.

Finally, testing of FM and PPM laser communication systems in the optical tunnel is described. Since these systems are still being developed, no detailed test procedures are presented. It is recommended that, at this time, an analog system and the Hughes PCM/PL system be used as "test beds" for most of the communication theory and system performance tests.

C. Task III - Power Model

This task was primarily concerned with implementing the power model shown in the Final Report[1] on HUD-38120. As such, it has more results than conclusions or recommendations. However, it can be concluded that a Power Model can be developed for use on a Univac 1108 computer and that results shown in the Final Report[1] for the effects of polarization errors on the performance of a PCM/PL system are in error. All other results given in the Final Report[1] agree with those derived during test runs of the program.

It is recommended that actual laser communication theory experiments be carried out to determine the validity of predictions computed by use of this Power Model on a Univac 1108.

D. Task IV-Ranging Analysis

During this task, it was concluded that a digital range tracking

system should be used for deep space ranging on a laser communication signal. It was also concluded that a digital range tracking transponder could be included as part of the laser communication system on board a spacecraft. Theoretical investigation of ranging performance showed that this system possessed rapid acquisition properties, and should perform well even when the ground based (or satellite based) receiver is operating near the quantum limit.

It is recommended that further investigation of the effects of the phased lock loop design on ranging performance be conducted, both in the laboratory and by theoretical analyses. It is also recommended that the relation between range codes bits/data bit and range tracking stability be investigated in a laboratory.

Section III

OPTICAL MATERIALS TEST PLAN

A. Statement of Task

A review is made of the requirements of the optical materials that would be used in a laser communication system for a MDSV. A review is also made of the environment that the materials would be subjected to for such a mission. Some known information about materials that indicate good application is presented. Using this, a basis is formed for the selection of materials for deep space application.

A list of materials is drawn up for future study purposes. Relevant material parameters are listed and in many cases combined for test purposes.

Tests are recommended to measure these parameters, with particular emphasis on material selection. Test philosphy is dealt with, and existing test facilities are recommended.

B. Material Selection

B.1 Basis of Selection

B.1.a According to Required Optical Equipment

The selection of optical materials depends, in part, on the use they would serve. The use they serve may make use of the material's transmission properties, its reflective properties, its polarizing abilities, etc. Some idea must also be had of what degree of deterioration of any of its properties constitutes a serious deterioration of the system. Further, knowledge must be had, or at least good

guesses must be made, as to where, physically, each of the components lie within the system. The interest here is mostly one of shielding. Later stage components are shielded against certain radiations, particularly UV and IR, if the intial stages are chosen to filter our these radiations. Also, later stage components can be inserted further into the vehicle for better shielding effects.

A final analysis will always have to be made of a particular optical system for the requirements of its components. A suggested, or typical system is described here. The system described here should include most of the components of any system that may finally be designed.

B.1.a.(1) Sample Optical Transmitting and Receiving System

Figure III-1 shows the essential components of an optical system, using most of them for both transmitting and receiving purposes. This system does not contain two channels of detection optics but, nevertheless, contains each type of component that such a system might contain.

B.1.a.(2) List of Optical Components

(A) Telescope Support Frame
(B) Secondary Mirror Supports
(C) Protective Covering
(D) Primary and Secondary Mirror Bank
(E) Reflective Coating
(F) Lens Mount
(G) Collimating Lens
(H) Antireflective Coating
(I) Interference Filter Substrate
(J) Interference Dielectric Coating
(K) Wollaston Prism
(L) Binder for Wollaston Prism
(M) Detector
(N) Supports for Quarter Wave Plate
(O) Quarter Wave Plate
(P) Modulator
(Q) Antireflective Coatings
(R) Mirror Blanks
(S) Mirror Coatings
(T) Multilayer Coatings
(U) Laser Oscillator

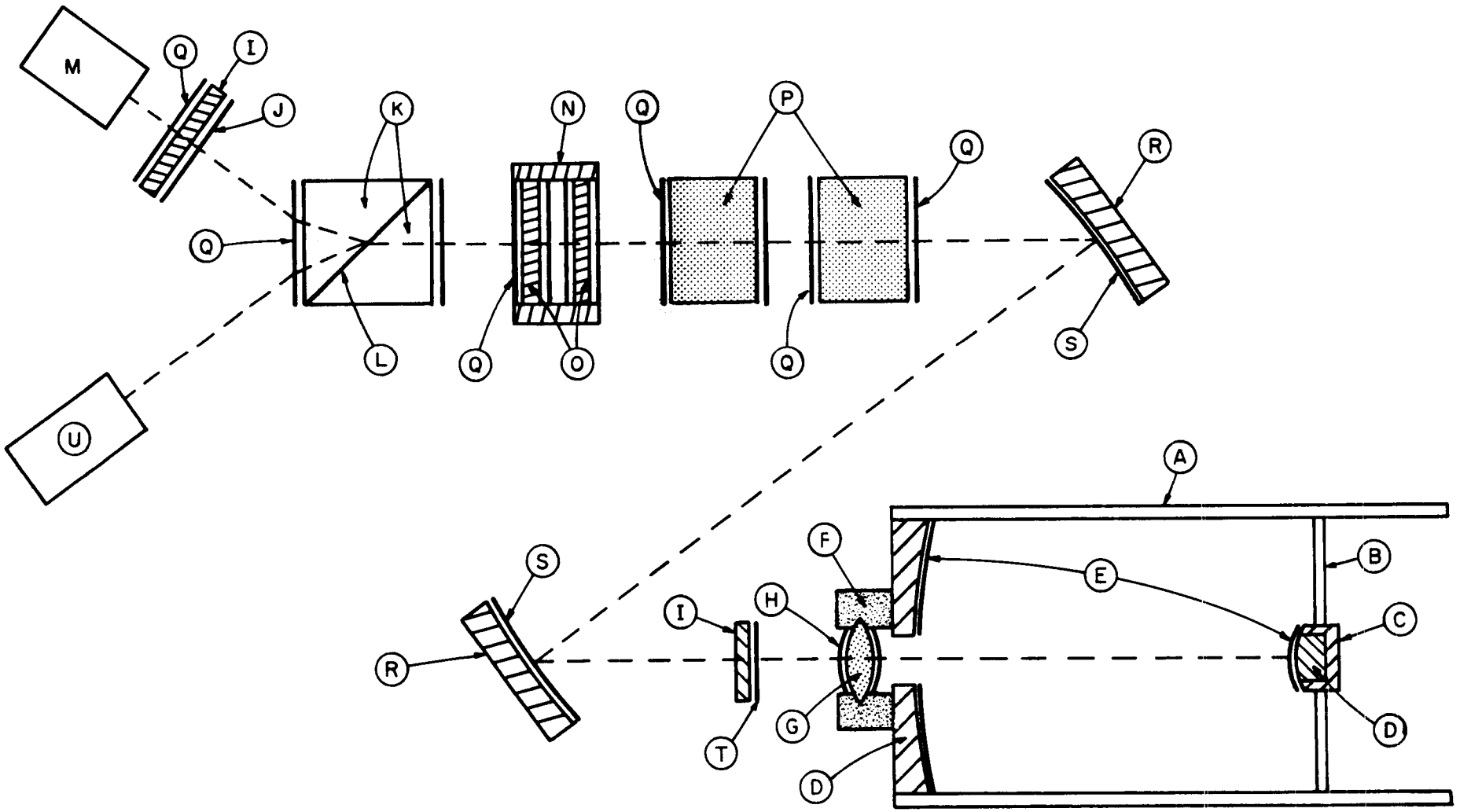

FIGURE III-1. Sample Optical Transmitting and Receiving System

B.1.a.(3) Requirements for Each Component

(A). Telescope Support Frame should be of solid construction, made of material capable of absorbing as much radiation as possible (i.e., protons, soft X-rays and electrons) while being light in weight and strong. In addition to these factors, a strong emphasis must be made on thermal stability in order to maintain mirror alignment. Mirror alignment could be made independent of the frame and secondary mirror if necessary.

(B). Secondary Mirror Supports should be strong and thermally stable {See (A) above}. Weight must be minimal.

(C). Protective Covering of secondary mirror should be made of metal. It should be designed of a material that will absorb a maximum amount of soft X-rays, alpha, electron, and proton radiation. The absorbing function of the protective covering is most important, as this element is the one most exposed to the space environment.

(D). Primary and Secondary Mirror Banks must have good radiation resistance to dimensional distortion and surface pitting. These mirror blanks must also have a very low expansion coefficient.

(E). Reflective coatings should have good resistance to radiation effects. The important factors that a reflective coating must maintain are a smooth surface (lack of surface erosion, pitting, etc.), a uniformly reflecting surface (at least for the wavelength of the useful reflected light) and the coating must, of course, remain adhered to the mirror blank. Besides the effects of radiation, the deteriorating effects of vacuum and micrometeorites must be low.

(F). Lens Mount should serve two purposes:

(1) It should be a thermally stable holder and insulator for holding a lens. It is important that if temperature gradients exist, they are at least radial.

(2) It also serves as an isolator between the space environment and environment of the internal optics (similar to internal space ship environment).

(G). Collimating Lens should be a simple lens, particularly sturdy against space environment. Note that this lens is the only transmission type optical component exposed directly to the space environment.

(H). Antireflective Coatings must be resistant to UV, soft X-rays, alpha rays (if used on outside of collimating lens). If not, the coating should at least be resistant to protons, electrons and gamma rays.

(I). Interference Filter Substrate - Fixed material.

(J). Interference Dielectric Coating designed to pass only desired bandwidth of radiation. Dielectric layers to be hard and durable.

(K). Wollaston Prism - Fixed material.

(L). Binder for Wollaston Prism must not be susceptible to damage by proton, electrons, or gamma rays. Best approach would be to air space components with anti-reflective coatings on surfaces.

(M). Detector (type not called out here) may require special shielding to prevent noise output. If a tube, such as a photomultiplier, employing a photocathode is used, the photocathode should be kept as small as possible. This reduces the possibility of the emission of an electron from the photocathode due to stray radiation.

(N). Supports for Quarter Wave Plates should be constucted of thermally stable material (structured plastics or metal).

(O). Quarter Wave Plates may best use two plates for thermal compensation.

(P). KDP Modulator should also use two elements for the necessary thermal stability. KDP must be in "dry" environment. Cell would probably require windows with anti-reflective coatings.

(Q). Anti-reflective coatings must be resistant to protons, electrons and gamma rays.

(R). Mirror Blanks must be thermally stable and radiation resistent.

(S). Mirror Coatings should be aluminum, overcoated with a protective coating. The aluminum should be stable under proton, electron and gamma ray bombardment.

(T) Multilayer Coating is used here as a filter. It must have a broadband transmission characteristics to maximize transmission at the required wavelength. It must be designed to reflect UV for wavelengths less than 3500Å (this provides UV protection for following components from wavelength region 2000 to 3500Å.)

B.1.b <u>According to Environment of Components</u>

B.1.b.(1) <u>Environment Summary</u>

B.1.b.(1).(a) <u>Environment Parameters</u>

The important space environments are:

(1) Electromagnetic Effects due to Solar Radiation
(2) Thermal Effects due to Solar Radiation
(3) Solar Wind
(4) Galactic Cosmic Rays

(5) Solar Cosmic Ray Events
(6) Meteroid Environments
(7) Vacuum Environment

B.1.b.(1).(b) Range of Parameters According to Partial or Photon Energies, Dosage, and Source*

(1) Electromagnetic

(a) 99% of the radiant energy has a wavelength between .3 and .4 microns.

(b) The total flux does not vary by more than .5%.

(c) The spectral distribution is that of a black body whose temperature is about 6000° K. (The peak intensity wavelength is at about 4700° A and has a power level of .22 watts/cm^2 • micro)^2 at earth radius in space. The total power between 2000Å AND 4 u is .14 watts/cm^2. At Mars, the solar radiation is about .4 that at the earth radius.

(d) The irradiance between 2000 Å and 100 Å (approximate black body at 4500°K).
- Most of the radiation with wavelengths less than 2000Å is in the Hydrogen Lymen Alpha emission at 1215.7Å (5 x 10^{-7} watts/cm^2 • Å)
- Second in intensity is the Helium line at 304Å (5 x 10^{-9} watts/cm^2 • Å)**

(e) Solar flares which last from 10 minutes to five hours.
- Class 2 + flares reach approximately 1.5x10^{-8} watts/cm^2 • Å between 20 and 80Å*** (X-rays).
- Maximum background is 2 x 10^{-8} watts/cm^2 • Å between 30 and 80 Angstroms.

*See 1st Report[2], Page 191.
**Ibid., page 192, Figure IV-88.
***Ibid., page 192, Figure IV-89.

(f) Electromagnetic radiation in the 2 to 8 Å wavelength region (X-rays).

- Background $\simeq 5 \times 10^{-11}$ w/cm^2
- Class 2 + Flare $\simeq 5 \times 10^{-5}$ w/cm^2 .
- Class 3, 3 + flare (less than 10 Å) - There is no knowledge, but it is thought important.

(2) Thermal

(a) Heat radiated from space craft (general)

$$H_r = E_S \sigma T^4$$

H_r = heat radiated

E_S = surface emissivity

σ = Stefan Boltzman constant

T = temperature in degrees Kelvin

(b) Average temperature determined by α_s/E_S (α_s = surface absorptivity).

(c) Average guide line $\alpha_s/E_S < 1$ (Approximately average earth temperature = 300°K) and $\alpha_s/E_S > .1$ (Approximate Mars temperature = 120°K) based on data of electromagnetic radiation.

(3) Solar Wind (Plasma particles)

(a) The solar wind consists mainly of protons, electrons and a small percentage of alpha particles.

	Earth	Mars
Average Velocity	5 X 10^2 km/sec	5 X 10^2 Km/sec.
Average Flux	5 X 10^6 p^+, e^-/cm^2.sec.	2.5 X 10^6 p^+,e^-/cm^2.sec.
Average Energy	p^+ 1 KeV, e^- 50 eV	p^+ 1 KeV, e^- 50 eV
Average p^+/e^-	10	5

(4) Galactic Cosmic Rays

(a) Consists of charged atomic nuclei (mainly Hydrogen) traveling at relativistic velocities.

(b) Consists of electrons and gamma rays (galactic in origin). These,however,are assumed to be negligible in quantity.

(c) The main contents of the cosmic rays are particles of Hydrogen and Helium. The ratio of Hydrogen particles/Helium particles = 100/7, i.e., Helium particles make up about 7% of the total number of cosmic ray particles.

(d) The average energy of these particles is 3.6 Bev. The flux density is about 1 nucleon/cm^2 · Sec.

(e) Cosmic ray flux varies inversely with solar activity.

(5) Solar Cosmic Ray Events*

(a) These events consists mainly of protons and alpha particles (small percentage of heavier particles).

(b) The energy distribution of protons (non-relativistic) is between 30 and 300 Mev.

(c) Maximum flux (big solar flares) is approximately 10^4 protons/cm^2. sec.

(6) Meteroid Environment

(a) It is mainly concentrated in ecliptic plane.

(b) Most of the meteroids have a velocity between 11 and 72 km/sec relative to the earth and between 5 and 58 km/sec relative to Mars.

(c) The range of densities of these particles is between 5g/cc and 8g/cc.

(d) Range of particles with respect to maximum flux rate, mass and approximate diameter:

*Ibid, page 200, Figure IV-93.

Flux (particles/cm^2. sec)	Mass (grams)	Diameter (density 5 gm/cc)
1.0	10^{-14}	2×10^{-5} cm
10^{-2}	10^{-9}	9×10^{-4} cm
10^{-9}	10^{-6}	9×10^{-3} cm
10^{-15}	1.0	0.9 cm
10^{-21}	10^{-4}	20 cm

(e) For 3-year mission the probable number of encounters of particles of a given size:

Particle Diameter	No. of Encounters/cm^2
2×10^{-5} cm	10^{8}
9×10^{-4} cm	10^{6}
9×10^{-3} cm	10^{-1}
0.9 cm	10^{-7}
20 cm	10^{-13}

B.2.a List of Materials

Materials to be tested, on the basis of their optical properties and potential immunity to the space environment, include:

Magnesium Flouride	Epoxy Glass (heat resistant type)
Silicon Monoxide	Lithium Niobate
Zinc Sulfide	KDP
Titanium Dioxide	KD*P
Cerium Dioxide	Cer-Vit (Owens-Corning)
Calcite	Aluminum Coatings
Natural Quartz	Fused Quartz (Corning 7940)
Balsam (Canada)	Laser Gases (Ar,He,Ne,Hg,CO_2,etc.)
Sapphire	Laser Solids (YAG:Nd^{+3},Glass:Nd^{+3},Ruby:Cr^{+3})
Phenolic Glass	Injection Lasers (GaAs,InAs, InP)
Epoxy Glass	Flash Lamps
	Tungsten Lamps

B.2.b. Summary of Known Information about Materials under Consideration

(1) In general, the stronger the molecular or atomic binding of the material, the greater is the resistance of the material to radiation.

(2) The main effect to metals of UV radiation (mirror coatings, etc.) is electron emission causing a charged surface which attracts negatively charged space dust.

(a). Damage by ionization or atomic displacement is negligible for solar radiation.
(b). Mirrors coated with Al or Au are not effects by UV.

(3) Good structural plastics are Phenolic glass and Epoxy glass (either the non-heat-resistant or heat-resistant type). These plastics are resistant to UV, vacuum and radiation. Temperature range is from -100°F to 250°F, except for the heat resistant epoxy glass, which is good up to 450°F.

(4) Main effect of UV and X-rays to inorganic materials is the formation of color centers, e.g.,

(a). NaCl forms an absorption band at .4 μ with half width of .1 μ.
(b). KBr forms an absorption band at .63 μ with half width approximately .1 μ.

(5) Non-browning glasses containing cerium resist coloration due to neutrons, gamma rays and solar radiation. Glasses have been developed to withstand 10^6 Roentgens.

(6) Fused Silica has good resistance to gamma radiation.

(a). It is very important that the material be pure (no Al or Li impurities).
(b). If pure, it has good gamma ray stability.
(c). If pure, it has good UV stability.
(d). If pure, it has good X-ray stability.
(e). All types of high energy radiation (which probably includes protons) develops absorption at 2140 Å.

(7) Aluminized mirrors undergo no change in reflectivity due to gamma radiation.

(8) Sapphire undergoes no change in IR transmission due to gamma radiation. Sapphire also has good proton stability.

(9) To date, one of the best window and transmitting optical materials is fused quartz (experimentally determined).

(10) Anti-Reflective coatings:

(a). MgF_2 - probably color center formation (UV and X-ray), and deteriorates under alpha radiation.
(b). ZnS, TiO_2, $BaTiO_3$ do not form color centers (color center formations). However, very pure materials are necessary.
(c). Si is uneffected by X-rays.

(11) It is estimated that proton bombardment would most greatly effect optical properties for MDSV. (Electrons to a much lesser degree).

(12) Sapphire and Fused Quartz produce no change in transmission due to electron bombardment.

There is little information on other materials. The best materials for transmission optical components, at this point, appear to be:

(1) Fused Quartz (Corning No. 7940)

(2) Sapphire, annealed (Linde Company)

though the sapphire may not be desirable where birefrigent materials are not wanted.

C. Test Parameters

C.1. The Basis for the Selection of Test Parameters

The two basic characteristics of an optical component is that it either transmit light or reflect it. Factors which hinder light transmission can be divided into those that take place within the optical component medium such as absorption, internal scattering, loss due to polarization where it is not wanted and those that take place at the surface of the optical medium, such as reflection, surface scattering, and changes in light path due to changes of material change of index of refraction and changes in the position or direction of the surface, i.e., surface distortion. Factors which hinder reflection are the loss of reflectance, i.e., a surface that transmits or absorbs or both when it should reflect. The reflecting surface may also roughen so that though all the light is either reflected or scattered, it is not in the desired direction out of the surface.

The primary functions of some of the optical components is not that of transmission or reflection but of filtering, light beam bending, polarizing wave retardation, etc. It is suggested, however, that most of the component materials be tested for transmission or reflectance even though this be their secondary function.

The factors that hinder transmission or reflection can be many. A more theoretical study might find the causes for the deterioration of transmission or reflection. It is suggested that universal transmission and reflectance tests be made. With this as the objective, this report devises transmission and reflection tests that will show any change

in a material that will hinder transmission or reflection, though the test will not name the cause of deterioration. It is assumed that the main purpose of the test is to accept or reject materials for space use.

Other tests are recommended for the measurement of other important parameters that some of the optics must maintain without significant deterioration. These include tests of the polarizing abilities of some materials, the wavelength dependent transmission or reflection of filters, and the wave retardation ability of some materials.

The basis of the selection of the environmental parameters , to which the materials are to be exposed during tests, is that of best simulating space environment near Mars.

C.2 Measured Parameters

Presented here is a list of parameters that are recommended for direct measurements. Those shown in the left column are parameters, whose change will show up in the direct measurements. Possible causes for these changes are subheaded in the right column.

TRANSMISSION	Absorption Reflection Internal Scattering Surface Scattering Dimensional Distortion Change of Index of Refraction
REFLECTANCE	Absorption Surface Scattering Dimensional Distortion

POLARIZABILITY	Absorption Reflection Internal Scattering Surface Scattering
WAVE RETARDATION	Transmission Reflection Internal Scattering Surface Scattering

The terms in the left column are not necessarily used in the same way as those in the right column. For instance, the parameter transmission in the left column includes all the subparameters in the right column, i.e., it is defined in terms of the test scheme as shown in Figure III-2 where as the term transmission in the right column refers to the material transmittance properties.

The environmental parameters to be used in the test are listed in Section D.2.a.

D. Measurements

D.1 Philosophy of Tests

For these tests, the materials must undergo two processes. The materials must first be subjected to one or more characteristics of the space environment and the materials must then be measure for physical changes that the space environment may have induced in them.

A number of choices present themselves at this point. The material samples may be subjected to actual space environment, the samples being placed on some space vehicle as a side experiment, or

the samples may be subjected to a simulated environment. In the simulation case the sample can be subjected to one characteristic of space at a time or may be subjected to a whole series of space characteristics at the same time.

The advantage of subjecting the material samples to actual space environment is that there is the best assurance that the samples are being subjected to the most "accurate" simulation. It has disadvantages of being time consuming, if a "meaningful" accelerated laboratory simulation is possible. (One which yields results that correlate with those observed during space flight).

There is some advantage to subjecting the samples to each space parameter separately if it is advantageous to determine the particular cause of a material deterioration. This would be particularly so if a more theoretical study were being made of the space effects on materials. The disadvantage of this procedure is the fact that a material may deteriorate a certain way only if a number of space effects act simultaneously on the material, i.e., the cause of deterioration may have to be synergistic - taken together.

So, unless it can be shown that space parameters can be applied to a given material separately and still simulate space, there is a great advantage in exposing the materials to space environment synergistically.

Placing of equipment for the adequate testing of optical materials for deterioration aboard a space craft would be difficult and expensive. It is not recommended, except perhaps for some special cases.

Ground laboratory measurements would generally be more flexible, more accurate and more economical.

The above seems to suggest that the best procedure would be to expose the material samples to actual space environment, retrieve the samples and measure their deterioration in a laboratory. This procedure is recommended. However, it is not a complete procedure and must be supplemented by other tests. A number of effects of space environment on optical materials exist only as long as the material is subjected to the environment. Examples of this are flourescence and scintilation. Other effects, such as coloration disappear or decrease after radiation ceases.

For this reason it is imperative that at least some test monitoring takes place while the materials are being subjected to some parameters of the space enviroment.

For those measurements that should be made at the same time the materials are subjected to space environment parameters, simulated space environment is recommended. Though placing materials in space for irradiation apparently gives greater assurance of their receiving a more typical radiation dosage, simulated space environment produced on the ground is becoming more reliable as both better means for developing simulated radiation in laboratories is improving (particularly the increased ability to produce synergistic space effects) and as a better knowledge of space environment develops.

Thus, a hybrid procedure is recommended for the determination of the suitability of given optical materials for use in space.

D.2 Test to be Performed

D.2.a Optical Configuration

In the following Figure, III-2, suggested optical schemes for the measurements of the important optical parameters of the optical components of interest are presented. Each of the test schemes is lettered and referred to in Chart III-1 and Chart III-2.

Note that in some of the optical schemes, light sources are called for that are collimated and in some the light source must be collimated and monochromatic. Those tests not requiring a monochromatic source may nevertheless use such a source if it is readily available. In most of these tests good collimation of the light source is required, the degree of test validity being proportional to the collimation of the light source.

In each test scheme, only the sample should be irradiated unless it has been clearly shown that some of the optical test components are stable in the presence of the radiation in which they are subjected.

The detector used in each of these test schemes should be a photomultiplier, so chosen and operated to produce as little noise as possible. As even placing the photomultiplier outside the irradiation chamber will not reduce irradiation of the detector to zero, the photocathode of the photomultiplier should have a very small area. Of course, shielding the photomultiplier may also be necessary.

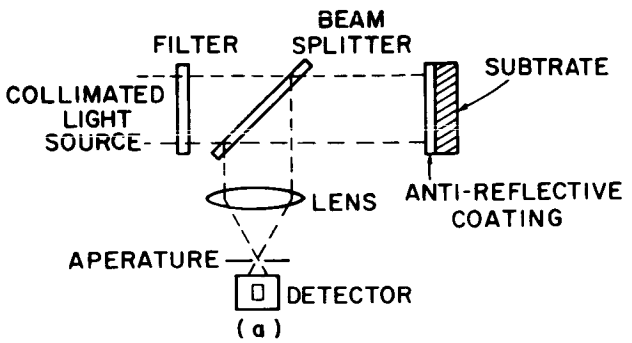

(a)

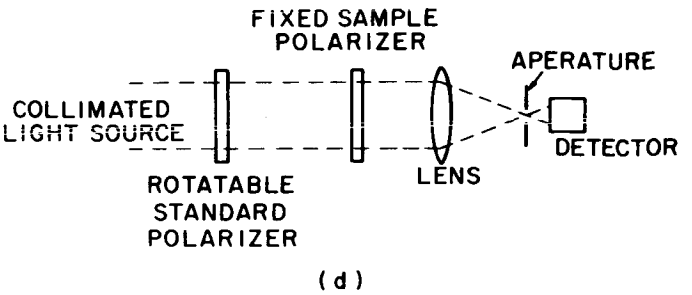

(d)

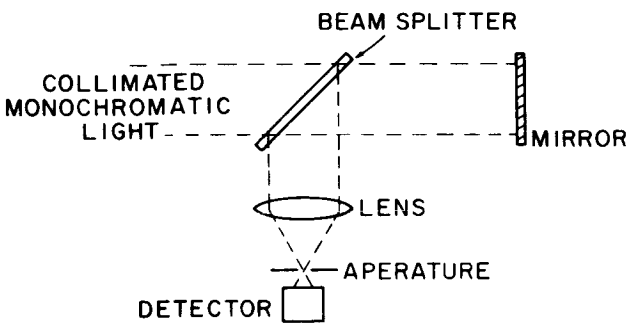

(b-1)

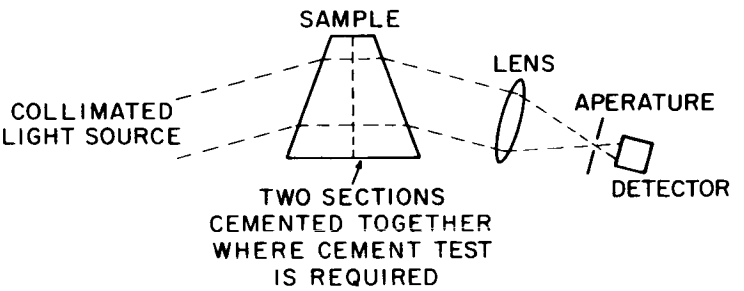

(e)

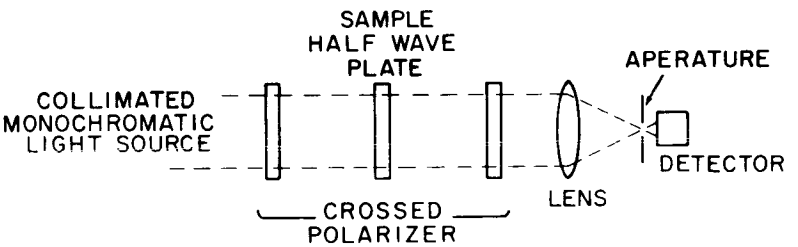

(f)

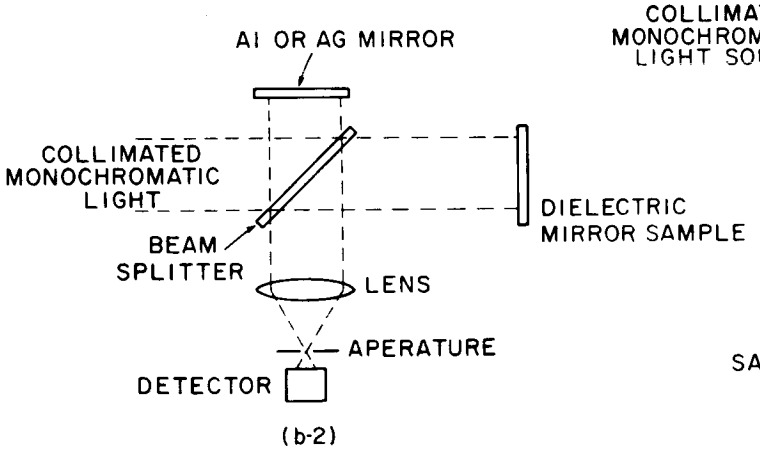

(b-2)

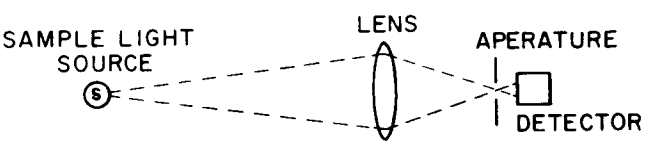

(g)

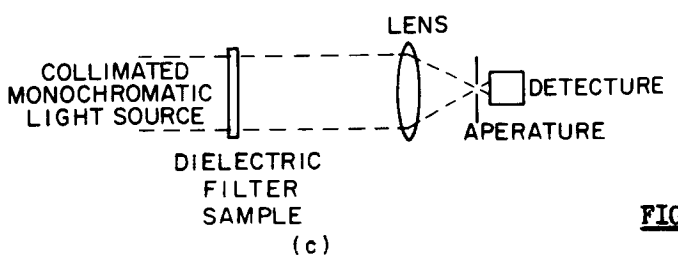

(c)

(h) LASER MATERIAL WOULD BEST BE CHECKED WHILE THAT MATERIAL IS OPERATING WITHIN A COMPLETE LASER

FIGURE III-2. Test Configurations

CHART III-1. ENVIRONMENT PARAMETERS

I. Proton (p^+) Bombardment

Simulation	Test No.	Time Integrated Flux**	Average Density
Solar Wind	I.A	5×10^{14} p^+/cm^2	1 Kev
Galactic Cosmic Ray's (relativistic)	I.B	1×10^{8} p^+/cm^2	3.6 Bev
Solar Flares	I.C-1	4×10^{11} p^+/cm^2	10 Mev $\lesssim \bar{E} \lesssim$ 100 Mev
	I.C-2	7×10^{9} p^+/cm^2	100 Mev $\lesssim \bar{E} \lesssim$ 1 Bev

II. Electron (e^-) Bombardment

Simulation	Test No.	Time Integrated Flux**	Average Energy
Solar Wind	II.A	5×10^{13} e^-/cm^2	50 ev
Solar Flares	II.B	2×10^{11} $e^-/cm2$	$1 \lesssim \bar{E} \lesssim$ 10 ev

III. Gamma (γ) Ray Bombardment

Simulation	Test No.	Radiation Flux
Galactic Cosmic Rays	III.A	Undefined (generally regarded as negligable)

** Time integrated flux is given here for a three year period. This time may be shortened for test purposes where it can be shown that the time interval is not of significance.

Chart III-1 Continued

IV. Ultra Violet (U.V., 200 Å - 3500 Å) Radiation

Simulation	Test No.	Radiation Flux	Wavelength Region
Solar Background	IV.A-1	2×10^{-5} watt/cm^2 3 yr exposure	100-2000 Å (roughly follows 4500°K Black Body
	IV.A-2	1×10^{-5} watt/cm^2 3 yr exposure	Hydrogen Lyman Alpha emission at 1215.7 A
	IV.A-3	1×10^{-2} watt/cm^2 3 yr exposure	2000-3500 Å (roughly follows 6000°K Black Body

V. X-Ray (10 Å - 100 Å) Radiation

Simulation	Test No.	Radiation Flux	Wavelength Region
Solar Flares	V.A	1.5×10^{-6} watt/cm^2 75 hr exposure	20-80 Å
Solar Background	V.B	1.5×10^{-7} watt/cm^2 3 yr exposure	20-80 Å

VI. Alpha (α) Particle Bombardment

Simulation	Test No.	Radiation Flux
Solar Flares	VI.A	Undefined, but may approach 10^{11} particles/cm^2 (Energy probably less than 10 Mev)≠
Solar Wind	VI.B	Undefined, but assumed small.

VII. Neutron (n) Bombardment

Simulation	Test No.	Time Integrated Flux	Energy Spectrum
Solar Flares	VII.A	2×10^{3} neutrons/cm^2	Undefined (probably on order of 10 Mev.)

≠ F. B. McDonald, Solar Proton Manual, Goddard Space Flight Center; NASA TRR-169; page 4, 114, December 1963.

Chart III-1 Continued

VIII. Meteoroid Bombardment (Density range 3 glcc-8g/cc)

Simulation	Test No.	Time Integrated Flux (for .4π Steradians)	Ave. Diam.	Velocity
Constant Environment	VIII.A-1	1 X 10^{7} particles/cm^{2}	2x10^{-5} cm	11-72 km/sec.
	VIII.A-2	1 X 10^{5} particles/cm^{2}	9X10^{-4} cm	11-72 km/sec.
	VIII.A-2	.01 particles/cm^{2}	9X10^{-3} cm	11-72 Km/sec.

IX. Thermal Environment

Simulation	Test No.	Temperature Range* (Kinetic)
Space	IX.A	100° K to 400° K (General) 120° K to 300° K (Most Likely)
Space Ship Interior	IX.B	200° K to 400°K (General)

X. Extreme Vacuum (~10^{-19} Torr)

Simulation	Test No.	Test Conditions
Space Vacuum	X.A	Experiments will probably have to be done in space.
Simulated Space Vacuum	X.B	10^{-10} to 10^{-11} Torr. Earth based vacuum stations. Materials surviving this test should then be subjected to space vacuum.

* The equilibrium temperature is drastically influenced by space ship design and materials, therefore, only general range will be considered.

CHART III-2

Materials	Use	Test	Test Exposure	Notes
1 Magnesium Flouride 2 Silicon Monoxide 3 Zinc Sulfide 4 Titanium Dioxide 5 Cerium Dioxide	Multi-layer coatings for Antireflection, Mirror, and Filter uses.	a,b,c	All tests I to IX (excluding IX. (3)	To be tested on fused quartz (Corning 7940) substrates in antireflection, mirror and filter combinations.
6 Calcite	Polarizers and Prisms(e.g.Wollaston)	d,e	I, II, III, VII, IX, B	
7 Natural Quartz	Polarizers and Prisms	d,e	I.A, IB, II, III, IX.B, I.C-1	5 X 10^{N} p^{+}/cm^{2}(240 Mev.)-negligable coloration. 2 X 10^{13} p^{+}/cm^{2}(22 Mev.)-Darkened 2 x 10^{14} e^{-}/cm^{2} (probably high energy - Brown striations
8 Silicon Monoxide	Protective Coating for Al Coated Mirrors	b	Stability and adherence properties: I - X (excluding IX.B)	
9 Balsam (Canada)	Lens and Prism Cement	e-2	Adhesion and Transmission I, II, III, VII and IX.B	Probably best to use air spaced components
10 Sapphire	Quarter & Half Wave plates and windows	e,f	I.A, I.B, I.C-2, II, III, IV, V, VI, VII, VIII, IX.A and X.	No less in transmission for: 3 X 10^{12} p^{+}/cm^{2} (19 Mev) 2.7 x 10^{15} e^{-}/cm^{2} (1.2 Mev).
11 Phenolic-Glass 12 Epoxy - Glass 13 Epoxy - Glass (Heat Resistant Type)	Structural Plastics, Lens supports Inside or outside of spaceship			No tests are recommended as these materials have proven themselves for all applicable environments.
14 Lithium Niobate 15 KDP and KD*P	Electrooptical Modulator Crystals	f	I, II, III, VII, IX.B	

CHART III-2 Continued

	Materials	Use	Test	Test Exposure	Notes
16	Antireflective Coatings for Lithium Niobate KDP and KD*P	Antireflection	a	Test for stability and adhesion: I, II, III, VII, IX.B.	
17	Index matching liquids for KDP and KD*P Modulators	Antireflection	a	I, II, III, VII, IX.B.	Imorganic Liquid should be used.
18	Cer-Vit (Owens-Corning)	Mirror Blanks	b	I, II, III, V, VI, VII, VIII, IX.A., X	Expansion coefficient 10^{-2} less than fused silica
19	Aluminum Coatings	Reflective Coatings for Mirror Blanks	b	I, II, III, V, VI, VII, VIII, IX.A, X	Good U.V. stability, probably not effected by space environment
20	Fused Quartz (Corning 7940)	Lenses, Filter Substrates and Windows	e	I, II, IV, V, VI, VIII	Must be ultra pure for good U.V., X-Ray and gamma ray stability. No transmission loss at 2.7×10^{15} e^-/cm^2 (1.5 Mev.) Probably good proton stability. Apparently good vacuum, temp., and gamma ray stability.
21	Laser Gases: Ar, He,Ne, Hg, CO^2, etc.	Active Laser Materials (RF or D.C. Pumped)	h	I, II, IX.B	Probably effect of p^+ and e^- would be to increase ionization rates. Effect to performance probably negligible. Temperature environment effect on Laser should be checked.

CHART III-2 Continued

	Materials	Use	Test*	Test Exposure**	Notes
22 23 24	YAG: Nd^{+3} Glass: Nd^{+3} Ruby: Cr^{+3}	Optically pumped Active Laser Materials	h	I, II, III, VII, IX.B	Material performance may be quite sensitive to p^+ and e^-. bombardment. Temperature sensitivity is also quite important.
25 26 27	Ga As In As In P	Injection Lasers	h	I, II, III, VII, IX.B	In general, those materials must be operated at 77° K
28 29	Xenon-Quartz Flash Lamps	Laser Pump Source	g	I, II, IX.B	Using in-line triggering and ignition type voltage hold-off, radiation effects on performance probably negligible.
30	Tungsten-Quartz C.W. Lamps	C. W. Exitation of Laser Materials	g	I, II, IX.B	Radiation effects probably negligible.

* Keyed to Figure III-2
** Keyed to Chart III-1

D.2.b Spaceborn Tests

Spaceborn exposure of optical materials is highly recommended. Though most material parameters cannot be practically measured in the spacecraft during flight, the materials can easily be exposed during flight, retrieved, and measured in ground laboratories. However, as pointed out above, it is recommended that the bulk of the radiation (and simultaneous measurement) be done on the ground using good space simulating facilities.

The spaceborn irradiation of the materials would serve two ends. The first would be to establish a good correlation between the effects of an actual space environment and a ground stimulated environment on the degradation of the materials. The second end space testing would serve would be as a final check on the results obtained by simulated irradiation of the materials.

Though the bulk of the material parameters changed by space and simulated environments can be correlated, there remains those material changes that are short lived, particularly flourescence and scintillation. If the space and simulated environment tests are to be correlated, some measuring equipment would have to be sent with the materials into space. This equipment, however, could be kept relatively simple as it does not have to measure most of the parameter changes measured during ground tests.

The type of equipment that could be used to contain and progressively expose material samples to the actual space environment is shown in Figure III-3, taken from a report by Kollsman Instrument

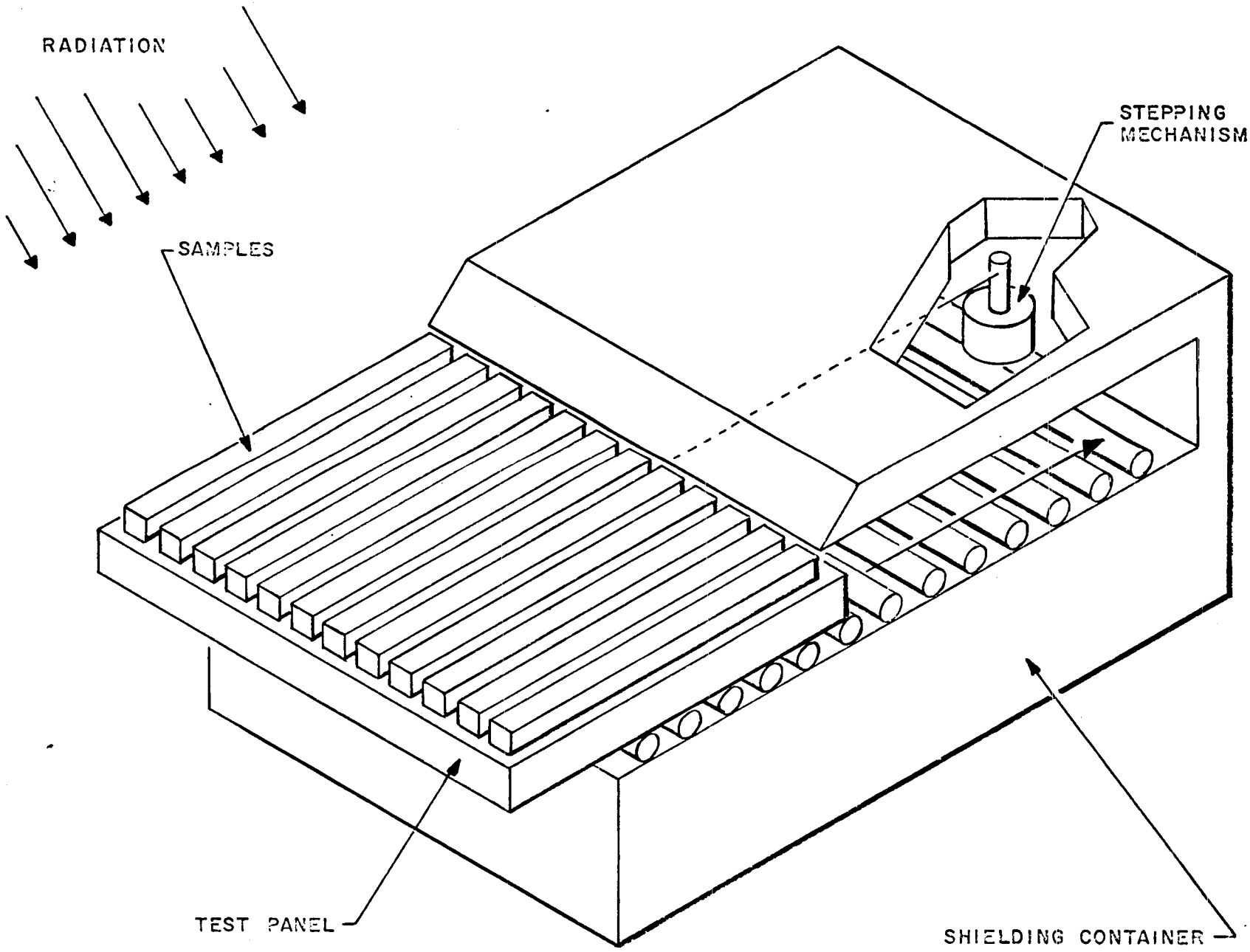

FIGURE III-3. Cumulative Exposure Experiment Box

Corporation.

E. Recommended Test Facilities

The degree that various existing radiation facilities simulate space environment varies with the facility, some being able to simulate one parameter or another. If the largest portion of material radiation exposure is to be done on the ground, it is important that the radiation source be capable of simulating all or nearly all the meaningful parameters attributable to actual space environment. As long as it has not been shown that synergistic irradiation of the materials has the same deteriorating effect as the sum of individual space parameters acting separately on the materials this will be true.

At least one such facility has been found. The Illinois Institute of Technology Physics Research Division operates a facility which is capable of simulating most space environment parameters and, what may be more important, these parameters may be applied to materials simultaneously.

It is recommended that this facility be considered for use in simulated testing.

Section IV

COMMUNICATION THEORY TEST PLANS

A. Statement of Task

The objectives of this task of the program has been to develop plans for experiments to verify the theory of laser communications when a laser communicator is operating near the quantum limit. Plans for testing laser communications both over an 11 mile field range and in the optical tunnel were to be devised. It was the intent of this task of the program to develop, whenever possible, plans for testing laser communication theory and laser communication system performance that could be implemented on NASA's laser communication equipment.

As part of this task methods to vary from quantum limited to noise limited system operation were to be devised. Methods for monitoring the error rate as the noise level and the data rate are varied were to be developed. For each test recommended, optical arrangements, methods of monitoring signal level, electronic test configurations, and the electronic test equipment required were to be described in detail. Methods of reducing test data to plots of probability of error as a function of signal and noise power per decision was the ultimate objective of these communication theory tests.

If possible, an analysis of the effects of atmospheric conditions on the performance of a laser communication system was to be carried out. The results of this analysis were to be included as part of this task.

B. Test Recommended

NASA has in its possession, or is developing, laser communicators that use PCM/PL modulation, PPM and wideband (50 MHz) analog FM modulation of a 125 MHz subcarrier. In addition, NASA has other equipment that can be assembled into communication systems, and it has optical test ranges. One of the ranges is 11 miles long, running from the desert floor at White Sands, New Mexico to the top of a mountain. The other range is in a controlled atmosphere, at NASA, Houston. This range is approximately 80 meters long, and the laser beam propagates within a cylindrical tube that is 4 meters in diameter.

Given this large selection of laser communicators, and two potential test ranges that are radically different in their optical characteristics, one of the most difficult portions of this task has been to select for development and recommendation those tests that would yield the greatest amount of information about laser communication theory and laser system performance. In general, tests have been selected for one of the four following reasons:

- they are basic, allowing system alignment, monitor calibration and test equipment calibration, while giving NASA personnel experience with system testing.
- they are tests of the basic theory of quantum limited operation, using existing digital data transmission systems.
- they are tests of the performance of a digital data transmission system, as distinguished from tests of theory of laser modem performance.
- Performance data obtained allows a partial characteristics of an unknown transmission medium, since this data is taken with a calibrated system.

Using these criteria, Westinghouse is recommending that NASA perform the following communication tests to determine, quantitatively, the performance of laser communicators and to characterize the effects of the atmosphere on this performance:

1. A monitor calibration experiment (See Part C) in the tunnel.
2. Testing of laser communication theory using analog modulation of a HeNe laser, to determine signal to noise ratios in the tunnel as a function of received signal level (See Part E).
3. The testing of the performance of a PCM/PL system in the tunnel, at a low data rate, to correlate test results with those predicted for PCM/PL modulation during Task III of this program (See Part F).
4. The testing of system performance for a 30 megabit/sec PCM/PL communication system in the tunnel (See Part G).
5. Measurement of the amplitude characteristics of an 11 mile test range at White Sands, New Mexico (See Part H).
6. Measurement of the phase characteristics of an 11 mile test range at White Sands, New Mexico (See Part I).
7. Measurement of system performance at 30 megabits/sec for a PCM/PL laser communicator operating over the 11 mile range (See Part J).

In addition to these specific tests, this part of the report suggests ways to test the digital performance of PPM and FM laser communication systems, details the optical configuration to be used for testing laser modulation theory and laser communication systems in the tunnel, explains the design and performance of monitors, investigates potential problems associated with high data rate testing, and recommends ways of reducing raw data to more meaningful formats.

C. Development of Monitors for Power Level Measurements

C.1 Performance of Photomultiplier Tubes as Optical Detectors

C.1.a General

Photomultiplier tubes (PMT's) will be used in monitors* to measure the average incident power on optical receivers during systems tests. It is also contemplated that the basic monitor will be used as a receiver in setting up a simple amplitude modulated communication link to be tested in the tunnel (See IV-E). The present section (IV-C) will discuss the performance of PMT's as optical detectors, the design of a monitor incorporating a PMT, and the calibration of the monitor. When used as a monitor the input to the PMT will be chopped at some low frequency like 90 hertz and the output will be measured on a wave-analyzer or synchronous detector. Because the monitor will be operating with a very narrow output bandwidth (2-10 hertz) its output S/N ratio should be high, even when the system receiver with an output bandwidth of some mega-hertz is operating quantum limited.

When the monitor is used as a simple optical reciver the input to the PMT will not be chopped. Instead, the PMT will act as a detector of the amplitude modulated transmitted beam. A single frequency sinusoid will be modulated on the optical carrier and this will constitute the signal in the receiver output. Measurements of output signal plus

*The term "monitor", as used in this section, means an optical power meter.

noise and noise will be made. From these one may calculate S/N ratios for comparison with theoretical predictions. More will be said about this under IV-E.

The anticipated dual use of the monitor necessitates the consideration of the PMT under two rather different modes of operation. As a monitor it operates with a chopper and a narrow output bandwidth (integration) to measure average incident power flux regardless of the modulation on the beam. Operating in this mode it may be used to measure the average power of a modulated beam, the power of an un-modulated beam, or the constant power flux due to background radiation in the optical bandwidth provided. When operating as a receiver it will be operated with the output circuit tuned to the modulation frequency. The bandwidth of the output circuit will be chosen to suit the purpose of the test. Varying the bandwidth should have no affect on signal power but will affect noise power and therefore S/N ratio, since the modulation is a single frequency.

C.1.b The PMT as a Simple Transducer

The PMT comprises a photoemissive surface, the photocathode, and a secondary-emission electron multiplier contained in a common evacuated glass envelope. Light striking the photocathode liberates electrons which are collected and guided through the multiplier section by properly applied electric fields. The amplified current flowing through the impedance of the output circuit produces a voltage which constitutes the output. Under normal operating

conditions the current liberated at the cathode is directly proportional to incident power and amplification is independent of current level. The PMT may therefore be viewed simply as a transducer which receives optical power and delivers an electrical output proportional to the power received. It will be instructive to formulate the relations between power (P) incident on the photocathode, current (I) liberated at the photocathode and the voltage (V) appearing across a resistance in the output circuit.

We know that the energy in electromagnetic radiation is quantized and if the radiation is monochromatic the energy quanta all have the same magnitude (hf) where (h) is Plancks constant and (f) is frequency in hertz. If the incident power is (P), the quantum efficiency of the photocathode (photoelectrons/photon) is ϵ, and the electronic charge is q, the current liberated at the photocathode is

$$I = \frac{\epsilon q P}{hf} \qquad (1)$$

This current is amplified by a factor (G), the gain of the dynode section of the PMT, and flows through an output resistance (R) to produce an output voltage,

$$V = \frac{\epsilon q G P R}{hf} \qquad (2)$$

These equations are in agreement with the simple transducer concept and describe the performance of the PMT quite adequately if (P) is high

enough and/or the bandwidth of the output circuit is so limited that noise in the output circuit is of no consequence. If we know quantum efficiency (ϵ), gain (G), and load resistance (R), we can calculate the proportionality factor between (V) and (P). Approximate values for these quantities are available in the descriptive literature provided by the supplier and suffice for general design purposes but not for absolute calibration where good accuracy is required.

But PMT's are used to detect very weak optical signals and may of necessity operate with output bandwidths of many megahertz. As a consequence, the noise characterics of the device are all important and must be considered.

C.1.c Quantum Limited S/N Ratio

We considered first the special case in which the S/N ratio in the output of the PMT is determined entirely by the quantum noise in the signal, i.e. the noise which the signal itself produces. To understand this condition consider a constant power (P) incident on the photocathode. The current leaving the photocathode is given by Equation (1) and constitutes a flow of electrons away from the photocathode. The noise in this current can be represented by the well-known and well-established shot-noise formula,

$$\overline{i^2} = 2qI\,df \qquad (3)$$

where q = electron charge

df = the increment of bandwidth contributing to $\overline{i^2}$.

Later we will determine the noise bandwidth of typical output circuits but for the present we simple use (B) to signify the bandwidth of the output circuit. The total noise current in the output circuit is then,

$$\overline{i_n^2} = 2eI_d G^2 B \qquad (4)$$

where (G) is the current gain of the PMT. Since the signal current is also amplified by the same factor (G) in the PMT, the output S/N ratio is,

$$S/N = \frac{I_s^2}{2eI_d G^2 B} \qquad (5)$$

This is the S/N ratio which would appear in the output of the PMT in the absence of all other noise sources. A higher S/N ratio obviously cannot be achieved. If the value of (I) is substituted from equation (1) the S/N ratio is expressed in terms of incident power (P) as,

$$S/N = \frac{\eta^2 P^2}{2eI_d B} \qquad (6)$$

If $\eta = 1$ (100 percent quantum efficiency) equation (6) becomes,

$$S/N = \frac{P^2}{2eI_d B} \qquad (7)$$

which is the S/N ratio inherent in the optical beam intercepted by the photocathode. We see that the S/N ratio realized in the output of the PMT is lower by a factor ( ) than the inherent S/N ratio in the incident beam.

This quantum noise limitation typical of many optical systems never arises in R.F. systems because the magnitude of the energy quanta (hf) is at least 1000 times smaller at radio frequencies and other noise sources (usually thermal noise) limits S/N ratio before the quantum limit is reached. Other noise sources are also present in PMT's and we procede now to consider the overall noise characterics of this device. Before leaving the quantum limited case it is interesting to note that a S/N ratio of unity is achieved in equation (5) when the current is 2qB which corresponds to an average of two electrons per hertz of bandwidth. Likewise from equation (6) the S/N ratio inherent in the incident beam is unity when the power (P) corresponds to two photons per hertz of bandwidth if 100% quantum efficiency is assumed.

C .1.d. Total Noise Considerations*

It is clear from the above discussion that any current originating at the photocathode has a noise component associated with it, and the noise component can be represented by equation (4) if the proper current is substituted.

The sources of noise in a PMT are 1) the signal noise already discussed, 2) the dark current noise associated with the current(I_d)

*This discussion assumes that the shot noise contributed by I_c is independent of the usable signal energy.

leaving the photocathode in the absence of optical input (primarily thermal emission), 3) background noise associated with the current (I_b) due to back ground radiation entering the system in the optical bandwidth provided, and 4) thermal noise generated by the resistance of the output circuit. The contribution of these noise sources will be considered and expressions for S/N ratio will be derived. For this analysis it will be assumed that the PMT receiver is looking at a laser transmitter, amplitude modulated at a single frequency (f_o), as illustrated in Figure IV-1a. (P_o) is the maximum possible output of the transmitter, $P_c = P_o/2$ is the average or carrier power level, and the peak modulation power, with a modulation index (m), is $P_m = mP_c$. The corresponding variation in photocathode current is shown in Figure 1b. Calculations will be made in terms of currents at the photocathode which are related to power incident on the photocathode by equation (1).

Let us now consider the noise sources and their contribution to total noise in the output circuit. The expressions for the contribution by the signal carrier (I_c), the dark current (I_d), and the background current can be written directly,

$$\overline{i_s^2} = 2qI_c G^2 \Delta f \tag{8}$$

$$\overline{i_d^2} = 2qI_d G^2 \Delta f \tag{9}$$

$$\overline{i_b^2} = 2qI_b G^2 \Delta f \tag{10}$$

The PMT is a pretty good approximation to an infinite impedance source supplying these currents in parallel to the output circuit. These currents have been amplified in the PMT. The thermal noise generated by the resistance of the output circuit also can be represented by an infinite impedance current source in parallel with the output circuit. The strength of this source is given by

$$\overline{i_t^2} = \frac{4kT\,p(f)\,df}{R} \qquad (11)$$

where (k) is Boltzmanns Constant, (T) is the temperature of the loss elements in the output circuit, p(f) is Plack's factor, df is the incremental frequency bandwidth contributing to $(\overline{i_t^2})$ and (R) is the equivalent shunt resistance of the output circuit. In the radio frequency range Plack's factor p(f) = 1 so the noise contributed by the output resistance is,

$$\overline{i_t^2} = \frac{4kT\,df}{R} \qquad (12)$$

All of these current sources equations 8, 9, 10 and 12 are expressed in differential form and represent the contribution to noise in the incremental bandwidth (df).

The average square of the signal current from Figure IV-1 is,

$$\overline{i_s^2} = \frac{m^2 I_m^2 \sigma^2}{2} = \frac{m^2 I_a^2 \sigma^2}{2} \qquad (13)$$

FIGURE IV-1. Input Signal to PMT

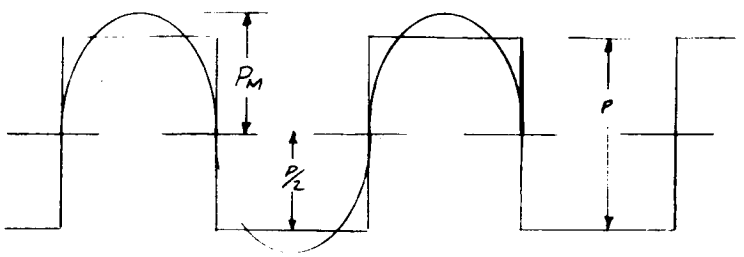

(a)

$P_M = \frac{P}{2} \cdot \frac{4}{\pi} = \frac{2P}{\pi}$

$Pm = mP_c$

m = modulation index

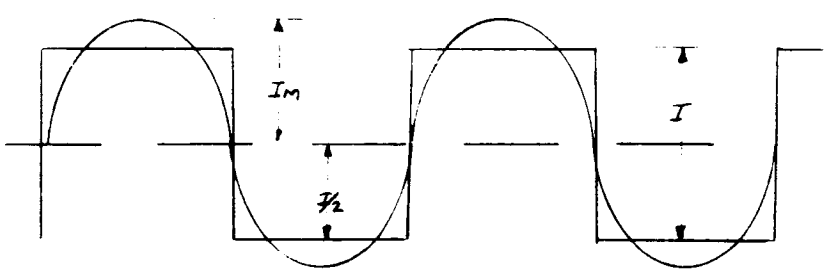

(b)

$I_M = \frac{I}{2} \cdot \frac{4}{\pi} = \frac{2I}{\pi}$

$Im = mI_c$

m = modulation index

This current, like the shot noise currents, is amplified in the PMT and acts like an infinite impedance current source in parallel with the output circuit. It should be noted that the signal current and the shot noise currents are amplified through the PMT but the thermal noise in the output circuit is not.

Fig.IV-2 shows the equivalent circuit of the signal and noise sources in parallel with an RLC tuned output circuit. The problem is to calculate the noise component of voltage $\overline{v^2}$ which each will produce across the output circuit and the S/N ratio at the output of the PMT.

The output circuit is assumed to be tuned to the frequency (f_o) of the modulation frequency. The $\overline{v^2}$ for the signal is therefore simply

$$\overline{v_s^2} = \frac{i_s^2}{2} \tag{14}$$

The noise currents contain all frequencies, and since the impedance of the output circuit is frequency dependent, the contribution of the several noise currents to the voltage across the output circuit must be determined by integration.

Consider first the thermal noise source (equation 12). The total voltage produce by this source is

$$\overline{v_t^2} = \int_0^\infty \frac{4kT}{R} |Z|^2 \, df \tag{15}$$

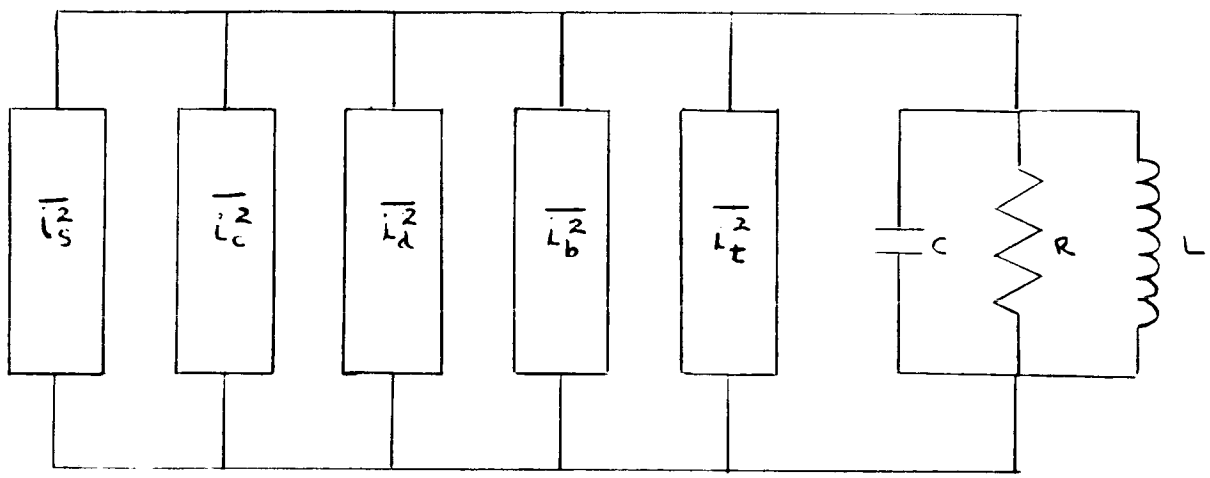

FIGURE IV-2. Equivalent Circuit of PMT

where $|Z|^2$ is the square of the absolute circuit impedance. This is a somewhat tedius integration but the result is simple

$$\overline{v_c^2} = \frac{kT}{C} \tag{16}$$

The result also follows from the assumption of the equipartition of energy

$$\tfrac{1}{2} L \overline{i^2} = \tfrac{1}{2} C \overline{v^2} = \tfrac{1}{2} kT$$

whence

$$\overline{v_c^2} = \frac{kT}{C}$$

Note that in the integral of equation (12) $|Z|^2$ at the point of resonance has the value R^2. We can define the noise bandwidth therefore by,

$$\frac{4kT}{R} \cdot R^2 \cdot B = \frac{kT}{C}$$

whence,

$$B = \frac{1}{4RC} \tag{17}$$

The spectral density function $\overline{i_t^2}$ is from equation (12) 4KT/R and the voltage contributed across the output circuit is KT/C. The ratio of $\overline{v^2}$ to the spectral distribution function is R/4C. This ratio must be the same for all noise currents because all have constant spectral density functions. We can therefore write immediately the total $\overline{v^2}$ contributed by all the shot noise currents, equations 8, 9, and 10.

$$\overline{v^2} = \frac{qG^2R^2}{2C^2}\left(I_c + I_d + I_f\right) \tag{18}$$

1.

The total noise voltage is obtained by adding the thermal noise (equation 13).

$$\overline{i_n^2} = \frac{kT}{C} + \frac{q G^2 R}{2C}\left(I_c + I_d + I_b\right) \quad (19)$$

and the S/N ratio at the output of the PMT is equation (13) divided by equation (15)

$$S/N = \frac{\frac{m^2 I_c^2 G^2 R^2}{2}}{\frac{kT}{C} + \frac{q G^2 R}{2C}\left(I_c + I_d + I_b\right)} \quad (20)$$

The noise bandwidth is given by equation (17) and is obviously the same for all noise sources. Dividing equation (16) by (R) and substituting RC = 1/4B gives,

$$S/N = \frac{\frac{m^2 I_c^2 G^2 R}{2}}{2kTB + 2qG^2 RB\left(I_c + I_d + I_b\right)} \quad (21)$$

This is a familiar form of the equation which could have been written from inspection. The rather rigorous procedure was followed to emphasize the nature of noise and it incidentally showed that the noise bandwidth of the tuned RLC circuit is 1/4RC. This is, at first glance, a rather surprising result because it shows that bandwidth is fixed by R and C without considering (L). This suggest that (L) may be made infinite and that the noise bandwidth of a simple RC output circuit is also 1/RC. This can be verified by carrying out the integration indicated in equation (12) for this simple case. It can also be

shown that the noise bandwidth (B) is related to the 3 db bandwidth (Δf) by,

$$B = \frac{\pi}{2} \cdot \Delta f \tag{22}$$

C .1.e. Thermal Noise is Generally Negligible in a PMT

One of the outstanding advantages of the PMT is the high post-detection gain which raises the signal power to such a level that thermal noise in the output circuit is negligible in comparison to the shot-noise which we have seen is inevitable in any photon detector. In a simple vacuum photodiode or solid state photodiode the thermal noise is generated ahead of the amplifier and is usually much greater than shot noise. The ratio of thermal noise to shot noise from equation (17) is,

$$\frac{N_t}{N_s} = \frac{2kT}{2eG^2R(I_c + I_d + I_b)} \tag{23}$$

The only current in the denominator which cannot be arbitrarily reduced is I_d so we will eliminate I_c and I_b and write,

$$\frac{N_t}{N_s} \simeq \frac{2kT}{2eG^2RI_d} \tag{24}$$

To eliminate R we will substitute bandwidth (B) and output capacity (C) through the relation $B = 1/4RC$, which gives

$$\frac{N_t}{N_s} \simeq \frac{8kTBC}{q^2 G^2 I_d} \qquad (25)$$

If we substitute

$G = 1.5 \times 10^5$

$I_d = 5 \times 10^{-14}$ RCA 7326 S-20 surface

$k = 1.38 \times 10^{-23}$ joules/degrees K.

$T = 300°K$

$C = 10^{-11}$ farads

$q = 1.60 \times 10^{-19}$ coulombs

$$\frac{Nt}{Ns} = 1.84 \times 10^{-9} B \qquad (26)$$

Thus we see that for any bandwidth within the capabilities of the tube, thermal noise is completely negligible in comparison to shot noise. (The usable bandwidth of a conventional PMT is limited to approximately 5×10^7 hertz by variations in transit time of electrons through the dynode structure.) The values of gain (G) and dark current (I_d) used are characteristic of the RCA 7326 PMT which will be used as a model throughout this analysis. It is chosen for its simplicity, its S-20 response which is suited for receiving both the He-Ne visable wavelength (6328 Å) and the 4047 Å and 5145 Å wavelengths of the argon ion laser.

Since thermal noise is negligible in comparison to shot noise with the RCA 7326 operating at its rated gain we will eliminate the 4kTB term in the denominator of equation (17) to obtain,

$$S/N = \frac{m^2 I_c^2}{4qB(I_c + I_d + I_{bg})} \qquad (27)$$

It should be kept in mind,of course, that if for some reason the tube is not operated at or near rated gain the magnitude of the ratio Nt/N_s as given by equation 21 should be checked to see if the thermal noise term can still be neglected.

If we assume that background noise is negligible in comparison to the sum of the carrier generated noise and the dark current noise, equation (18) is further simplified to,

$$S/N = \frac{m^2 I_c}{2qB\left(1 + \frac{I_d}{I_c}\right)} \qquad (28)$$

The relationship of (S/N), I_c and (B) represented by this equation are plotted in Fig. IV-3. The dark current level is indicated and it will be noted that the (S/N) ratio drops off rather rapidly when I_c falls below I_d. The curves are arbitrarily terminated at 10 db because it is felt that an analogue system is not particularly useful below this value. The termination was quite arbitrary and the curves may be extended to 1 db if desired. A modulation index m = 1 was assumed in plotting the curves. The effect of a lower modulation index is clearly indicated by the equation.

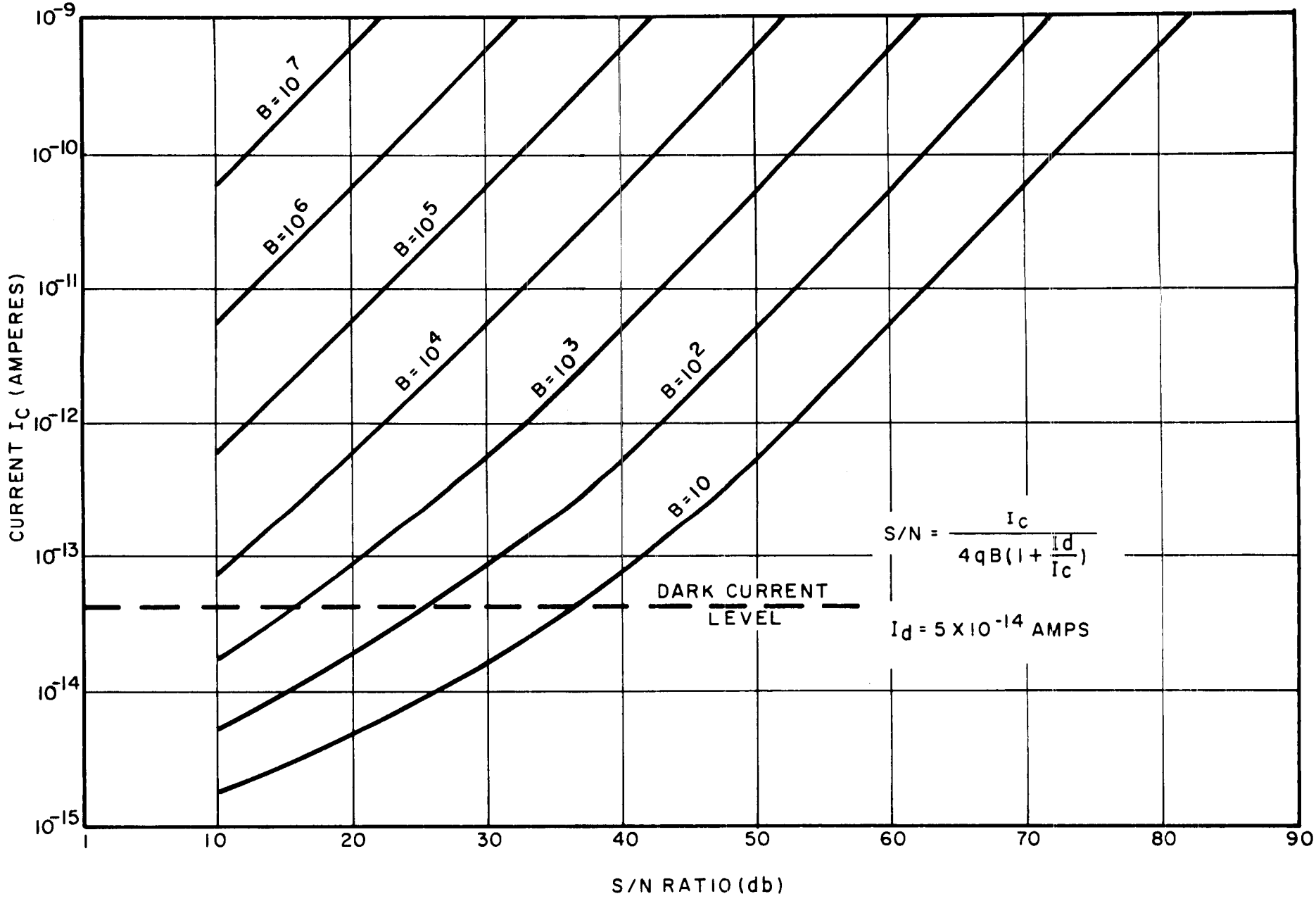

FIGURE IV-3. Sine Wave Modulation

Equation (1) was used to convert from (I_c) to carrier power (P_c) and the resulting curves are plotted in Figure IV-4. These curves are suited to experimental verification because a calibrated monitor can be used to measure the power density at the receiver and from this one can calculate the average carrier power incident on the photocathode.

It should be emphasized that the I_c values plotted in Figure IV-3 are current values at the photocathode. The highest value of I_c plotted in the curves is 10^{-9} amperes which corresponds to $1.5 \times 10^{5} \times 10^{-9} = 150 \times 10^{-6}$ amperes which is at least close to the limit of linearity for the electron multiplier. The corresponding upper limit for P_c in Figure 4 is 3.14×10^{-8} watts incident on the photocathode. The region of linearity and other characteristics should be run on any PMT to be used in the quantitative testing of theory.

C.1.f. Square-Wave Modulation

Thus far we have considered only a sinusoidally modulated carrier. Since it is planned to use PMT's as monitors to measure average power density (irradiance) in the place of a receiver and since the optical input to the PMT will be interrupted with a mechanical chopper, it is necessary to consider the case of a square-wave modulated input. Quantities are defined in Fig. IV-5 and we can write an expression for S/N ratio on the basis of equations already developed for a sinusoidally modulated carrier. Only the fundamental frequency component of the chopped input will be selected and measured in the output of the PMT. As in the sinusoidal case we will write equations in terms of currents

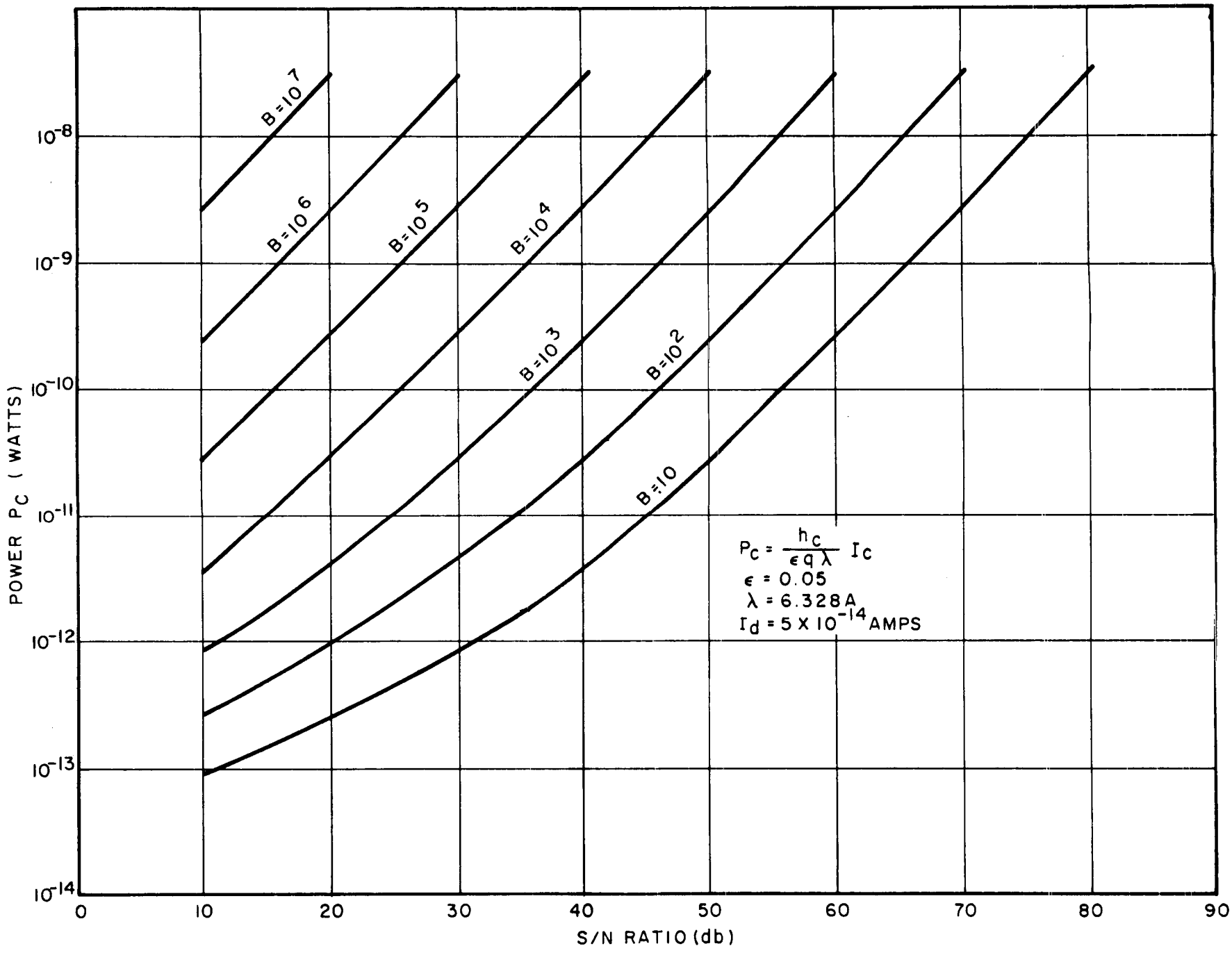

FIGURE IV-4. Sine Wave Modulation

$$Pm = \frac{P}{2} \quad \frac{4}{\pi} = \frac{2P}{\pi}$$

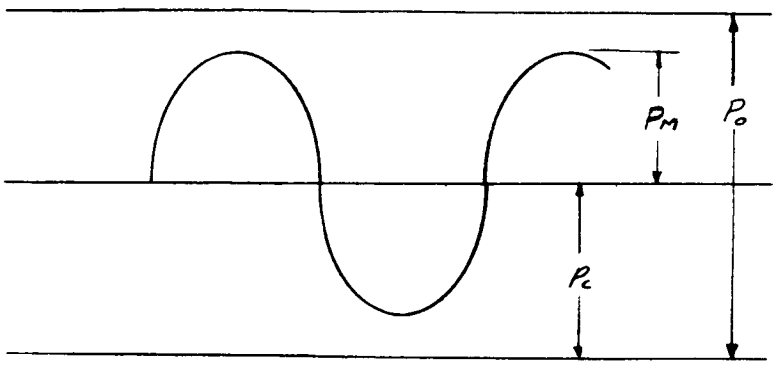

(a)

$P_M = M P_c$

M = MODULATION INDEX

$$Im = \frac{I}{2} \quad \frac{4}{\pi} = \frac{2I}{\pi}$$

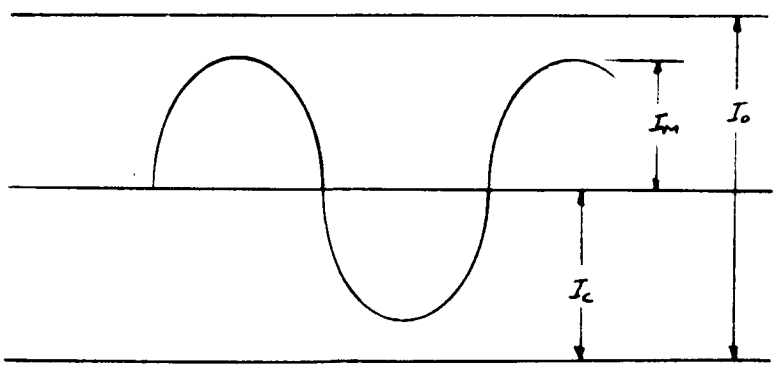

(b)

$I_M = M I_c$

M = MODULATION INDEX

FIGURE IV-5. Square Wave Modulation

at the photocathode and convert to power at the photocathode by equation (1).

If we go back to equation (17) and neglect the 4KTB term in the denominator it can be written as

$$S/n = \frac{i_m^2/2}{2qB(I_c + I_d + I_b)} \qquad (29)$$

The peak current (I_m) for the square wave (chopped wave), Figure 5, is $I_m = 2I/\pi$, and the carrier current I_c is I/2. Substituting these values in equation (20) we obtain for the square wave case,

$$S/n = \frac{I^2}{\pi^2 qB(I/2 + I_d + I_b)} \qquad (30)$$

which if we neglect (I_b) can be written,

$$S/n = \frac{2I}{\pi^2 qB\left(1 + \frac{2I_d}{I}\right)} \qquad (31)$$

This is analogous to equation (19) for the sinusoidal case and is plotted in Fig. IV-6. Fig.IV-7 shows the same curves plotted in terms of power. It should be noted that for the sinusoidal case the current (I_c) and power (P_c) are the true carrier values of these quantitites whereas in the square-wave case the power (P) is the power incident on the photocathode when the chopper is open and (I) is the corresponding current. It seemed desirable to write the equations and plot the curves in this way because sinusoidal modulation will be used

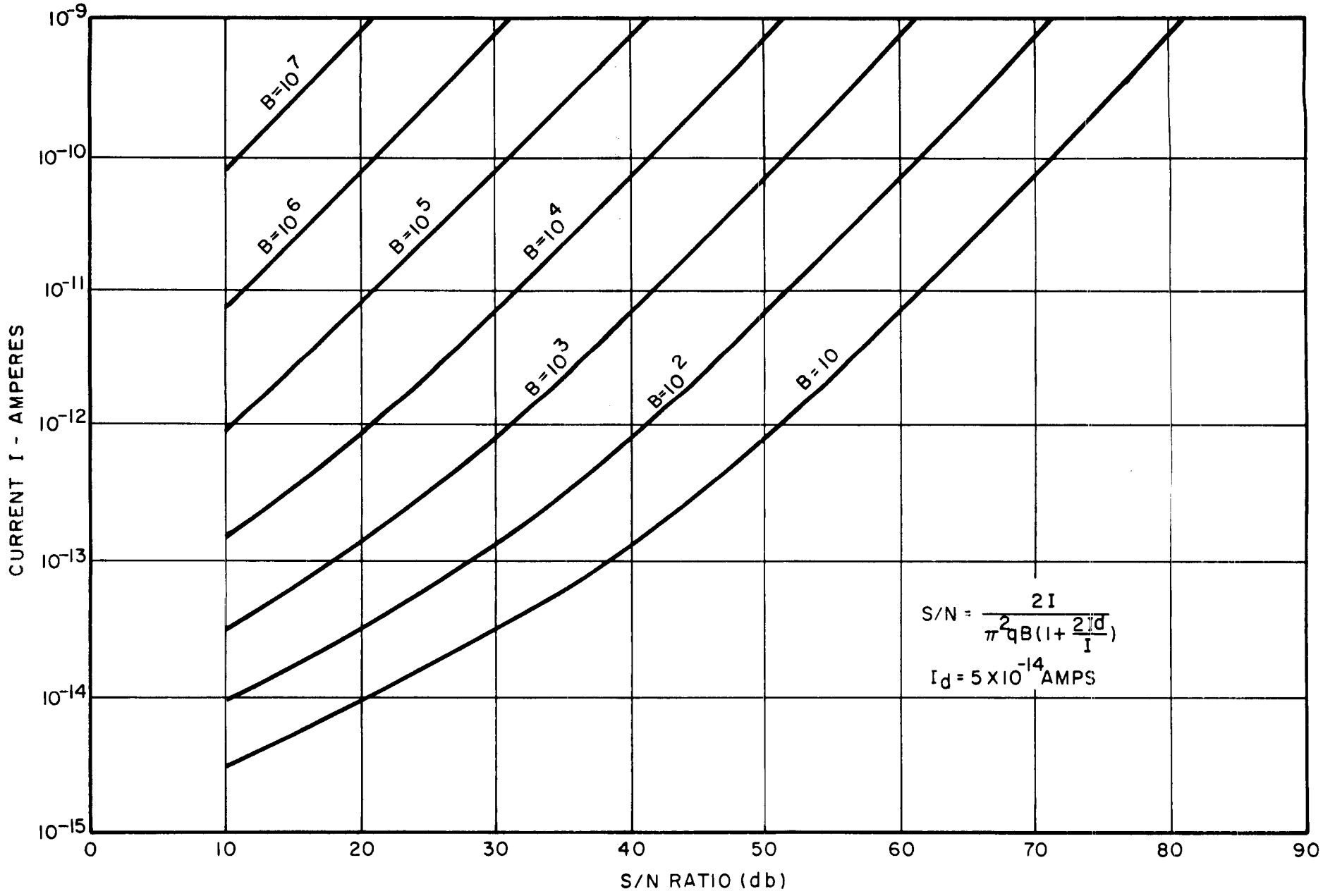

FIGURE IV-6. Square Wave Modulation

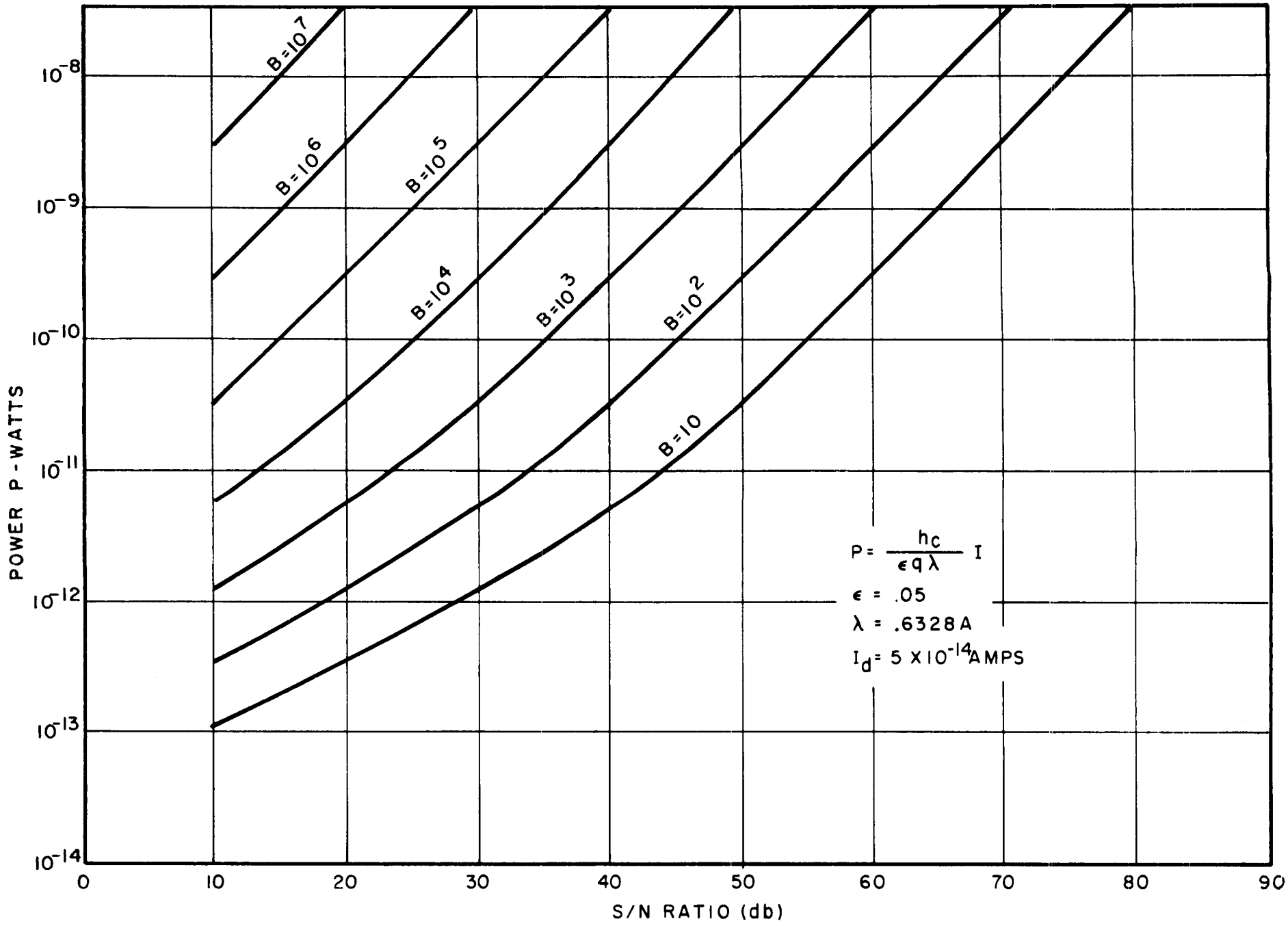

FIGURE IV-7. Square Wave Modulation

primarily in communications experiments and square wave modulation will be used primarily in the monitoring application. Considering the fact that the monitor will operate characteristically with a narrow output bandwidth it is probably superfluous to plot the curves for a range of bandwidths. This was done simply for the sake of completeness and just in case one might want to test a PMT receiver in conjunction with a square-wave modulated transmitter.

There is not much difference in the equations and curves for sinusoidal and square-wave modulation, as one would expect. At first glance the operating range of current and power shown by the curves appears to be limited for larger bandwidths. The reader will probably realize that this is not a real limitation. The upper limit of the curves is fixed by maximum allowable anode current on the basis of a constant gain in the amplifier. (S/N) ratio, according to the simple model used is not dependent on gain, so when the input level is such that anode current is excessive one should reduce the voltage on the PMT to reduce gain. This condition arises only when noise due to dark current is negligible. Reduced gain allows one to increase power input and photocathode current well beyond the range plotted. Thermal noise in the output circuit will eventually become appreciable in comparison to shot noise as gain is reduced and must therefore be considered. There are also precautions to be taken in reducing voltage. The noise figure of the electron multiplier is not unity as we have assumed in the simple model but depends on the ratio of secondary

electrons to primary electrons at a dynode. This ratio should be maintained at the first few dynodes by operating these at full voltage. The overall reduction in gain is accomplished by operating the remaining dynodes at reduced voltage.

C.2 PMT Monitors

C.2.a General

The PMT monitor to be described will have a dual purpose and use. It will be used to measure the irradiance in the plane of a test receiver so that the average power intercepted by the receiver and delivered to the photo surface of the receiver PMT can be calculated. Knowing total average power the energy per decision in the case of digital transmission or energy per cycle of bandwidth in an analog transmission may be calculated. Theoretically predicted performance may thus be determined and checked by experiment. In this mode of operation the optical input to the monitor will be mechanically chopped at some low frequency like 90 hertz and the output of the PMT will be read on a wave-analyzer or synchronous detector. Mechanical chopping of the optical input and reading out on a wave-analyzer or synchronous detector enhances the desired signal relative to dark current in the PMT because the latter is not chopped. Noise associated with the dark current appears in the output circuit but this is minimized through integration in the narrow-band output circuit. The effective narrow bandwidth of the PMT also discriminates against extraneous electromagnetic disturbances like 60 cycle hum and other circuit noise. The monitor will usually employ a narrow bandpass optical filter in front of the PMT to minimize background radiation which would otherwise limit the sensitivity and usefulness of the monitor. The monitor operating in this mode can obviously be used

to measure background radiation falling in the passband of the optical filter. The monitor will be calibrated by use of a calibrated light source, as will be described later.

The monitor will also be used as a simple optical receiver for use in conjunction with a laser transmitter (See IV-E). The design concepts of the monitor will be described and it is suggested that at least two prototypes of the final design be built so that one may be used as a monitor with the other operating as a simple optical receiver.

C.2.b Description of Monitor Design

Experience may indicate the desirability of building a number of monitors because calibrated monitors will find many uses, some no doubt which are not even anticipated in the planning stage. The heart of the monitor is the PMT with its housing, its voltage divider and the necessary regulated power supply. The RCA type 7326 PMT was selected as a model for the discussions and analyses presented in the last section. It is proposed to use this tube or its equivalent in the construction of the monitor. It is a relatively cheap and unsophisticated PMT, quite adequate for our purpose. It incorporates an S-20 photosurface suited for operation at the visible HeNe laser wavelength (6328Å) and at the argon ion laser wavelengths (4880 Å and 5145Å). The 10 stage electron amplifier provides a current gain of 1.5×10^5, more than adequate to make thermal noise in the output circuit negligible in comparison to shot-noise. A higher gain PMT

would be more temperamental and more difficult to use. As shown in the last section it will actually be necessary to reduce the gain of the type 7326 PMT under certain operating conditions to prevent excessive output current. Although the monitor is to be a portable instrument, size is not a controlling factor, and it is felt that the standard size PMT is preferable to a miniature version.

Various suppliers can provide shielded housings for PMT's of most makes and sizes. It is usually preferable to obtain the shielded housing from the tube supplier and alter it as necessary to fit into the design of the ultimate equipment. There would seem to be no reason for a coolable housing in the presently anticipated use of the monitor.

Fig.IV-8 shows schematically one possible monitor configuration. The sketch is strictly illustrative and will be referred to in the following discussion of the functions to be performed. A small reflecting telescope with folded optics is shown as the optical collector. This is envisioned as a "Questar" (field model) telescope or equivalent. The Questar telescope has a 4" aperture and an effective focal length of 50". The physical length of the barrel of the telescope is approximately 10". It employs a primary mirror (M_1) and a secondary mirror (M_2). The light collected by (M_1) converges on (M_2) which redirects it back through (M_1) to a prime focus. A field stop (S) located at the prime focus will be used to limit the field of view of the telescope. From (S) the collected light in the

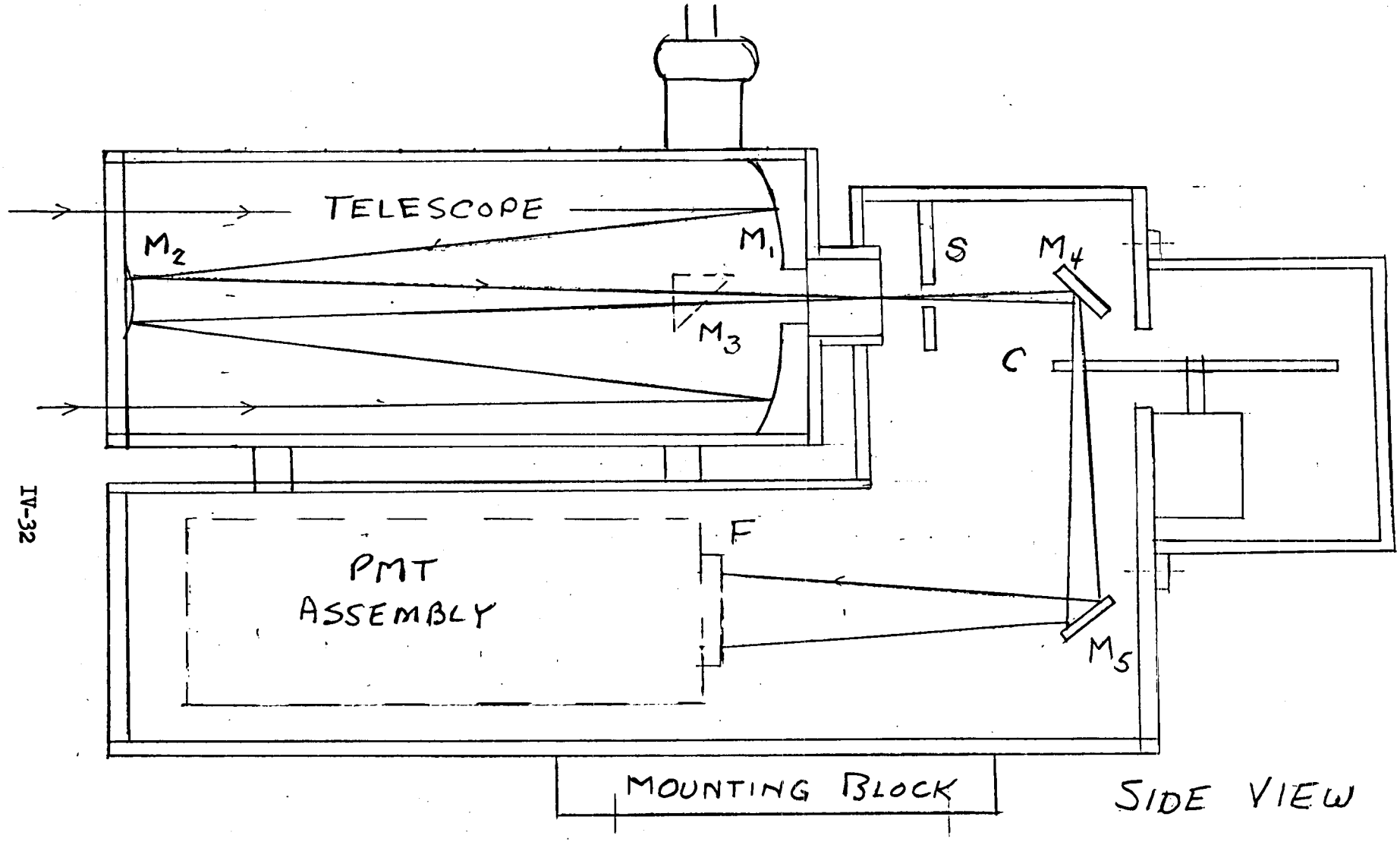

FIGURE IV-8. Illustrative Design Sketch of Monitor

divergent beam is reflected off 45° plane mirrors (M_4) and (M_5) and onto the face of the PMT. A chopper (C) is located between (M_4) and (M_5) to interrupt the light fed to the PMT. For the dimensions shown (half scale) the spot on the photocathode will be a little less than 1" in diameter. In the telescope there is a totally reflecting prism (M_3) which can be moved so as to intercept and redirect the beam from (M_2) to form an image in front of the eyepiece on top of the telescope. By the use of adjustable cross-hairs in the eye-piece one can collimate the visable field in the landscape with the laser beam from a transmitter when the telescope is oriented so that the received signal passes through the field stop (S). When the system is thus collimated the eyepiece may be used to aim the monitor at a distant transmitter. Depending on use it may be desirable to reduce the acceptance angle of the system to less than one milli-radian.

A filter holder (F) is located in front of the PMT. Bandpass and neutral density optical filters will be inserted in this holder as required. Typical bandpass and neutral density filters which can be obtained from the Ealing Corporation, 2225 Massachusetts Avenue, Cambridge, Mass, 02140, among others, are as follows:

Ealing TFP Interference Filters

Cat.No.	Price	λ	$\Delta\lambda$	t	t_s
26-525	$60.50	6328Å	100Å	50%	10^{-3}%
26-527	90.50	6328Å	30Å	70%	10^{-3}% (2)
26-528	185.50	6328Å	10Å	60%	10^{-3}% (2)
26-520	185.50	5145Å	10Å	50%	10^{-3}% (2)

(2) Free filter range ends at 1 micron.

λ = wavelength

$\Delta\lambda$ = bandwidth

t = transmission in band

t_s = spurious transmission outside band.

Ealing TFP Neutral Density Filters

Cat.No.	Price	Density	2500Å	5000Å	1.2 μ
26-575	$40.50	.30 ± .03	46.8%	50%	53.7%
26-576	40.50	.60 ± .03	23.5%	25%	26.9%
26-577	40.50	1.00 ± .03	9.3%	10%	10.7%
26-578	50.50	2.00 ± .10	.8%	1.0%	1.2%
26-579	60.50	3.00 ± .10	.08%	0.10%	0.12%
26-580	70.50	4.00 ± .10	.008%	0.010%	0.012%

The mechanical chopper is mounted external to the main enclosure and is provided with a separate removable light tight enclosure. It is anticipated that the chopper will be removed when the monitor is used as a simple optical receiver although one may choose to provide a means for locking the chopper in the open position.

It is suggested that the main enclosure be fabricated from 1/8" thick aluminum sheet with all seams welded to make it light tight. Only the side view is shown. Overall dimensions should be approximately

8" high x 4" wide x 18" long. One side should be removable with quick acting screw fasteners to permit access to interior components. A heavy aluminum alloy block welded to the bottom will be drilled and tapped for mounting on tripod or otherwise. Variable adjustments in azimuth and elevation should be provided for alignment purposes.

The mechanical chopper can be constructed from a suitable synchronous motor and a slotted disc. A motor speed of 600 rpm appears favorable from the standpoint of noise and vibration. For a chopping frequency of 90 hertz, the disc must be provided with 9 slots. Assuming a diameter of 4" and a slot width equal to a tooth width the slot width is about 0.7". The diameter of the beam at the chopper is approximately .32". The chopped output will not be a very good square-wave but this should be of little or no consequence.

The sensitivity inherent in this monitor is greater than needed in some phases of systems testing. This will be particularly true when attenuation (neutral density filters) is introduced in a receiver under test in the tunnel. On the other hand the sensitivity* of this monitor can also be reduced by the introduction of neutral density filters along with the narrow-band optical filter and the sensitivity is available when needed. It is anticipated that a calibrated lamp will be permanently installed where it can be used to perform a quick calibration on the monitor. With this facility the change in sensitivity of the monitor and recalibration are easily accomplished. Operating with high sensitivity the monitor may be used to measure

*Monitor sensitivity is the ratio of the output current from the monitor to the flux incident on its receiving optics.

weak signals, background due to sunlight and other sources, the strength of isolated sources like the moon, the stars, the planets, etc.

The power supply for the PMT has not been mentioned. It is assumed that this item will be purchased. Good regulation is essential and the output voltage should be adjustable in order that the sensitivity of the PMT may be adjusted by varying the voltage applied to it. It will connect to the monitor head through a suitable flexible lead. A flexible lead from the monitor will also be required for convenient metering of the output. Another lead will be required to supply power to the chopper motor and still another to bring out a synchronizing signal if the output measuring equipment requires it.

The Telewave Laboratories, Inc., 43-20 34th Street, Long Island City 1, N.Y. make a line of stock and custom built choppers and motor power supplies. Some of their component parts may be useful in constructing the chopper for the monitor, especially if for some reason it is decided that a regulated adjustable speed drive is desirable.

C.3. CALIBRATION OF MONITOR

C.3.a General

We will consider first the general theory and procedure to be used in calibrating a monitor, then procede with a discussion of calibrated light sources and other practical details. It will be obvious as we proceed that the thing which remains constant is the power output of the calibrated source. The monitor is simply a detector of optical radiation which can be expected to hold its calibration only so long as something is not changed to affect its sensitivity. Changes in the sensitivity of a PMT can arise from a variety of causes, some of which may not be understandable. Thus, a recalibration is in order if there is any reason to suspect a change. Fortunately recalibration can be as simple as turning on the calibrated lamp, pointing the monitor toward it, and taking a reading of output.

The monitor will normally be calibrated with a narrow band optical filter in front of the PMT, because it will be so used to monitor and measure the power delivered by a laser transmitter. Even when it is used to measure background or other non-signal power sources we will be interested only in the power which these sources can deliver in the passband of the filter.

C.3.b. Theory of Calibration

The theory of calibration is quite simple. The standard lamp used in calibrating the monitor will have a known output. This can

be described in either of two ways, 1) the radiance (N) of the source in watts/cm^2/sterradian/unit wavelength interval at various wavelengths or 2) the irradiance (H) produced on a plane perpendicular to the line joining it to the source in watts/cm^2/unit wavelength interval at various wavelengths. In either case the orientation of the lamp will be specified because it does not emit uniformly in all directions. Let us consider in more detail the concepts of radiance and irradiance and some other terms used in discussing radiation.

The total radiation from an emitting body is described as "radiant flux" and will be measured in watts. Radiant flux density at the surface of the emitter is called "radiant emittance" and will be measured in watts/cm^2. The radiation from a source into unit solid angle is called "radiant intensity" and will be measured in watts/ster. The radiation from unit area of an emitting body into unit solid angle is called "radiance" and will be measured in watts/cm^2/ster. The flux density on an irradiated surface is called "irradiance" and will be measured in watts/cm^2. These radiometric terms with units and symbol are listed below.

Quantity	Symbol	Unit
Radiant flux	P	watts
Radiant emittance	W	watts/cm^2
Radiant intensity	J	watts/ster.
Radiance	N	watts/cm^2/ster.
Irradiance	H	watts/cm

For reference the corresponding photometric terms are:

Quantity	Symbol	Unit
Luminous flux	F	lumen
Luminous emittance	L	lumens/cm^2
Luminous intensity	I	lumens/ster. (candle)
Luminance (Brightness)	B	lumens/cm^2/ster. (candles/cm^2)
Illuminance	E	lumens/cm^2

In calibrating the monitor we will work entirely with radiometric units but some of the data on PMT's is given in photometric units so the listing of these units may be helpful.

Fig.IV-9 shows the standard lamp & monitor separated by some distance (d). A narrow band optical filter (passband = B_o angstroms) is inserted in front of the PMT of the monitor. The calibration curve of the standard lamp shows that it produces an irradiance (H_o) watts/cm^2/Å at distance (d_o). The inverse square law applies when $d > d_o$ so the irradiance at the monitor in the bandwidth of the optical filter is,

$$H = H_o B_o \left(\frac{d_o}{d}\right)^2 \qquad (32)$$

A simultaneous reading of (H) and monitor output (amperes or volts) establishes a calibration of the monitor at one particular power level. By varying distance (d) calibration will be accomplished at various power levels. It is anticipated that this calibration will be accomplished in the optical tunnel with the monitor fixed at one end and the lamp carried on the cart which can be located at various points along the tunnel. The range of calibration may be extended as desired by the use of suitable neutral density filters in the monitor. The calibration curve will plot irradiance in watts/cm^2 versus monitor output. A plot of the calibration will show at a glance the range of linearity and any abnormalities which may exist. It will be advisable to make calibrations with normal voltage on the PMT and also with reduced voltage. The resulting family of calibration curves plus the use of neutral density filters will permit the setting of monitor sensitivity in subsequent use. A re-check of a

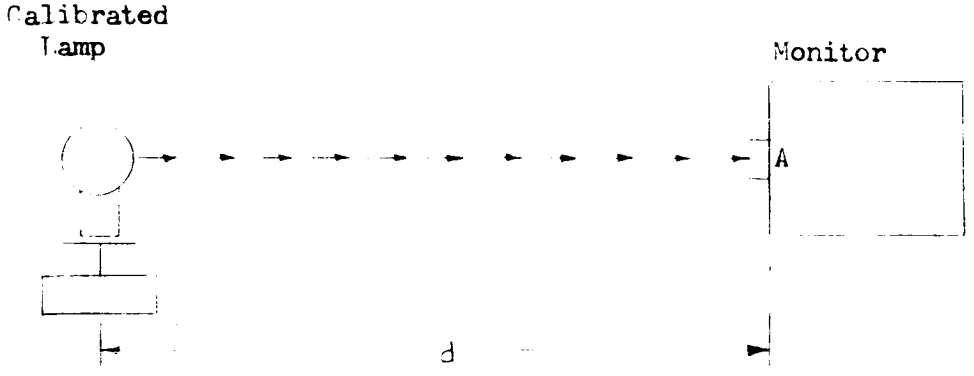

FIGURE IV-9. Calibration of Monitor

few points of calibration should be made each time the monitor is used. One should not trust the original calibration curves in terms of voltage applied to the PMT, neutral density filters used, etc. because unexpected changes in the PMT characteristics can occur. It is suggested that the calibration curves show watts/cm^2 versus monitor output.

In the above discussion it was assumed that the irradiance produced by the standard lamp at a given distance is known. One may alternately know the radiance of a diffuser placed in front of the standard source. This arrangement has the advantage that the irradiance produced by the source at a certain distance can be varied over a wide range by exposing varying amounts of area on the emitting surface. Consider, in Fig. IV-9, that the lamp is enclosed and that several spaced sheets of opal glass are used as a diffuser on the side next to the monitor. The radiance of this surface is (N) watts/cm^2/ster./Å. If A_s is the area of the surface exposed and B_o is the passband of the optical filter in the monitor, the total effective flux radiated into a solid angle (Ω) is

$$P = N A_s B_o \Omega \text{ watts} \qquad (33)$$

The area through which this flux passes in the plane of the monitor is A = (Ω d^2) and the power density or irradiance at the monitor is

$$E = \frac{A_s L}{d^2} \quad \text{watts/cm}^2/\text{nm} \qquad (34)$$

Thus we see that one may vary the irradiance at the monitor either by varying distance (d) or by aperturing the source.

C.3.c. Available Sources

Available calibrated sources are offered by Gamma Scientific Inc., 5841 Mission Gorge Road, San Diego 20, California, and Electro Optics Associates, 3335 Birch St., Palo Alto, California, 94306. The Gamma Scientific system is known as Model 220 Calibrated Optical Source System (Data Sheet No. 361A). It consists of a tungsten filament lamp and a regulated power supply. Two types of heads are available: 1) the bare lamp which is calibrated in terms of irradiance (microwatts/cm^2/nm) at specified distance, and 2) the lamp in an enclosure with a diffuser which is calibrated in terms of radiance at the diffuser. The Electro-optics Associates unit is known as L-101 Spectral Irradiance Standard and P-101 Current Supply. The lamp used in this system is a quartz-iodine lamp with tungsten filament. The iodine vapor in the quartz envelope minimizes evaporation of the tungsten filament which operates at about 3000°K and prevents blackening of the quartz envelope. Whereas this system has the advantage of good output in the UV, it has no particular advantage over the Gamma Scientific system in the wavelength region of the argon-ion and HeNe lasers. The Gamma Scientific system

has the advantage of providing a standard of radiance and it is recommended that this source be used for calibrating the monitor.

C.3.d. Calibration Procedure

The output curve for the Gamma Scientific radiance standard Model 220-1 is reproduced in Fig. IV-10. To calibrate the monitor the following procedure is followed.

1. Set up radiance standard at distance d = 262' = 8000 cms from the monitor so that the radiating surface of the standard is perpendicular to the line joining the monitor and the standard.

2. Cover the face of the standard with an opaque card or sheet of metal with a small (approximately 1" diameter) hole in the center of it to establish a definite source area (A_s).

3. Insert a 0.1" diameter stop at the principal focus of the monitor telescope. This, with the 50" focal length, limits the field of view of the monitor to two milliradians. The 1" diameter aperture at the source subtends an angle of 1/3 milliradian so the focussed image will easily pass through the stop opening.

4. Use the bore-sighted eyepiece on the telescope to align the telescope axis with the line joining the source and the telescope. If the eyepiece has not been previously boresighted with the axis of the telescope this may be easily done at this time by centering the image of the source in the field stop of the telescope and setting the cross-hairs in the eyepiece to fall in the center of the visual image of the source.

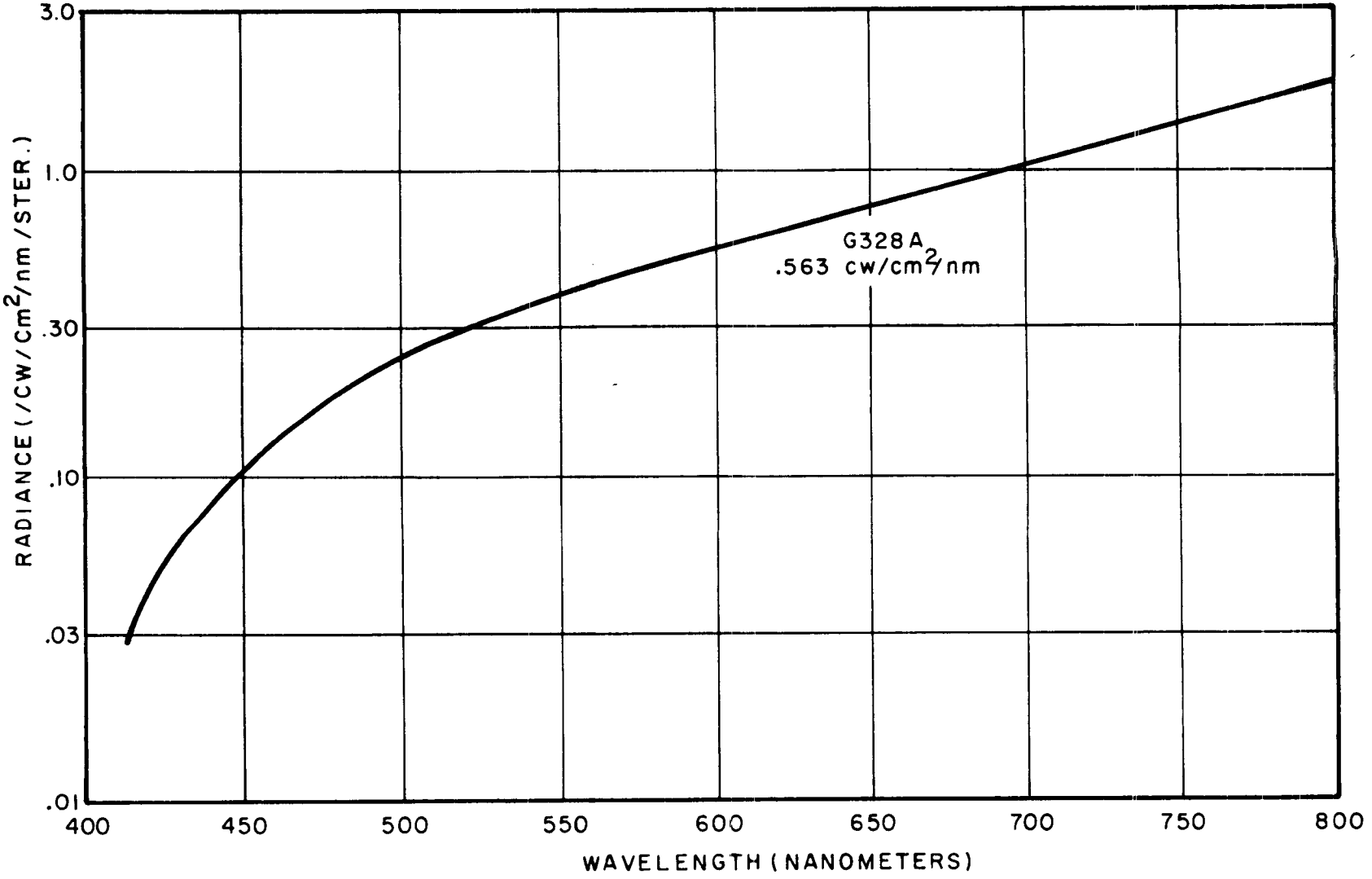

FIGURE IV-10. Radiance of Diffuser on Gamma Scientific Luminance Standard Head Model 220-1.

5. Check out the optical chopper and connect the output metering equipment (wave analyzer or synchronous detector).

6. Apply voltage to the PMT with chopper running and measure output (current or voltage) of the PMT and calculate irradiance at the monitor. The irradiance in watts/cm^2 in the passband of the optical filter permanently installed in the monitor is calculated from the standard source information, the area of the source (A_s), the bandwidth of the optical filter B_o, and the distance (d) from the source to the monitor, according to equation (34).

7. Vary irradiance at the monitor by varying the aperture area of the source and record corresponding values of irradiance and monitor output. Change (d) also if necessary.

8. Plot Calibration curve of irradiance N(watts/cm^2) versus monitor output.

B.3.e Investigation of Magnitudes

The PMT is inherently a sensitive device and when combined with a 4" diameter telescope as it is in the monitor it provides an extremely sensitive radiometer. Things will go more smoothly in the initial calibration if one knows approximately what to expect.

The curves of Fig.IV-7 show that with a noise bandwidth of 10 hz., the minimum power which we expect to measure at the photocathode is 10^{-13} watts. The maximum power that we will be able to measure without exceeding allowable anode current with normal voltage on the

tube is 10^{-8} watts. This is a range of 50db. If we assume a 40 percent efficiency in the optics including the narrow band optical filter and assume a 4" telescope aperture, the limiting values of irradiance at the monitor will be 3.1×10^{-15} watts/cm^2 and 3.1×10^{-10} watts/cm^2 respectively in the passband of the monitor. We will assume this to be 100 Å. The radiant source has a radiance of 0.563×10^{-6} watts/cm^2/nm/ster. or 5.63×10^{-8} watts/cm^2/ster/Å. If we substitute this value of (N) is equation (34) along with (A_s) in cms^2 based on a 1" diameter source, B_o = 100 Å, and d = 262' = 8000 cms, the irradiance (H) at the monitor is found to be 4.47×10^{-13} watts/cm^2 in the 100 Å optical passband of the monitor. This is about midway between limiting values of (H) which the monitor can accept; namely 3.1×10^{-15} watts/cm^2 and 3.1×10^{-10} watts/cm^2. The choice of a 1" diameter aperture at the source and a separation of 262' (through the tunnel) are good choices; i.e., they are compatible with the sensitivity of the monitor. The monitor can be calibrated over the complete range of powers by varying (A_s) and/or (d) as necessary.

D Optical Configuration for All Tunnel Testing

D.1 General

Several optical communications links are to be tested in the tunnel. The most natural arrangement is the location of the transmitter at one end of the tennel and the receiver at the other. This arrangement is also satisfying because we are transmitting information from one point to another in the usual manner. It would appear, however, that some definite advantages result from placing the transmitter and receiver side by side at one end of the tunnel and using retro-optics to return a fraction of the transmitted beam to the receiver. Connections can be made directly between transmitter and receiver for any purpose whatsoever and in particular a short length of coax between transmitter and receiver can be used instead of a hard line running the length of the tunnel for comparing transmitted and received signals. The side by side arrangement also places all operating personnel at one location thus facilitating communication and permitting flexibility in performing tasks. It's only disadvantage is that it inverts "ones" and "zeros" but this can be accounted for in the receiver. It is assumed that the retro-optics, once setup and adjusted, will need little or no attention in subsequent systems testing.

The purpose of this section of the report is to describe the optical arrangement for systems testing in the tunnel with special emphasis on the design of the retro optics. Basically, it is proposed to diverge the transmitted beam so that the beam diameter at

the retro end of the tunnel is 6' and to so design the retro-optics that the returned beam is 6' in diameter at the receiver. The size of the spots is obviously not critical so long as they are large enough to comfortably include the retro optics at the one end and the receiver optics at the other. Since range is limited in the tunnel ($2 \times 262' = 524'$) attenuation of some kind must be introduced. It seems logical to use divergent beams to provide part of the needed attenuation and at the same time allow maximum freedom in the location of optical components in the beams.

Although the monitor described earlier will be used to measure the absolute power level at the receiver under test, a knowledge of the beam structure at the receiver will be of interest. It is suggested that this information may be obtained by scanning the beam with a monitor or a simple uncalibrated optical sensor.

D.2 Optics for Expanding Transmitted Beam

It is anticipated that the standard optics in the transmitter might be adjusted to provide the desired divergence in the transmitted beam. If this is not practical, a combination of lenses to be described may be inserted in the output beam to perform this function.

In Figure IV-11, assume a parallel beam entering lens (L_1) from the transmitter. Lens (L_1) focuses the beam at (P_1) and the diverging beam beyond (P_1) is intercepted and partially recollimated by a second lens (L_2). The exit beam has the desired divergence angle (α) radians. To accomplish this, (P_1) must fall inside the focal distance for (L_2)

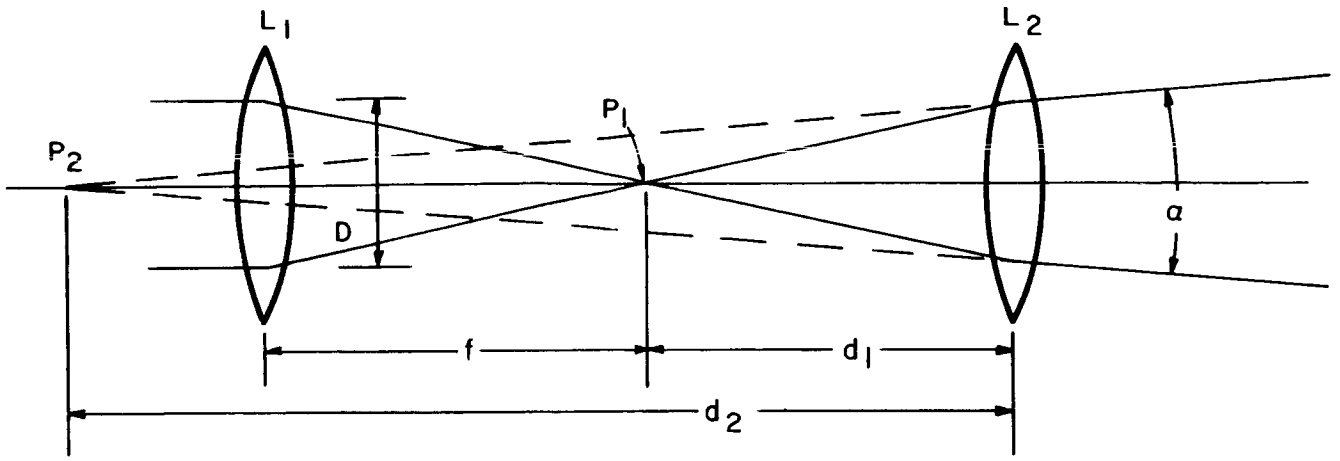

FIGURE IV-11. Beam Diverging Optics

and it is convenient to write $d_1 = f(1-\Delta)$ where $\Delta << 1$. The virtual image formed by (L_2) is at (P_2), a distance (d_2) to the left of (P_1) where $d_2 = D/\alpha$. We will neglect the fact that the diameter of the beam at (L_2) is slightly less than (D) because it does not affect the result appreciably. From the standard lens equation,

$$\frac{1}{d_1} + \frac{1}{d_2} = \frac{1}{f} \tag{35}$$

we obtain

$$\frac{1}{f(1-\Delta} - \frac{\alpha}{d} = \frac{1}{f}$$

The minus sign on the second term results because (P_1) and (P_2) are on the same side of (L_2), and (d_2) is therefore negative. Solving for (1-Δ) we have,

$$(1-\Delta) = \frac{D}{D+\alpha f} = 1 - \frac{\alpha f}{D} + \left(\frac{\alpha f}{D}\right)^2 - \left(\frac{\alpha f}{D}\right)^3 + \cdots$$

and since $\Delta << 1$,

$$\Delta \cong \frac{\alpha f}{D} \tag{36}$$

The ratio f/D is the f number of the lens and a reasonable value, regardless of diameter, is f/D = 4. We can therefore finally write

$$\Delta = 4\alpha \tag{37}$$

We want a beam diameter of 6' at a distance of 262' which corresponds to α = .023 radians, or Δ = .092. Thus with L_2 located so that (P_1) is about 10% inside the focal distance of (L_2), the desired beam divergence will be obtained. The length of this assembly is about eight times the beam diameter which is not prohibitive. It can be shortened by using one negative and one positive lens of different focal lengths.

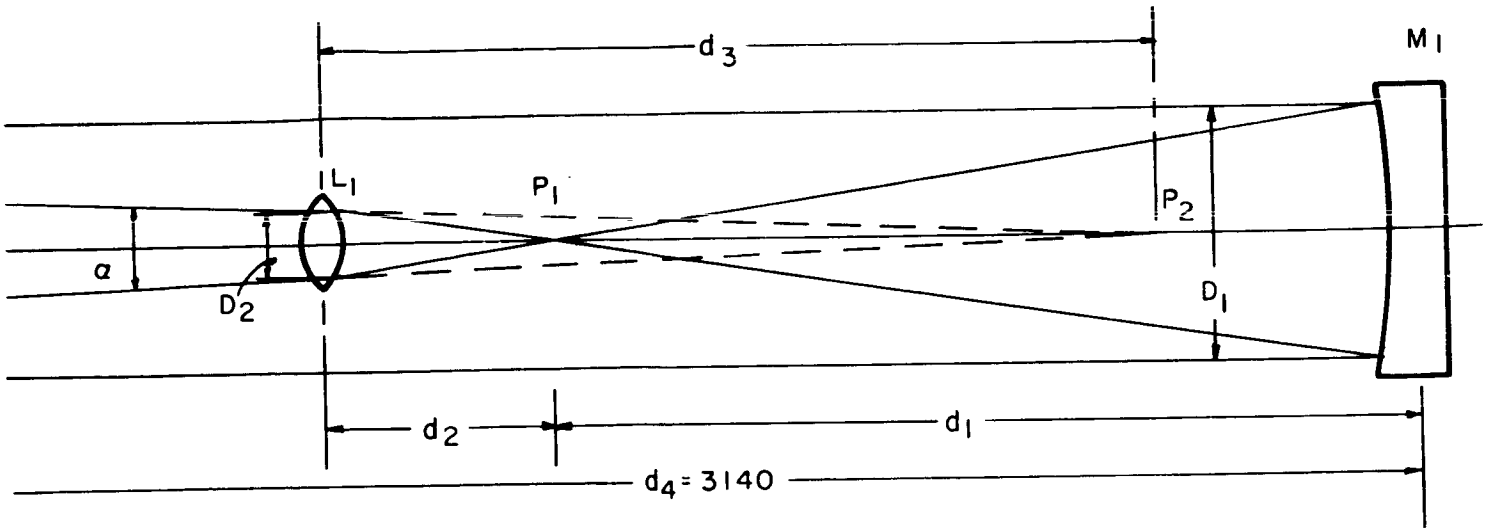

FIGURE IV-12. Retro-Optics

D.3 Retro Optics

A diagram of the retro optics is shown in Figure IV-12. A front surface spherical concave mirror M_1 is used to intercept and redirect a fraction of the transmitted beam. The flux intercepted by M_1 is focussed at point (P_1). The divergent beam from (P_1) is intercepted by a short focus positive lens (L_1) which recollimates the beam partially to provide the desired beam angle (α) in the beam directed back to the receiver. We will establish the size and spacing of the optical elements. The focal point (P_1) will remain fixed in space and the spacing of (L_1) relative to (P_1) may be used as a means of adjusting beam divergence. Calculations will be based on obtaining a spot 6'

in diameter at the far end of the tunnel, 262' or 3140" from the mirror (M_1).

The mirror (M_1) is assumed to have a diameter of 6" and a focal length of 48" because this is a standard size used by amateur astonomers and is readily available at low cost. In fact one can simply buy a standard telescope and modify the front end to mount lens (L_1) on a bracket similar to the one normally used to mount the star diagonal.

The location of (P_1) is determined by applying the standard lens formula

$$\frac{1}{d_4} + \frac{1}{d_1} = \frac{1}{f} \qquad (38)$$

$d_4 = 3140"$

$f_m = 48"$

$d_1 = 48.8"$

To obtain a divergent beam to the left of (L_1) we place (L_1) a distance $d_2 < f$ from (P_1) where (f_L) is the focal length of (L_1). Lens (L_1) then forms a virtual image of (P_1) at (P_2) distance (d_3) behind (L_1). Because (P_1) and (P_2) are on the same side of (L_1) the applicable lens formula is,

$$\frac{1}{d_2} - \frac{1}{d_3} = \frac{1}{f} \qquad (39)$$

We are free to choose the focal length of (f_L) and a reasonable

value is $f_L = 4"$. Other relationships, obvious from the geometry are,

$$\frac{D_2}{D_1} = \frac{d_2}{d_1}$$

$$D_1 = 6"$$

$$d_1 = 48.8"$$

Therefore $D_2 = .123\ d_2$

$$\frac{D_2}{d_3} = \alpha = \frac{6}{262} = .0229$$

Substituting, $D_2 = .123\ d_2$

gives, $d_2 = .186\ d_3$

Using this relationship in equation (39) with $f_L = 4"$ gives,

$D_3 = 17.5"$

$d_2 = 3.24"$

The diameter of the beam at (L_1) can now be calculated and is found to be 0.40".

We are now able to completely describe the retro optics. (M_1) is a 6" diameter spherical mirror with a focal length of 48". Lens (L_1) is a positive lens with a usuable aperture of 0.40" and is to be located a distance $d_1 + d_2 \cong 52.0"$ in front of (M_1).

These optics should be mounted in a tube approximately 7" in diameter provided with a base adjustable in azimuth and elevation. In systems tests this assembly will be used to collect light from the transmitted beam and redirect it to the receiver. The alignment is not particularly critical because the only requirement is that the returned spot shall cover the receiver. The receiver must, of course, be aimed so that the image of the source falls in the field stop aperture of the receiver.

The total power attenuation resulting from the fact that only part of the beam power is intercepted by the retro optics and only part of the returned beam power is intercepted by the receiver is easily calculated. If the receiver, as well as the retro optics, has a 6" diameter aperture, the attenuation is 2.08×10^4 or 43.2 db. This does not appear to be a prohibitive amount of attenuation for any of the contemplated systems tests, but if it should prove so, the attenuation can be reduced by reducing beam divergence. This is easily accomplished by increasing slightly the spacing between (L_1) and (M_1). The lens (L_1) should be adjustably mounted, in any case.

The simplest test configuration obtains when the doors of the tunnel can be left open. This is possible only when the transmission medium is room air at atmospheric pressure. The effects of turbulent air or temperature gradients can be studied in this mode of operation and one can conceive of simulating clouds or fog by various methods

to study their effect on the transmission of the optical path. When it is desired to operate the tunnel at low pressure or with atmospheres other than air, it will be necessary to operate either with the transmitter and receiver inside the tunnel or operate these outside the tunnel by use of the optically flat windows provided in the doors of the tunnel. There appears to be no reason why the retro optics cannot be located in the tunnel. A possible problem might be the reflection of light from the inside surfaces of the door at the retro end of the tunnel. Reflections off diffusing surfaces tend to destroy the polarization of polarized optical beams and this could show up as noise when testing the PCM/PI high data rate system. In any case, a highly absorbing backdrop should be provided behind the retro optics assembly.

E Test of Simple Optical Communication System in Tunnel

1. Configuration and Test Equipment

It is proposed that NASA set up a simple amplitude modulated optical communication link in the tunnel using the available Spectra-Physics Model 125 HeNe laser and Model 320 Pockel's cell modulator as a transmitter and one of the PMT monitors described in earlier sections as a receiver. The monitor will be used without the chopper and a relatively broadband tuned output circuit will be provided. The HeNe laser is to be operated at the visable (6328Å) wavelength. The transmitter and receiver will be operated side by side with retro optics at the far end of the tunnel to return a portion of the transmitted beam to the receiver. The testing of such a system is recommended because it will provide experience in quantative testing which will be valuable in the subsequent testing of more sophisticated systems and will also provide valuable information on the characteristics of PMT's operating near the quantum limit. It is essential to know that the PMT performs according to theoretical predictions in the quantum limit before one tries to analyze the performance of more complicated systems like the NASA-Hughes PCM/PL high data rate system. A separate monitor operating in the normal monitor mode will be located alongside the monitor-receiver and will be used to measure average power density incident on the receiver. The monitor will have been previously calibrated using the standard lamp and procedure discussed in section IV.C.3. The standard lamp should be permanently mounted so that it can be used to recheck the calibration of the monitor from time to time.

Pockel cell modulators are discussed extensively in the literature but a short discussion will be given here for the sake of completeness.

The arrangement used to amplitude modulate a light beam is shown in Figure IV-13. It consists of a first polarizer (P) an electro optic crystal (C), and a second polarizer called the analyzer (A). The polarizer and analyzer have their polarizations crossed so that no output is obtained when the crystal is inactive, i.e., when no voltage is applied. The application of voltage to the crystal changes the situation so that at least some of the light passed by the polarizer can also pass through the analyzer. By varying the applied voltage, varying amounts of light output can be achieved and the device can therefore operate as a modulator. The applied voltage does not simple shift the plane of polarization of the plane-polarized beam as it passes through the crystal as one might suspect, but rather produces an elliptical polarization with a component having the correct polarization to pass through the analyzer. This action will be explained by reference to Figure IV 14. The S-F axes shown are the so-called slow and fast axes of the crystal. The velocity of propagation of a plane polarized wave through the crystal depends on the plane of polarization. A wave whose plane of polarization coincides with the (S) or slow axis will have the minimum velocity of propagation and a wave whose plane of polarization coincides with the (F) or fast axis will have the maximum velocity of propagation. There are other axes which correspond to intermediate propagation velocities but it is convenient to use the two axes specified and any plane polarized wave can be resolved into two components - one component parallel to each of these axes. The plane of polarization passed by the polarizer is indicated by the 45° dotted line marked (P) (Fig. IV-14). The plane of polarization

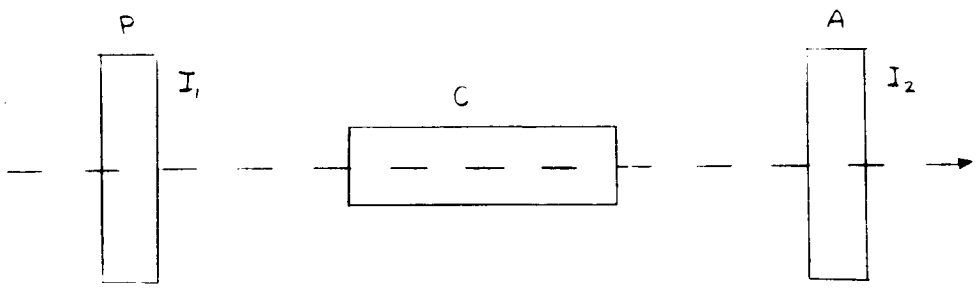

FIGURE IV-13. Pockel's Cell Modulator

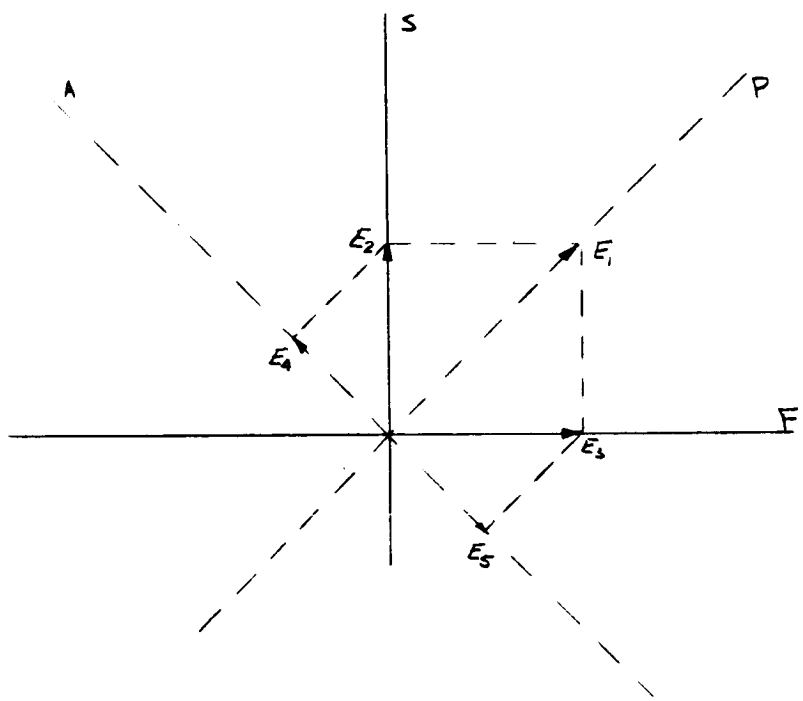

FIGURE IV-14. Space Vector Diagram

passed by the analyzer is indicated by the other dotted line marked (A). It is desired to calculate the output intensity (I_2) in terms of the output of the polarizer (I_1) and the voltage (V) applied to the crystal. We are purposely a little vague about how this voltage is applied becuase various arrangements may be used and it is undesirable at this time to get into such a detailed discussion. By using I_1 as the output of the polarizer we make the analysis sufficiently general to apply to the modulation of an ordinary unpolarized (randomly polarized) source or a plane polarized source like a laser. The reader has probably already observed that the first polarizer is actually not essential when a laser source is used. It can, however, help to improve the extinction ratio (ratio of maximum to minimum output signal) and is therefore generally used. When it is used it and the other components in the modulator must be lined up with the polarization of the source. Consider now the quantitative relationships which can be derived.

The intensity (I_1) can be expressed in terms of electric field strength (E_1) and vice versa.

$$I_1 = k E_1^2 \tag{40}$$

$$E = \sqrt{\frac{I_1}{k}} \tag{41}$$

where,

E_1 = peak value of the sinusoidally varying field strength.

I_1 = optical intensity or power.

k = a constant of proportionality.

The quantity E_1 (a space vector) can be resolved into components E_2 and E_3 along the slow and fast axes. We can write time varying functions corresponding to E_2 and E_3 as,

$$e_2 = \frac{E_1}{\sqrt{2}} \sin \omega t \tag{42}$$

$$e_3 = \frac{E_1}{\sqrt{2}} \sin \omega t \tag{43}$$

If these propagate through the crystal at the same velocity they reach the analyzer in phase and reconstruct the plane polarized wave

$$e_1 = E_1 \sin \omega t \tag{44}$$

coinciding with the plane of the polarizer. This plane-polarized wave obviously cannot pass through the analyzer which is polarized at 90° to this plane. The same conclusion is reached if we think of E_2 and E_3 being projected on the dotted line (A), corresponding to the polarization plane of the analyzer. In this case we write two time functions,

$$e_4 = \frac{E_1}{2} \sin \omega t \tag{45}$$

$$e_5 = -\frac{E_1}{2} \sin \omega t \tag{46}$$

The sum of these is a wave polarized in the (A) plane which can be passed by the analyzer and contribute to output (I_2). We will write this as,

$$e_2 = e_4 + e_5 \tag{47}$$

and note that it is zero as it must be if there is no phase shift through the crystal. If we take into account the fact that E_4 arises from E_2 and E_5 arises from E_3 and that in general E_2 and E_3 will not be in time phase because of the difference in propagation velocity for the two polarizations, we get a general expression for e_2 which is not patently zero, i.e.,

$$e_2 = \frac{E_1}{2}\left[\sin \omega t - \sin(\omega t - \phi)\right] \tag{48}$$

which can be transformed by a trigonometric identity to

$$e_2 = E_1 \sin\frac{\phi}{2} \cdot \cos\left(\omega t + \frac{\phi}{2}\right) \tag{49}$$

We note that this is a sinusoidally varying function of amplitude ($E_1 \sin \frac{\phi}{2}$). The fact that the time varying function has shifted to a cosine function and contains a phase angle is inconsequential. We can write the output intensity as,

$$I_2 = \frac{E_1^2 \sin^2\frac{\phi}{2}}{2} \tag{50}$$

and from eq. (40)

$$\frac{I_2}{I_1} = \frac{k E_1^2 \sin^2\varphi}{k E_1^2} = \sin^2\varphi$$

or $$I_2 = I_1 \sin^2\varphi \qquad (51)$$

where (φ) is the relative phase shift in radians between the slow and the fast components. The Pockel's effect shows that phase shift is proportional to voltage (V) applied to the crystal and if we use (V_o) to indicate the voltage required to cause a shift of π radians, eq. (51) becomes

$$I_2 = I_1 \sin^2\left(\frac{\pi}{2}\frac{V}{V_o}\right) \qquad (52)$$

This output function is plotted in Figure IV-15. To obtain symmetrical operation as a modulator it is clear that one should bias the modulator to the voltage $V_o/2$. The same effect can be accomplished by inserting a quarter-wave plate anywhere between the polarizer and the analyzer and this is generally done. Sometimes a voltage bias is used and automatically varied to maintain the proper operating point O' in spite of the effect of temperature variations, etc., which tend to shift the point of operation.

The monitor used as receiver of the amplitude modulated transmission will be provided with an output circuit as shown in Figure IV-16. This is a simple parallel tuned circuit which will be tuned to resonate at the modulation frequency. The bandwidth of the circuit will be arbitrarily varied

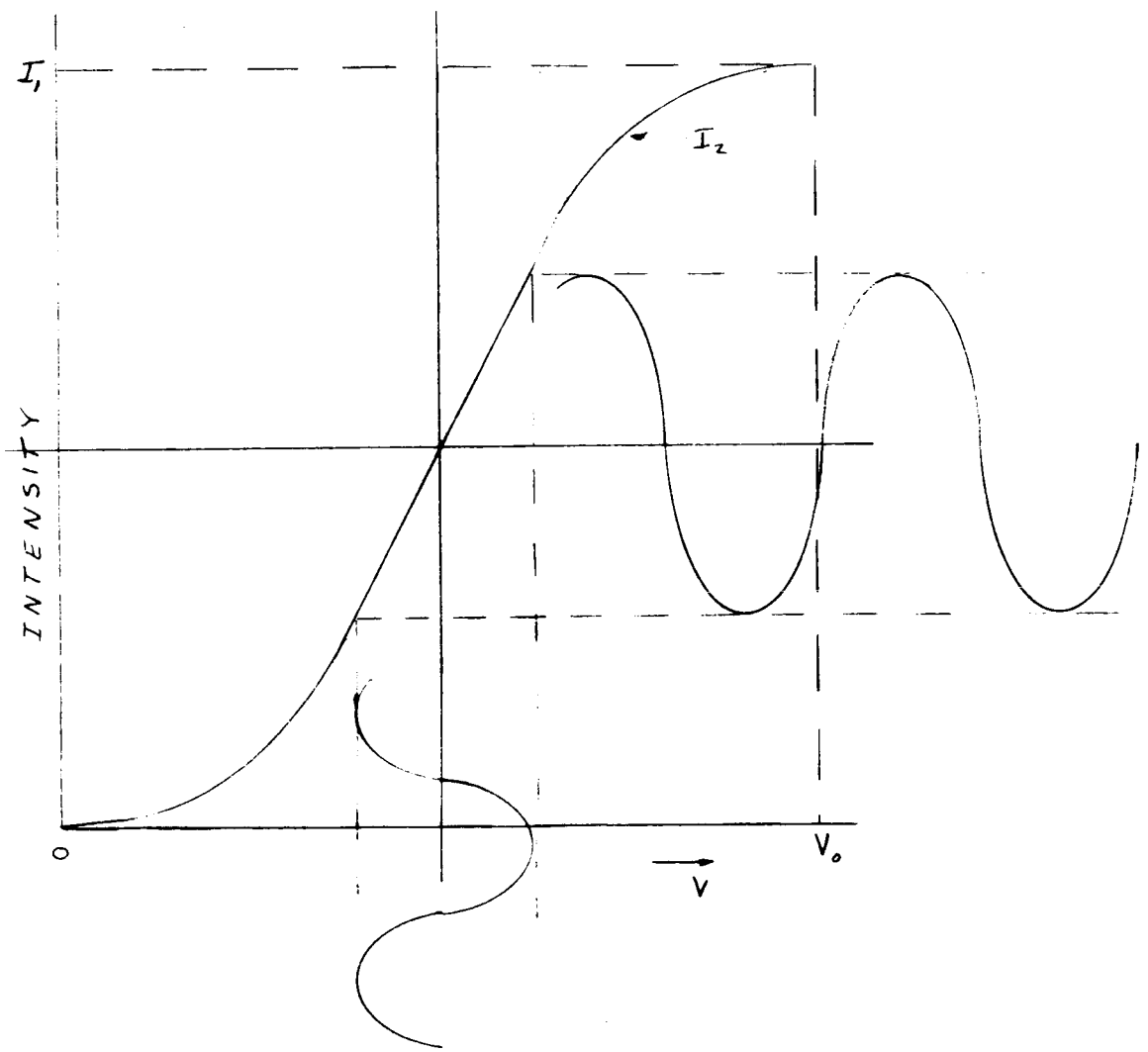

FIGURE IV-15. Amplitude Modulation Using Pockel's Cell Modulator

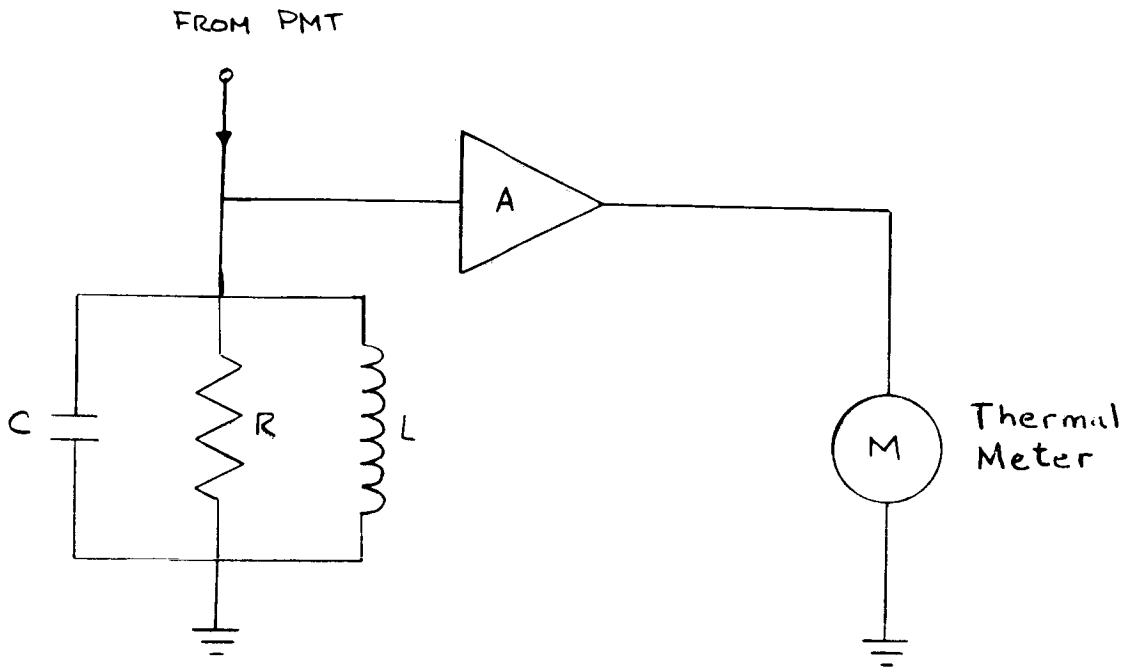

FIGURE IV-16. Measurements of Receiver Output

by varying (R) and (C), with (L) chosen to maintain the desired resonant frequency. An amplifier is used to prevent loading of the output circuit of the PMT and to provide amplification as needed. It will be recalled from an earlier section that the signal bandwidth of the parallel tuned circuit is,

$$\Delta f = \frac{f}{Q} \tag{53}$$

and that the noise bandwidth is,

$$B = \frac{1}{4RC} \tag{54}$$

Also it can be shown that (B) is related to (Δf) by

$$B = \frac{\pi}{2} \cdot \Delta f \tag{55}$$

In testing this simple link we will be primarily interested in quantitative measurements of signal and noise levels and S/N ratio in the output circuit as a function of average optical power input, modulation index, etc. Since in general noise will always be present in the output it will be necessary to measure signal plus noise (S + N) and noise (N) separately and from these calculate (S/N) ratio for comparison with predicted values. The measurable quantities are current or really average squares of current.* Thus, when we measure (S + N) we measure $\overline{I^2_{S+N}}$ and when we measure (N) we measure $\overline{I^2_N}$. Since we think of (S) and (N) in

* Using a thermal ammeter, as shown in Figure IV-16.

terms of power,

$$S+N \sim \overline{I_{S+N}^2}$$

and

$$N \sim \overline{I_N^2}$$

Also, since there is no correlation between signal current and noise current

$$S+N \sim I_S^2 + \overline{I_N^2}$$

and we obtain signal by subtraction

$$S \sim \overline{I_{S+N}^2} - \overline{I_N^2}$$

and the measured S/N ratio is calculated from

$$S/N = \frac{\overline{I_{S+N}^2} - \overline{I_N^2}}{\overline{I_N^2}} \qquad (56)$$

We are not interested in absolute power levels in the output so long as the power is adequate for making measurements and at such a level that subsequent circuits do not degrade the S/N ratio at the output of the PMT. The contribution of noise by the resistance of the output circuit was discussed in detail in Section IV.B.1.

D.2 Optical Noise Sources

Although optical noise sources might well be included under test equipment they are discussed under a separate heading because reference will be

made to this section in other parts of the report.

An optical noise source is easily provided. Any black body or grey body emitter capable of putting out sufficient power in the narrow bandwidth of the receiver may be used as an optical noise generator. A tungsten filament lamp has the advantages of being readily available in suitable sizes and convenient to use. With the noise source located at an appropriate distance from the receiver, the irradiance at the receiver can be measured by use of the monitor. Knowing the irradiance at the receiver and receiver aperture as well as the transmission of the receiver optics one may calculate the power incident on the photocathode of the PMT. The reader is reminded that this is not all noise power. The constant optical input signal liberates a current (I) at the photocathode and it is only the shot noise associated with (I) which shows up as noise in the output of the PMT. This duplicates exactly the condition which we are trying to simulate, i.e., the noise introduced by a constant background such as that provided by scattered sun light or the light from a planet in the view of the receiver. Obviously, we simulate the condition accurately if the total power from the lamp source falling in the optical pass band of the receiver is equal to the total power supplied by the natural noise source in the same band of optical frequencies. In considering extended sources the field of view of the receiver must also be considered.

D.3 Test Procedure

No attempt will be made to specify a strict test procedure beyond a few obvious steps which must be taken to get under way. The ultimate goal is to gain experience in the quantitative checking of a simple system and to verify the results predicted in Section IV.B and particularly the S/N

ratio curves of Fig. IV-4 or similar curves calculated for the PMT finally chosen for use in the monitor and the monitor-receiver. Even if the RCA 7326 PMT is used, the curves of Fig. IV-4 should be recalculated on the basis of the most accurate obtainable values of quantum efficiency and dark-current.

The single frequency modulated onto the optical carrier may be thought of as a sub-carrier which may in turn be frequency modulated or amplitude modulated for the transmission of information. The measurement of signal bandwidth available and (S/N) ratio, or carrier/noise (C/N) ratio, which will be approximately equal to (S/N) ratio, determines, according to information theory, the amount of information which can be transmitted over the channel in a given time.

A tentative test procedure will now be outlined.

1. Set up transmitter, receiver, and retro optics in the tunnel.
2. Use diverging optics as necessary to obtain a beam diameter of 6' at the retro end of the tunnel. (Extreme caution should be excercised to guard against eye damage to personnel.) It will be helpful to observe the transmitted beam on a white card held in the beam, first at close range, then progressively further down the tunnel. At a distance of 20' a 5.5" diameter spot will correspond to a 6' (72") diameter spot at the far end of the 262' long tunnel. Since beam divergence does not enter in any critical way into the quantitative testing, adjustments based on such an observation should be adequate. The beam should next be centered on the retro optics and this can be

accomplished by a combination of sighting and viewing the spot at 20' on the white card.

3. Adjust retro optics to return a 6' diameter beam in the plane of the receiver and centered on the receiver. The card and sighting technique used above should be adequate for the purpose.

4. Set up monitor by the side of the receiver. Allign the monitor so that the image is in the beam (retro optics create an apparent point source at distance of 262' from monitor). Do not look into telescope eye-piece when transmitter is operating. A flood light in the vicinity of the transmitter and directed toward the far end of the tunnel may be safely used. The image in the beam should be located in the cross hairs in the telescope by adjusting the aximuth and elevation of the monitor.

Final adjustment can be accomplished by observing monitor output with transmitter energized. It is assumed that the monitor has been previously calibrated using the standard lamp (see Section IV.C.3) Whereas the divergent beams provide some attenuation over the link, neutral density filters will probably be required in the monitor to prevent overloading.

5. We are now in a position to make a quantitative check on the system. Using the E.G. & G Light Mike set the transmitter output (unmodulated) at 10 VW. Neglecting losses in the system, use beam divergence and the apertures of retro optics and monitor to calculate the power which should be collected by the monitor. Introduce neutral density filters to bring the power incident on the PMT within the operating range and take a reading. Compare the observed and calculated values. They should not

differ by more than a factor of two and the measured value should be lower because of losses. A number of simple experiments like this may be undertaken to gain familiarity and establish the validity of procedures.

6. Align receiver so that the image in the received beam falls in the field-stop aperture. Measure S/N ratio as a function of average power incident on PMT, modulation index, etc., to check predictions. Greatest emphasis will be on results in the region of near quantum limited operation. In these tests the optical carrier will be amplitude modulated at a single frequency (1-4 mc) and the output circuit of the receiver will be tuned to be resonant at the modulating frequency. There is considerable freedom in procedure. One may, for instance, set a constant power level at the transmitter and measure (S/N) ratio as the modulation index is varied from zero to 100%, or one may hold transmitter power and modulation index constant and vary bandwidth at the receiver output. Or one may simply measure noice output with a constant C.W. noise signal (any tungsten lamp or one of the calibrated lamps if this is more convenient) as bandwidth is varied. Absolute noise measurements can be made by providing a known sinusodially varying signal from the transmitter for comparison.

Clearly one may operate the receiver in the near quantum limited mode with low S/N ratios and low power input or with high input levels and high S/N ratios. He may also operate the receiver with large signal input and low S/N ratio by the use of a strong background noise source. The optical receiver will usually be equipped with a narrowband optical filter.

D.4 Data Collection and Processing

The tests considered here were so simple and the data so easily plotted in curve form that special consideration of methods seems almost superfluous. After some of the preliminary testing is over and the system parameters have

been established it may be desirable to provide for automatic variation of some parameters and automatic recording of results. Such a decision should be made after testing is underway.

D.5 Predicted Test Results

The methods for predicting results are described in Section IV.C. The predicted results will be calculated values of S/N ratio at the output of the receiver under various conditions of operation as discussed under D.3, Test Procedures. Test results should agree fairly well with predicted results. If they do not it becomes necessary to examine things more closely to ascertain the reason. Followed to an extreme this can be an unending and unprofitable undertaking. One must therefore decide on the basis of common sense when the agreement between predictions and test results is good enough.

F. Test of Laser Communication Theory in the Tunnel, Using PCM/PL Modulation

This test is designed to allow testing of the actual performance of PCM/PL modulation of a laser transmitter, and to obtain results which can be compared with those predicted in the Final Report on NAS 9-3650 for PCM/PL at various modulation indicies. The basic system that will be used in this test is the Hughes 30 megabit/second laser communicator, but it will be modified to operate a a bit rate compatible with the limitations of existing "off the shelf" test equipment. Complete details of this modification are contained in Paragraph 3 of this test plan.

1. Configuration

The optical configuration for this test will be the same as that used for other tunnel tests, as described in Part D of this Section. However, the electronic test configuration is different from that used for analog testing of a laser communication system, since the objective of this test is to measure error rate as a function of the average signal energy and average noise energy/decision.

The basic test configuration is shown in Fig. IV-17. It will be noted that the transmitter clock is connected directly to the decision circuitry in the receiver and that the modulating signal at the transmitter is used as a reference for detecting bit errors at the output of the digital portion of the Hughes receiver. The clock output and the modulating signal are delayed, in coaxial cables, before they are applied to the receiver and comparator, respectively, to allow for the time delay introduced by the two way transmission of the laser beam through the tunnel and to allow for the reversal in sense of polarization that occurs when the optical signal is reflected at one end of the tunnel (transmitted "ones" are received as

FIGURE IV-17. Test Configuration

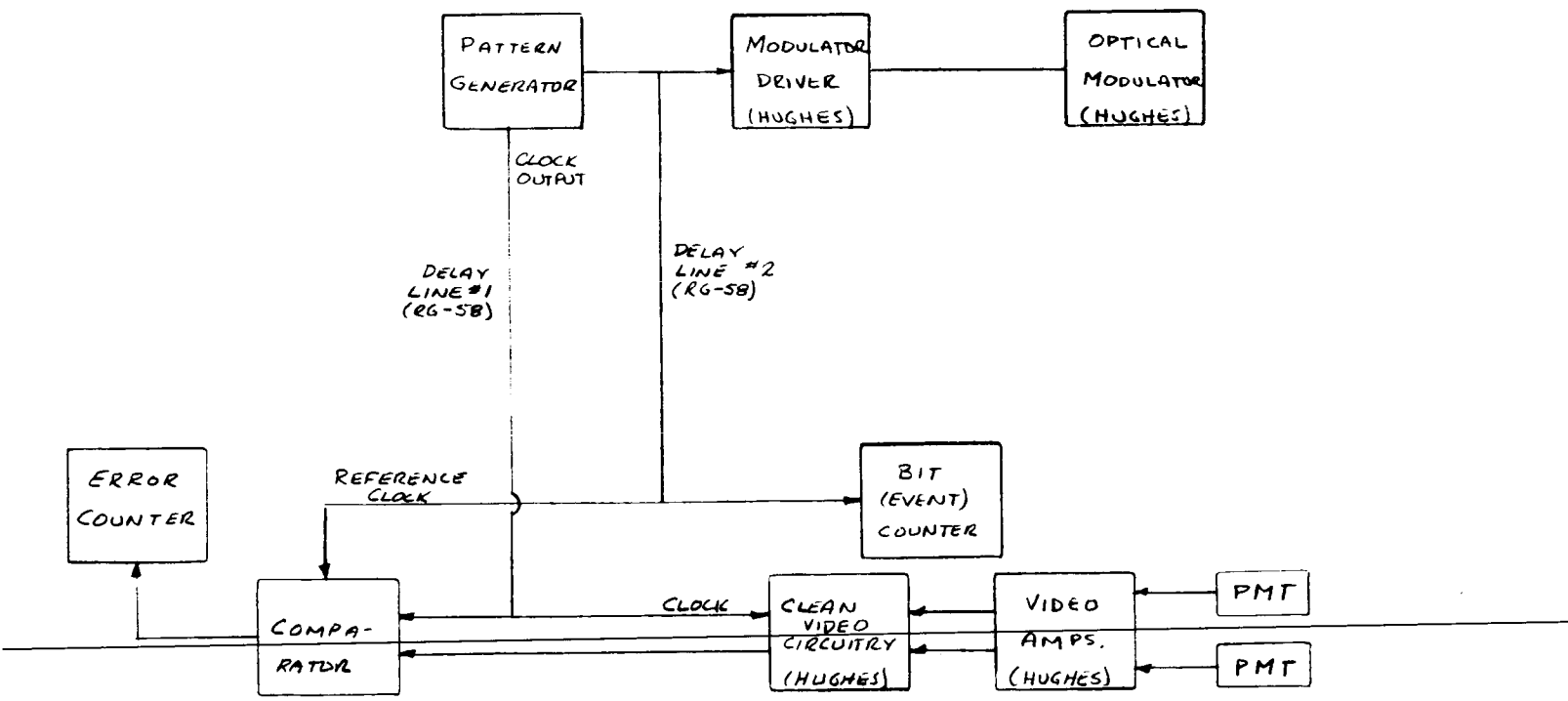

"zeros" and "zero" are received as "ones").

The comparator, which is shown as a block in the test configuration, is actually an exclusive OR circuit. It detects, at the time of a clock pulse, whether or not the received signal and the reference signal are of the same polarity. If they agree, the comparator does not generate an output signal. However, if the polarities of the received signal and the reference signal disagree (an error), the comparator generates a pulse whose width is a small fraction of a bit time. The necessity for these short error pulses, as compared with a bit time, comes from a requirement that the error counter be able to count successive errors. If the comparator output were as long as a bit, or longer, two adjacent errors would look like a single error (event) to the error counter.

All the basic electronic elements in this test configuration, with the exception of the comparator are available as standard test equipment, provided the bit rate is held to less than 1 megabit/sec. Also, at digital data rates of less than 1 megabit/sec the comparator can be implemented with standard test equipment and system calibration is relatively insensitive to the exact lengths of the delay lines. As will be seen later, at 30 megabits/second some of the test equipment is not available, system calibration becomes critical, and implementation of the comparator represents a major development program. Since this test is intended to provide information pertinent to the theoretical performance of PCM/PL modulation, and is not intended to test the digital performance of the Hughes system at high data rate, Westinghouse is recommending that the pattern generator be operated at 1 megabit/second, or less.

The comparator will be implemented with standard digital gate circuits and flip-flops, as shown in Fig. IV-18. It operates in the following manner:

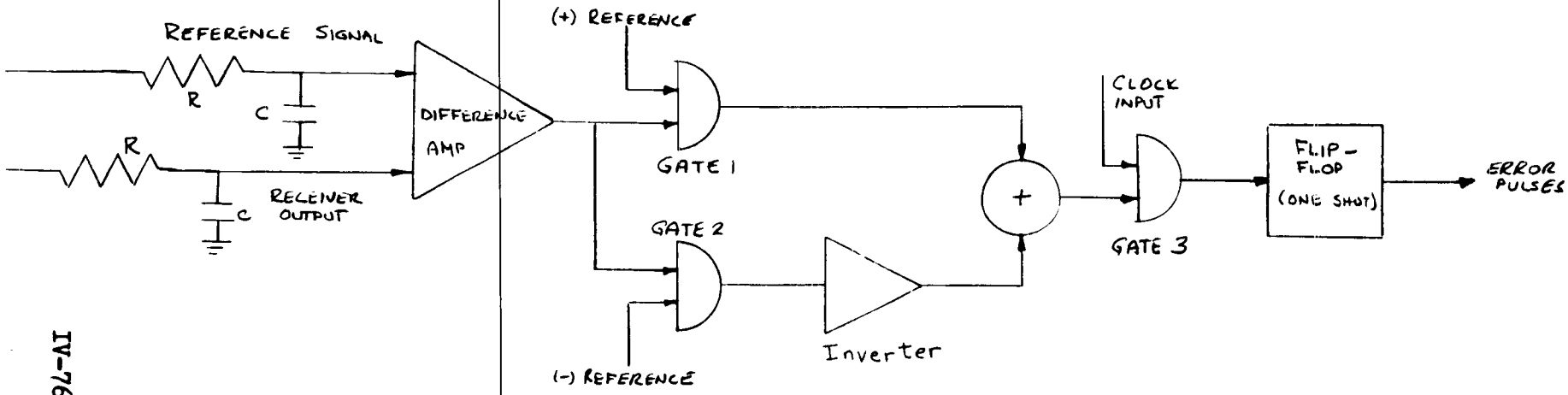

FIGURE IV-18. Comparator

1) If the reference signal and the receiver output correspond, the output of the difference amplifier is zero (essentially) at the end of a received bit. In this case, both gates 1 and 2 are disabled, so the combination of the clock input to gate 3 and zero volts results in no drive for the flip-flop. No error pulse is generated.

2) If the reference signal is a "one", while the receiver output is a "zero", the difference amplifier has a positive output. This positive output signal enables gate 1, supplying a positive voltage to gate 3. This voltage, and the clock pulse, enable gate 3, and a drive is supplied to the one-shot flip-flop. This flip-flop then cycles, generating an error pulse. Note that the length of the error pulse, which should be less than one half the duration of a bit, is determined by time constants in the flip-flop. Its shape is independent of the shape of the received pulse or the clock pulse.

3) If the reference signal is "zero", while the receiver output is a "one", the difference amplifier has a negative output. This enables gate 2, supplying a negative signal to the inversion amplifier. There, the sense of the signal is reversed, so that a positive signal is supplied to gate 3. This positive signal, in combination with the clock pulse, enables gate 3. This drives the flip-flop producing an error pulse.

The RC circuits shown at the input to the difference amplifier are used in place of the conventional integrate and dump matched filters to maximize the signal to noise ratio of each signal at the input to the difference amplifier. These circuits should have their 3 db bandwidths adjusted so that they are equal to the bit rate. No specific values

of R and C are quoted, as these depend upon source impedance and load impedance. RC filtering, rather than the "ideal" matched filter, is being recommended for inclusion in the comparator on the basis that in simpler to implement and more reliable than the ideal filter, while being within 1 db of it in performance.

2. Test Equipment

Now that the basic electronic configuration for testing of a PCM/PL laser communicator at 1 megabit/second, including the comparator, has been discussed, specific equipment for implementing this test will be defined. The requirements for the bit counter and the error counter are that they can count events that are less than 1/2 microsecond in duration and that they have good long term stability, to allow accurate counting of the total number of bits transmitted in a test and the errors detected in a given test. These requirements can be met, at data rates of less than 2 megabits per second with Hewlett Packard 5233L Electronic Counters, or equivalent commercial test equipment. At very low error rates, two of these counters will be required for instrumentation, as shown in Fig. IV-17. At somewhat higher error rates, as would be expected in noise limited or quantum limited testing, only one 5233L counter is required. The output of the pattern generator is connected to "Input B" of the counter and the output of the comparator is connected to "Input A". Then the counter is set in a ratio mode, to read the ratio of errors to events (or bits).

The recommended delay lines are standard RG-58 coaxial cable. The basic test setup shows two delay lines, each of which has a delay equal to twice the propagation delay in the optical tunnel. Therefore, these lines are approximately twice as long as the tunnel. If a simple

101010 .... test pattern, rather than a code word is generated by the pattern generator, delay lines much shorter than these can be used, and we recommend this arrangement to minimize pulse distortion on the delay lines. Using this simple pattern, the delay lines are trimmed to the proper length by observing, on a dual trace oscilloscope, the time relation between transmit pulses and clock pulses at the receiver. A Techtronics 585 oscilloscope with a dual trace preamplifier can be used to make this adjustment. Proper line length is achieved when a clock pulse out of the delay line and the end of a bit coincide, as described in the operations manual for the Hughes PCM/PL receiver.[37]

Finally, we come to the test pattern generator. This is, in theory, a 1 megabit/second square wave generator. However, we have an additional requirement. It must also supply the clock pulse that drives the decision circuitry in the PCM/PL receiver, and this pulse should occur near the end of a bit. This requirement, and the 1 megabit/second pulse repetition rate can be met by using a Hewlett-Packard 215A Pulse Generator, or equivalent, as the pattern generator. Using the HP 215A, the time relation between a pulse and a trigger pulse* can be controlled. Since the trigger pulse is related to one polarity pulse, only, while we need two polarities and a trigger pulse for each polarity, the following modifications to this generator must be made:

Add a one stage JK (bistable) flip-flop to the output of the pulse generator. This flip-flop will produce a positive output voltage for the first 10 in a sequence, with a trigger pulse associated with the one. Then, during the next 10 period, it produces zero output voltage with the trigger pulse associated with the 1. Delay internal to the

*The terms "clock pulse" and "trigger pulse" are used interchangibly in this report.

pulse generator allows alignment of the trigger pulse with the output of the flip-flop. This flip-flop is a standard divide by two, unipolar output, 2 megacycle piece of digital electronic equipment. It is available as on "off-the-shelf" item.

3. Additional Instrumentation and Equipment Modifications

In parts of 1 and 2 of this this test plan, we have described the modifications of test equipment and the non-standard test equipment required for electronic instrumentation of this test. The significant modifications and developments for the electronic equipment are as follows:

a) Develop a bit comparator, capable of working at 1 megabit/second, for detection of errors.

b) Add a divide by two, unipolar flip-flop to the output of the pulse generator.

c) Cut delay lines to the proper length, so that the time delay for two way transmission of the optical signal in the tunnel is compensated.

In addition, certain modifications of the Hughes PCM/PL system are required. The test has been designed to minimize these modifications, but the analog input, digital transmission, analog output format cannot be used for testing of the theory of laser communications. It is proposed that the following changes be made to the Hughes equipment:

a) Disconnect the present coaxial cable input to Q1 on the modulator driver, and connect the output of the pulse generator to the same points.

b) Disconnect the BNC input to the phase locked clock from the threshold detector. Connect the delayed clock from the pattern generator to this connector on the phased locked clock.

c) Disconnect the BNC PCM Video Output Line from the Matched Filter. Connect this Video Output (Clean Video) to the Bit Comparator.

All other circuitry in the Hughes PCM/PL system should be left in its present configuration, for tests of optical communication theory at modulation indices of less than 50%. For those tests where a modulation index of more than 50% is desired, further modifications will be required at the transmitter. During those tests, the output of the pattern generator should be connected to the input of a DC to 2 MHz BW power amplifier, that can deliver at least 75 volts peak (push-pull) into a 120 pfd load. The output of this amplifier is then connected (through a bias) to the modulator's drive terminals, in place of E_1 and E_2 from the modulator driver. The bias, a direct current source, should be used in series with the amplifier output to bias the modulator with 68 volts. In this mode of operation the modulator mode servo is inoperative, so care must be taken to ensure a symmetric polarization and a constant percent modulation. This will be elaborated on in the next part of our recommended test plan.

In addition to the electronic test equipment required for this test, optical signal level monitors (described in Part C), neutral density filters for controlling the received signal level, and a calibrated noise source for injecting a known amount of noise power into the receiver optics (over the spectral band of the receiver's optical filter) are required.

4. Noise Sources

A separate noise source for reducing the system to noise limited operation will only be required for those tests of communication theory where modulation of the laser is greater than 50%. The Hughes PCM/PL system, in its present configuration, does not permit a modulation index of more than .5, so all tests carried out without a new modulator driver can be conducted without a separate noise source. In these tests, the self-noise in the system introduced by the unmodulated portion of the laser energy will act as the background noise that limits the system performance (both during quantum limited and noise limited tests). It is expected that during these tests, with $m \leq .5$, quantum limited operation will not be observable. The noise in the signal and the noise in the photomultiplier detectors will probably limit significant testing to a noise limited operating level. This prediction is based on observation of the operation of the Hughes system at 30 magebits/second, where detector noise is significant, but theoretical predections for large polarization errors (Polarization error $\geq 45°$) agree with this conclusion.

At higher modulation indices ($m > .5$), a separate noise source must be supplied for varying the system conditions from quantum limited operations to noise limited operations. Typical background noise sources are discussed in Part E of this Section. They can be used for operating the 1 megabit/second PCM/PL system in a controlled noise environment, at the higher modulation indices. It should be noted that a background noise source is not really needed for quantum limited testing of laser communication theory, even at 1 magebit/second and $m = 1$. The photodetectors contribute enough noise to an input signal at the receiver to make quantum limit system operation difficult, according to theoretical predictions.

5. System Alignment and Calibration

Optical System alignment for all tunnel testing was discussed in part D of this section. Optical alignment is the same for all tunnel testing.

Electronic alignment consists primarily of adjusting the lengths of delay lines 1 and 2 so that received "ones" correspond in time with transmitted "ones" and so that the trigger pulse into the phase locked clock is positioned near the end of a bit. It is suggested that alignment of the electronic system should be done at high signal levels, with no background noise source, and at the highest possible per cent modulation. All alignment is done with a Tectronics 585 dual trace scope, or equivalent. In order, the electronic alignment steps are as follows:

1. Connect one trace of the oscilloscope to the output of delay line 2, and connect the other trace to the video input jack of the matched filter in the Hughes PCM/PL receiver. Do not connect the trigger pulse to the phase locked clock input. Adjust the length of delay line 2, using a variable delay line, similar to a General Radio 314 - S86, until the two patterns are in time synchronism.

2. Connect one trace of the oscilloscope to the output of delay line 1, leaving the other connected to the video input jack of the matched filter. Using a second variable delay line, adjust the time of occurrence of the clock pulse out of the delay line until it coincides with the end of a pulse.

3. Connect the outputs of each delay line as shown in Figure IV-17, and check the error rates counted on the error counter. If this is greater than one error/10^6 bits, readjust the length of delay line 1 to minimize

the error rate, as measured by the electronic instruments.

Next, we come to system calibration. Optical calibration is essentially the same as that used in part E of this section, except that the percentage modulation must be monitored while running tests at modulation indices greater than .5. Other optical calibrations include:

a) Measurement of the absolute background noise power density at the optical receiver

b) Measurement of the absolute laser power density at the optical receiver.

These calibrations will be done at a reasonably high received power level, and then the received signal level will be decreased by using calibrated neutral density filters in the transmitter and in the receiver.

Electronic calibration consists of the measurement of the noise power density at the output of the photomultipliers, as described in parts C and F.7 of this section. This noise power must be added to the noise in signal and intentionally added noise power in calculating the noise energy/decision. The use of this information in determining the signal and noise energy/decision for a given error rate will be explained in part 7 of this section.

6. Test Procedure

First, the electronic and optical systems must be aligned and calibrated, at a reasonable power level, as explained in part 5. Then, measurements of the background light noise power (in the spectral width) and photomultiplier noise power in a bandwidth of 0 to 2 MHz must

be made, with the laser turned off. These noise sources set an absolute lower limit on the range of noise powers/decision that can be used during any test run. This measurement of the absolute power limit on noise power will be made with a calibrated monitor, as described in part C of this section.

Then, the laser is turned back on, and the modulation is applied. Neutral density filters are inserted in the transmitter and receiver until a desired error rate (approximate) is obtained. The following measurements are then made:

1) Percent Modulation (Using the Hughes Monitor)

2) Signal Power at the Receiver (Using the Monitor Described in part C), Tuning Background Noise Source Off

3) Background Noise Power at the Receiver, if an external Noise Source is Used, Turning the Laser Off.

In general, it is better to put a shield over the laser in step 3 and over the noise source in step 2, as percent modulation and absolute power may vary when these items are turned off and on.

While continuing to monitor these parameters, to ensure that they remain with 10% of the original measured values, restart the event counter and the bit error counter. Continue to count events and errors until the desired confidence that error rate has been measured with a given tolerance has been obtained. The number of bits that must be transmitted, and the number of errors that must be read, before these criteria are satisfied is a function of the error rate. The exact relation between error rate, tolerance, confidence, and events counted is described in part F of this section.

Once the desired confidence and tolerance are reached, the test is ready to be repeated for different noise powers, percent modulation, and received signal power. Any combination of these values, for normal operating points, background noise limited, noise in signal limited, or even quantum limited operation (provided an external modulator driver is used to increase the percent modulation) can be used. Using the Hughes modulator driver, tests at the quantum limit do not have much meaning, as the noise in signal overrides any controlled noise sources.

7. Data Collection and Processing

The purpose of this series os tests is to test the laser modulation theory for polarized light communications developed under contract NAS 9-3650, and presented in the Final Report on that contract.[1] To obtain meaningful test date for each test in this series, the following parameters must be known:

a) Polarization error (mathematically equivalent to percent modulation)

b) Received noise energy/decision (other than noise in signal)

c) Receiver signal energy/decision (total)

d) Bits, or events transmitted

e) Bits in error

The calibrated monitor, described in Part C, has been used to measure noise power density due to its own photomultiplier, and due to background noise, over a 3.5 Hz bandwidth. The total noise power in the signal bandwidth is then

$$N_{BW} = \frac{N_{measured}}{3.5} \times B W_{signal}$$

Since we are interested in the noise energy/decision, not the total noise power in the signal bandwidth, we multiply N_{BW} by the duration of a bit. Doing this, we have

$$\text{Noise Energy/Decision} = \frac{N \text{ measured}}{3.5} \times BW_{\text{signal}} \times \text{Bit Time}$$

But $$BW_{\text{signal}} \text{ (one sided)} \cong \frac{1}{\text{Bit Time}}$$

Therefore, all noise and signal power measurements made with the monitor can be converted to noise energy/decision and signal energy/decision by dividing them by 3.5 (assuming a HP 302A Wave Analyzer is used with the monitor). This result, although not exact, is within the limits of measurement accuracy.

Next the signal energy/decision and the noise energy/decision must be separated. This is done by determining the absolute power associated with the photomultiplier in the monitor. Placing a cap on the monitor's input lens removes all other sources of noise. Calling this (N_M) we have the following:

$$(N \text{ measured}) \text{ Background} = N \text{ measured} - N_M = N_B$$

$$S = S \text{ measured} - (N_B + N_M) = S \text{ measured} - N \text{ measured}$$

Using these relations, we obtain

$$N_B \text{ (energy/decision)} = \frac{N \text{ measured} - N_B}{3.5}$$

$$N \text{ (energy/decision)} = \frac{N_M + N_B}{3.5}$$

$$\text{and } S \text{ (energy/decision)} = \frac{S \text{ measured} - (N_B + N_M)}{3.5}$$

These values then are converted to equivalent average numbers of signal photoelectrons/decision and average number of noise photoelectrons/decision, as explained in part C of this section.

The next step in data reduction is to determine the confidence in the data error rate measurement to a given tolerance. Figure IV-19 shows the mathematical relation between confidence, tolerance, and bit errors counted. Take the number of errors counted and divide by the number of bits transmitted. This gives a number

$$\hat{P} = \frac{\text{number of errors}}{\text{number of bits}}$$

Multiplying $\hat{P}$ by the number of bits transmitted, one obtains the ordinate value on this figure. Reading to the right of this, one obtains the confidence that $|P \text{ error} - P| <$ a given tolerance. Drawn on the figure is a sample of this, where the number of errors is 100, $\hat{P}$ is 10^{-3}, and the required tolerance is 10%. One sees that, under these conditions, the confidence that the actual error rate lies within 10% of $\hat{P}$ is 67%.

These curves were drawn on the basis of the following relation

$$n = \frac{C^2 (1 - \hat{P})}{\hat{P}\, T^2}$$

where:

n = Number of bits in a test

$\hat{P} = \frac{\text{errors}}{\text{bits transmitted}}$

T = tolerance (T = .25 for 25% tolerance)

C = confidence interval (C = 1.96 for 95% confidence)

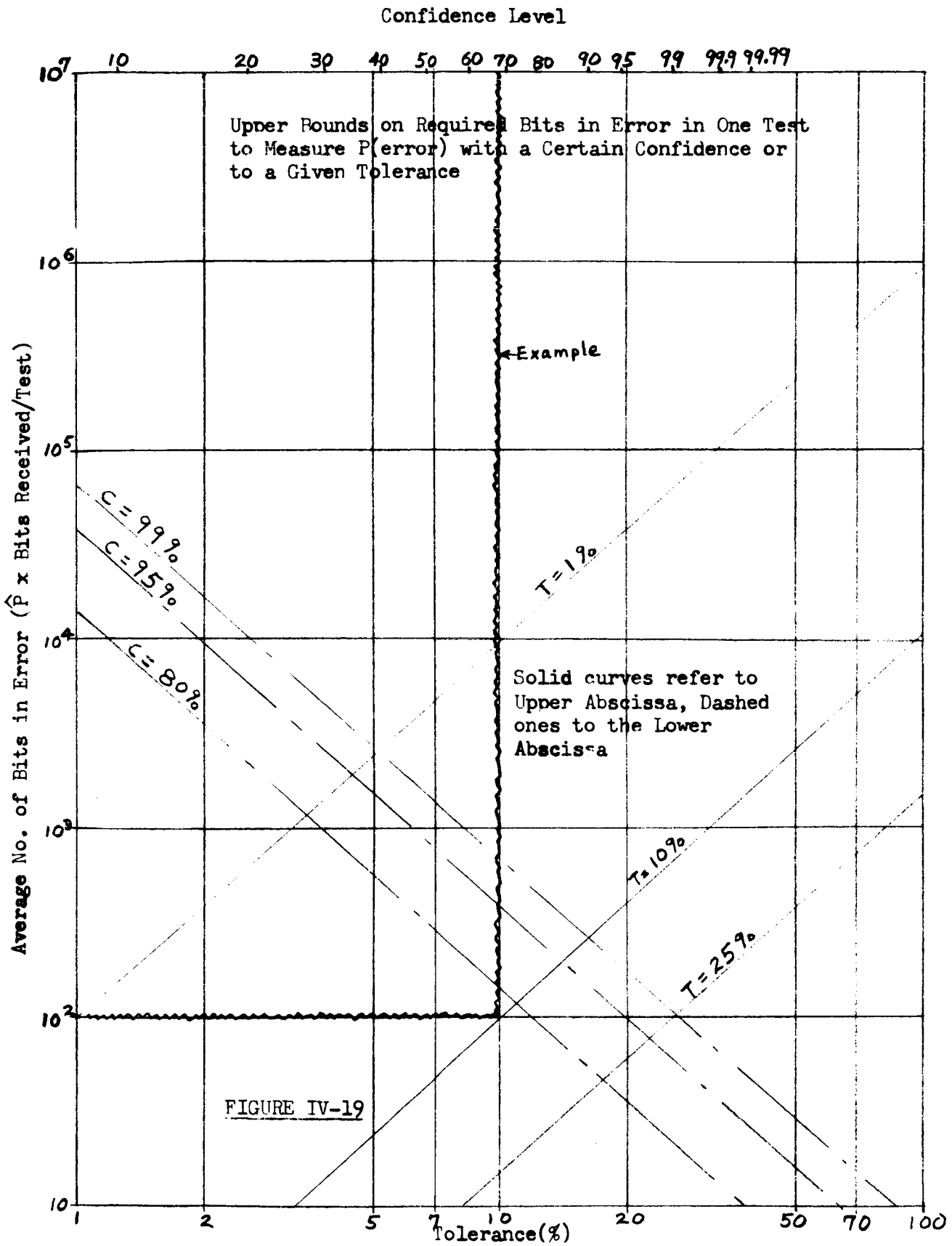
Confidence Level
10
20
30
40
50
60
70
80
90
95
99
99.9
99.99
Upper Bounds on Required Bits in Error in One Test to Measure P(error) with a Certain Confidence or to a Given Tolerance
Example
C=99%
C=95%
C=80%
T=1%
T=10%
T=25%
Solid curves refer to Upper Abscissa, Dashed ones to the Lower Abscissa
Average No. of Bits in Error (P̂ x Bits Received/Test)
Tolerance(%)
1
2
5
7
10
20
50
70
100

FIGURE IV-19

Finally, to correlate test data at modulation indices less than 1, the equivalent polarization error must be determined.*

Modulation indices less than 1 in polarized light modulated transmission systems are not physically equivalent to the polarization error discussed in the Second Interim Report[3] (pp. 74-75) on this contract. With a modulation index less than one, noise is injected into both channels of a polarized light receiver by the transmitted laser signal. With a polarization error, signal energy is diverted from the correct channel to the incorrect one. However, there is a mathematical equivalence, that can be used to convert results of theoretical analyses for the effects of polarization errors to similar ones for the effects of modulation indices less than 1.

In the case of polarization error, $(SNR)^1$ (as defined in the Second Quarterly Report) is

$$(SNR)^1 = \frac{2 S \cos^2 \phi}{N + S \sin^2 \phi} \qquad (1)$$

where:

S = signal power

N = noise power

ϕ = polarization error

In the case of percentage modulation less than 100%

$$(SNR)^1 = \frac{2 S M}{N + (1-m) S} \qquad (2)$$

---

*Polarization error, rather than "noise in signal", is introduced here because the Computer Program (Section V) uses this factor to correct for modulation indicies less than 1.

There are two cases of interest, both of which are treated in the Power Model (See Section V) of this report. These are the cases of high percentage modulation and low percentage modulation.

If m = 1, equation 1 simplifies to

$$(SNR)^1 = \frac{2 S \cos^2 \phi}{N} \tag{3}$$

while equation (2) simplifies to

$$(SNR)^1 = \frac{2 S M}{N} \tag{4}$$

At high modulation indices, or more specifically, where (1 - m) S is negligible with respect to N, the mathematical relation between ϕ and m becomes

$$m = \cos^2 \phi \tag{5}$$

or

$$\phi = \cos^{-1} m \tag{6}$$

At low modulation indices, or more specifically where (1 - m) S > N, equation (1) simplifies to

$$(SNR)^1 = \frac{2 S \cos^2 \phi}{S \sin^2 \phi} \tag{7}$$

while equation (2) simplifies to

$$(SNR)^1 = \frac{2 S M}{S (m - 1)} \tag{8}$$

Under this condition (low modulation index), the following relation holds:

$$\frac{1}{\tan^2 \phi} = \frac{m}{1 - m} \tag{9}$$

or $$\phi = \tan^{-1} \left(\frac{1 - m}{m} \right) \tag{10}$$

Although relations (6) and (10) are identical in form ($\phi = \cos^{-1} m$) it should be remembered that (6) only applies when $(1-m) \ll 1$ and (10) only applies if $(1-m)\ S \gg N$. In the general case, where $(1 - m)\ S$ and $m\ S$ are approximately equal, ϕ should be determined for calculations from the relationship.

$$\frac{\cos^2 \phi}{1 + \left(\frac{S}{N}\right) \sin^2 \phi} = \frac{m}{1 + \left(\frac{S}{N}\right)(1 - m)} \tag{11}$$

The approximate relation between polarization error and percent modulation is shown in Figure IV-20.

8. Predicted Results for 50%, 70% and 100% Modulation

Having the signal photons/bit, and the polarization error, one can then measure the effect of each of these parameters on system performance, and compare it with the results of theoretical studies of laser communication. This part of Section IV presents the predictions, for a 10^{-3} error rate and modulation indices of 1 ($\phi = 0°$), .7($\phi = 30°$), and .5 ($\phi = 45°$), as summarized in Figure IV-21.

The abscissa on this curve is the number of signal photons/decision (signal energy/decision) and the ordinate is the total number of noise photons/decision.

FIGURE IV-20. Percent Modulation Versus Polarization Error

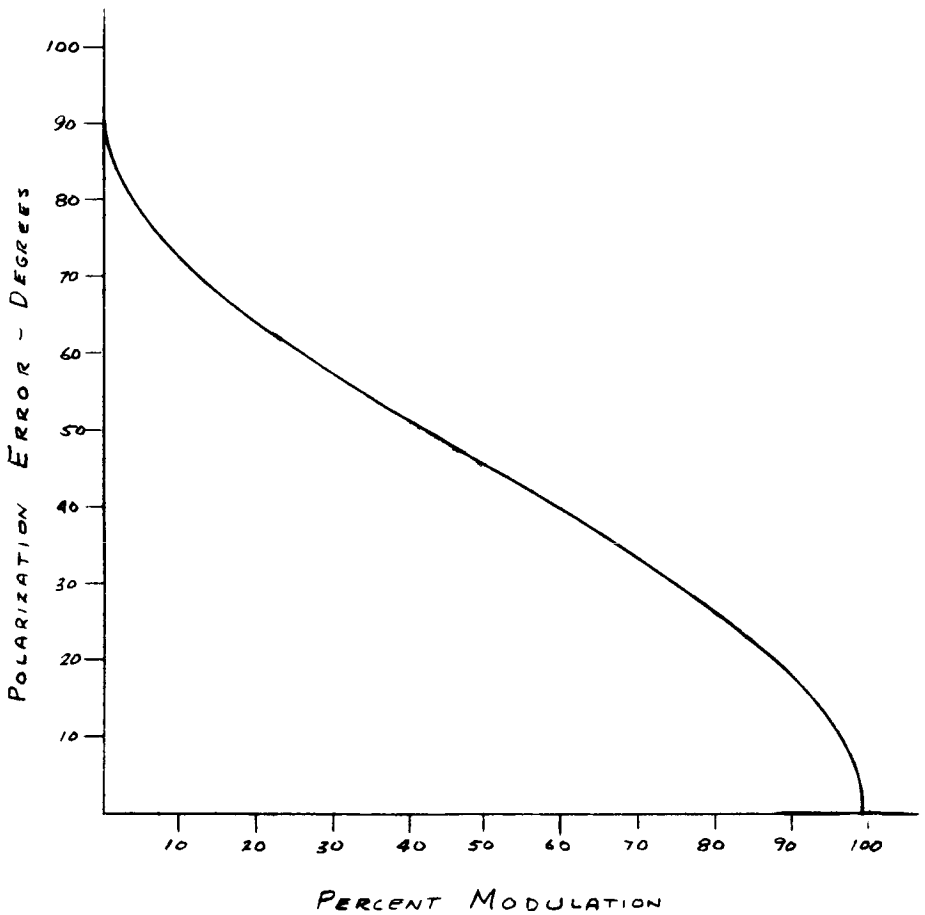

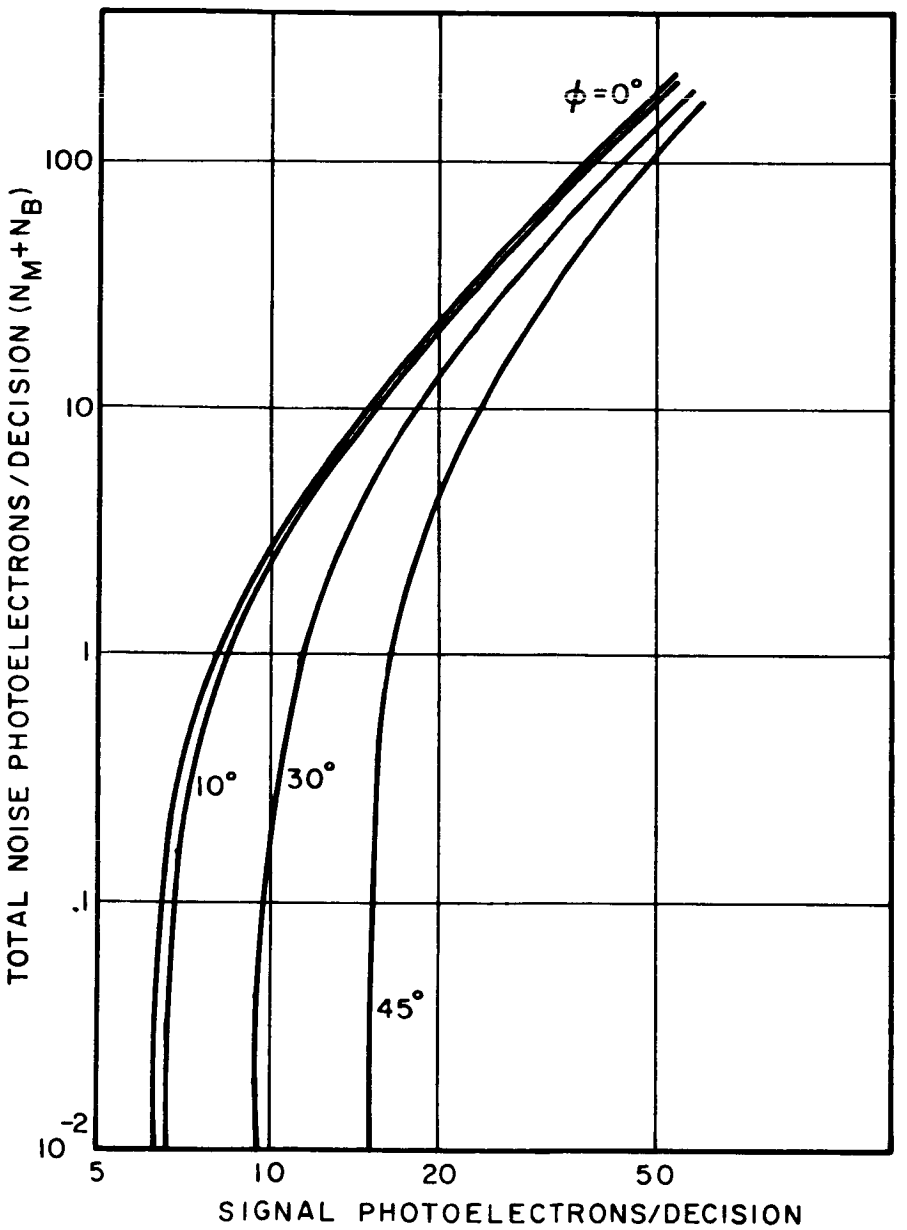

FIGURE IV-21. Signal Polarization Errors PCM/PL ($P_e = 10^{-3}$).

G. Test of a 30 Megabit PCM/PL System's Performance in the Tunnel

This test is not recommended for use in verifying the theory of quantum limited laser communications. It has been included as part of the tests to allow testing of the Hughes PCM/PL system at its maximum data rate. As will be seen, implementation of this test will require development of special purpose, extremely high speed, digital logic equipment. Even with this equipment, tests of quantum limited operation will not be possible, as the noise in signal is large enough to obscure most of the quantum effects on the performance of a laser communicator.

1. Test Configuration

The electronic and optical configuration for this test will be, basically, the same as those shown in parts D and F of this section. The differences between this test, and the 1 megabit/second test of the PCM/PL system (part F) lie in the implementation of test system, and not in the basic concept of a digital error rate measuring system.

Part F.1 of this section describes a bit error detector (or comparator) to be used during that testing. The differences between that one and the one used for 30 magebit/second testing, are that for 30 magebit/second testing:

1. There will be no RC integrators used at the inputs of the difference amplifier. There is enough stray capacity at these inputs to integrate both the reference signal and receiver output signal.

2. Gates 1, 2 and 3 must have switching times that are less than 5 nanoseconds. They must also operate with pulse of less than 30 nanoseconds in length.

3. The difference amplifier bandwidth must exceed 70 megahertz.

4. The inverter's bandwidth must be at least 70 megahertz.

5. The one shot flip-flop should produce error pulse that are approximately 20 nanoseconds long.

The logical operation of this high speed comparator is identical with that of the low speed comparator described in part F.1 of this section.

2. Test Equipment

At this digital data rate, it is difficult to obtain the necessary test equipment. The bit counter must be able to count at a rate of 30 megabits/second and the bit error counter must count events that last only 20 nanoseconds (50 megabits/seconds). They are also required to have good long term stability, to allow running tests for significant periods of time before drifts in these counters upset the system calibration. These requirements can be met by using Hewlett-Packard 5244L Electronic Counters (or equivalent commercial test equipment). It is recommended that two of these counters be used, as shown in part F.1.

The recommended delay lines are General Radio 314-S86 Variable Delay Lines, or their equivalents. These lines offer the bandwidth and resolution necessary for high speed testing of the PCM/PL system. These lines do not offer enough delay to compensate for transmission time in the tunnel, but they are sufficient for the proposed 101010 .... test pattern. A Tectronics 585 oscilloscope, with a wide band, dual channel preamplifier should be used to adjust the lengths of these lines, as described in part F.2 of this section.

There are many high speed pattern generators available for use during this test. It is recommended that a Hewlett Packard 216 A Pulse Generator,

or equivalent, be used because it also supplies the trigger pulse needed to operate the Hughes receiver and the comparator. The following modification to this generator should be made:

Add a one stage JK flip-flop to the output of the pulse generator. This flip-flop must be capable of operating with input pulse only 16.5 nanoseconds long. The flip-flop will produce, at its output terminals, a positive voltage for the first "10" in the sequence. Then, the next "1" causes the flip-flop to change state, and produce zero output. It is not necessary to align the output of the flip-flop with the "trigger output", since delay line 1 will compensate for any fixed time difference.

It should be noted that the pulse generator must operate at 60 megabits/second, with this modification, to produce a 30 megabit 101010 ... test sequence. An alternate approach would be to use a "times two" digital multiplier in series with the trigger pulse, and operate the pulse generator at 30 megabits/second. The "divide by two" circuit in series with the pulse output was chosen because the trigger pulse is only 3.5 nanoseconds long. This requires excessive speed in a "times two" network.

The "divide by two" JK flip-flop and the gates needed for the comparator are within the state-of-the-art, but they are not commercially available as complete operating systems.

3. Additional Instrumentation and Equipment Modifications.

All additional instrumentation and equipment modifications are the same as those described in part F.4 of this section. It is not recommended that an external modulator driver be used, as this test is designed to test

the performance of the driver used in the existing equipment. This means that the modulation index cannot exceed .5, but it also means that the modulation index will be kept constant by the "mode servo" in the Hughes equipment.

4. System Alignment and Calibration

The basic system alignment and calibration procedures for these high data rate tests are the same as those described in parts C.3 and F.5 of this section. All delay lines, and other coaxial cables carrying the 30 megabit/second test pattern and the trigger (clock) pulses, should be kept short. This will minimize the amount of pulse distortion caused by these cables.

5. Test Procedures

Procedures for conducting this test were described in part F.6 of this section.

6. Data Collection and Processing

A technique for reducing the raw data to statistically significant results was presented in part F.7 of this section. Section F also presented the relation between polarization error and percent modulation. Predicted performance results are presented in part F.7 of this section and in section V.E.2.

H. Measurement of Link Characteristics with an Analog System.

1. Objectives

The objectives of testing the characteristics of the 11 mile test link with an analog optical communications system are to:

1. Measure the optical transmission properties of the link as a function of time.

2. Correlate atmospheric conditions with optical transmission characteristics.

3. Determine the time interval during which test conditions remains essentially constant, allowing meaningful system testing.

4. Determine the time delay variations in the arrival of a laser signal, which is a measure of the phase coherence of the link.

The data derived from these analog tests will be used in later testing over the link to determine characteristics of certain test equipment, test durations, and meaningful atmospheric parameters that must be monitored during the tests. It also influences the methods of data reduction that should be used to obtain meaningful test data from these tests (See parts I and J of this section).

An analog system was chosen for these initial outdoor tests because of its simplicity. Meaningful test data can be obtained with a relatively simple test system. There is no need for maintaining time synchronism between the transmitter and receiver, or for generating a reference test code in the receiver. Since this is a preliminary test, designed to obtain as much data as possible about atmospheric effects on laser transmissions at a minimum cost, the analog test system is recommended for this work.

2. System Configuration

There are two general types of analog measurements of a transmission channel that can be conducted. One is with an unmodulated carrier. The

received signal level is recorded. This data is then converted to amplitude correlation functions for the channel and to power spectra for channel transmission.

Unmodulated transmissions can be used to obtain the first three objectives of this test, provided the background noise is constant. Because it is believed that the fourth objective is important, and that the assumption of a constant background noise may not be valid, we are recommending the use of a modulated transmitter during analog testing of the 11 mile link. The modulation allows observation of "time jitter" in the detected signal and it allows narrowing the post-detection bandwidth enough to reject most of the background noise.

The transmitter to be used during this test was described in part E of this section. It consists of a Spectra-Physics #125 Laser with a Spectra Physics #320 Modulator used to amplitude modulate the laser beam. No specific modulating frequency will be recommended, but it should be between 1. and 4 MHz, for reasons discussed in part E of this section. The modulator driver can be any high frequency, high power, push-pull amplifier, in series with a low impedance bias source.

In addition to transmitter equipment mentioned in part E, a collimator should be placed at the output of the modulator. This lens is used to narrow the transmitter beamwidth as much as possible after the beam divergence has been increased in the laser modulator.

The receiver configuration used for these tests was also described in parts C and E of this section. It consists of an optical telescope, a PMT

detector which is preceded by an optical filter, a tuned circuit, a high input impedance amplifier, and a true RMS voltmeter.

During setup of the test configuratinn, some problems may be encountered with optical alignment due to beam bending. This can be minimized by using a large aperture receiver. We recommend the use of NASA's 30" field receiver for these tests, to minimize this problem. Alignment can be accomplished by aiming the transmitter, optically, at the receiver and then transmitting an unmodulated signal. The receiver should then be aimed, optically, at the transmitter, and the average receive level monitored. Then, by slight adjustment of the transmitter alignment, the average receive level can be maximized.

At this point, the transmitter and the receiver should be locked in position. If at any time during the analog tests the system alignment is questioned, these steps must be repeated and new sets of test data must be obtained. Extreme care should be taken when working around the transmitter and receiver, as any change in the absolute aiming of these elements can invalidate tests.

3. Test Configuration and Instrumentation

The configuration that is recommended for this series of tests, and the test instrumentation for the electronic system are shown in figure IV-22. This figure does not show the optical power monitors, which are described in part C of this section.

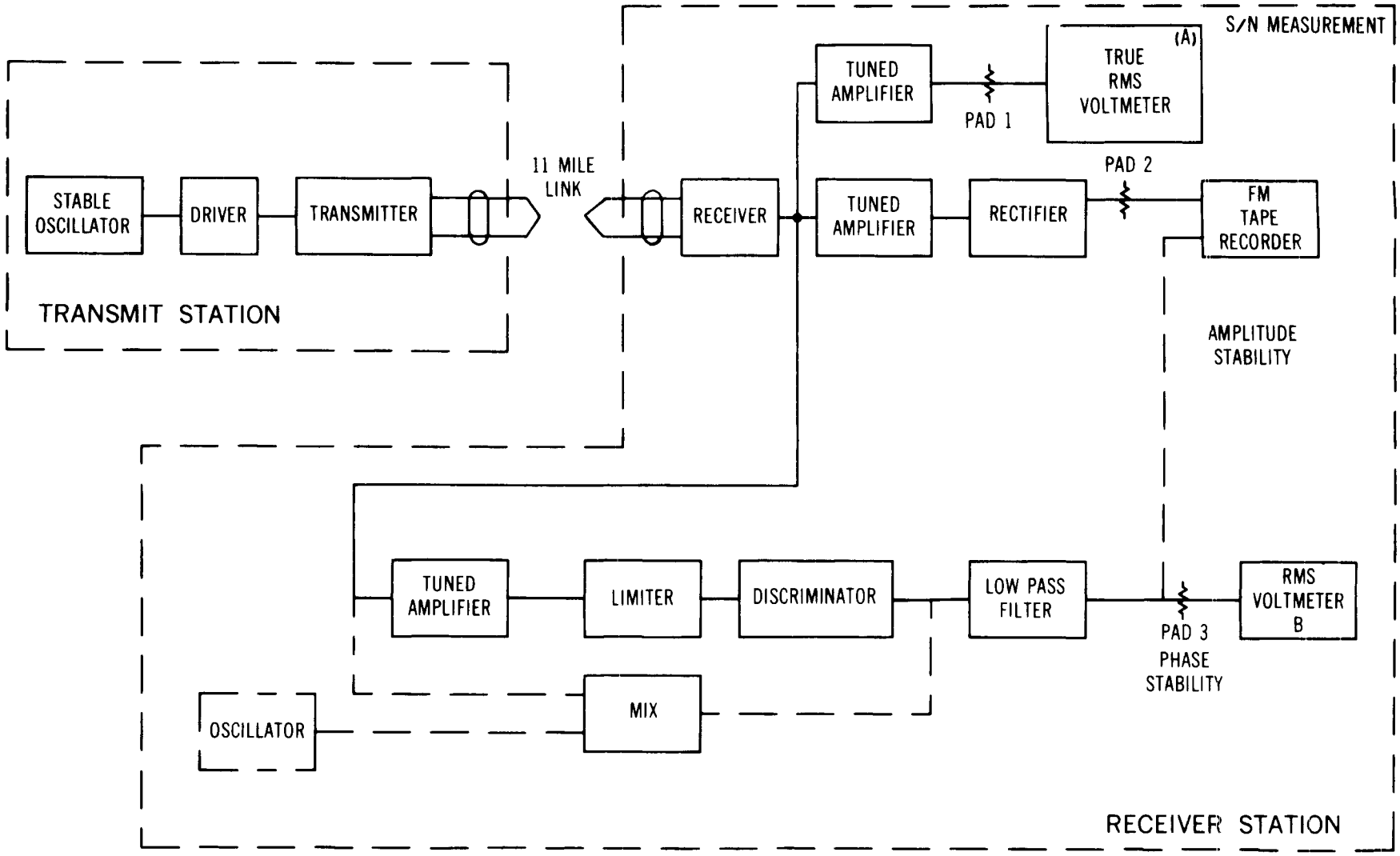

FIGURE IV-22. Test Set-Up, Analog Range Tests

The oscillator used in the transmitter should be as phase stable as practical, to allow measurement of the random effects of the atmosphere on the path delay. If possible, a Hewlett-Packard 106AR, or equivalent, quartz oscillator should be used, as it introduces a negligible phase noise. If an oscillator with poorer phase stability is used, an approximate compensation for its effects will have to be included in the date reduction portion of these tests (see H.3).

The tuned amplifiers, limiter, and discriminator are commercially available systems, or they can be breadboarded. They should be tuned to the frequency of the oscillator in the transmitter. A bandwidth of a few thousand cycles is desirable for the amplifiers and limiter, but this bandwidth is not critical. The discriminator should have a linear frequency-voltage characteristic for frequency changes up to the maximum passed by the tuned amplifier.

The low pass filter is used as an averaging device. It should have a variable bandwidth. The maximum recommended bandwidth of this device should be a few thousand cycles/second, but it should be possible to reduce this to approximately 2 cycles/second.

The RMS voltmeters shown in Fig. IV-22 are thermal voltmeters, available from Weston or other meter manufacturers. Its purpose is to average the output of the low pass filter, which will resemble noise (phase noise).

Any commercially available dual channel FM tape recorder that has a pass band from DC to at least 500 Hz can be used. Standard AM tape recorders cannot be used because they have no DC response, and strip chart recorders cannot be used because their maximum frequency response is less than 200 Hz.

As will be mentinned during part H.4 of this section, it may be found that the transmission medium is too stable to allow phase variation measurements with the test setup shown in figure IV-22. If this proves to be true during testing, the oscillator at the transmitter should be replaced by a HP 106 AR, and another HP 106 AR should be placed at the receiver. These oscillators will then be synchronized by using a piece of RG-58 coaxial cable as a delay line in the receiver. Finally, the output of the receiver and of the delay line will be mixed, to produce a zero center frequency. The output of the mixer will then be read, after it passes through the low pass filter, with the same type of meter that is used in the receiver. This potential test configuration is shown as the dotted portion of figure IV-22. The homodyne mixer is commercially available, or can be breadboarded with existing electronic equipment.

The pads are GR 1454 Decade Voltage Dividers, or equivalent.

4. Test Procedure

A. Align the system, as described in part H.2, under conditions of good visibility, thermal stability, and low wind velocity. This should probably be done at night, after the air and the earth have reached thermal equilibrium. Lock transmitter and receiver in their positions, before doing any testing. Unless these elements have been moved, they should not be realigned during subsequent tests.

B. Turn off the laser, and monitor the noise current (I_n) at the receiver with the RMS meter (A). If this cannot be read, increase the gain of the amplifier until a satisfactory meter reading is obtained. During this, pad 1 should be set for zero attenuation (Voltage ratio = 1). Record this

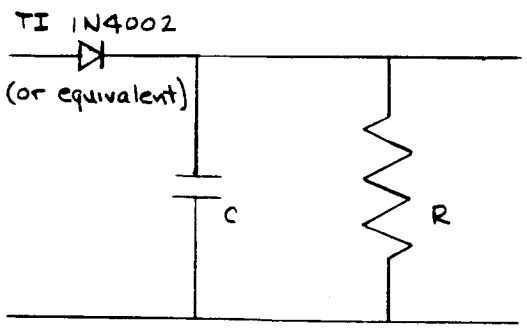

$RC \geq 500$

Where: C is in microfarads
R is in ohms

FIGURE IV-23. Rectifier

reading.

C. Turn on the laser, with modulation, and monitor meter A. The reading should be at least 10 db (above) that obtained in part B. Set pad 1 to keep the meter on scale. Record both the pad setting and the meter reading.

The system is now ready for testing under representative atmospheric conditions. The choice of conditions is at the operator discretion, but during a given test the following parameters should be monitored.

1. Wind speed at both the transmitter and receiver.
2. Visibility (in miles)
3. Temperature
4. Humidity

Also, general atmospheric conditions (cloud cover, rain, etc.) should be recorded before a test run is conducted.

Having chosen a "representative" link condition, test data recording is started. This begins with step D of this procedure.

D. With the laser off, monitor the noise power, as in step A. Set pad 2 to achieve a resonable recording level in the tape recorder. Turn the tape recorder on, and tabulate the setting of pad 2 and the reading on meter A. After a few minutes, stop the recorder.

E. Turn the laser on, with modulation, and set pads 1 and 2 to give proper levels. Restart the recorder, and tabulate the settings of the pads and the readings on meter A. The percent modulation is somewhat arbitrary, but is is recommended that this be as high as possible to prevent noise in signal from obscuring channel effects. Continue to run for at least 15 minutes, tabulating changes in the reading of meter A as they are noted, along with the time of the measurement.

F. At the same time, tabulate the reading on meter B, which is measuring the total phase noise in the signal. This should be done at a number of bandwidths, from the narrowest allowed by the low pass filter to the widest allowed by the amplifier. If it is noted that this measurement drops 6 db for each octave reduction in the filter bandwidth, the alternate phase measuring system shown in figure IV-22 will have to be used for measuring phase noise.

G. Finally, turn off the modulation at the transmitter, but leave the laser on. Readjust pads 1 and 2 for proper signal levels at the meter and the recorder. Tabulate the pad settings and the meter reading.

This concludes one analog test of the link. Steps A and B do not have to be repeated for each atmospheric condition of interest. On these subsequent tests, only steps D through G need be repeated.

There is no way of predicting how long a test should be run, as this depends on the effects that one is attempting to measure. "Steady state" tests should be kept relatively short, as atmospheric conditions are always changing. On the other hand, when attempting to measure the effects of rain or temperature gradients on atmospheric transmission, the tests should be long enough to include good periods of time, transition times, and times where the atmospheric changes have reached their extremes.

5. Data Processing

A way of processing the test data is to obtain S/N ratios at the receiver, as a functinn of time, is included in part E of this section. This procedure assumes that the noise powers, as measured during steps C and F of the test procedure, are essentially constant over the measuring interval. During periods of operation in a "steady state" atmosphere this is a reasonable assumption, so the procedure presented in E can be used.

If, as measured in step G, the noise power is not constant, this test arrangement can not be used to directly measure S/N. However, it can still be used to measure variations in the amplitude and phase of the modulating signal as a function of time. It is expected that the signal power will be large enough, at a high modulation index, to make the effects of noise power on the readings taken during steps E and F negligible. Steps D and G are taken to verify this assumption.

The amplitude test data taken during step D should be reduced to an approximate amplitude correlation for each test condition by taking uniformly spaced sample values and using them in the relation:

$$\phi_{11}(\tau) \cong \phi_{11}(n\,T) = \frac{1}{N} \sum_{\text{SAMPLES}} f(t)\ f(t + n\,T)$$

where N = the number of samples

T = the time spacing between samples

τ = nT= the value of time shift for which $\phi_{11}(\tau)$ is calculated

t = an arbitrary starting line for sampling

ϕ_{11} = autocorrelation functinn

This quantized correlation function should then be transformed to an amplitude power density function, using the relation

$$\Phi_{11}(\omega) \cong F\left[\phi_{11}(nT)\right]$$

The approximations in both these expressinns result from the fact that sample values of the received signal, and not the Analog recorded values, are being used in calculating $\phi_{11}(\tau)$. It is expected that frequencies as high as

1000 Hz will be of interest in the reduced data. To achieve this resolution, samples (taken from the tape recording) should be spaced by no more than .5 milliseconds. With this requirement, the number of samples used to compute $\phi_{11}(\tau)$ depends on the nature of the equipment used to perform the indicated calculations. It is not recommended that these calculations be made by hand, as they are extremely lengthy.

If available, a correlator is recommended for this work. It's input would be the data recorded during step E of a test. Such correlators are available at universities (MIT, for example), and special purpose correlators can be purchased.

The data recorded during step F of a test is, ideally, a measure of the phase noise. Unfortunately, it also contains some noise power generated in the receiver and by the transmission link. It is known that the noise power from "white noise sources" should reduce at a rate of 6 db/octave as the bandwidth of the low pass filter is reduced. Plot values obtained on meter B at various bandwidths on log-log paper. At the higher frequencies, this plot should approach a straight line, with a slope of 6 db octave. Draw this straight line on the plot. Anything above is represents phase noise. Subtract the value of the lines at a measurement bandwidth from the measured value. This leaves phase noise as a separate quantity, since it is not correlated with the other noise source.

As the final step in data reduction, this information should be converted to a power density spectrum. The adjusted reading at the minimum bandwidth represents the phase noise power in that bandwidth. Subtracting this from the adjusted value for the next larger bandwidth gives the total phase noise power between these points. Proceeding in this way, one can construct an approximate phase noise power density spectrum.

With the alternate phase stability measuring system, phase noise data can be reduced to a power density spectrum in the same way. This more precise phase noise measurement will be required if the measurements made using the original system all lie on the 6 db/octave line.

6. Predicted Results

Results of these tests, for a constant noise power, are predicted in part C of this section. These results are directly applicable to these tests, since most of the noise power is associated with signal currents. As the received signal level varies, the S/N ratio should vary as predicted therein.

A gross prediction of the results of the amplitude transmission characteristics can also be made. The power density spectrum will be centered at zero frequency, but it will be significant at frequencies as high as 500 Hz.

No firm prediction can be made for the phase stability measurements (phase noise) since these has never been attempted over a range of this length.

I. Measurement of the Characteristics of an 11 mile link at Low Data Rate

1. Selection of Test System

The analog tests have determined the amplitude and phase power spectra for the 11 mile outdoor link. From these results, theoretical predictions of the performance of PPM and FM subcarrier systems can be made. However, these tests have not determined the effects of the propagation mechanism on the polarization of a light carrier.

Since polarization loss, or polarized noise sources, seriously affect the performance of a PCM/PL laser communication system, we recommend the use of a modified version of the Hughes PCM/PL system for initial digital testing over the range. Data obtained with this system will allow gross prediction of the performance of a high data rate PCM/PL system on the range.

The Hughes system, modified for testing at 1 megabit/second, was also chosen for this test sequence because of its relatively high power output. This insures a good average signal to noise ratio at the receiver. The only major modification recommended for these tests is to replace the existing receiver telescope with the 30" field receiver's telescope. Its large aperture minimize the effects of "beam steering" on system performance.

2. Test Configuration

The recommended test configuration, along with the necessary electronic test equipment, are shown in figure IV-24. This is essentially the same as shown in part F.1 of this section, with the following modifications:

a. Addition of clocks at the transmitter and receiver

b. Addition of a tape recorder to the output of the comparator

TRANSMITTER 1

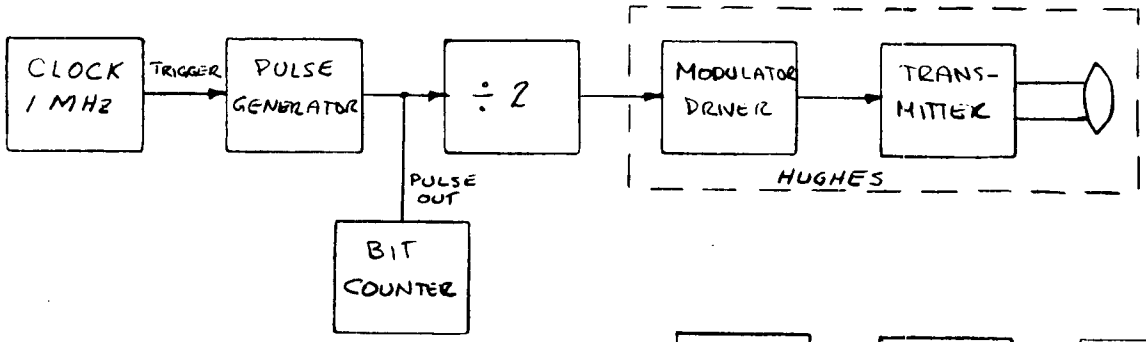

or,

TRANSMITTER 2

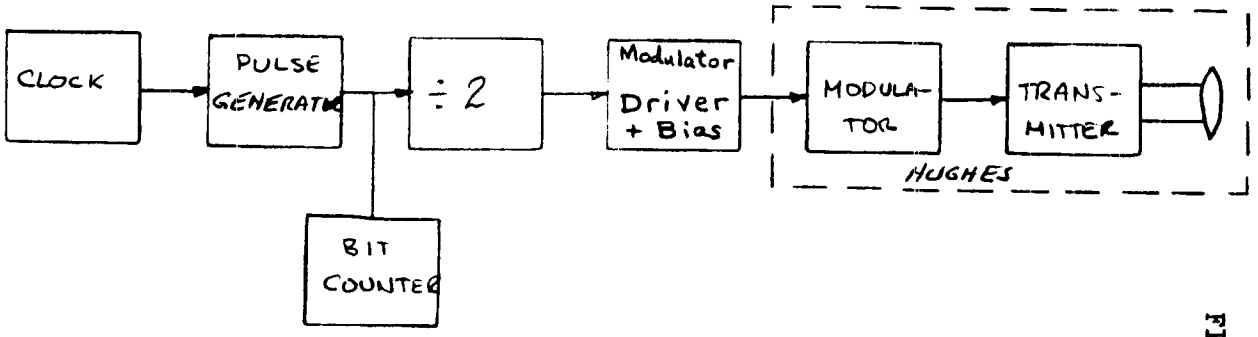

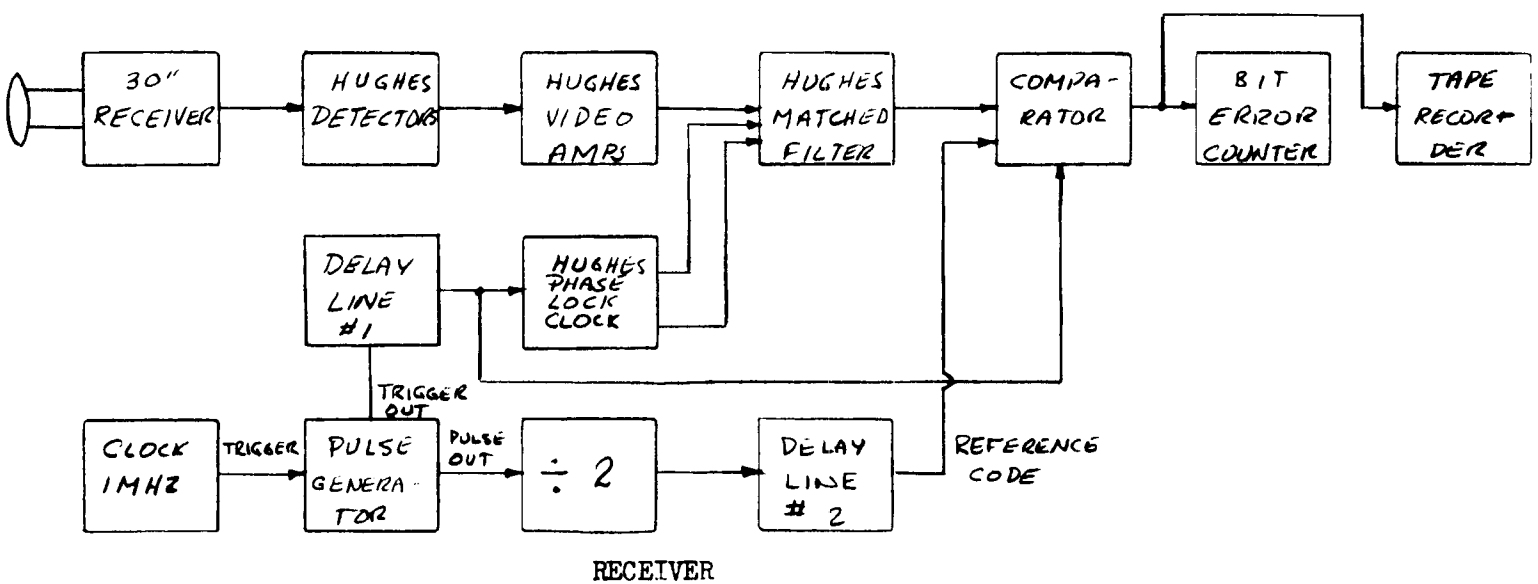

RECEIVER

FIGURE IV-24. Test Set-Up, Test of Low Data Rate System over 11-Mile Link.

c. Addition of a pulse generator at the receiver.

The comparator shown is the same one used in part F of this section, as are the dividers, which were described in part F.2.

3. Instrumentation

In addition to the electronic test equipment shown in figure IV-24, atmospheric monitoring equipment (part H) and optical monitors (part C) are required. The use of this additional instrumentation has already been discussed.

The second transmitter configuration uses a high power amplifier, rather than the Hughes modulator driver, to obtain modulation indices greater than .5. The characteristics of this biased amplifier, and the reasons for using it in testing laser communication theory, were discussed in part F.

4. Test Equipment Required

Both the transmitter and receiver clock must be highly stable to prevent synchronization errors in the electronic system. It is recommended that quartz oscillators, similar in performance to HP 107AR, be used for these clocks. They should have a 1 MHz output sine wave, as shown.

The pulse generator must be able to produce pulses at 2 megabits/second, as explained in part F. The receiver pulse generator must also produce a trigger pulse which drives the Hughes "phase locked clock". It is recommended that HP222A Pulse Generators, or equivalent, be used for generation of the test pattern and the reference code.

The delay lines can be RG-58 coaxial cables, but it is recommended the General Radio 314-S86 Variable Delay Lines be used if they are available. The lengths of these lines should be kept as

small as practical, to avoid distortion of the Reference Code and the Trigger Pulse.

The bit counter and bit error counter can be any stable 1 MHz counters. It is recommended that HP 5233L, or equivalent, counters be used.

The modifications that must be made to the Hughes PCM/PL system were detailed in part F.3 of this section.

The tape recorder shown should be a wide band (at least 2 MHz) FM recorder. Commercially available video tape recorders can be used for this purpose.

In addition, it is recommended that a strip chart recorder be connected to the optical monitor's output to record fluctions in average received power level with time. The monitor and recorder are not shown.

The choice between the two transmitter configurations depends on the desired modulation index. It is recommended that, if possible, the second one be used. However, meaningful test data can be obtained using the first configuration. This choice was discussed in part F.

5. System Alignment

Alignment of the optical system was discussed in part H. Since only the electronics are changed for this test, only a minor realignment should be required.

Timing alignment should be made at night, with maximum transmitter power. Start the clocks and pulse generators at both sites, and allow them to warm up for at least 15 minutes. Then, without connecting delay line 1 to the phase locked clock, connect one channel of a dual trace oscilloscope, Tectronics 585 or better, to the output of the video amplifier. Connect the other channel across the output of delay line 2,

where it enters the comparator. Adjust the length of delay line 2 until the received sequence of ones and zeros is in synchronism with the reference sequence.

Next, connect delay line 1 to the phase locked clock. Remove the oscilloscope lead from the video output, and bridge it across the delay line input to the phase locked clock. Adjust the length of delay line 1 until this pulse occurs near the trailing edge of each one or zero. This positioning of the timing pulse is explained in the Hughes Maintenance Instructions.[37]

The system is now aligned, and ready for error rate testing.

6. Test Procedure

The procedure for conducting this test was detailed in part F. The only change in test procedure is to run the tape recorder and strip chart recorder during a test. These recorders should also have provisions, either manual or electronic, for noting the time of a test and what signal level corresponds to what error counting condition.

Choose an atmospheric condition that is desired, as explained in part H, and start the test by restarting the bit counter and bit error counter. Do not turn the oscillators off between tests, or allow at least 15 minutes for warmup. If they have been shut down, or the system has not been aligned for several hours, realign the electronics, as explained in H.5.

Turn the tape recorder and the strip chart recorder on, and then proceed with the test procedure described in part F.6 of this section.

7. Data Processing

There are two basic types of data as to channel characteristics that can be derived during this test. One is the probability of error, or error rate, at a constant received signal level. This data will be

obtained by reducing the readings accumulated on the bit counter and bit error counter during a period where the signal level is essentially constant to a $\hat{Pe}$. Then, estimates of the confidence in this measurement for a given tolerance should be obtained, using the data contained in part F.7 of this section. The only difference between the data reduction used here, and that described in part F, is that tolerances and confidences will now be limited by the length of constant signal amplitude data available.

The second way in which this data can be reduced is to determine a probability density for the probability of n adjacent errors. The raw data is contained on the magnetic tape. This tape should be played back to determine how many times during a test, at a given signal level, or at varying signal levels, two errors are adjacent, three errors are adjacent, an error is isolated, four errors occur in a row, etc. This data can then be plotted, and compared with the theoretical prediction that if Pe is the average probability of error, then

$$P \text{ (n errors adjacent)} = Pe^{n-1}$$

This measurement allows one to determine the amount of correlation in errors introduced by the transmission medium.

8. Predicted Test Results

Predictions of test results, at constant signal levels for a Pe of 10^{-3} were presented in part F.8 for various modulation indicies. Predictions for other error rates can be obtained by using the power model described in Section V of this report.

It is not possible to predict results of error correlation studies and varying signal levels. There is not enough data on the channel characteristics available to make these predictions.

J. System Performance Measurements at 30 magabits with PL Modulation

This test is designed to measure the performance of the Hughes PCM/PL system at maximum bit rate over the 11 mile range. It is not recommended for initial testing, because of its cost and problems with maintaining station timing. It is included here for completeness. It is believed that more data about the range's properties can be obtained with test series H and I than with this test.

1. Test Configuration

A potential test configuration is shown in figure IV-25. This is identical with the one proposed in part G, except for the inclusion of separate clocks and pulse generators in the transmitter and the receiver, and the X6 multipliers, which are solid state multipliers designed to give 30 MHz outputs when driven by a 5 MHz clock.

The performance requirements, and potential design, of the dividers and comparator were discussed in parts F and G.

The optical configuration includes the NASA 30" field receiver, for reasons discussed in parts I and J. This configuration does not show the signal level monitors and strip chart monitors, which are used here as they were in part I.

2. Station Timing

It is not practical to keep the transmitter and receiver in time synchronism, within the few nanoseconds allowed by the data rate, by using a hard line tie between the transmitter and receiver. Therefore, we are recommending the use of separate clocks at the receiver and the transmitter. If it is found that pulse timing, as measured during the first step of the alignment, has a jitter that exceeds 10 nanoseconds (RMS), it is recommended that this series of tests be terminated. Station timing, and atmospheric jitter, will have such a gross effect

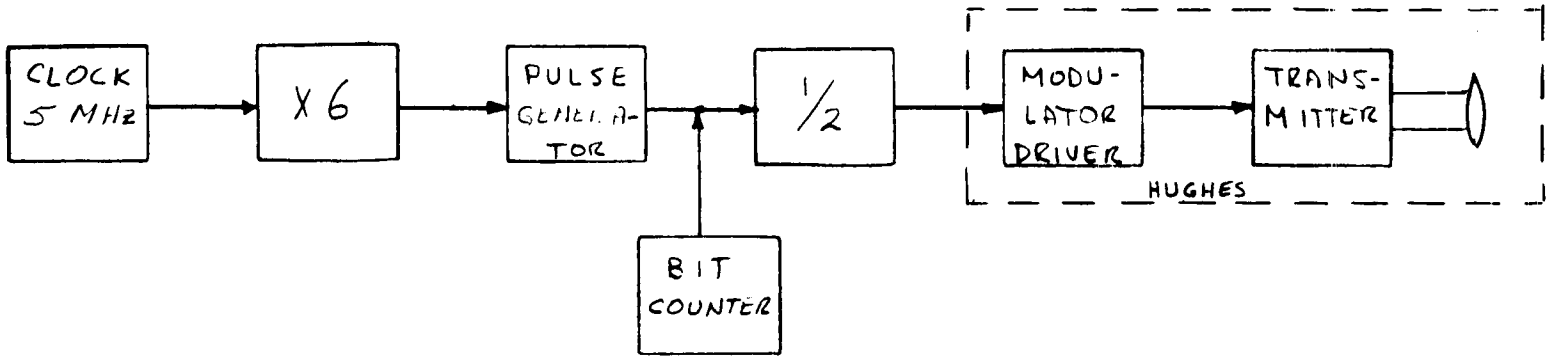

TRANSMITTER

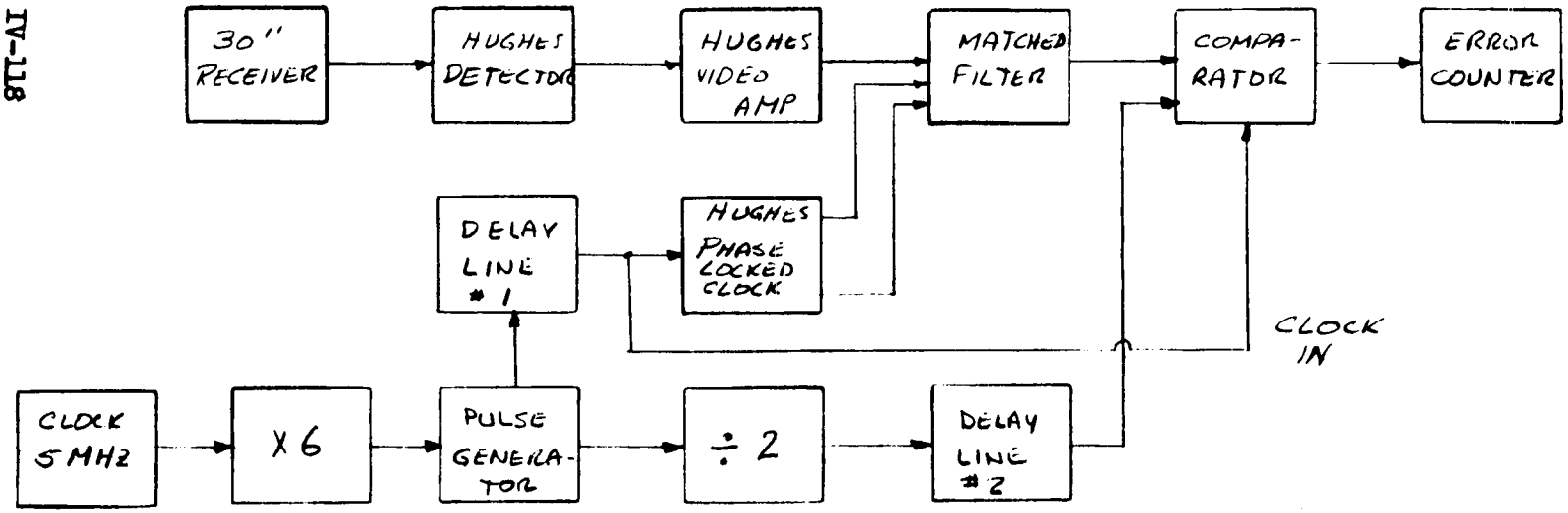

FIGURE IV-25. Test at 30 Megabits/Second

on system performance that the test data is invalid.

Even if the pulse jitter is small,it is recommended that the video output to the matched filter and the receiver reference be continually monitored (as in the first step of the alignment) to insure that they do not drift out of time synchronism. It will probably be necessary to realign the system every few minutes.

3. Test Equipment Required

It is recommended that HP 107AR Quartz Oscillators, or their equivalent, be used as clocks because of their highly stable 5 MHz outputs (.4 milliradians RMS over 1 second).

The bit counter and bit error counters should be HP 5244L, or equivalent, electronic counters capable of counting at rates in excess of 50 magabits/second.

It is recommended that a pulse generator similar to the HP 216A be used at both the transmitter and the receiver. The delay lines should be General Radio 314-S86 variable delay lines. All other test equipment, including the monitors, were described earlier in this section.

4. System Alignment

Basic alignment, both optical and electronic, for digital data testing of the PL modulated system were detailed in parts F and I of this section. The additional requirements for alignment for high data rate testing were explained in part G.4. The only modification of these procedures, monitoring of time synchronization, was explained as item 2 of this part. Once aligned, the system is ready for testing under various atmospheric conditions. The choice of these conditions is left to the test system's operator.

5. Test Procedure

The procedure for these tests, and modifications to them based on phase jitter measurements, is explained in item 2 of this part, and in parts G and I, of this section. As before, signal levels, starting times, test conditions, error counts, and bit counts should be logged for each test run.

6. Data Processing

It should be noted that the use of neutral density filters during field tests has not been described. This is because it is felt that variations in received signal level will be enough to allow determination of error rate as a function of signal level. In this test, background noise will probably be masked by noise in signal, as described in part G. If the signal level received is well above the quantum limit, it is suggested that neutral density filters be used to reduce the received signal level to a satisfactory level. Once this has been done, a plot of $\hat{Pe}$ (measured probability of error) versus noise power and signal power can be obtained by varying the percent modulation. This is explained in part F.

Given a run with a constant signal level, we have four basic measured quantities:

m = per cent modulation

N + S = signal power + background noise power (measured with a monitor)

Ne = number of errors counted in a test

Nb = number of bits in a test

Using m, and assuming $N + S \cong S$, we can compute the noise energy and signal energy/decision (see part F).

Next, one forms an estimate of the probability of error/decision, which is

$$\hat{Pe} = \frac{Ne}{Nb}$$

Finally, using the figure or the relation given in part F.7 of this section, one determines the confidence with which $\hat{Pe}$ is within a given tolerance interval of the actual probability of error.

Part F.8 of this section gives theoretical predicitions of performance, for comparison with the measured results. In using those predictions, it should be remembered that the noise energy is mostly (1-m)S. This means that the noise energy per decision is $\frac{(1-m)S}{30 \times 10^6}$. If predictions for the Gaussian noise region, or for $Pe \neq 10^{-3}$, are needed, they can be obtained by using the program described in Section V of this report.

K. Testing of PPM and FM digital data transmission systems.

There will be no attempt made here to detail tests of PPM and FM digital laser communication systems to the extent that the testing of the analog system and the PCM/PL system have been documented. This is because most of the basic test procedures have already been explained and because the PPM and FM systems are still undergoing development. This part of Section IV will, instead, discuss basic configurations for testing these systems with digital signals and the differences in data reduction from that already described.

1. Test Configuration for FM System

For testing digital FM laser systems in the tunnel, the test configuration used in part F or part G of this section can be used, with the same electronic test equipment. It may be necessary to use a bipolar driver, rather than a unipolar one, if the FM modulator requires bipolar drive.

The system should be set up in the tunnel, with the transmitter and receiver side by side. The timing pulse is connected to the decider in some, undetermined, manner.

An optical monitor is used to determine the received signal power (see Part C). A retroreflector reflector (part D) is located at the other end of the tunnel, and is aligned as in part D. If desired, a chart recorder can be connected to the monitor to insure that the signal level remains constant during a test. Finally, a variable power noise source (part E) is placed in the tunnel to allow measurement of system performance at various signal to noise ratios.

Calibration of the system, with the exception of measuring the FM

subcarrier modulation index, has been explained in parts D, E, and F of this section. The subcarrier modulation index should be measured with a deviation meter.

2. Test Equipment for FM Testing

In addition to the test equipment described in parts F and G, and that described in part C, a FM deviation meter is required. This is a standard piece of test equipment, available from Boonton and other companies.

3. Parameters to be Varied in FM Testing

During testing of an FM system, it is important to vary signal level, noise level, and deviation. This is because an FM laser system can be expected to have two thresholds. One result from the receiver falling below a limiting threshold and the other results from the quantum nature of the laser energy. At high modulation indices, it is expected that the quantum threshold will become apparent before the limiting threshold. At low modulation indices the limiting threshold may occur first as the signal level is reduced or the noise level is increased.

4. Data Reduction for FM Testing

Data reduction for these FM tests is identical to that discussed in part F of this section, except that carrier to noise measurements should be made at the input of the decider. These are made with a true RMS voltmeter.

5. Predicted Results for FM Tests.

Signal to noise is not one of the output parameters in the Computer Model (Part V). However it can be inputed to the program, and results of tests runs on the computer can be compared with test data taken during an experiment. Figure IV-26 shows the predicted probability of error, as a function of the

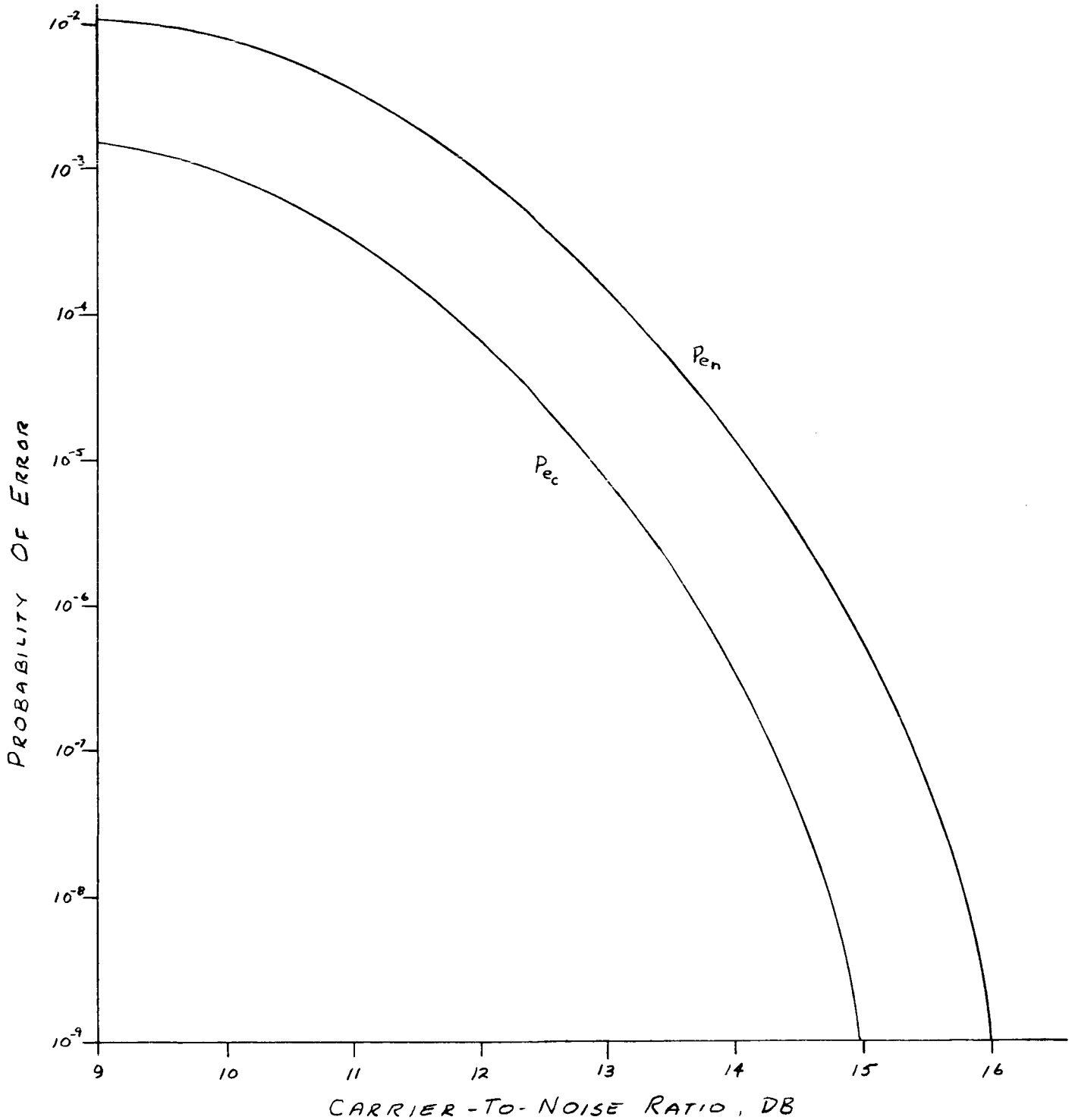

FIGURE IV-24. Probability of Error in Binary FSK System: P_{e_n} = Probability of Error for a Non-Coherent FSK System: P_{c_c} = probability of error for a Coherent FSK system.[52]

carrier to noise ratio, which should be measured as part of any FM test. Although these results are independent of the modulation index, it should be remembered that they only hold when the system is above threshold.

A way of measuring the carrier to noise ratio, and prediction of it as a function of the received signal level, was presented in part C of the section.

6. Test Configuration for PPM System

If we assume that a PPM laser communicator has been designed to accept digital data at the transmitter and to deliver digital data from the receiver, the test configuration shown in parts F and G can be used to measure error rate for various transmission speeds and at various signal powers. Even the optical monitors (part C) can be used, provided the duration of a pulse and the duration of a frame are known.

7. Data Reduction for a PPM System

Let T_1 = length of a pulse

T_2 = length of a frame.

Then the signal power/decision is $\frac{T_2}{T_1}$ S, where S is the signal power as measured by a monitor. The noise power per decision is simply N, where N is the noise power as measured on a monitor.

Given these two quantities, and P_e as measured during a run, one can plot the average probability of error as a function of the noise power and signal power per decision. This can then be compared with theoretical predictions, as generated during computer runs.

It is of interest, if possible, to see how P_e varies with the alphabet level. It is recommended that tests be made at the same signal energy/decision and noise energy/decision but at varying alphabet levels. These can then be

compared with predictions of performance generated on the computer.

Section V

COMPUTER MODEL USED TO CALCULATE POWER REQUIREMENTS FOR DEEP SPACE OPTICAL COMMUNICATIONS

A. Statement of the Task

The purpose of this task was to generate a FØRTRAN IV computer program to perform calculations of the power requirements for deep space optical communications. A sample set of output data for an eleven mile earth surface link was to be generated, complete with a set of desired test case parameters. This was to be supplied to NASA. The documentation for the program was to include a Fortran listing,* deck,* and instructions for exercising the program for any set of system parameters.

B. The Power Model

The mathematical model for the power model implemented for use on a UNIVAC 1108 computer is summarized on the flow chart shown on pages 10-7 through 10-10 of the Final Report[1] on NAS 9-3650. This flow chart is based on mathematical analyses of the performance of laser communication systems that were presented in the Second Interim Report[3] on that contract (pp 66 through 100). The complete flow chart for calculation of laser power requirements is shown in Flow Chart V-1.

It has been assumed, during development and testing of this program that all noise sources are unpolarized. If a polarized noise source is present in the background field view of a PCM/PL receiver,its noise power adds a bias in either the "zero" channel of the "one" channel. The effects of this type of noise source on system performance are not calculated by the Power Model.

Each subroutine used in the Power Model is described in Part C of this section. For most of the subroutines, flow charts of the computer coding are also presented. In addition, complete FØRTRAN IV listing for

* Only one listing and one deck are included. Additional listings can be obtained from the source deck.

FLOW CHART V-1. POWER MODEL

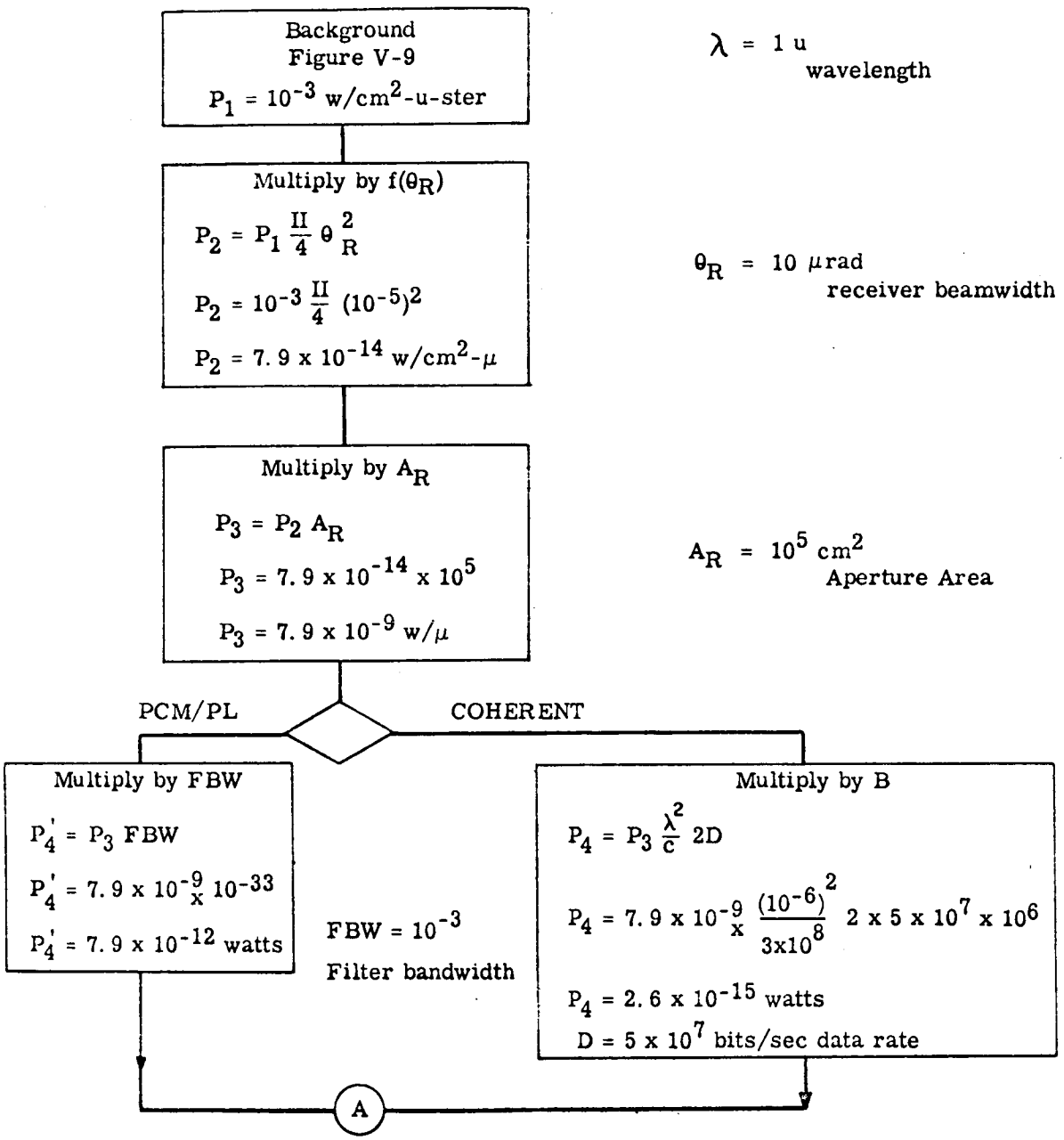

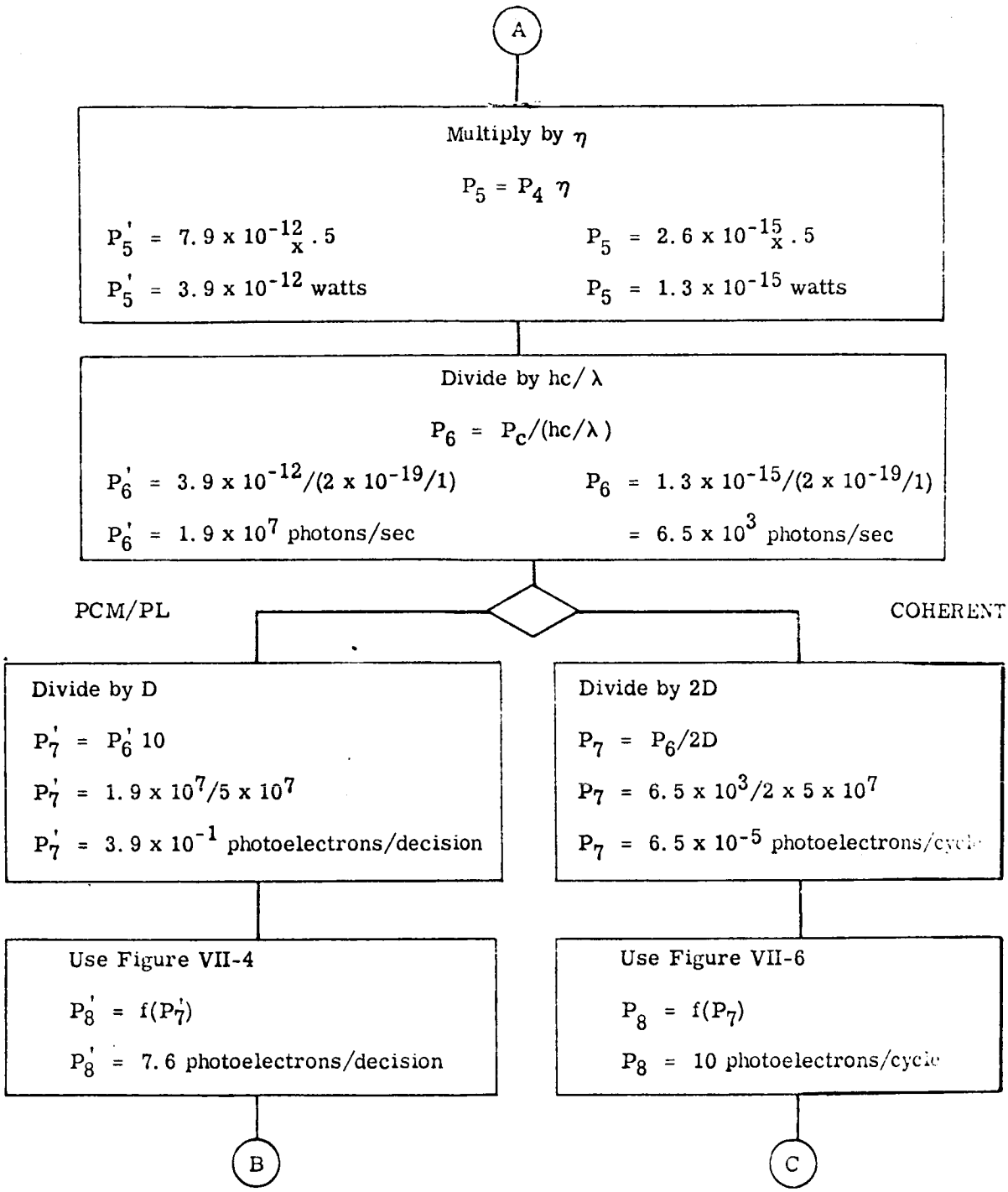
A
Multiply by η
$P_5 = P_4 \eta$
$P_5' = 7.9 \times 10^{-12}_{x} . 5$
$P_5' = 3.9 \times 10^{-12}$ watts
$P_5 = 2.6 \times 10^{-15}_{x} . 5$
$P_5 = 1.3 \times 10^{-15}$ watts
Divide by hc/λ
$P_6 = P_c/(hc/\lambda)$
$P_6' = 3.9 \times 10^{-12}/(2 \times 10^{-19}/1)$
$P_6' = 1.9 \times 10^{7}$ photons/sec
$P_6 = 1.3 \times 10^{-15}/(2 \times 10^{-19}/1)$
$= 6.5 \times 10^{3}$ photons/sec
PCM/PL
COHERENT
Divide by D
$P_7' = P_6' 10$
$P_7' = 1.9 \times 10^{7}/5 \times 10^{7}$
$P_7' = 3.9 \times 10^{-1}$ photoelectrons/decision
Divide by 2D
$P_7 = P_6/2D$
$P_7 = 6.5 \times 10^{3}/2 \times 5 \times 10^{7}$
$P_7 = 6.5 \times 10^{-5}$ photoelectrons/cycle
Use Figure VII-4
$P_8' = f(P_7')$
$P_8' = 7.6$ photoelectrons/decision
Use Figure VII-6
$P_8 = f(P_7)$
$P_8 = 10$ photoelectrons/cycle
B
C

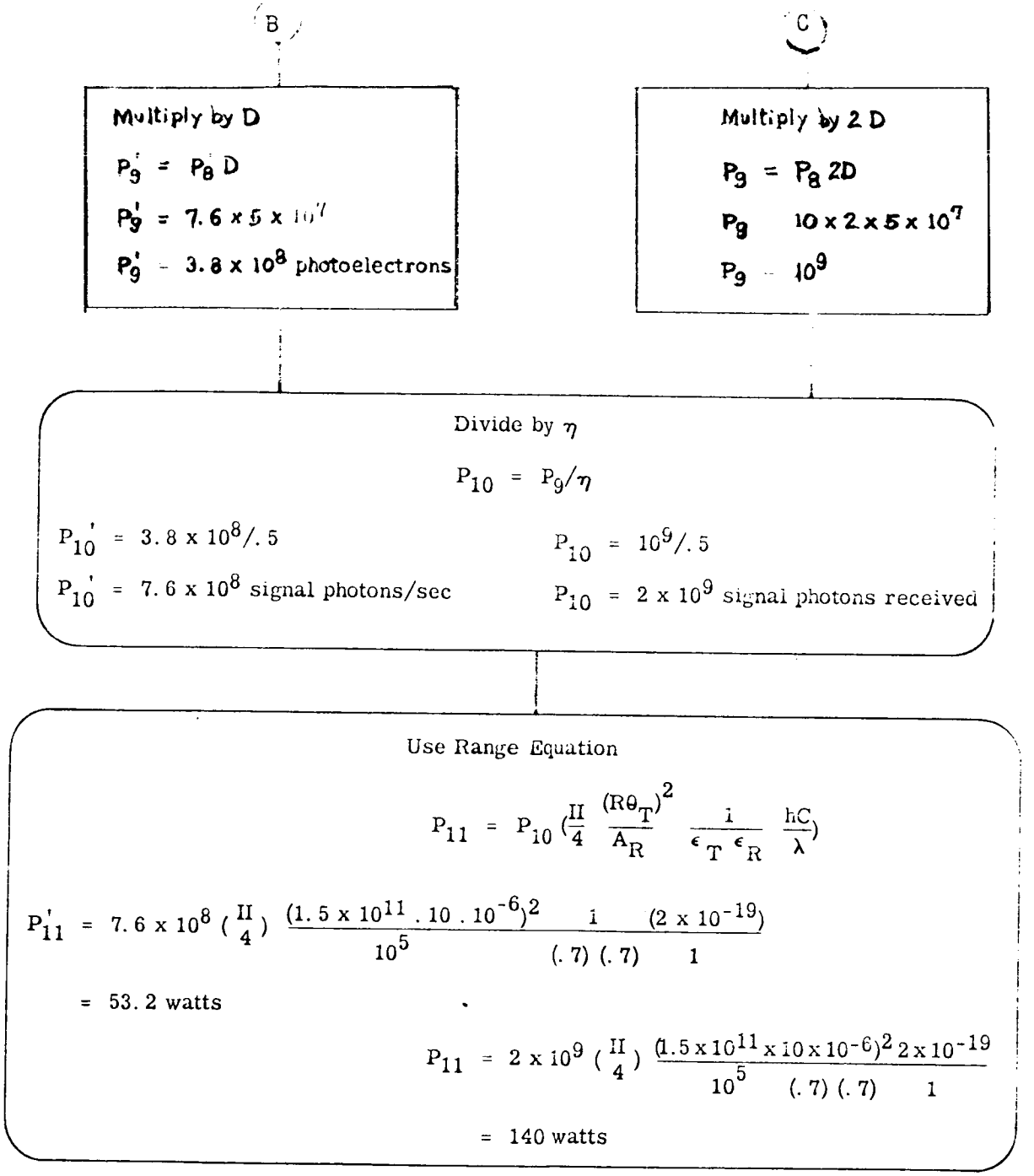

R = 1.5×10^8 km range

θ_T = 10 μrad transmit beamwidth

$E_T = E_R$ = .7 optics efficiency

FLOW CHART V-1. Calculation of Laser Power Requirements

these subroutines are contained in Appendix I of this report,* and a set of program cards are supplied as a separate item.*

Part D of this Section explains how input variables are entered into the program, and gives the units in which each variable should be stated. This part of the section also shows typical cards for inputing data to the program.

Part E of this section shows several computer runs for cases of interest during the design of the ranging system, at various percentage modulations for correlation with the results of the communication theory test program, and at various wavelengths to assist in the design of a laser communication system with deep space application.

It was found that test runs could not be made for the 11 mile test range. There is not enough data available on the transmission characteristics of such a path to allow mathematical modeling of a laser system operating through this length of atmosphere. As a result, the recommended communication theory test plan for this range are intended to determine the phase and amplitude characteristics of this 11 mile test range.

C. Computer Programs

This part of Section V contains flow charts and explanations for the operating subroutine of the Power Model. A listing of these subroutines, and of the Input and Output is contained in Appendix I.*

1. DPSP

DPSP is the entry point into the Power Model and serves primarily as an incrementing routine for the Receiver and Transmitter Beamwidth, the wavelength, and the data rate. Subroutine MAIN, which serves as the primary calling routine, is called from DPSP after variables are set or incremented.

Flow Chart V-2 outlines DPSP and is divided into two main parts. The first section, which extends to the bottom of the "DO 106" loop

* Only one copy of each of these items is supplied.

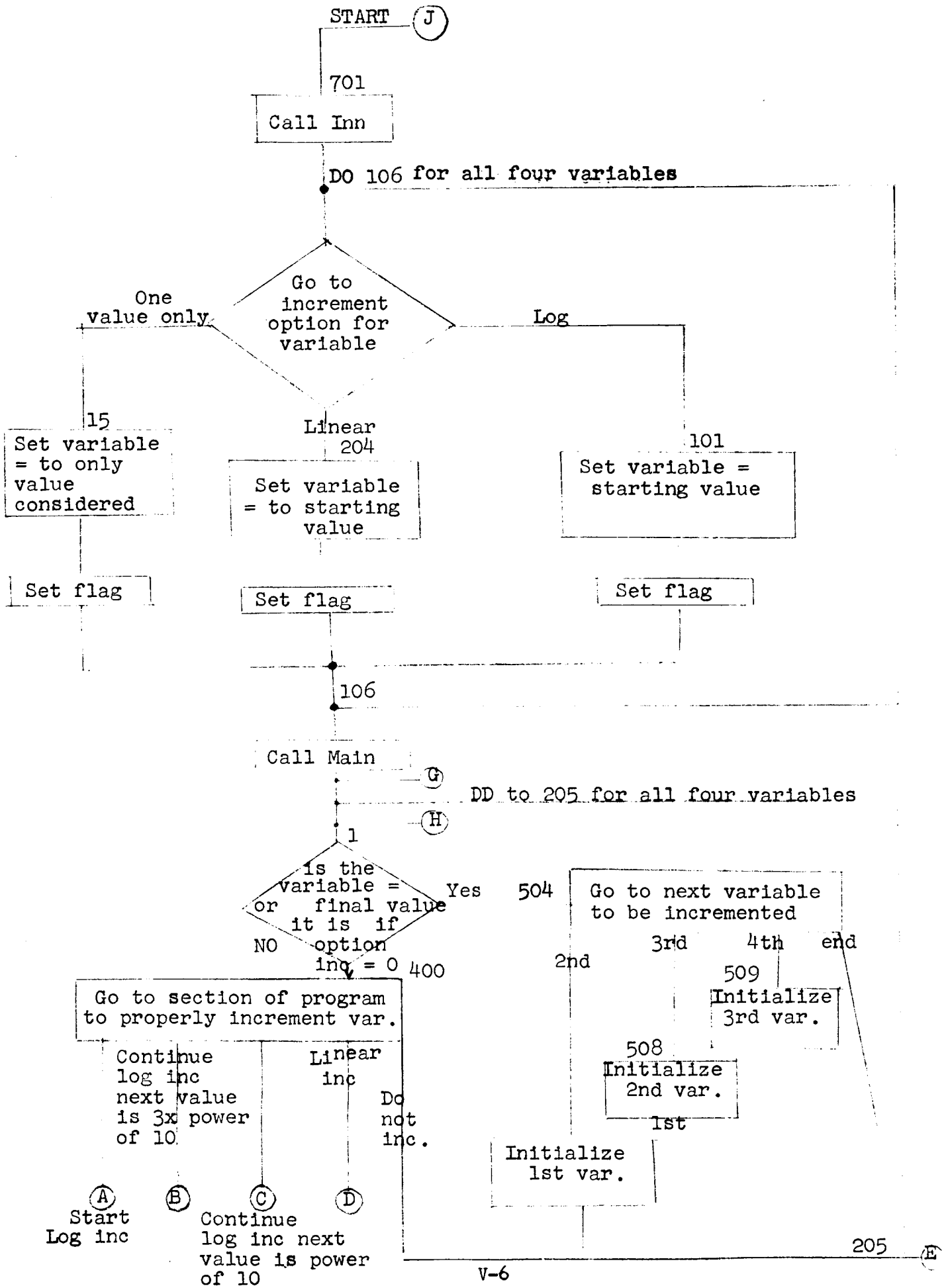
START
J
701
Call Inn
DO 106 for all four variables
Go to increment option for variable
One value only
Linear
Log
15
Set variable = to only value considered
204
Set variable = to starting value
101
Set variable = starting value
Set flag
Set flag
Set flag
106
Call Main
G
DD to 205 for all four variables
H
1
Is the variable = or final value it is if option inc = 0
Yes
NO
504
Go to next variable to be incremented
2nd
3rd
4th
end
509
Initialize 3rd var.
508
Initialize 2nd var.
1st
Initialize 1st var.
400
Go to section of program to properly increment var.
Continue log inc next value is 3x power of 10
Linear inc
Do not inc.
A
Start Log inc
B
C
Continue log inc next value is power of 10
D
205
E

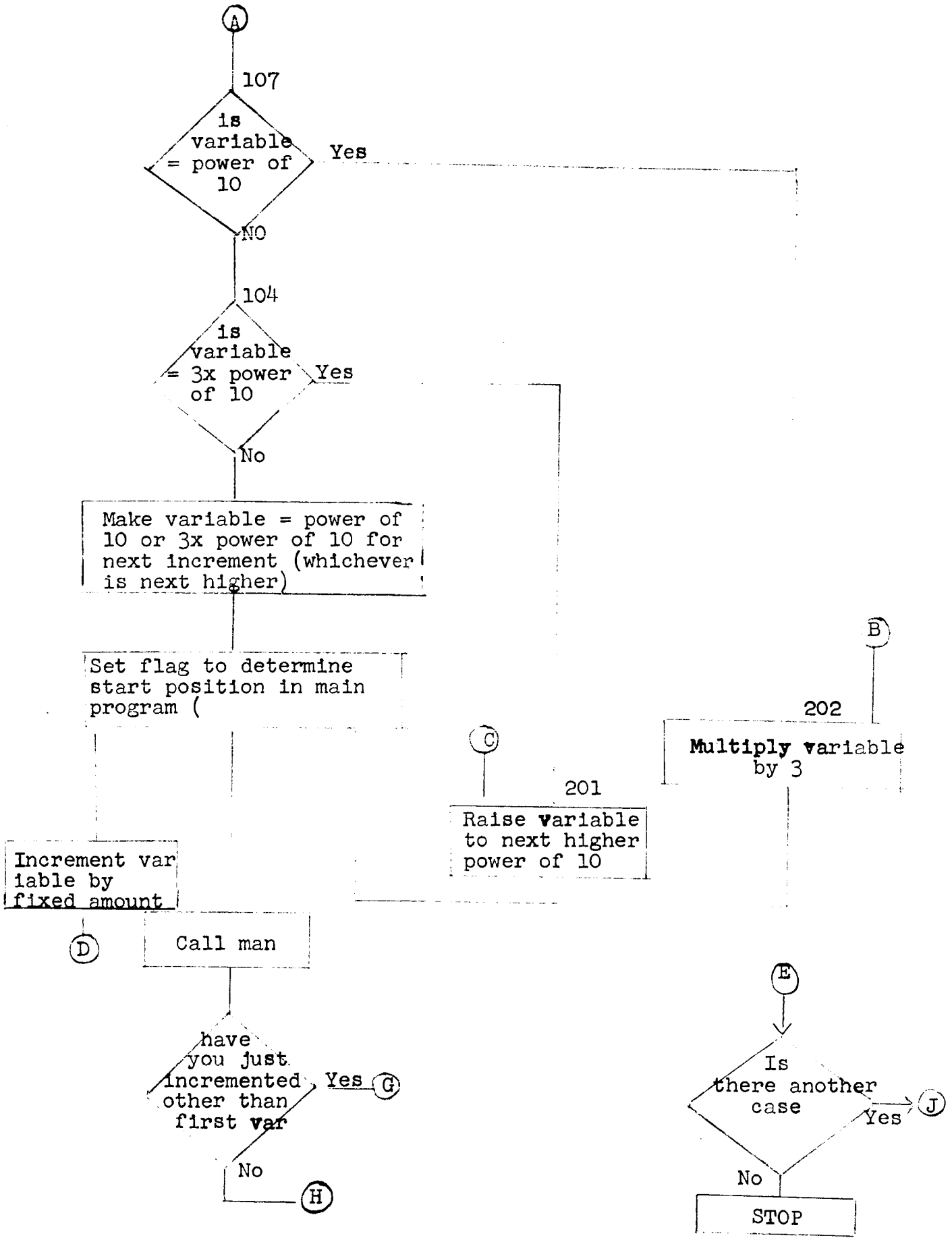

FLOW CHART V-2, DPSP

calls the input subroutine to start the run and then initializes the four incrementable variables. The remaining section, which begins after returning to DPSP and terminates at "call exit", tests the variables and increments them when instructed.

Two types of incrementing are possible in the program, exponential and linear. A single valued case, of course, is also possible. The exponential option starts at the starting value specified by the input and systematically increases it to powers of ten and 3 times powers of ten until the stopping value is reached (introduced by input). An example of this option is below:

Starting value 1
Stopping value 100 } input

1, 3, 10, 30, 100 - values used.

If other than a power of 10 or 3 times a power of 10 is inserted as the starting value the first increment will raise the variable to the next higher 1×10^x or 3×10^x and increment normally.

Starting value 7
Stopping value 300

7, 10, 30, 100, 300 - values used.

The variable used for computational purposes in DPSP is D(1,2,3, and 4). This is related to the working variables for beamwidth, wavelength, and data rate in subroutine MAIN.

D(1) = Transmit Beamwidth
D(2) = Data Rate
D(3) = Receive Beamwidth
D(4) = Wavelength

The variables are arranged in this order to allow the least amount of calculations to be made while incrementing.

Since the variables it is possible to increment are entered on separate cards it is possible to use a separate option for each, if desired. When all of the incrementing has been accomplished for a given case the program is either terminated or returns to INN for

more data cards.

The linear incrementing option increments the variable from the given starting value to the stopping value at a fixed rate.

Starting value = 1
Stopping value = 10
Increment = 2

1, 3, 5, 7, 9, 11 - values taken.

Note that the stopping value does not have to be a number the variable uses since the stopping test involves an equal to or greater than decision.

2. Subroutine MAIN

Subroutine main is the primary calling subroutine in the program. In this routine the basic equations of the power model, pages 10-7 through 10-9 of the final report[1], are solved. During the execution of the subroutine BKG, which finds the background noise, and PHOTON, which relates the signal photons/decision, noise photons/decision, and the bit error probability, are called. Subroutine OUT is called late in the subroutine to print the output for the case considered. A flow chart (gross) of MAIN is shown in flow chart V-3.

3. BKG

Subroutine BKG calculates the background noise from planets and stars within the beamwidth of the receiver and adds this to any input noise entered on the data cards (BK6N), using flow chart V-4.

Noise due to planets is calculated either from stored experimental curves or from grey-body curves approximating the reflected and self-emitted radiation from the planets. The experimental curves are entered as data in subroutine ALLUMF, whereas constants allowing use of grey-body equations are entered as data in this subroutine. The radius of the planets, effective temperatures, and C_1 (used in $W(\lambda,T) =$

$$\frac{C_1}{\lambda^5(e^{C_2/\lambda T}-1)} \quad (\frac{R}{D})^2$$

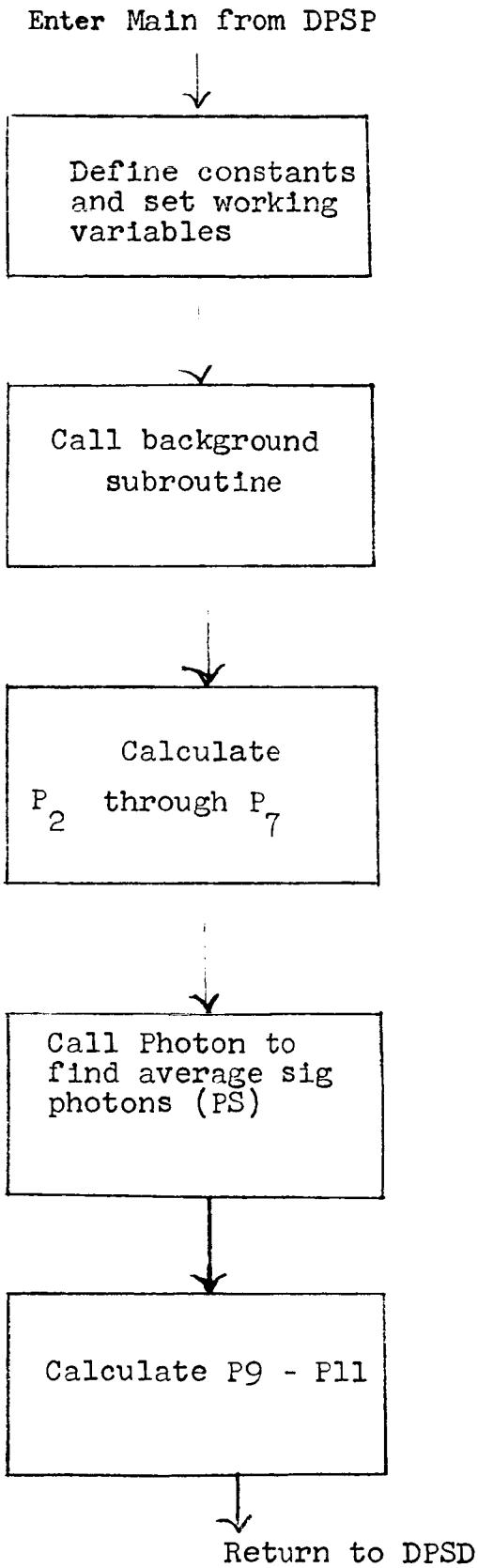

FLOW CHART V-3 MAIN

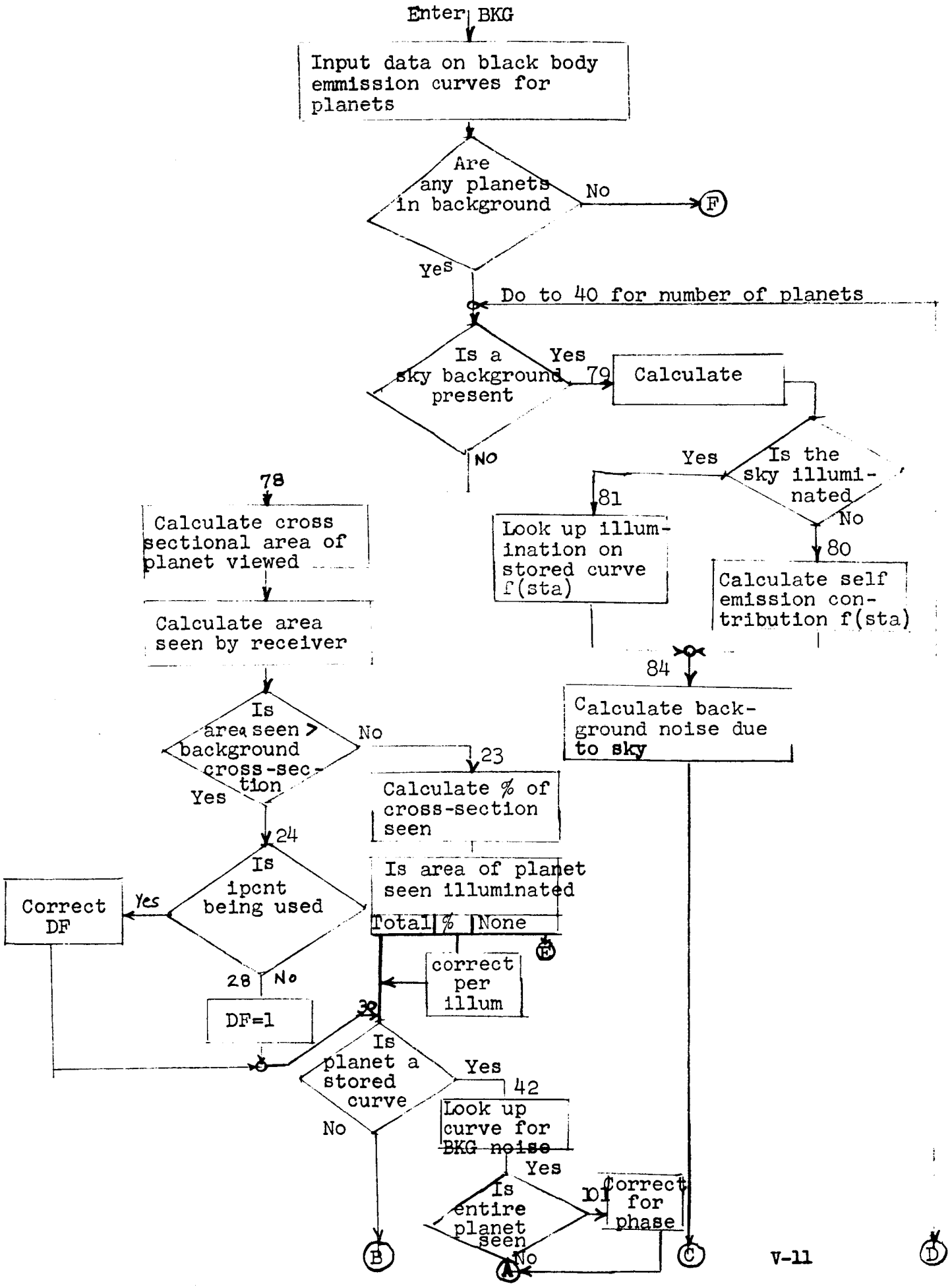
Enter BKG
Input data on black body emmission curves for planets
Are any planets in background
No
F
Yes
Do to 40 for number of planets
Is a sky background present
Yes
79
Calculate
NO
Is the sky illuminated
Yes
81
Look up illumination on stored curve f(sta)
No
80
Calculate self emission contribution f(sta)
78
Calculate cross sectional area of planet viewed
Calculate area seen by receiver
84
Calculate background noise due to sky
Is area seen > background cross-section
No
23
Calculate % of cross-section seen
Yes
24
Is area of planet seen illuminated
Total
%
None
Is ipcnt being used
Yes
Correct DF
28
No
DF=1
correct per illum
30
Is planet a stored curve
Yes
42
Look up curve for BKG noise
No
Yes
Is entire planet seen
No
Correct for phase
B
C
D
A

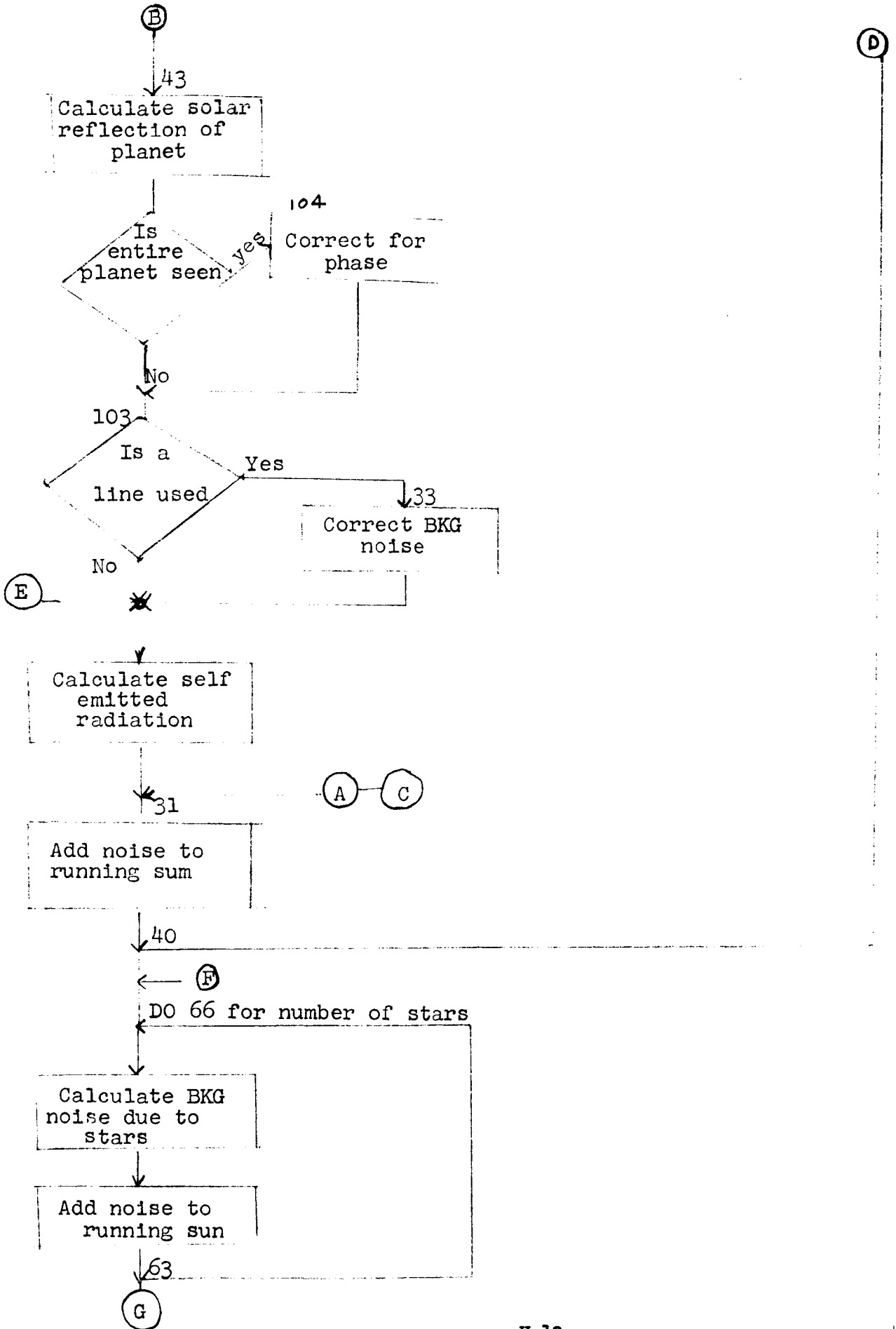
B
43
Calculate solar reflection of planet
104
Is entire planet seen
yes
Correct for phase
No
103
Is a line used
Yes
33
Correct BKG noise
No
E
Calculate self emitted radiation
A
C
31
Add noise to running sum
40
D
F
DO 66 for number of stars
Calculate BKG noise due to stars
Add noise to running sun
63
G

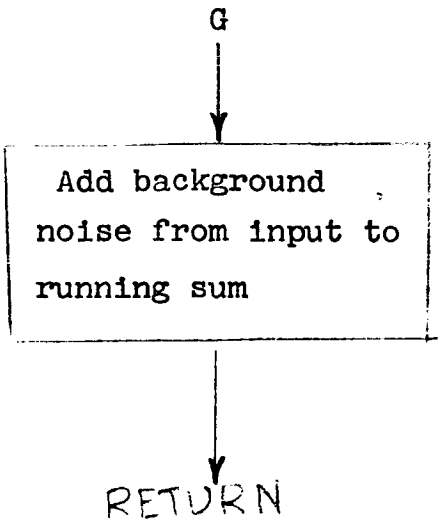

FLOW CHART V-4 BKG

are examples of these constants.

The first major do-loop in the subroutine considers each planet in the background sequentially. Radiation from each planet in the solar system can be calculated using grey-body equations. The Earth, sky, and moon also have stored experimental curves. The planet number entered as input determines whether grey body or experimental curves are used (see input explanation for further details).

The background planet is first tested to determine if it is a sky background for an earth receiver. It is is, a determination is made as to whether it is daylight or not. If it is lighted the stored experimental curve is called and the result multiplied by the solid of the receiver. If it is dark, the grey-body curve is used. (Note: parameters for grey body curve were obtained from dotted plot inside experimental curve in final report[1]).

If a sky background is not being considered the cross-section of the planet is calculated and this is compared with the area the receiver beamwidth allows to be seen. If the receiver can view the entire planet a test is made to determine if IPCNT is being used. IPCNT allows for off-center viewing of the planet and represents the percent of the planet which cannot be seen. (see below)

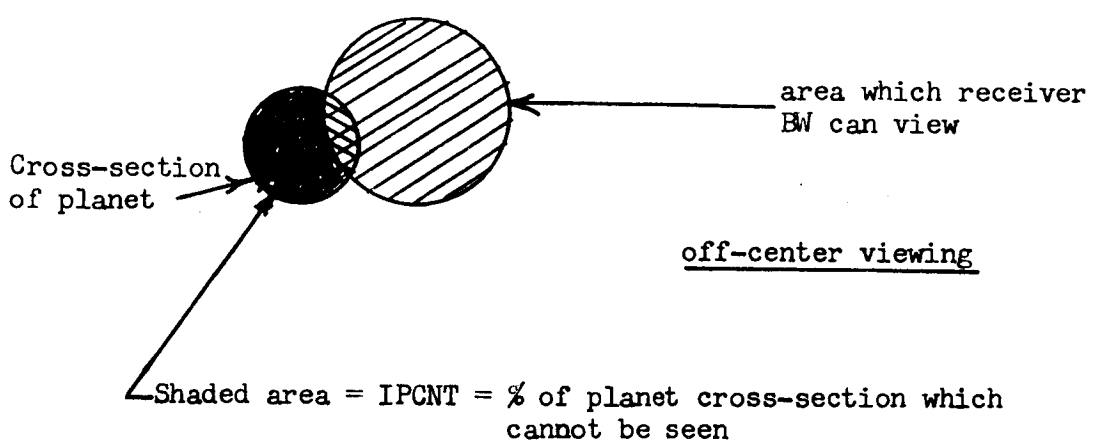

It must be remembered that if the receiver BW is not large enough to allow the entire planet to be seen IPCNT will be bypassed (see flow chart).

If the BW of the receiver does not allow the entire planet cross-section to be seen a variable, DF, is set which represents the percent of cross-sectional area which can be seen. A test is then made to determine if the area of the planet seen is illuminated. If it is not illuminated the reflected radiation from the planet is neglected. If it is partially illuminated DF is corrected to reflect this. The input variable ILLUM determines the illumination of the area seen in this case (see below).

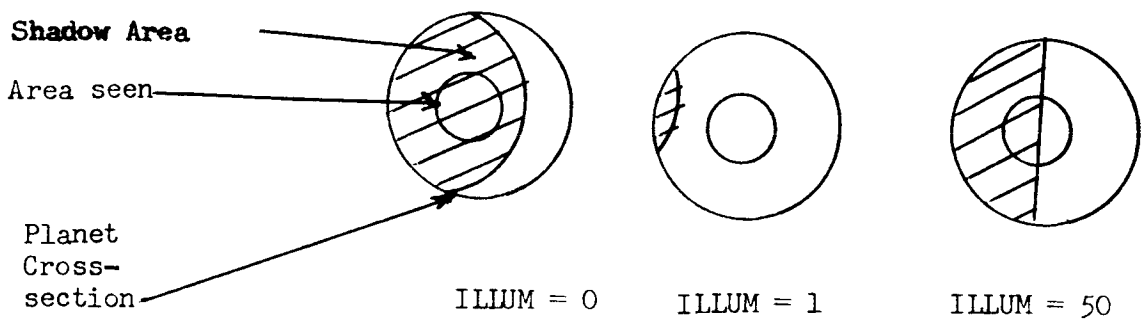

ILLUM is used only if the area seen is smaller than the planet cross-section -- otherwise it is bypassed (see flow chart).

The background noise from the albedo of the planet is calculated next using either stored curves or grey-body equations. If the entire planet is seen, a phase correction is then made based on the phase of the planet.

Finally background noise due to the self-emission of the planets is calculated for those cases using grey body curves or for areas viewed which are not illuminated.

The second major do loop in the subroutine accounts for stars in the background. Since they are considered as point sources, the beamwidth

of the receiver is not a factor. The noise due to the stars is calculated using the visual magnitude of the star and its temperature.

A running sum of the background noise is maintained throughout the subroutine and Fraunhofer lines are considered, when desired, in the calculation.

4. Subroutine EXTRAP

Subroutine EXTRAP is used when it is desired to calculate the average signal level for noise levels in the gaussian region. Since Poisson statistics, upon which the central equations are based, are reasonably calculated only for relatively small numbers of photons, it is necessary to extrapolate these into the gaussian region.

When an average noise is arrived at that would place the signal in the gaussian region, the signal level required is automatically calculated for a noise level of 25 which is near the upper limit of the computer's capability without scaling. When the signal required for 25 noise photons/decision has been calculated in PPMPCM, EXTRAP then extrapolates this to the desired value using the procedure outlined in the Second Interim Report[3] of the initial study.

In this routine an extrapolation constant is first arrived at and this is incorporated into a calling program for NEWTON by which the desired value of the signal is found.

5. Subroutine PPMPCM

Subroutine PPMPCM is a subroutine used to find the average number of signal photons required for PPM and PCM/PL, given the error rate and the character error probability. This routine expresses the equation for the average number of signal photons in terms of itself and uses subroutine NEUTON, a variation of Newton's iteration technique, to find the value of signal photons satisfying the equation. Variables used in Newton are first set and a value of the average signal is approximated

to begin the iteration process. Using the central probability equation for PPM or PCM/PL, a value of the average signal is then obtained using the stored constants. When polarization errors exist in PCM/PL the average signal and noise are corrected, although the constants, which are a function of the average noise, are not being changed in this routine. If the corrected noise differs from the starting noise by more than 2% the average signal arrived at will be significantly in error and the coding program is returned to for determination of corrected constants followed by a recalling of PPM/PCM.

If more than 50 iterations of Newton are required it is assumed that it will not converge and exit is called. This is a safety feature and should never be the case.

If extrapolation is required because of the signal lying in the gaussian region subroutine EXTRAP is called before returning to the main program.

The coding for PPMPCM is shown in Flow Chart V-5.

6. Subroutine KONST

Subroutine KONST is used to determine the value of the inner portions of the central probabilities equations. Since a considerable amount of mathematics is involved in obtaining these values, and since they don't change as the signal is changed, it is advantageous to calculate these once and store them for future use. Once these values have been calculated there is no need to calculate them again, unless the value of AVN or the alphabet level is changed (AVN is changed when a polarization error occurs in PCM).

7. Function MAXF

Function MAXF is used to determine the maximum number of terms that have to be considered in the central probablistic equations. The criteria for determining KMAX was set forth in the second interim report of the initial study[3] (or in Entwistle's paper).

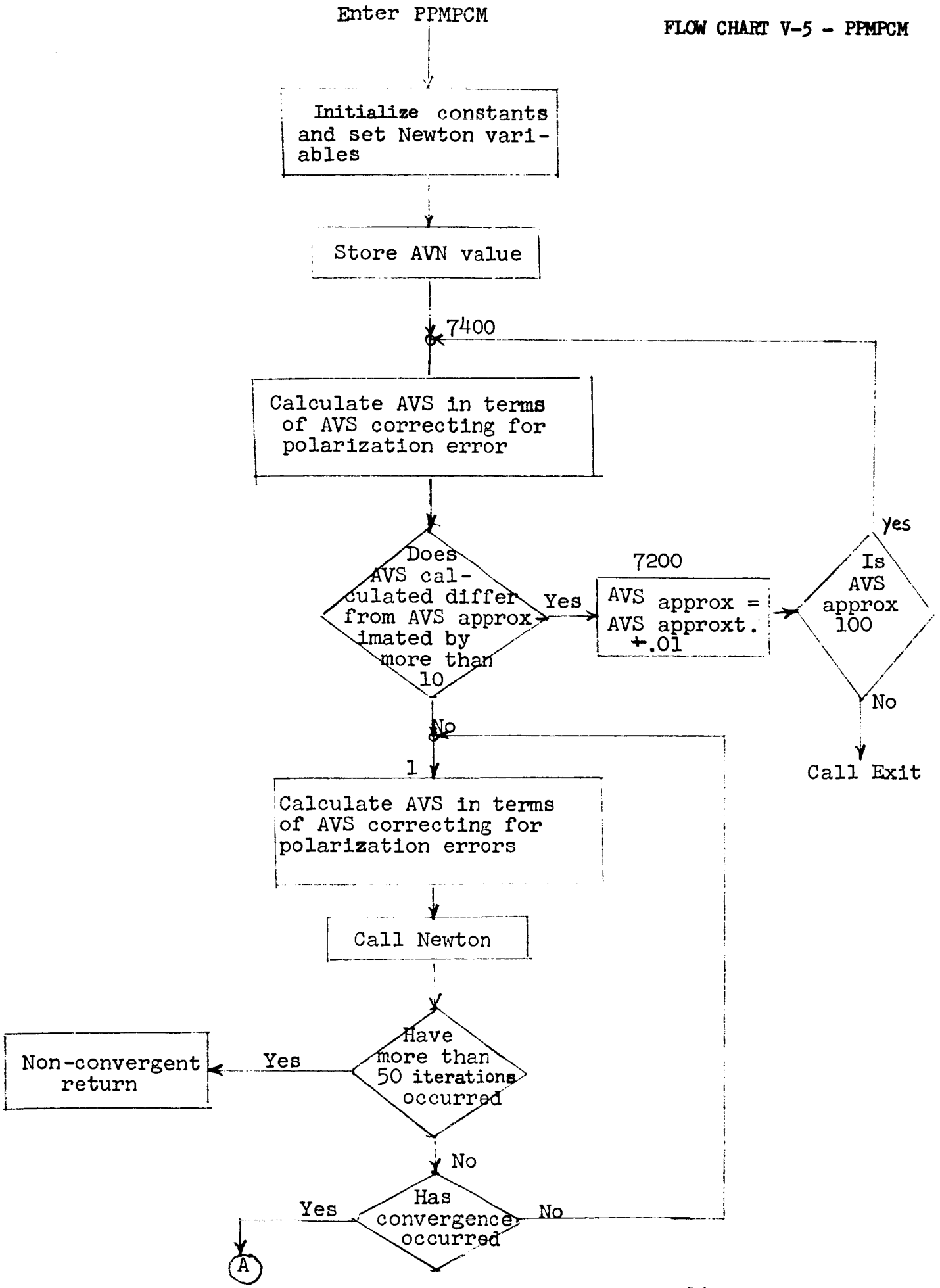
Enter PPMPCM
Initialize constants and set Newton variables
Store AVN value
7400
Calculate AVS in terms of AVS correcting for polarization error
Does AVS calculated differ from AVS approximated by more than 10
Yes
7200
AVS approx = AVS approxt. +.01
Is AVS approx 100
yes
No
Call Exit
No
1
Calculate AVS in terms of AVS correcting for polarization errors
Call Newton
Have more than 50 iterations occurred
Yes
Non-convergent return
No
Has convergence occurred
Yes
No
A

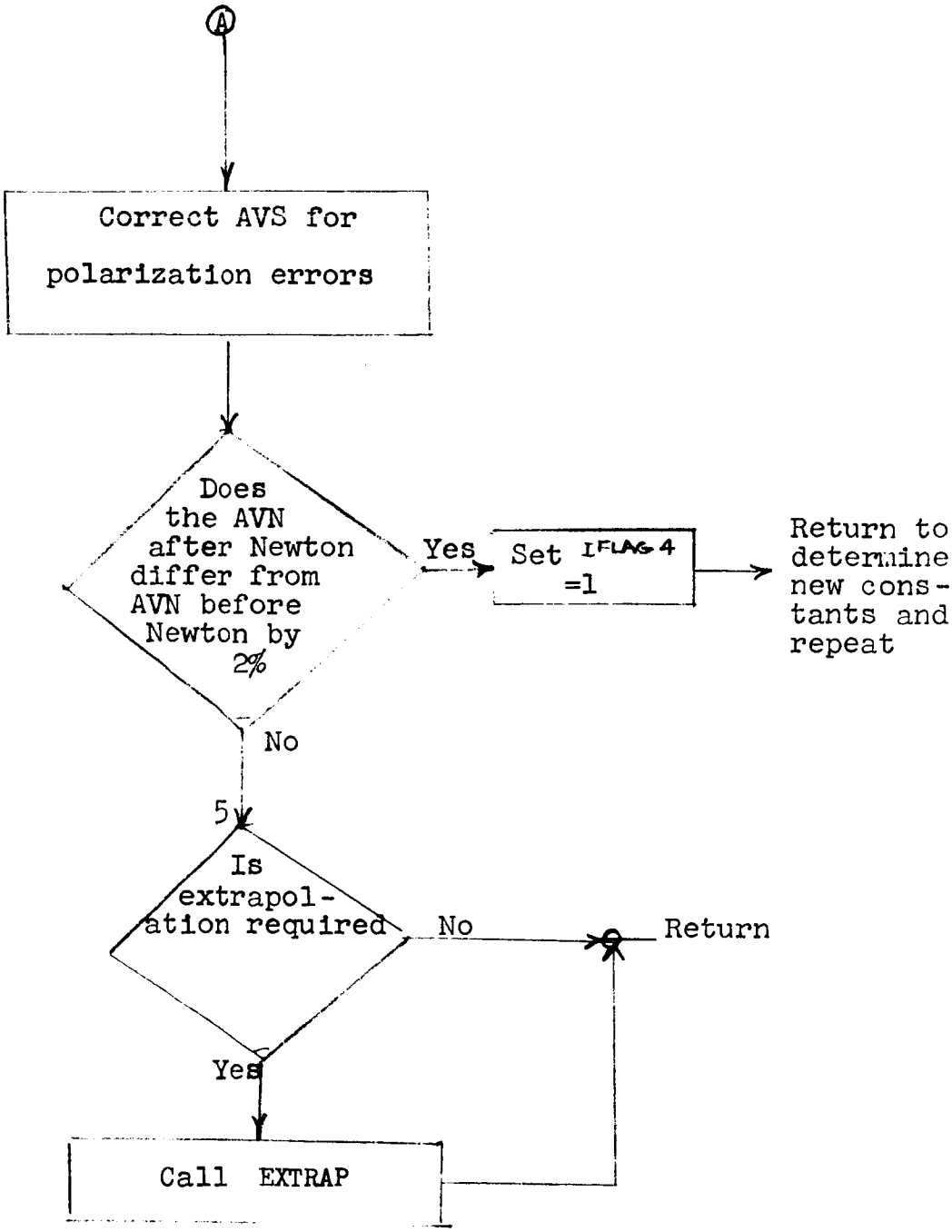

FLOW CHART V-5 PPMPCM

Upon entering the function the average signal, AVS, must be approximated. This is done by approximating the AVS/AVN curves with a logarithmic relationship for AVN >15 and a constant value for AVN ≤ 15. A value of AVS = 15 is assumed for AVN ≤ 15 since this is higher than the asymptotic value of AVS for any practical case and therefore will give a safe value for KMAX. The logarithmic relationship chosen for the remainder of the range of AVN is such that it will also approximate the AVS slightly higher than its actual value for the same reason.

Using the approximation for AVS, the trial and error solution outlined in the interim report[3] is next obtained. When a value for KMAX is reached, the do loop is terminated (whether or not it has reached the 1500 limit) and the calling subroutine is returned to.

The coding for MAXF is shown in Flow Chart V-6.

8. BICOEF

Subroutine BICOEF determines the binominal coefficients necessary in the solution of the central probabilistic equations for PPM and PCM/PL. Since a symmetry exists in the binominal coefficients used, only half of them need actually be computed. The values found are stored and called later in KONST. If the alphabet level has not changed since the last case run there is no need to compute the value of the coefficients again and subroutine PHOTON is returned to immediately.

9. PHOTON

Subroutine PHOTON is used as a calling routine for the determination of the average signal required/decision (cycle) with a given noise level. If coherent detection is employed, the actual signal required is determined. For PCM/PL and PPM, constants necessary for the solution of the probabalistic equation are found by calling BICOEF and KONST and the equations themselves are solved by calling PPMPCM. Function MAXF is called to determine the maximum number of terms that the Poisson probability equation must be carried to to get an error rate as small as

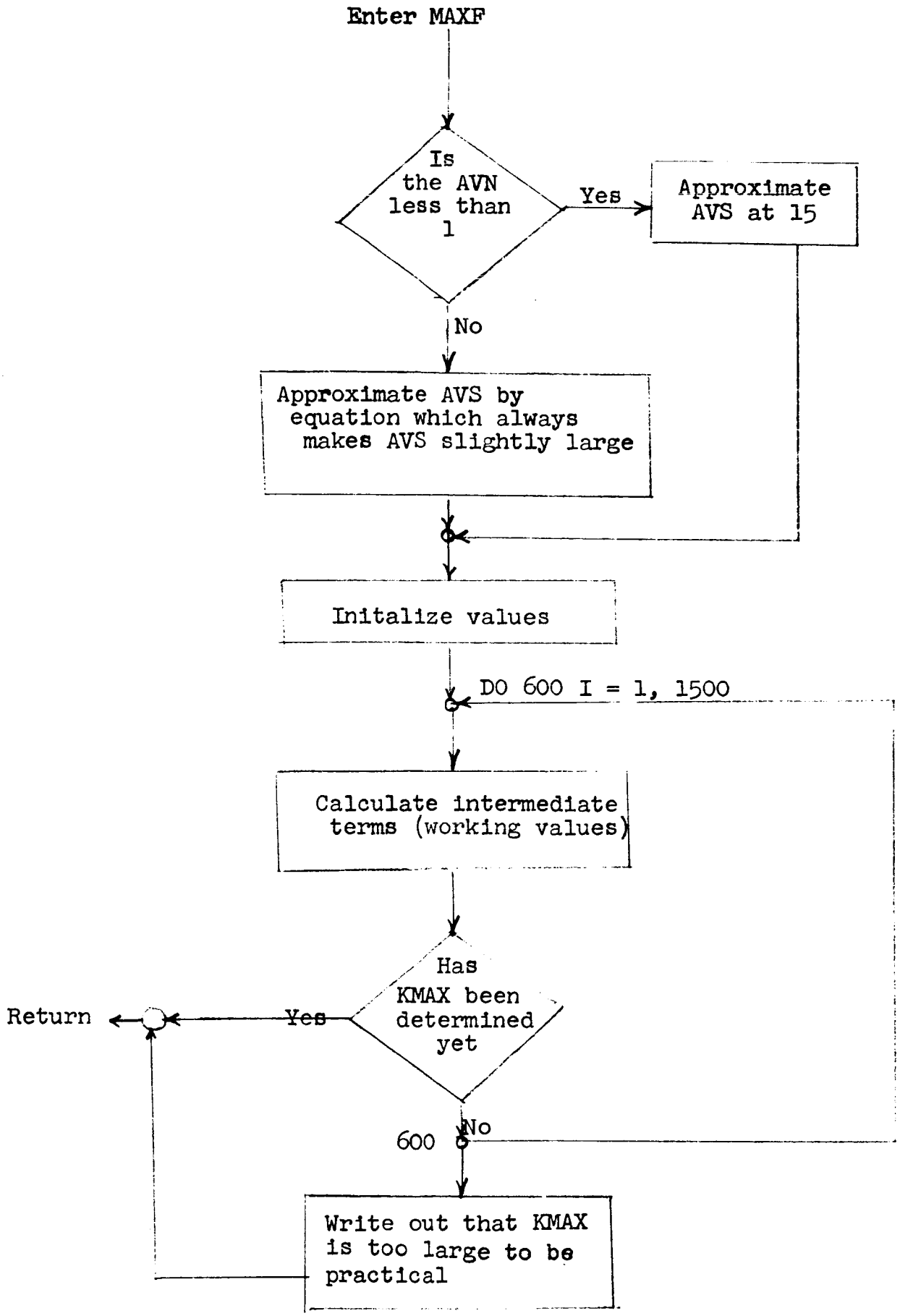

FLOW CHART V-6. MAXF

necessary. Redundant calculation checks to see if KMAX must be called for the case under consideration.

Computer coding for PHOTON is shown is Flow Chart V-7.

10. ALLUMF

Function ALLUMF is used to interpolate the stored curves representing background noise from the earth, sky, and moon. Data points for these curves are entered at the beginning of the function and an order of interpolation = 1 is set (linear). Since extrapolation of these curves is invalid, an indication is printed in the output when extrapolation is used.

D. Data Cards and Input Quantities

Input variables are entered into the computer program using subroutine INN. There is no fixed number of data cards required for each case under consideration since the complexity of the case and previous cases in the same computer run will alter the number needed. The minimum number of data cards needed is two, while the maximum has no set limit. All input parameters must be entered for the first case in a run, whereas for subsequent cases only changed cards need be entered.

An explanation of the input variables and the use of subroutine INN follows. The field of the cards and the variables contained are shown in Figures V-1 through V-5. The E's and I's shown indicate the number expected (exponential or integer). It should be remembered that f type (fixed) numbers may be used with an E format. The number in the upper-right hand corner of the cards will be referred to as the card number throughout this discussion.

Card number one must be present in all cases run. The purpose of this card is to indicate if other cases follow this one in the run and which data cards follow for the case being considered. (A case is defined here as the calculations resulting from one group of data cards. More than

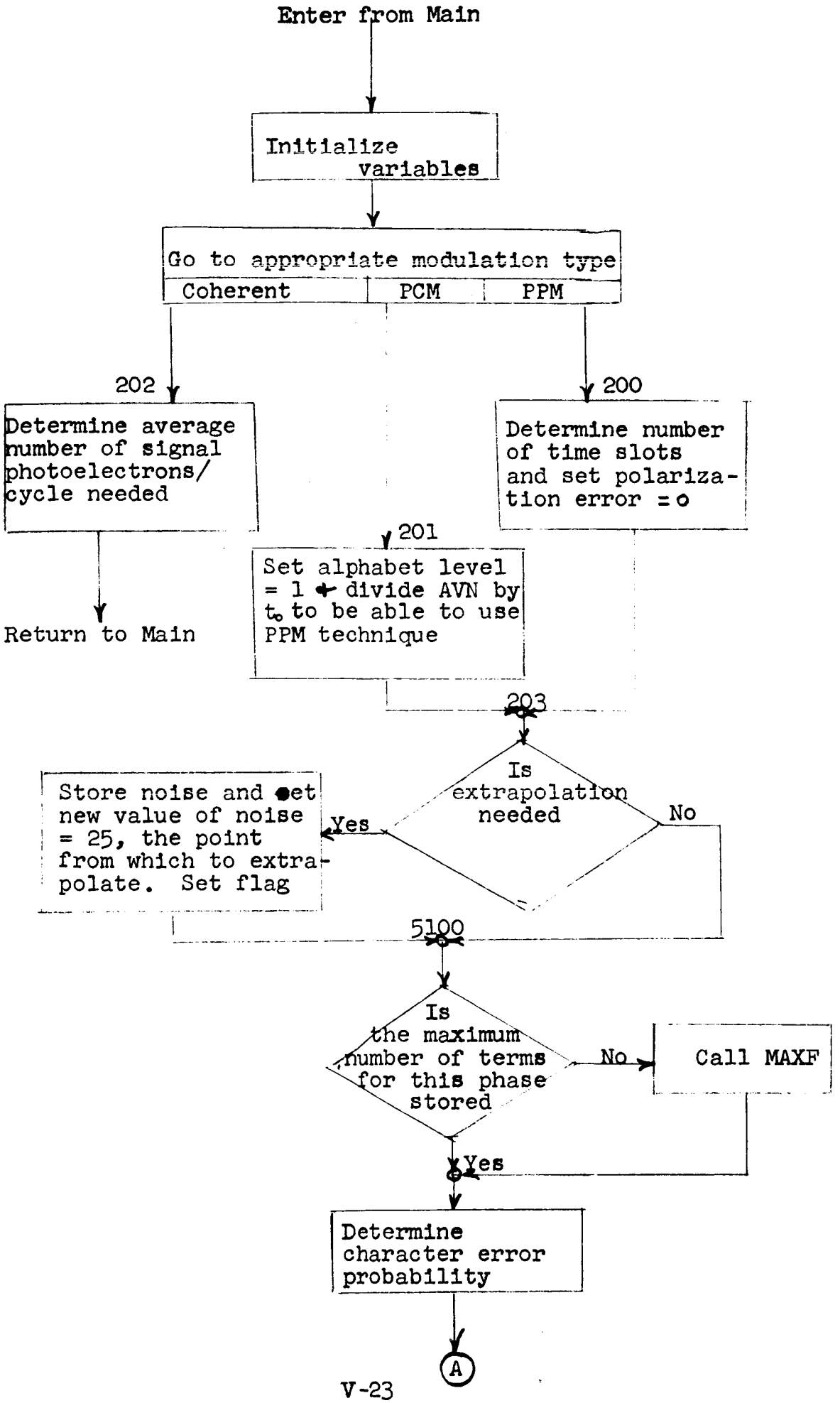
Enter from Main
Initialize variables
Go to appropriate modulation type
Coherent
PCM
PPM
202
Determine average number of signal photoelectrons/ cycle needed
Return to Main
200
Determine number of time slots and set polarization error = 0
201
Set alphabet level = 1 ÷ divide AVN by t_o to be able to use PPM technique
203
Is extrapolation needed
Yes
No
Store noise and set new value of noise = 25, the point from which to extrapolate. Set flag
5100
Is the maximum number of terms for this phase stored
No
Call MAXF
Yes
Determine character error probability
A

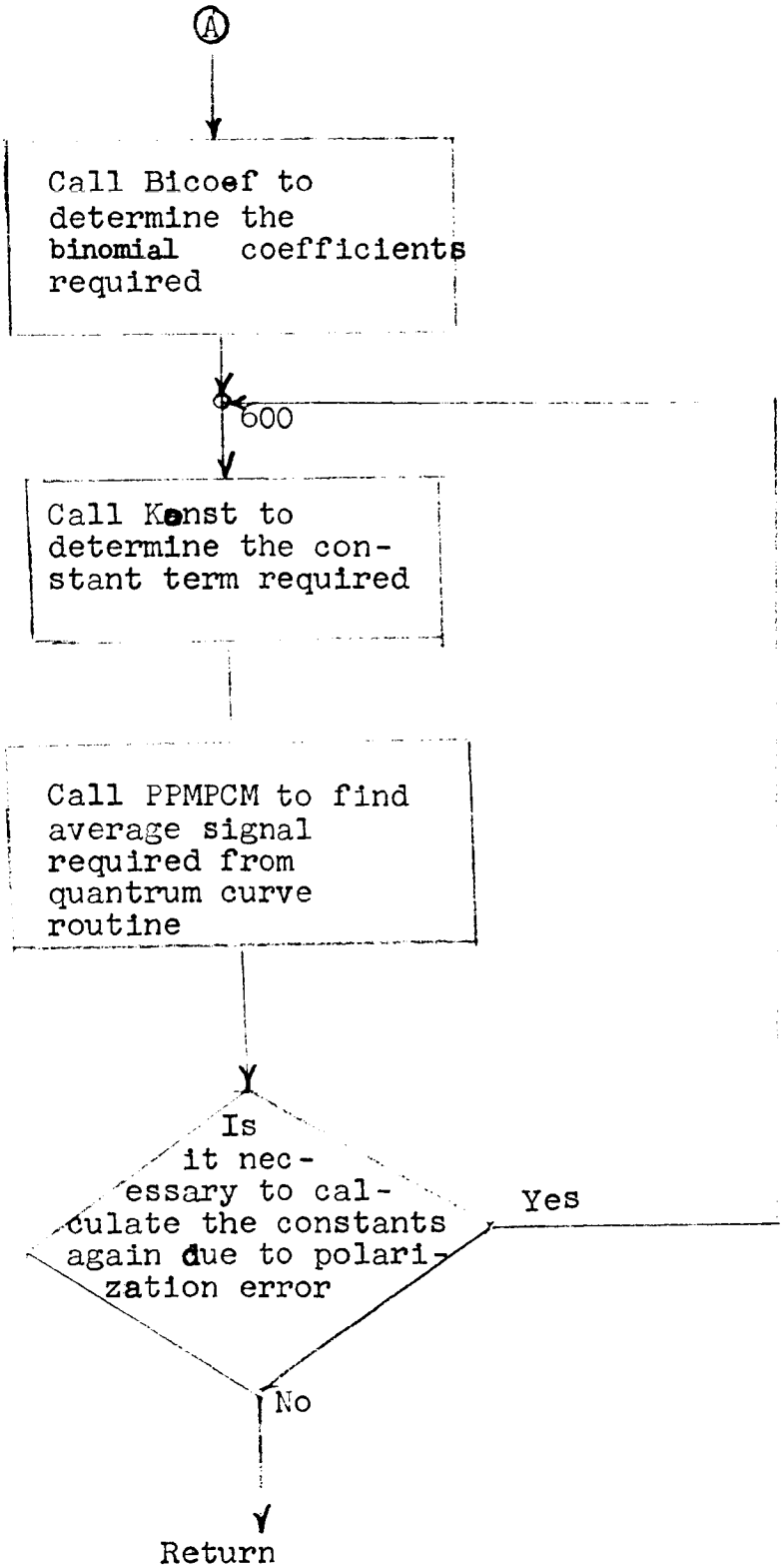

FLOW CHART V-7 PHOTON

1

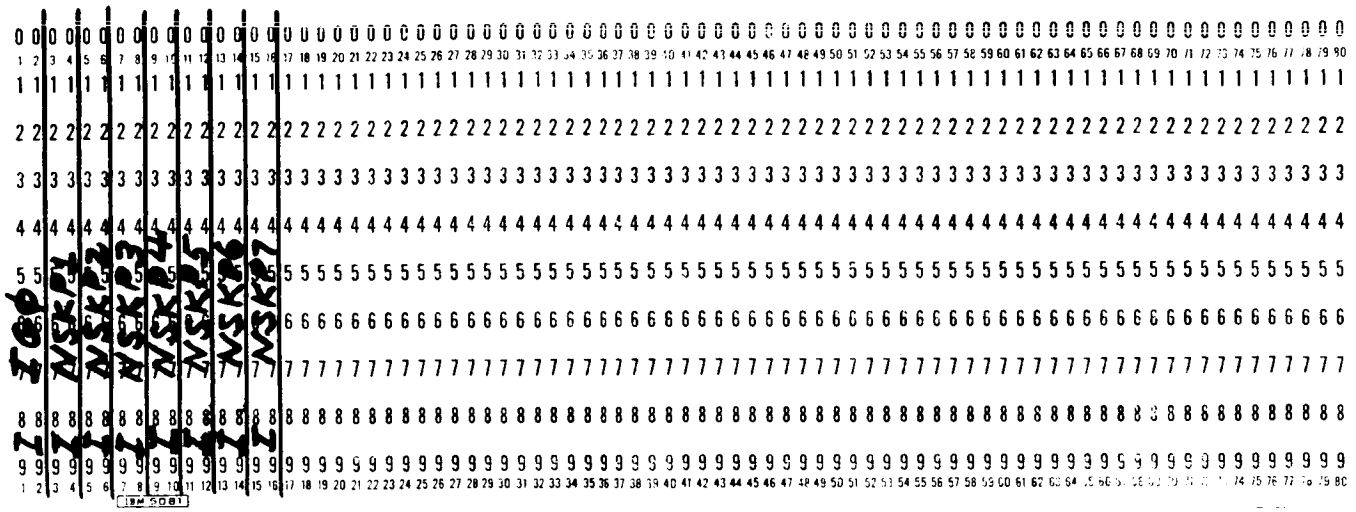

2

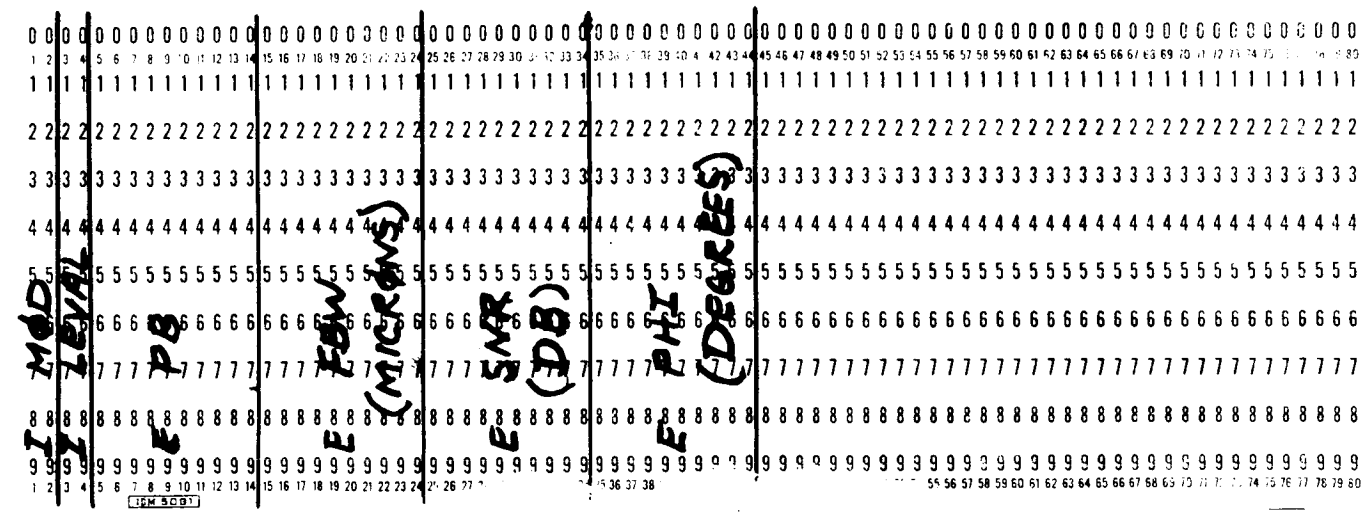

FIGURE V-1. Data Cards 1 and 2

3

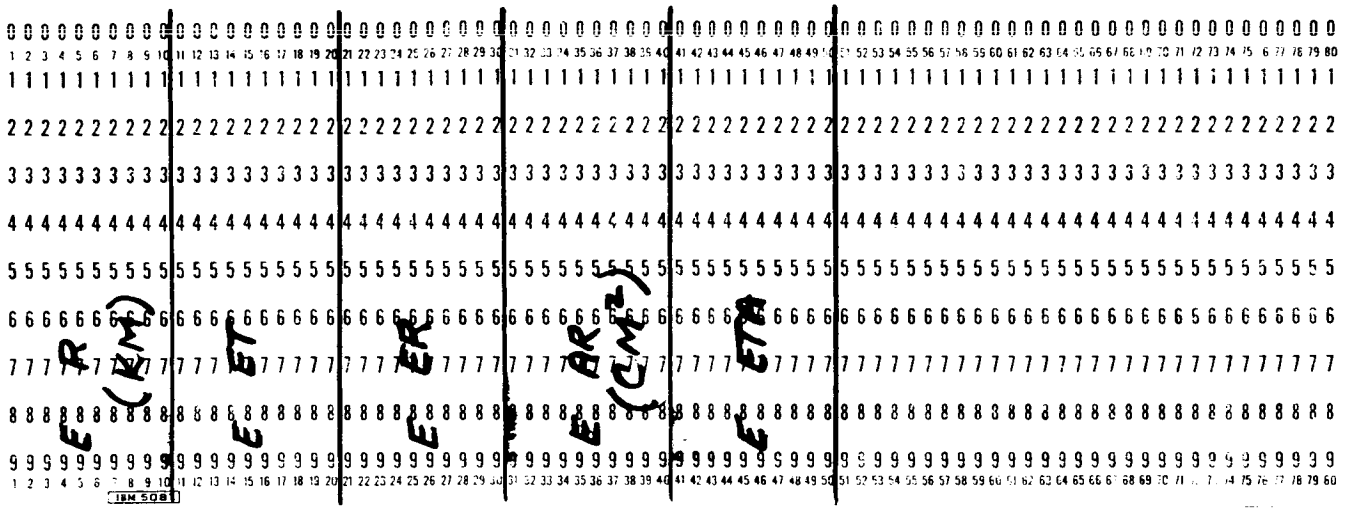

4

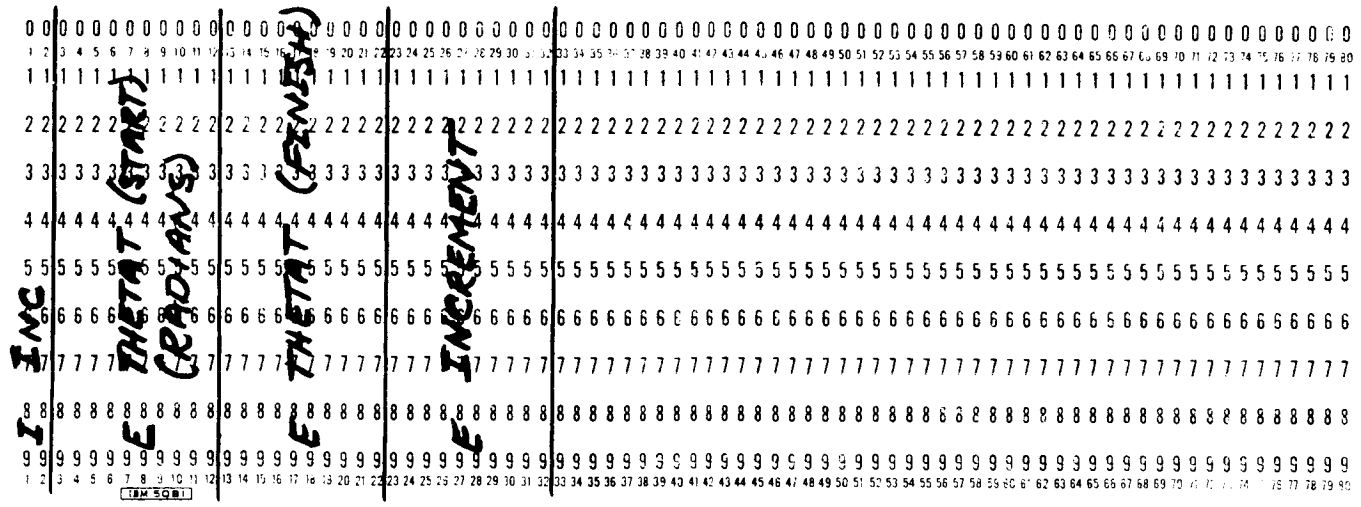

FIGURE V-2. Data Cards 3 and 4.

5

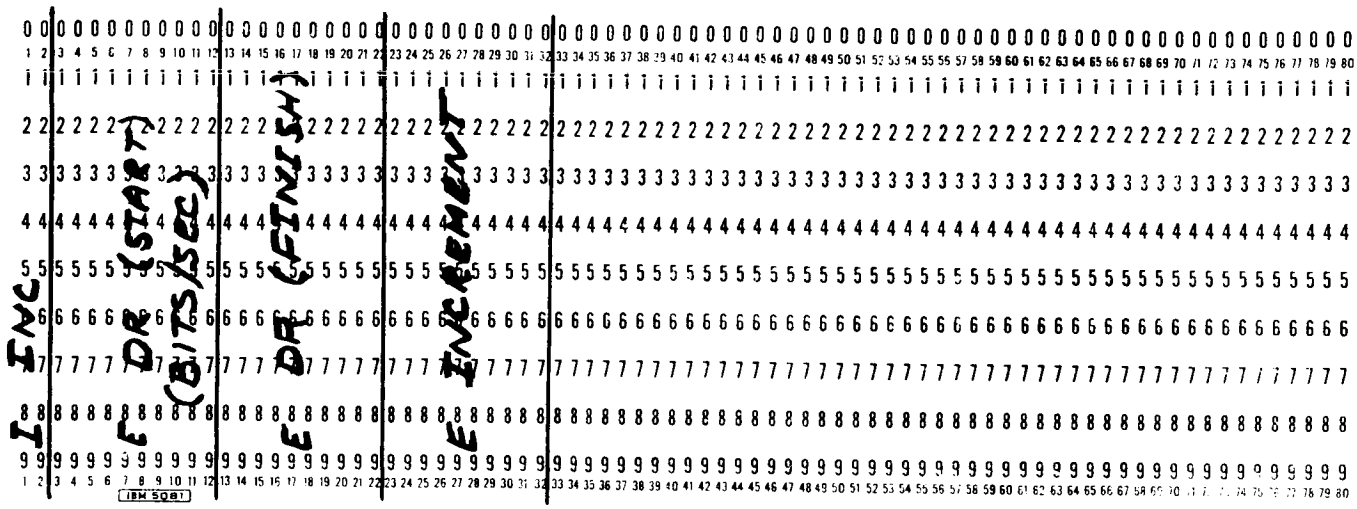

6

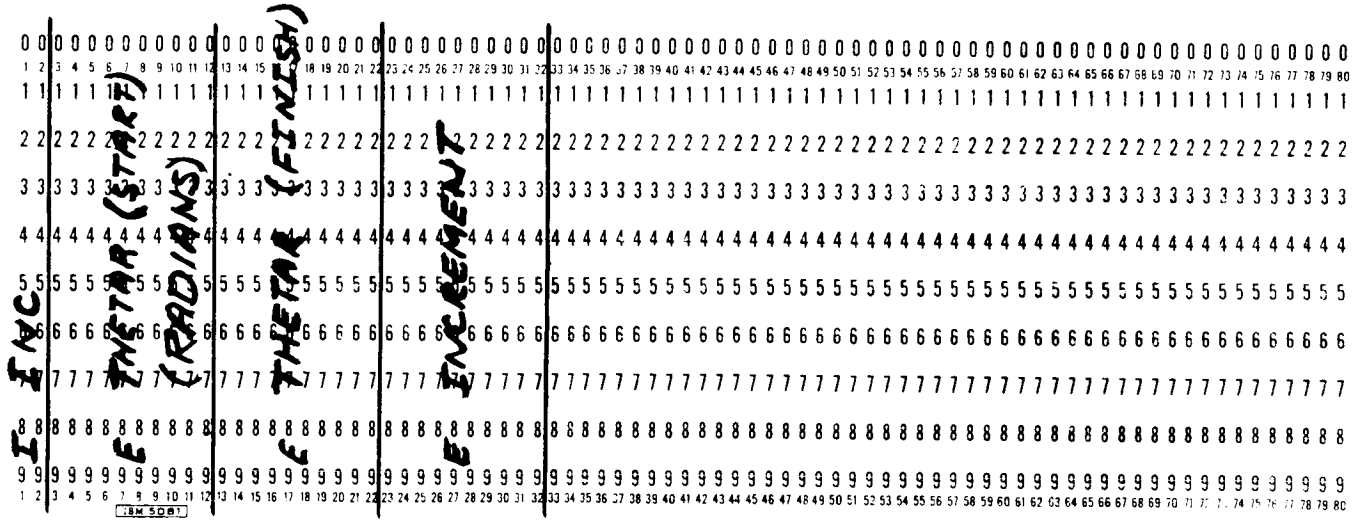

FIGURE V-3. Data Cards 5 and 6.

7

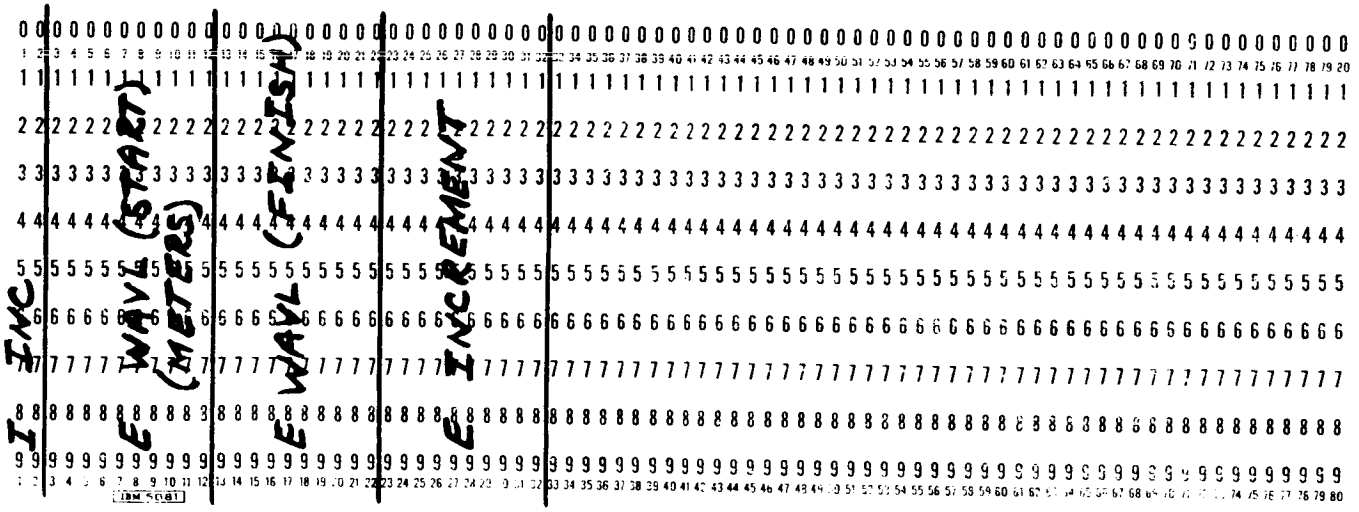

8

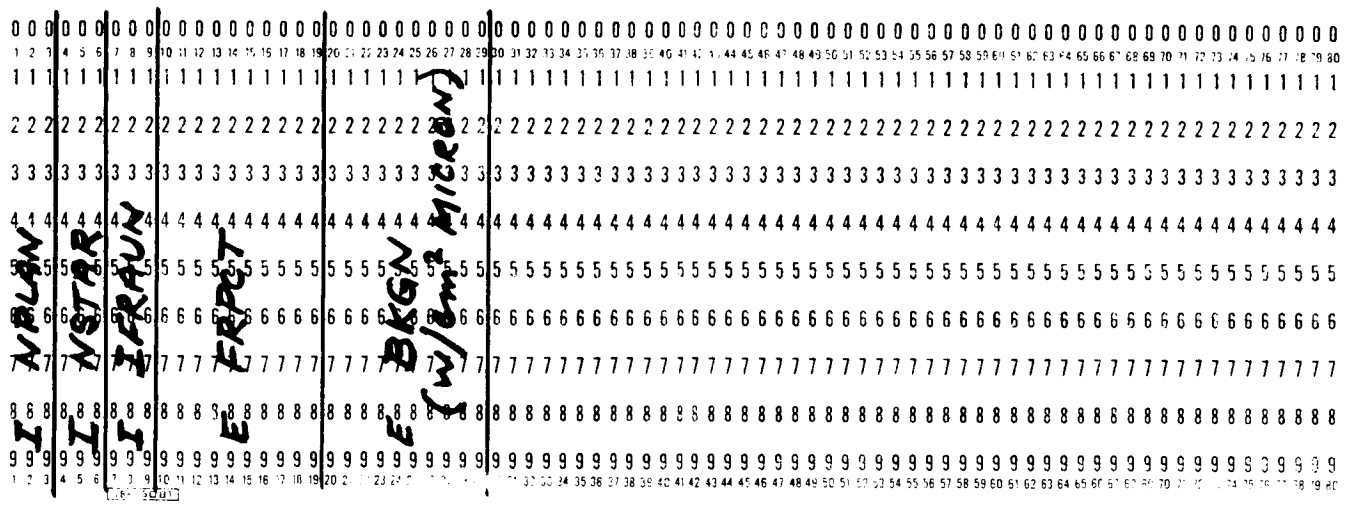

FIGURE V-3. Data Cards 7 and 8.

9

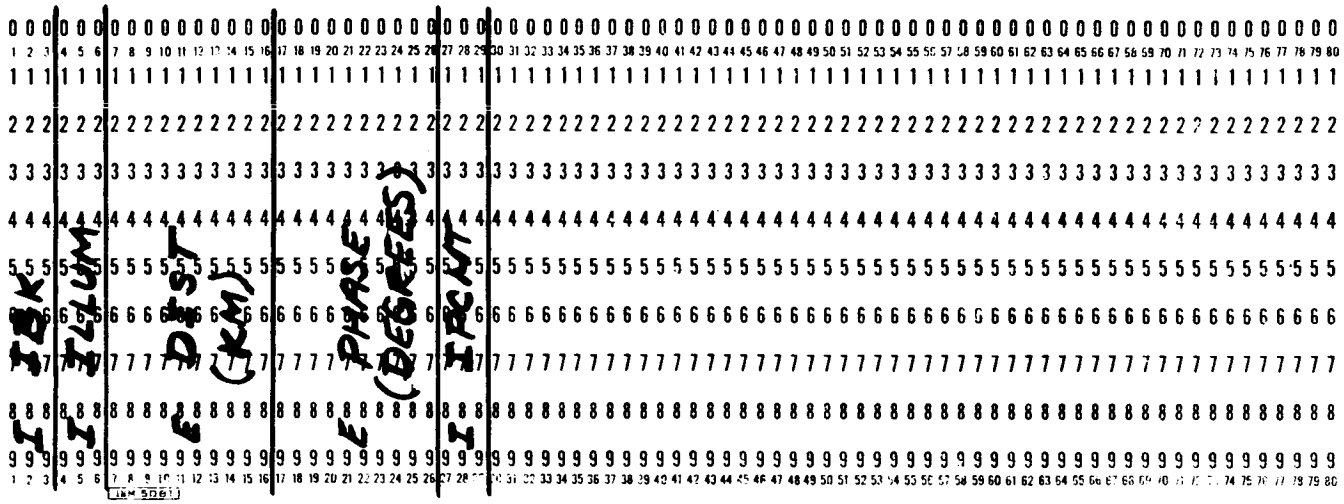

10

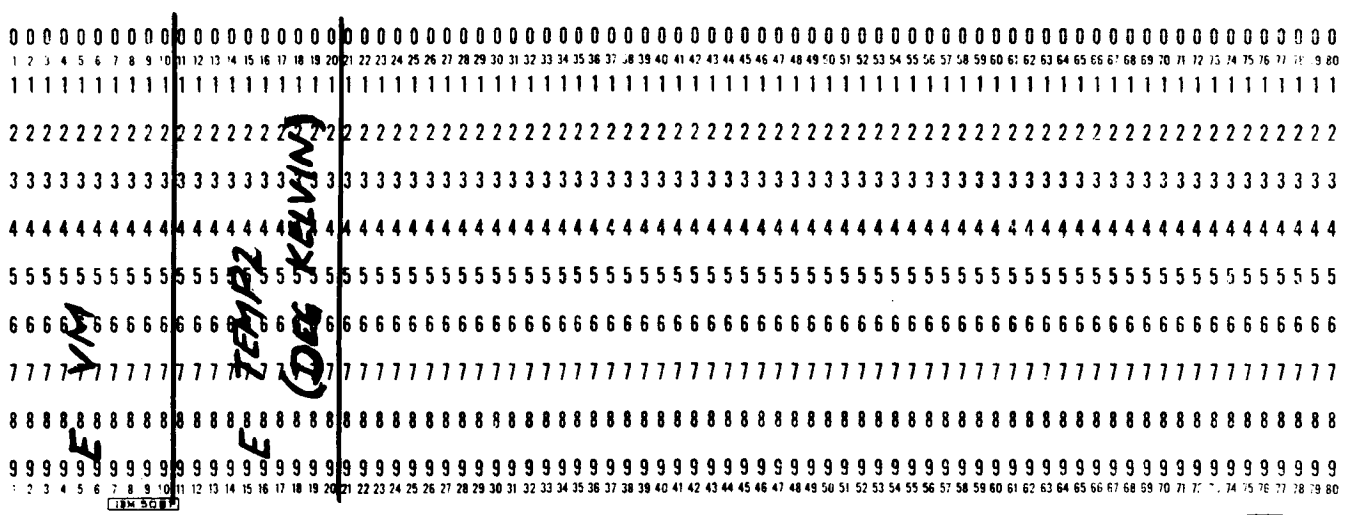

FIGURE V-4. Data Cards 9 and 10.

one group of data cards may be placed on the program deck for a single computer run).

Card Number 1

The variables entered in the first card are IGØ and NSKP1 through NSKP7. If IGØ is zero the run will terminate after this case, if it is one, another case will be expected after completion of the one under consideration. NSKP1 through NSKP7 are flags used to determine which of the following data cards have been omitted. For the first case in a run NSKP1 through NSKP7 must be 1 (meaning that all cards must be read) since the computer has no input variables stored. In the following cases, however, a zero for any of the NSKP's indicates that the values on various cards have not been changed and the program will use the values for the last case. If any input variable on a card is changed, the entire card must be read in for the new case. The following is a breakdown of the cards and their relationshop to the NSKP numbers.

NSKP	Card Number Controlled
NSKP1	2
NSKP2	3
NSKP3	4
NSKP4	5
NSKP5	6
NSKP6	7
NSKP7	8-9-10

From this it can be seen that at least two cards are needed for a new case.

Card Number 2

The variable MØD determines the modulation technique used:

1 - PPM
2 - PCM/PL
3 - Coherent

LEVAL indicates the alphabet level used and is entered only when using PPM.

PB is the bit error probability and is always entered.

FBW is the filter bandwidth and is entered only when using PPM or PCM/PL. Units are microns.

SNR is the Signal/Noise Ratio, and is needed for coherent modulation (dimensionless).

PHI is the polarization error, and is used only for PCM/PL. Unit is degrees.

Card Number 3

R is the range-distance from transmitter to receiver. Units are KM.

ET is the transmitter optics efficiency (dimensionless).

ER is the receiver optics efficiency (dimensionless).

AR is the area of the receiver aperture. Units are cm^2.

ETA is the quantum efficiency (dimensionless).

All of the values on card 3 must be entered regardless of the modulation type.

Card Number 4

This card specifies the value of the Transmitter beamwidth in radians (THETAT) and whether it is to be automatically incremented for different values. If the incrementing option is used, transmitter power for each value of THETAT is calculated with no increase in the number of cases required. Values INC may take the following meanings:

INC	Meaning
0	Do for only one value of THETAT
1	Automatically increment logarithmically for THETAT between specified limits (use values of 1 and 3)
2	Automatically increment at a fixed interval between specified limits.

Theta T (start) is the starting value of the XMTR beamwidth. For INC = 0 it is the only value of Theta T considered. This field must always have a value when this card is used.

Theta T (stop) is the stopping value and is used only for INC = 1 or 2 options.

Increment is used only for INC = 2 and specifies the increment by which Theta T is stepped.

Card Number 5

This card is similar to card 4 in that it allows the analyst to automatically increment an input parameter, the data rate in this case. The INC option for this card is the same as for card 4 and the other fields take on similar meanings.

Card Number 6

This card is similar to 4 and 5 also. This time the input value is the receiver BW.

Card Number 7

Card 7 is similar to 4, 5, and 6, with the wavelength being entered. Cards 4, 5, 6 and 7 may be incremented using any of the desired options and are not interdependent. The sequence of incrementing allows all possible combinations of the four to be considered without redundancy. The incrementing sequence these variables are stepped in uses a minimum of calculations for each case.

Card Number 8

This card gives background noise information from which the total background noise may be determined.

NPLAN is the number of planets in the background.

NSTAR is the number of stars in the background.

IFRAM indicates if a Fraunhofer line is used. An "0" indicates it is not, while a 1 indicates that it is being used.

FRPCT is the fractional percent of the reflected radiation remaining when the line is considered. No value is entered in the field if no Fraunhofer line is used.

BICGN is background noise introduced into the system which is not contributed directly by stars and planets. This input is particularly useful in a laboratory environment where a known value of noise is introduced.

Card Number 9

Card numbers 9 and 10 are used only if planets or stars are present, respectively.

IBK represents the number of the planet in view. The planet numbers are given below:

Planet No.	Planet
1	Earth (experimental)
2	Moon (experimental)
3	Sky (experimental)
4	Mercury
5	Venus
6	Mars
7	Jupiter
8	Saturn
9	Uranus
10	Neptune
11	Pluto
12	Earth (Grey-body)
13	Moon (Grey-body)

The radiation from all planets other than Earth and Moon are grey-body curves.

ILLUM is a flag which indicates whether the area viewed of the planet is illuminated. An "0" indicates that it is not illuminated. A "1" indicates that it is totally illuminated. A number < 100 indicates the percent of the area illuminated. This value differs from the phase in that the area of the planet viewed may be smaller than the entire planet (due to receiver beamwidth) and therefore the area viewed may be entirely dark even though a part of the planet facing the MDSV is illuminated. This option allows the analyst to specify whether the area seen is in the illuminated portion of the planet, not in it, or partially in each.

DIST is the distance in KM to the planet in view.

PHASE is the phase of the planet in degrees. IPCNT is the percent of the area seen not containing the planet. This allows neither the self-emission or albedo to be considered for this area.

Any number of planets may be considered for background, although a separate data card must be included for each.

Card Number 10

This card contains information relating to stars in the background. Any number of stars may be considered, with a separate data card for each.

VM is the visual magnitude of the star.

TEMPZ is the effective temperature of the star in degrees Kelvin.

E. Results for Cases of Interest

This part of Section V contains results of computer runs made for cases of interest in the prediction of laser communication performance at two (100 and 50) percentage modulations for PL modulation, for PPM modulation with an alphabet level of 3, and for a coherent laser communication system. Parts E.1, E. 2, and E.3 shows results for severl cases of interest in deep space laser communications. Part E.4 shows results of the study of requirements for range tracking with a 100% modulated PCM?PL system. System characteristics for each basic test are presented first. Although not mentioned in parts C and D of this report, the quantity "Percent Modulation" printed as part of the output listing is actually the polarization error "45 Percent Modulation" = 45° Polarization Error). A method for converting from Polarization Error to actual percent modulation is given in Section IV. F. 7 of this report.

After system characteristics and results are presented for a given condition, the program increments to different optical wavelengths. The results for these other wavelengths, with all other system parameters constant, are presented under the titles "After Incrementing".

All calculations have been made for an error rate of 10^{-3}, because this is a reasonable one for actual measurement of a system performance.

E.1 PPM Modulation, Alphabet Level of 3

E.2 50% Modulation, PCM/PL

The printout saying "45% Modulation" means a 45° polarization error, or m = .5.

E.3 Coherent Modulation

E.4 Requirements for Range Tracking on a Polarized Light Modulated Laser Signal (100% Modulation)

Results presented here were generated to determine the optical transmitter power required by the ranging system described in Part VI of this report. These results are also applicable to predicting laser communication performance for 100% modulation.

F. Program Limitations

The only known limitations to this program for computing laser power requirements have been set by our inability to model certain laser communication phenomena and by the storage limitations inherent in a UNIVAC 1108 computer.

Those major effects for which we have not been able to form mathematical models are as follows:

1) The effects of the Earth's atmosphere on any type of laser communication.

2) The effects of spatially non-coherent received signals on the performance of a coherent laser communication system.

3) The effects of doppler, and doppler rates on the performance of laser communication systems. As was shown in the Final Report[1] on NAS 9-3650, these effects are negligible in PL and PPM systems. However, they have an important effect on the performance of a coherent system.

The only limitation on the use of this Power Model program is set by the storage capability of the UNIVAC 1108. This has no effect on the use of the model for PL and coherent laser communication systems. In the case of PPM, alphabet levels greater than 8 (2^8 information position/frame) will frequently cause the computer to overflow when performing subroutine BICOEF. There are ways of preventing this overflow, but it is felt that in any practical PPM laser communication system this will never be more than 2^7 information positions/frame.

E.1 PPM, ALPHABET LEVEL = 3

SYSTEM CHARACTERISTICS

PULSE POSITION MODULATION

DATA RATE = .500+08 BITS/SEC

BIT ERROR PROBABILITY = .100-01

ALPHABET LEVEL = 3

WAVELENGTH = .100-05 METERS

RANGE = .150+09 KM

QUANTUM EFFICIENCY = .50

* * * * *

RECEIVER CHARACTERISTICS

BEAMWIDTH = .100-04 RADIANS

AREA OF APERATURE = .100+06 SQ CM

OPTICS EFFICIENCY = .70

FILTER BANDWIDTH = .100-02 MICRONS

* * * * *

TRANSMITTER CHARACTERISTICS

BEAMWIDTH = .100-04 RADIANS

POWER = 28.0 WATTS

OPTICS EFFICIENCY = .70

* * * * *

BACKGROUND

3 PLANET(S) ARE IN BACKGROUND

PLANET	DISTANCE (KM)	PHASE (DEGREES)	ILLUMINATION OF AREA SEEN
JUPITER	.100+07	-0.	NONE
MARS	.100+07	30.	NONE
VENUS	.100+07	-0.	NONE

1 STAR(S) ARE IN BACKGROUND

STAR NUMBER	TEMPERATURE (DEGREES KELVIN)	VISUAL MAGNITUDE
1	5000.	-1.

NO FRAUNHOFER LINE IS USED

NOISE CONTRIBUTIONS OF PLANETS AND STARS = .457-10 WATTS/SQ CM-MICRON

NOISE CONTRIBUTION FROM INPUT = -.000 WATTS/SQ CM-MICRON

TOTAL NOISE = .457-10 WATTS/SQ CM-MICRON

* * * * *

QUANTUM INFORMATION

TOTAL NOISE PHOTOELECTRONS/DECISION (CYCLE) = .181-07

TOTAL SIGNAL PHOTOELECTRONS/DECISION (CYCLE) = .391+01

AFTER INCREMENTING

TRANSMITTER BEAMWIDTH = .100-04 RADIANS DATA RATE = .500+08 BITS/SEC

RECEIVER BEAMWIDTH = .100-04 RADIANS WAVELENGTH = .300-05 METERS

TRANSMITTER POWER = .935+01 WATTS NOISE(TOT) = .158-11 WATTS/SQ CM-MICRON

QUANTUM INFORMATION

TOTAL NOISE PHOTOELECTRONS/DECISION (CYCLE) = .188-08

TOTAL SIGNAL PHOTOELECTRONS/DECISION (CYCLE) = .391+01

AFTER INCREMENTING

TRANSMITTER BEAMWIDTH = .100-04 RADIANS DATA RATE = .500+08 BITS/SEC

RECEIVER BEAMWIDTH = .100-04 RADIANS WAVELENGTH = .100-04 METERS

TRANSMITTER POWER = .280+01 WATTS NOISE(TOT) = .148-11 WATTS/SQ CM-MICRON

QUANTUM INFORMATION

TOTAL NOISE PHOTOELECTRONS/DECISION (CYCLE) = .586-08

TOTAL SIGNAL PHOTOELECTRONS/DECISION (CYCLE) = .391+01

E.2 50% MODULATION, PCM/PL

SYSTEM CHARACTERISTICS

PULSE CODE MODULATION (PL)

DATA RATE = .500+07 BITS/SEC

BIT ERROR PROBABILITY = .100-02

PERCENT MODULATION =45.

WAVELENGTH = .100-05 METERS

RANGE = .161+09 KM

QUANTUM EFFICIENCY = .50

* * * * *

RECEIVER CHARACTERISTICS

BEAMWIDTH = .100-04 RADIANS

AREA OF APERATURE = .100+06 SQ CM

OPTICS EFFICIENCY = .70

FILTER BANDWIDTH = .100-02 MICRONS

* * * * *

TRANSMITTER CHARACTERISTICS

BEAMWIDTH = .100-04 RADIANS

POWER = 119.9 WATTS

OPTICS EFFICIENCY = .70

* * * * *

BACKGROUND

3 PLANET(S) ARE IN BACKGROUND

PLANET	DISTANCE (KM)	PHASE (DEGREES)	ILLUMINATION OF AREA SEEN
JUPITER	.100+07	-0.	NONE
MARS	.100+07	30.	TOTAL
VENUS	.100+07	-0.	50 PERCENT

1 STAR(S) ARE IN BACKGROUND

STAR NUMBER	TEMPERATURE (DEGREES KELVIN)	VISUAL MAGNITUDE
1	5000.	-1.

NO FRAUNHOFER LINE IS USED

NOISE CONTRIBUTIONS OF PLANETS AND STARS = .489-10 WATTS/SQ CM-MICRON

NOISE CONTRIBUTION FROM INPUT = -.000 WATTS/SQ CM-MICRON

TOTAL NOISE = .489-10 WATTS/SQ CM-MICRON

* * * * *

QUANTUM INFORMATION

TOTAL NOISE PHOTOELECTRONS/DECISION (CYCLE) = .967-08

TOTAL SIGNAL PHOTOELECTRONS/DECISION (CYCLE) = .145+02

AFTER INCREMENTING

TRANSMITTER BEAMWIDTH = .100-04 RADIANS DATA RATE = .500+08 BITS/SEC

RECEIVER BEAMWIDTH = .100-04 RADIANS WAVELENGTH = .300-05 METERS

TRANSMITTER POWER = .400+02 WATTS NOISE(TOT) = .172-11 WATTS/SQ CM-MICRON

QUANTUM INFORMATION

TOTAL NOISE PHOTOELECTRONS/DECISION (CYCLE) = .102-08

TOTAL SIGNAL PHOTOELECTRONS/DECISION (CYCLE) = .145+02

AFTER INCREMENTING

TRANSMITTER BEAMWIDTH = .100-04 RADIANS DATA RATE = .500+08 BITS/SEC

RECEIVER BEAMWIDTH = .100-04 RADIANS WAVELENGTH = .100-04 METERS

TRANSMITTER POWER = .120+02 WATTS NOISE(TOT) = .148-11 WATTS/SQ CM-MICRON

QUANTUM INFORMATION

TOTAL NOISE PHOTOELECTRONS/DECISION (CYCLE) = .293-08

TOTAL SIGNAL PHOTOELECTRONS/DECISION (CYCLE) = .145+02

SYSTEM CHARACTERISTICS

PULSE CODE MODULATION (PL)

DATA RATE = .500+08 BITS/SEC

BIT ERROR PROBABILITY = .100-02

PERCENT MODULATION =45.

WAVELENGTH = .100-05 METERS

RANGE = .810+08 KM

QUANTUM EFFICIENCY = .50

* * * * *

RECEIVER CHARACTERISTICS

BEAMWIDTH = .100-04 RADIANS

AREA OF APERATURE = .100+06 SQ CM

OPTICS EFFICIENCY = .70

FILTER BANDWIDTH = .100-02 MICRONS

* * * * *

TRANSMITTER CHARACTERISTICS

BEAMWIDTH = .100-04 RADIANS

POWER = 30.4 WATTS

OPTICS EFFICIENCY = .70

* * * * *

BACKGROUND

3 PLANET(S) ARE IN BACKGROUND

PLANET	DISTANCE (KM)	PHASE (DEGREES)	ILLUMINATION OF AREA SEEN
JUPITER	.100+07	-0.	NONE
MARS	.100+07	30.	TOTAL
VENUS	.100+07	-0.	50 PERCNET

1 STAR(S) ARE IN BACKGROUND

STAR NUMBER	TEMPERATURE (DEGREES KELVIN)	VISUAL MAGNITUDE
1	5000.	-1.

V-44

NO FRAUNHOFER LINE IS USED

NOISE CONTRIBUTIONS OF PLANETS AND STARS = .489-10 WATTS/SQ CM-MICRON

NOISE CONTRIBUTION FROM INPUT = -.000 WATTS/SQ CM-MICRON

TOTAL NOISE = .489-10 WATTS/SQ CM-MICRON

* * * * *

QUANTUM INFORMATION

TOTAL NOISE PHOTOELECTRONS/DECISION (CYCLE) = .967-08

TOTAL SIGNAL PHOTOELECTRONS/DECISION (CYCLE) = .145+02

AFTER INCREMENTING

TRANSMITTER BEAMWIDTH = .100-04 RADIANS DATA RATE = .500+08 BITS/SEC

RECEIVER BEAMWIDTH = .100-04 RADIANS WAVELENGTH = .300-05 METERS

TRANSMITTER POWER = .101+02 WATTS NOISE(TOT) = .172-11 WATTS/SQ CM-MICRON

QUANTUM INFORMATION

TOTAL NOISE PHOTOELECTRONS/DECISION (CYCLE) = .102-08

TOTAL SIGNAL PHOTOELECTRONS/DECISION (CYCLE) = .145+02

AFTER INCREMENTING

TRANSMITTER BEAMWIDTH = .100-04 RADIANS DATA RATE = .500+08 BITS/SEC

RECEIVER BEAMWIDTH = .100-04 RADIANS WAVELENGTH = .100-04 METERS

TRANSMITTER POWER = .304+01 WATTS NOISE(TOT) = .148-11 WATTS/SQ CM-MICRON

QUANTUM INFORMATION

TOTAL NOISE PHOTOELECTRONS/DECISION (CYCLE) = .293-08

TOTAL SIGNAL PHOTOELECTRONS/DECISION (CYCLE) = .145+02

SYSTEM CHARACTERISTICS

PULSE CODE MODULATION (PL)

DATA RATE = .500+08 BITS/SEC

BIT ERROR PROBABILITY = .100-02

PERCENT MODULATION =45.

WAVELENGTH = .100-05 METERS

RANGE = .150+09 KM

QUANTUM EFFICIENCY = .50

* * * * *

RECEIVER CHARACTERISTICS

BEAMWIDTH = .100-04 RADIANS

AREA OF APERATURE = .100+06 SQ CM

OPTICS EFFICIENCY = .70

FILTER BANDWIDTH = .100-02 MICRONS

* * * * *

TRANSMITTER CHARACTERISTICS

BEAMWIDTH = .100-04 RADIANS

POWER = 104.1 WATTS

OPTICS EFFICIENCY = .70

* * * * *

BACKGROUND

3 PLANET(S) ARE IN BACKGROUND

PLANET	DISTANCE (KM)	PHASE (DEGREES)	ILLUMINATION OF AREA SEEN
JUPITER	.100+07	-0.	NONE 50% Total
MARS	.100+07	30.	NONE
VENUS	.100+07	-0.	NONE

1 STAR(S) ARE IN BACKGROUND

STAR NUMBER	TEMPERATURE (DEGREES KELVIN)	VISUAL MAGNITUDE
1	5000.	-1.

NO FRAUNHOFER LINE IS USED

NOISE CONTRIBUTIONS OF PLANETS AND STARS = .457-10 WATTS/SQ CM-MICRON

NOISE CONTRIBUTION FROM INPUT = -.000 WATTS/SQ CM-MICRON

TOTAL NOISE = .457-10 WATTS/SQ CM-MICRON

* * * * *

QUANTUM INFORMATION

TOTAL NOISE PHOTOELECTRONS/DECISION (CYCLE) = .904-08

TOTAL SIGNAL PHOTOELECTRONS/DECISION (CYCLE) = .145+02

AFTER INCREMENTING

TRANSMITTER BEAMWIDTH = .100-04 RADIANS DATA RATE = .500+08 BITS/SEC

RECEIVER BEAMWIDTH = .100-04 RADIANS WAVELENGTH = .300-05 METERS

TRANSMITTER POWER = .347+02 WATTS NOISE(TOT) = .158-11 WATTS/SQ CM-MICRON

QUANTUM INFORMATION

TOTAL NOISE PHOTOELECTRONS/DECISION (CYCLE) = .939-09

TOTAL SIGNAL PHOTOELECTRONS/DECISION (CYCLE) = .145+02

V-48

AFTER INCREMENTING

TRANSMITTER BEAMWIDTH = .100-04 RADIANS DATA RATE = .500+08 BITS/SEC

RECEIVER BEAMWIDTH = .100-04 RADIANS WAVELENGTH = .100-04 METERS

TRANSMITTER POWER = .104+02 WATTS NOISE(TOT) = .148-11 WATTS/SQ CM-MICRON

QUANTUM INFORMATION

TOTAL NOISE PHOTOELECTRONS/DECISION (CYCLE) = .293-08

TOTAL SIGNAL PHOTOELECTRONS/DECISION (CYCLE) = .145+02

E.3 COHERENT MODULATION

SYSTEM CHARACTERISTICS

COHERENT MODULATION

DATA RATE = .500+08 BITS/SEC

BIT ERROR PROBABILITY = .100-03

SIGNAL/NOISE =10.0 DB

WAVELENGTH = .100-05 METERS

RANGE = .150+09 KM

QUANTUM EFFICIENCY = .50

* * * * *

RECEIVER CHARACTERISTICS

BEAMWIDTH = .100-04 RADIANS

AREA OF APERATURE = .100+06 SQ CM

OPTICS EFFICIENCY = .70

* * * * *

TRANSMITTER CHARACTERISTICS

BEAMWIDTH = .100-04 RADIANS

POWER = 143.4 WATTS

OPTICS EFFICIENCY = .70

* * * * *

BACKGROUND

3 PLANET(S) ARE IN BACKGROUND

PLANET	DISTANCE (KM)	PHASE (DEGREES)	ILLUMINATION OF AREA SEEN
JUPITER	.100+07	-0.	NONE
MARS	.100+07	30.	NONE
VENUS	.100+07	-0.	NONE

1 STAR(S) ARE IN BACKGROUND

STAR NUMBER	TEMPERATURE (DEGREES KELVIN)	VISUAL MAGNITUDE
1	5000.	-1.

NO FRAUNHOFER LINE IS USED

NOISE CONTRIBUTIONS OF PLANETS AND STARS = .457-10 WATTS/SQ CM-MICRON

NOISE CONTRIBUTION FROM INPUT = -.000 WATTS/SQ CM-MICRON

TOTAL NOISE = .457-10 WATTS/SQ CM-MICRON

* * * * *

QUANTUM INFORMATION

TOTAL NOISE PHOTOELECTRONS/DECISION (CYCLE) = .301-11

TOTAL SIGNAL PHOTOELECTRONS/DECISION (CYCLE) = .100+02

AFTER INCREMENTING

TRANSMITTER BEAMWIDTH = .100-04 RADIANS DATA RATE = .500+08 BITS/SEC

RECEIVER BEAMWIDTH = .300-04 RADIANS WAVELENGTH = .100-05 METERS

TRANSMITTER POWER = .143+03 WATTS NOISE(TOT) = .457-10 WATTS/SQ CM-MICRON

QUANTUM INFORMATION

TOTAL NOISE PHOTOELECTRONS/DECISION (CYCLE) = .271-10

TOTAL SIGNAL PHOTOELECTRONS/DECISION (CYCLE) = .100+02

AFTER INCREMENTING

TRANSMITTER BEAMWIDTH = .100-04 RADIANS DATA RATE = .500+08 BITS/SEC

RECEIVER BEAMWIDTH = .100-03 RADIANS WAVELENGTH = .100-05 METERS

TRANSMITTER POWER = .143+03 WATTS NOISE(TOT) = .457-10 WATTS/SQ CM-MICRON

QUANTUM INFORMATION

TOTAL NOISE PHOTOELECTRONS/DECISION (CYCLE) = .301-09

TOTAL SIGNAL PHOTOELECTRONS/DECISION (CYCLE) = .100+02

E.4 REQUIREMENT FOR RANGE TRACKING ON A POLARIZED LIGHT MODULATED LASER SIGNAL (100 % MOD.)

SYSTEM CHARACTERISTICS

PULSE CODE MODULATION (PL)

DATA RATE = .500+03 BITS/SEC

BIT ERROR PROBABILITY = .100-02

WAVELENGTH = .100-05 METERS

RANGE = .161+06 KM

QUANTUM EFFICIENCY = .50

PERCENT MODULATION = 0

* * * * *

RECEIVER CHARACTERISTICS

BEAMWIDTH = .100-04 RADIANS

AREA OF APERATURE = .100+06 SQ CM

OPTICS EFFICIENCY = .70

FILTER BANDWIDTH ± .100-02 MICRONS

* * * * *

TRANSMITTER CHARACTERISTICS

BEAMWIDTH = .100-04 RADIANS

POWER = 51.3 WATTS

OPTICS EFFICIENCY = .70

* * * * *

BACKGROUND

3 PLANET(S) ARE IN BACKGROUND

PLANET	DISTANCE (KM)	PHASE (DEGREES)	ILLUMINATION OF AREA SEEN
JUPITER	.100+07	-0.	NONE
MARS	.100+07	30.	TOTAL
VENUS	.100+07	-0.	50 PERCNET

1 STAR(S) ARE IN BACKGROUND

STAR NUMBER	TEMPERATURE (DEGREES KELVIN)	VISUAL MAGNITUDE
1	5000.	-1.

NO FRAUNHOFER LINE IS USED

NOISE CONTRIBUTIONS OF PLANETS AND STARS = .489-10 WATTS/SQ CM-MICRON

NOISE CONTRIBUTION FROM INPUT = -.000 WATTS/SQ CM-MICRON

TOTAL NOISE = .489-10 WATTS/SQ CM-MICRON

* * * * *

QUANTUM INFORMATION

TOTAL NOISE PHOTOELECTRONS/DECISION (CYCLE) = .967-08

TOTAL SIGNAL PHOTOELECTRONS/DECISION (CYCLE) = .621+01

AFTER INCREMENTING

TRANSMITTER BEAMWIDTH =	.100-04 RADIANS	DATA RATE =	.500+08 BITS/SEC
RECEIVER BEAMWIDTH =	.100-04 RADIANS	WAVELENGTH =	.300-05 METERS
TRANSMITTER POWER =	.171+02 WATTS	NOISE(TOT) =	.172-11 WATTS/SQ CM-MICRON

QUANTUM INFORMATION

TOTAL NOISE PHOTOELECTRONS/DECISION (CYCLE) = .102-08

TOTAL SIGNAL PHOTOELECTRONS/DECISION (CYCLE) = .621+01

AFTER INCREMENTING

TRANSMITTER BEAMWIDTH =	.100-04 RADIANS	DATA RATE =	.500+08 BITS/SEC
RECEIVER BEAMWIDTH =	.100-04 RADIANS	WAVELENGTH =	.100-04 METERS
TRANSMITTER POWER =	.513+01 WATTS	NOISE(TOT) =	.148-11 WATTS/SQ CM-MICRON

QUANTUM INFORMATION

TOTAL NOISE PHOTOELECTRONS/DECISION (CYCLE) = .293-08

TOTAL SIGNAL PHOTOELECTRONS/DECISION (CYCLE) = .621+01

SYSTEM CHARACTERISTICS

PULSE CODE MODULATION (PL)

DATA RATE = .500+08 BITS/SEC

BIT ERROR PROBABILITY = .100-02

WAVELENGTH = .100-05 METERS

RANGE = .810+08 KM

QUANTUM EFFICIENCY = .50

PERCENT MODULATION = 0

* * * * *

RECEIVER CHARACTERISTICS

BEAMWIDTH = .100-04 RADIANS

AREA OF APERATURE = .100+06 SQ CM

OPTICS EFFICIENCY = .70

FILTER BANDWIDTH = .100-02 MICRONS

* * * * *

TRANSMITTER CHARACTERISTICS

BEAMWIDTH = .100-04 RADIANS

POWER = 13.0 WATTS

OPTICS EFFICIENCY = .70

* * * * *

BACKGROUND

3 PLANET(S) ARE IN BACKGROUND

PLANET	DISTANCE (KM)	PHASE (DEGREES)	ILLUMINATION OF AREA SEEN
JUPITER	.100+07	-0.	NONE
MARS	.100+07	30.	TOTAL
VENUS	.100+07	-0.	50 PERCNET

1 STAR(S) ARE IN BACKGROUND

STAR NUMBER	TEMPERATURE (DEGREES KELVIN)	VISUAL MAGNITUDE
1	5000.	-1.

NO FRAUNHOFER LINE IS USED

NOISE CONTRIBUTIONS OF PLANETS AND STARS = .489-10 WATTS/SQ CM-MICRON

NOISE CONTRIBUTION FROM INPUT = -.000 WATTS/SQ CM-MICRON

TOTAL NOISE = .489-10 WATTS/SQ CM-MICRON

* * * * *

QUANTUM INFORMATION

TOTAL NOISE PHOTOELECTRONS/DECISION (CYCLE) = .967-08

TOTAL SIGNAL PHOTOELECTRONS/DECISION (CYCLE) = .621+01

AFTER INCREMENTING

TRANSMITTER BEAMWIDTH =	.100-04 RADIANS	DATA RATE =	.500+08 BITS/SEC
RECEIVER BEAMWIDTH =	.100-04 RADIANS	WAVELENGTH =	.300-05 METERS
TRANSMITTER POWER =	.433+01 WATTS	NOISE(TOT) =	.172-11 WATTS/SQ CM-MICRON

QUANTUM INFORMATION

TOTAL NOISE PHOTOELECTRONS/DECISION (CYCLE) = .102-08

TOTAL SIGNAL PHOTOELECTRONS/DECISION (CYCLE) = .621+01

AFTER INCREMENTING

TRANSMITTER BEAMWIDTH =	.100-04 RADIANS	DATA RATE =	.500+08 BITS/SEC
RECEIVER BEAMWIDTH =	.100-04 RADIANS	WAVELENGTH =	.100-04 METERS
TRANSMITTER POWER =	.130+01 WATTS	NOISE(TOT) =	.148-11 WATTS/SQ CM-MICRON

QUANTUM INFORMATION

TOTAL NOISE PHOTOELECTRONS/DECISION (CYCLE) = .293-08

TOTAL SIGNAL PHOTOELECTRONS/DECISION (CYCLE) = .621+01

Section VI

RANGING SYSTEM FOR USE WITH HIGH DATA RATE LASER COMMUNICATOR

A. Statement of the Task

The purpose of this task was to formulate a ranging system for use with a deep space laser communicator. The ranging system was to be applicable to PCM/PL, PPM, and coherent laser communicator, and was to use the received signal as the ranging signal. The spacecraft receiver/transmitter design for each type of modulation was to be considered. The effects of doppler, frequency drift, and other influncing factors were to be considered. Range and range rate accuracies were to be determined. Finally, the recommended ranging techniques were to be compared with those DSIF/spacecraft procedures and equipments used on past and future deep space and lunar missions.

B. Data Format Considerations

The following types of ranging systems were investigated for their applicability to this problem:

1. A laser radar.
2. An analog subcarrier ranging system.
3. Various digital ranging systems.

It was decided that laser radar systems did not appear to have the range capability necessary for tracking a deep space probe at ranges of 100 million nautical miles. Analog subcarrier ranging systems were also discarded, beacuse they are not compatible with the constraints imposed on a laser communication system by the requirement for high data rate digital communications. There was no way of supplying the necessary ranging tones on the same channel as that used for digital laser communications.

The only promising ranging systems used digital range coding, as are now used for deep space radio ranging on space vehicles. Unfortunately, existing digital range trackers use a separate carrier for the spaceborne repeater in the tracking loop. Since the proposed laser communication system has only one transmitter carrier frequency, these existing techniques were not directly applicable to the problem. The range code had to be fitted into the existing digital format, as proposed in the Final Report[1] on HUD-38120.

At first, consideration was given to placing the ranging code, along with the voice data and telemetry in the television flyback time. An analysis of this showed that the probability of falsely recognizing a portion of the video data as the range code was excessively large, due to the short range code that could be fitted into the flyback time. This short range code also led to undesirable ambiguities in range.

Next, consideration was given to using a long range code, with only a portion of the code transmitted during the flyback time for each line. It was proposed that the code could be reconstructed from these samples at a ground receiver. Analysis of the system showed that reconstruction of the range code could be done, but it would require excessive amounts of space-borne electronics to note the time of arrival of the code, and retransmit this information along with the range code itself to an Earth based receiver.

As a consequence, a novel ranging and information carrying system was developed. Although it requires modification of the Earth based transmitter to allow transmission to the spacecraft at 50 megabits/second, it requires a minimum of spacecraft modification. This system, its operation, and its

expected performance are discussed in the rest of this Section. It is completely compatible with the data format recommended for transmission from the deep space vehicle to Earth.

It was found that doppler and doppler rate have almost no effect on the tracking performance. At its worst, the doppler causes a 1 part in 10^5 change in the baseband bit length. This is an insignificant error, and has not been compensated. If necessary, compensation of this error could be incorporated in the ranging system.

C. Digital Range Tracking Techniques

The use of pseudo-random sequences for range tracking and range determination is by no means new. As early as 1958 coded waveforms were used by the Millstone Hill Radar for measuring the distance to Venus. Since that time numerous "space shots" have used pseudo-random sequences for determining range and tracking. The development of "acquirable codes" was, to a certain extent, responsible for the wide acceptance of this technique for space applications, due to the much improved acquisition times of these type codes over the "maximal length" linear type codes.

The factors influencing the selection of a digital type ranging system are:

(1) The ease with which very long waveform periods can be realized, thereby eliminating range ambiguity problems.

(2) The ease with which the digital ranging code can be acquired if the code is properly constructed.

(3) The requirement for digital data transmission from the spacecraft over the laser system.

(4) The fact that no separate carrier or subcarrier is available from the proposed laser system solely for ranging purposes.

(5) The fact that laser radar ranging with retro-reflectors is not, at present, felt practical for ranges in excess of about 1000 miles.

(6) The requirement of the contract for ranging on the communication signal.

Considering these factors, it is felt that a digital ranging system in which a spacecraft transponder is used to enhance the returned pseudo-random transmitted sequence offers the most practical way of accomplishing laser ranging. The transponder will improve the signal-to-noise ratio of the coded sequence to a usable level, and also provide capability for changing the up or down link frequencies.

An acquirable code is a pseudo-random sequence which is generated by combining codes of a given period in a non-linear (logic) manner. Very long sequence periods may be obtained with desirable auto correlation properties, which allow the total code to be acquired in steps (i.e., by alignment of the individual components of the code). Each time a code component of the overall code is properly aligned with the incoming sequence, the correlation is improved. Another code component of the overall code may then be aligned, until the total code is finally "acquired". By maintaining bit synchronization of the doppler shifted incoming sequence, the codes may be kept in alignment, (i.e., normalized correlation equal 1). A measurement on the time displacement between the aligned codes provides a value proportional to the range of the space craft.

1. Required Additional Periodicity in a Sequence for Ranging

The requirement for very long pseudo-random sequence periods is due to the ambiguity in range which arises when the transmitted signal period is less than twice the return period. To remove the ambiguity problem, it is necessary to have periodic sequence with many digits. Sequences have been developed which have period lengths suitable for ranging measurement of distances to the limits of our solar system. The ranging code developed for the deep space optical communication ranging system has a period length of 68, 363, 477, 446 digits. Since the maximum range to be measured by this system is 100×10^6 miles, at 50 $\frac{MB}{SEC}$, the 18 minute round trip time would require a period length greater than 54×10^9 digits. A period length of 68×10^9 will therefore be satisfactory. The equipment for generation of this code is described in Part E.

Assuming the ranging code to be properly aligned, the resolution of the system is approximately 20 feet at the 50 $\frac{M\ BIT}{SEC}$ rate. The accuracy of the overall system is, however, not so good. Assuming the velocity of light is known to 1 part in 10^7, over a path of 100×10^6 miles or approximately 18 minutes round trip time, the time uncertainty is $(1 \times 10^{-7})(1080\ sec) = \pm 1.08 \times 10^{-4}$ sec. This corresponds to a distance uncertainty of $(1.08 \times 10^{-4} sec)\ (186000\ \frac{miles}{sec}) = \pm 20$ miles.

2. Maximal Length Code Sequence Generators

A maximal length pseudo-random sequence is defined as a binary sequence of length 2^n-1, where in each period the number of 1's differs from the number of 0's by at most 1.

In the subsequences within the period one-half the subsequences of each kind are of length 1; one-quarter of each kind are of length 2; one-eighth of each kind are of length 3; etc., and if the sequence is compared with a cyclic shift of itself, the number of agreements differs from the number of disagreements by at most 1.

The number (Ns) of maximal length sequences possible for a given n stage linear shift register may be determined from the following relationship:

$$Ns = \frac{\varphi(2^n-1)}{n}$$

Where $\varphi(2^n-1) = \varphi(k) =$ Euler's φ function which may be calculated from:

(For k Prime)

$$\varphi(k) = k-1$$

(For k containing factors)

$$\varphi(k) = k \times \prod \frac{(P_i-1)}{P_i}$$

Where P_i are the prime factors of k

This means that for a given maximal length there are $\frac{\varphi(2^n-1)}{n}$

arrangements which can be used to generate the maximal length period defined by n. All of these sequences will have the same basic properties specified previously.

Example:

$$n = 10$$

$$2^n - 1 = 1023$$

therefore $$k = 1023 = 3 \cdot 11 \cdot 31$$

$$N_s = \frac{\varphi(1023)}{n}$$

$$\varphi(1023) = 1023 \cdot \left(\frac{3-1}{3}\right)\left(\frac{11-1}{11}\right)\left(\frac{31-1}{31}\right)$$

$$N_s = \frac{(1023)(2)(10)(30)}{(10)(3)(11)(31)} = 60$$

In many applications maximal length pseudo-random sequence are not used but some modification to a maximal length code. One reason for using a modification of a maximal length sequence is in the desirable autocorrelation properties of the acquirable codes.

3. Auto Correlation Properties and Advantages of Non-linear Ranging Codes

The advantages of using non-linear random codes rather than linear maximal length linear codes for ranging purposes is quickly appreciated when the auto correlation properties of the two types of codes are compared. The normalized auto correlation function of a typical pseudo-random binary sequence of length P is shown in Figure VI-1.

The cross-correlation function of two relatively prime binary sequences is everywhere very small, therefore said to be uncorrelated. If the periods of the sequences are not relatively prime to one another, relatively minor peaks will start showing up in the cross correlation function. The same phenomenon can be observed in sequences which are made up of component codes of smaller lengths. The normalized correlation, P, may be determined from:

$$P = \frac{\text{number of agreements - number of disagreements}}{\text{number of agreements + number of disagreements}}$$

When the overall code is made up of sequences of smaller length, a number of situations arise corresponding to which subsequences happened to be in or out of alignment. The effects on the normalized correlation coeficient of a code made up of subsequences and the manner in which these subsequences are combined can be illustrated by considering the following example. Consider code X and code Y and the phase shifted versions code X^1 and code Y^1. Code X has a period of 11 and code Y has a period of 31, as shown in Fig. VI-2.

A method of generating code Y is shown in Figure VI-3.

The auto correlation function of code X is shown in Figure VI-4.

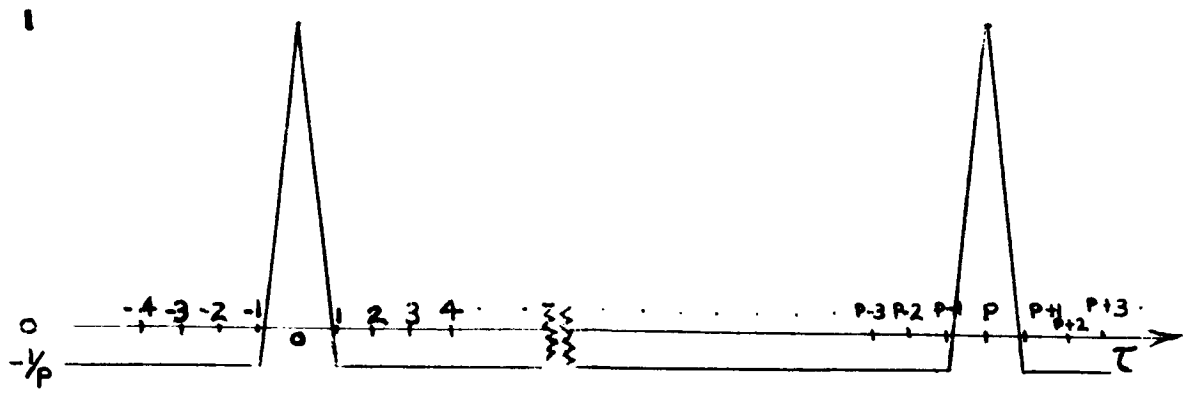

FIGURE VI-1. Autocorrelation Function of Ranging Code

CODE X 1 0 0 1 1 0 1 0 1 1 1 . . . L=11

CODE Y 0 0 0 0 1 0 0 1 0 1 1 0 0 1 1 1 1 1 0 0 0 1 1 0 1 1 1 0 1 0 1 . . . L=31

CODE X' 0 1 0 1 1 1 1 1 0 0 1 1 PHASE (CODE X) ≠ PHASE (CODE X')

CODE Y' 1 1 0 1 1 1 0 1 0 1 0 0 0 0 1 0 0 1 0 1 1 0 0 1 1 1 1 1 1 0 0 0 PHASE(CODE Y) ≠ PHASE(CODE Y')

FOR CODE X P(0) = 4/11
P(1) = 7/11

FOR CODE Y P(0) = 5/31
P(1) = 16/31

CODE (X·X') 0 0 0 1 1 0 1 0 0 1 1 . . . P(00) = 2/11
P(01) = 2/11
P(10) = 2/11
P(11) = 5/11

CODE (Y·Y') 0 0 0 0 1 0 0 1 0 1 0 0 0 0 1 0 0 1 0 0 0 0 0 0 1 1 1 0 0 0 0 . . . P(00) = 7/31
P(01) = 8/31
P(10) = 8/31
P(11) = 8/31

FIGURE VI-2. Cross-Correlation of Codes

TRUTH TABLE (STATES) OF A 5 BIT MAXIMAL LENGTH SHIFT REGISTER
(PERIOD = 31)

A	B	C	D	E	
1	0	0	0	0	
0	1	0	0	0	
0	0	1	0	0	
1	0	0	1	0	
0	1	0	0	1	
1	0	1	0	0	
1	1	0	1	0	
0	1	1	0	1	
0	0	1	1	0	
1	0	0	1	1	
1	1	0	0	1	
1	1	1	0	0	
1	1	1	1	0	Portion of Sequence During Which Phase Shifting is Accpmplished
1	1	1	1	1	
0	1	1	1	1	
0	0	1	1	1	
0	0	0	1	1	
1	0	0	0	1	
1	1	0	0	0	
0	1	1	0	0	
1	0	1	1	0	
1	1	0	1	1	
1	1	1	0	1	
0	1	1	1	0	
1	0	1	1	1	
0	1	0	1	1	
1	0	1	0	1	
0	1	0	1	0	
0	0	1	0	1	
0	0	0	1	0	
0	0	0	0	1	
1	0	0	0	0	← 31 = PERIOD
					← OUTPUT SEQUENCE

$$A^{t+1} = (C \oplus E)^{t}$$

Controlling Equation

FIGURE VI-3 GENERATION OF CODE Y

^1 0 0 1 1 0 1 0 1 1 1^1 0 0 1 1 0 1 0 1 1 1^1 0 0 1 1 0 1 0 1 1 1^

CODE (X X) $\tau = 0$	1 0 0 1 1 0 1 0 1 1 1	7-1 ORIGINAL CODE	P = 1
CODE (X X') $\tau = 1$	1 0 0 0 1 0 0 0 0 1 1	4-1	P = 5/11
$\tau = 2$	1 0 0 0 0 0 1 0 1 0 1	4-1	P = 5/11
$\tau = 3$	1 0 0 1 0 0 1 0 0 1 0	4-1	P = 5/11
$\tau = 4$	0 0 0 1 1 0 0 0 1 0 1	4-1	P = 5/11
$\tau = 5$	1 0 0 1 1 0 0 0 1 1 0	5-1	P = 7/11
$\tau = 6$	0 0 0 1 1 0 1 0 0 1 1	5-1	P = 7/11
$\tau = 7$	1 0 0 0 1 0 1 0 0 0 1	4-1	P = 5/11
$\tau = 8$	1 0 0 1 0 0 1 0 1 0 0	4-1	P = 5/11
$\tau = 9$	0 0 0 0 1 0 1 0 1 1 0	4-1	P = 5/11
$\tau = 10$	0 0 0 1 0 0 0 0 1 1 1	4-1	P = 5/11

FIGURE VI-4

AUTO-CORRELATION FUNCTION, PERIOD 11 CODE

The period of overall code is 11 x 31 = 341 bits. The value of the correlation function for the cases when the overall sequence is in phase, the correlation when X is in phase, the correlation when Y is in phase, and the correlation when neither X and Y is in phase can be determined from the Probabilistic Karnaugh Maps as shown in Figure VI-5 and VI-6.

$$A \oplus B = A\bar{B} + \bar{A}B$$

Let $A = X \cdot Y$ $\qquad$ $B = XY'$

$$XY \oplus XY' = XY \cdot \overline{XY'} + \overline{XY} \cdot XY'$$

$$= XY(\bar{X} + \bar{Y}') + (\bar{X} + \bar{Y})XY'$$

$$= X\bar{X}Y + XY\bar{Y}' + X\bar{X}Y' + X\bar{Y}Y'$$

$$= XY\bar{Y} + X\bar{Y}Y'$$

X \ YY'	00	01	11	10
0				
1		1		1

P(X) \ P(YY')	7/31 00	8/31 01	8/31 11	8/31 10
$4/_{11}$	$\frac{28}{341}$	$\frac{32}{341}$	$\frac{32}{341}$	$\frac{32}{341}$
$7/_{11}$	$\frac{49}{341}$	$\frac{56}{341}$	$\frac{56}{341}$	$\frac{56}{341}$

$$P_1 \cdot P_2 = 11 \cdot 31 = 341$$

$$P(0) = \frac{28 + 3(32) + 49 + 56}{341} = \frac{229}{341}$$

$$P(1) = \frac{2(56)}{341} = \frac{112}{341}$$

$$P = \frac{229 - 112}{341} = \frac{117}{341} \approx .343$$

FIGURE IV-5. CORRELATION WHEN X IN PHASE, Y OUT OF PHASE

Determination of the correlation coefficient when neither X or Y is in phase is shown below:

Let $A = X\bar{Y}$

$B = X'Y'$

$$XY \oplus X'Y' = XX'Y + X\bar{Y}Y' + \bar{X}X'Y' + X'\bar{Y}Y'$$

XX', YY'	00	01	11	10
00				
01		1	1	
11		1		1
10			1	1

$P(XX')$ \ $P(YY')$	7/31 00	8/31 01	8/31 11	8/31 10
2/11 00				
2/11 01		$\frac{16}{341}$	$\frac{16}{341}$	
5/11 11		$\frac{40}{341}$		$\frac{40}{341}$
2/11 10			$\frac{16}{341}$	$\frac{16}{341}$

$$P(1) = \frac{2(16) + 2(40) + 2(16)}{341} = \frac{144}{341} \quad .422$$

$$P(0) = \frac{341-144}{341} = \frac{197}{341} = .578$$

$$P = \frac{197-144}{341} = \frac{53}{341} = .1565$$

FIGURE VI-6. Calculation of Correlation When Neither Code X or Code Y are in Phase.

Not all combination sequences have autocorrelation functions with sub-peaks at multiples of the component sequence lengths. This can be illustrated by considering the linear logical combination of component codes X and Y.

The effect of using linear combining of sequences is shown in Figure VI-7. For this situation both components X^1 and Y^1 must be in phase with X and Y, respectively, for the correlation to be other than a very small value. For example, if the phases of X^1 and X are equal, the normalized correlation is still a very small value. This is an undesirable condition since the time required to "acquire" the code can be greatly reduced by acquiring components of the code. This requires a significant correlation "jump" in the correlation as each component of the overall code is brought into proper phase.

The computation of the correlation value for various phase alignments can be simplified if the assumption if made that the sub-sequences have equally as many ones and zeros. This leads to the approximation that for an out-of-phase code component, the four situations 00, 01, 10 and 11 occur equally after. With this approximation all the entries on the Karnaugh Map are equal and only the number of 1's and 0's need be counted to determine the correlation.

D. Range Tracking System Proposed for Laser Communication System

1. Description of the System Block Diagram

The ranging system which has been designed for the laser deep space communication system is shown in Figure VI-8. Operation of the system is as follows: The non-linear code generator KS1 is clocked

$X \oplus Y \oplus X' \oplus Y'$

$(X\bar{Y} + \bar{X}Y) \oplus (x'\bar{y}' + \bar{x}'y)$

$(X\bar{Y} + \bar{X}Y) \cdot \overline{(x'\bar{y}+\bar{x}'y')} + \overline{(X\bar{Y}+\bar{X}Y)} \cdot (x\bar{y}'+\bar{x}'y)$

$(X\bar{Y}+\bar{X}Y) \cdot \left[\overline{(x'\bar{y}')}\ \overline{(\bar{x}'y')}\right] + \left[\overline{(X\bar{Y})}\ \overline{(\bar{X}Y)}\right] \cdot (x'\bar{y}'+\bar{x}'y')$

$(X\bar{Y}+\bar{X}Y)\left[(\bar{x}'+y')\ (x'+\bar{y}')\right] + \left[(\bar{X}+Y)\ (X+\bar{Y})\right] \cdot (x'\bar{y}'+\bar{x}'y')$

$(X\bar{Y}+\bar{X}Y)\left[\bar{x}'x'+\bar{x}'\bar{y}'+\bar{x}'\bar{y}'+y'\bar{y}'\right] + \left[\bar{X}\bar{X}+\bar{X}\bar{Y}+XY+Y\bar{Y}\right](x'\bar{y}'+\bar{x}'y')$

$X\bar{Y}\bar{x}'y'+X\bar{Y}x'y'+\bar{X}Y\bar{x}'\bar{y}'+\bar{X}Yx'y'+\bar{X}\bar{Y}x'\bar{y}'+\bar{X}\bar{Y}\bar{x}'y'+XYx'\bar{y}'+XY\bar{x}'y'$

$X\bar{x}'\bar{Y}\bar{y}'+Xx'\bar{Y}y'+\bar{X}\bar{x}'Y\bar{y}'+\bar{X}x'Yy'+\bar{X}x'\bar{Y}\bar{y}'+\bar{X}\bar{x}'\bar{Y}y'+Xx'Y\bar{y}'+X\bar{x}'Yy'$

P(Xx') \ P(Yy')	4/31 3/15 00	8/31 4/15 01	8/31 4/15 11	8/31 4/15 10
2/11 1/7 00		16/341		16/341
2/11 2/7 01	14/341		16/341	
5/11 2/7 11		40/341		40/341
2/11 2/7 10	14/341		16/341	

Phase x' ≠ Phase X

Phase y' ≠ Phase Y

Xx' \ Yy'	00	01	11	10
00		1		1
01	1		1	
11		1		1
10	1		1	

$P(1) \approx 1/2$

$P(0) \approx 1/2$

$P \approx \frac{8-8}{16} \approx 0$

$P = \frac{4-4}{8} = 0$

$P = \frac{4-4}{8} = 0$

IF: $\varphi(X) = \varphi(X')$ Delete Rows 2 & 4

$\varphi(Y) = \varphi(Y')$ Delete Columns 2 & 4

∴ No peaks @ multiples of the periods of the component sequence lengths

FIGURE VI-7 SUBPEAK CALCULATION

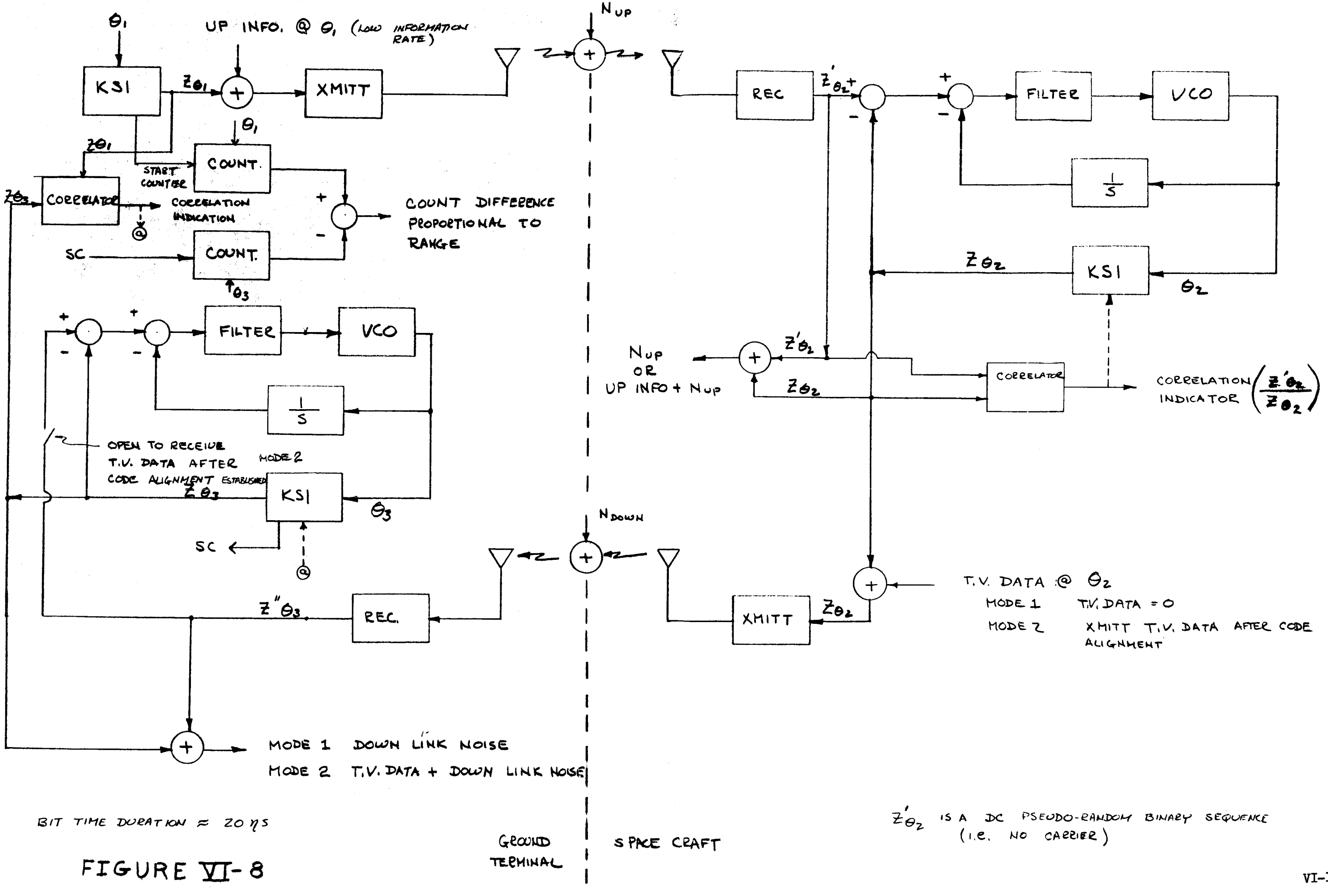

BIT TIME DURATION ≈ 20 ηs

Z'_{θ_2} IS A DC PSEUDO-RANDOM BINARY SEQUENCE (i.e. NO CARRIER)

FIGURE VI-8

by Θ_1 (50 $\frac{MC}{SEC}$) and modulates the laser carrier frequency. The transmitted signal plus up link noise is received in the spacecraft receiver at rate Θ_2 due to doppler shift. For non-coherent reception, the laser receiver can be considered as a bandpass limiter, its output being +1 or -1, with the carrier frequency removed. A coherent laser receiver is not felt feasible at this time.

The pseudo-random sequence from the laser receiver $Z'\Theta_2$ is sent to phase locked loop and the correlator. Since the code has as one code component the clock, no difficulties are encountered as the incoming code sequence slides past the locally generated code. In effect, the inner loop is free to lock up fairly quickly. It can slip any number of bits while aligning the remaining components of the code. This procedure has a number of advantages over other technqiues. First there is a basic clock component in the received code on which the inner loop can be locked, and secondly, there are no quasi-stable nulls on which the loop could mistakenly lock, as are present in some other methods. As indicated in Figure VI-8, Mode 1 is when the ranging code is being transmitted and received, and Mode 2 is when T. V. Data is being transmitted from the spacecraft after the range codes have been aligned and range measurements obtained. With a clock component in the incoming sequence the standard early gate - late gate technique could be used to establish "Bit Lock". Since the proposed ranging system is to also handle down-link T.V. Date, this information will also need clock component. However, since KS1 in the spacecraft is keying the T.V. Data, a clock component will be present in the T.V. Data stream and can be bit locked by

the ground station early-gate - late-gate arrangement. In effect, secure T.V. Data is provided by the KS1 keying. In Mode 1 the codes $Z\Theta_1$ and $Z\Theta_2$ are correlated. When the codes are aligned, a code word is decoded from the two KS1 ground station code generators which start two counters, one counting Θ_1, the up-link clock, and the other Θ_3, the received clock rate. Any time after the counters have been started the difference in count is proportional to the range and the rate at which the difference in count is changing is proportional to the range rate. The code words for starting the counters should be such that no ambiguities are generated in the starting times of the two counters.

If bit synchronization is for some reason lost while operating in mode two, the code must be acquired again by the ground station receiving pseudo-random generator. In Mode 2, the T.V. information is being clocked by the spacecraft clock and, for the keying code to be properly removed from the T.V. Data, ground terminal tracking of the code is essential.

When bit sync is lost while in Mode 2, the T.V. Data transmission is stopped and the ground station receiving pseudo-random generator is aligned code component by code component until it is in-phase with the spacecraft code. T.V. Data transmission may then be resumed. Notice that the spacecraft code generator need not be realigned with the transmitted code sequence unless additional range measurements are needed.

2. Phase Locked Loop Requirements

a. Desirable Loop Characteristics

Since the bandwidth requirement of the phase locked loops is primarily determined by the doppler frequency shift, a loop bandwidth of approximately 4 $\frac{kc}{sec}$ (at 50 $\frac{MB}{SEC}$) should be sufficient. The reference

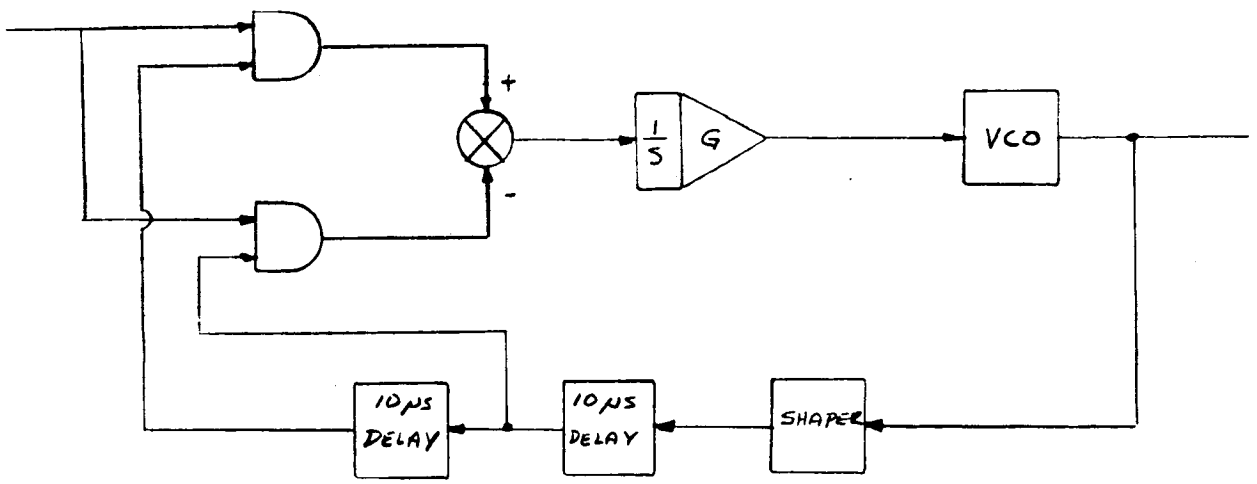

FIGURE VI-9. Early-Gate/Late Gate Digital Tracking Loop.

signal from the photomultiplier tube in the receivers, to the phase-locked loop is identical to that which would be obtained from a band-pass limiter. It has been theoretically and experimentally shown that a phase locked-loop preceded by a bandpass limiter approximates, over a wide range of input signals and noise levels, the optimum obtainable performance. The inner loops should correspond to a Type 2 continuous control system (i.e., two integrations) with sufficient loop gain and lead compensation to insure satisfactory transient response. A typical linear approximation of the asympotic frequency characteristic of a continuous inner loop is shown in Figure VI-10.

Circled intersections of the real axis frequency plot with the unity gain line are the closed loop roots (poles). As can be seen from this typical plot, of this gain the loop would have four real roots. As the gain is raised (lowered on the plot) the closed loop roots are shifted as shown with a breakaway point (i.e., a complex root) occurring as indicated. The same phenomenon would occur at a different location if the gain were lowered. It is essential therefore that the phase locked loops be carefully designed to insure satisfactory system performance. A treatment of the non-linear analysis of phase locked loops is given in "Functional Techniques for the Analysis of the Non-linear Behaviour cf Phased-Locked Loops" by H. L. Van Trees.[60]

Lead compensation, which has the advantages of improving the transient response with small network components and the disadvantages of additional amplification with increased high frequency components of the noise, should be satisfactory due to the high signal-to-noise ratio from the photomultiplier tube in the receiver.

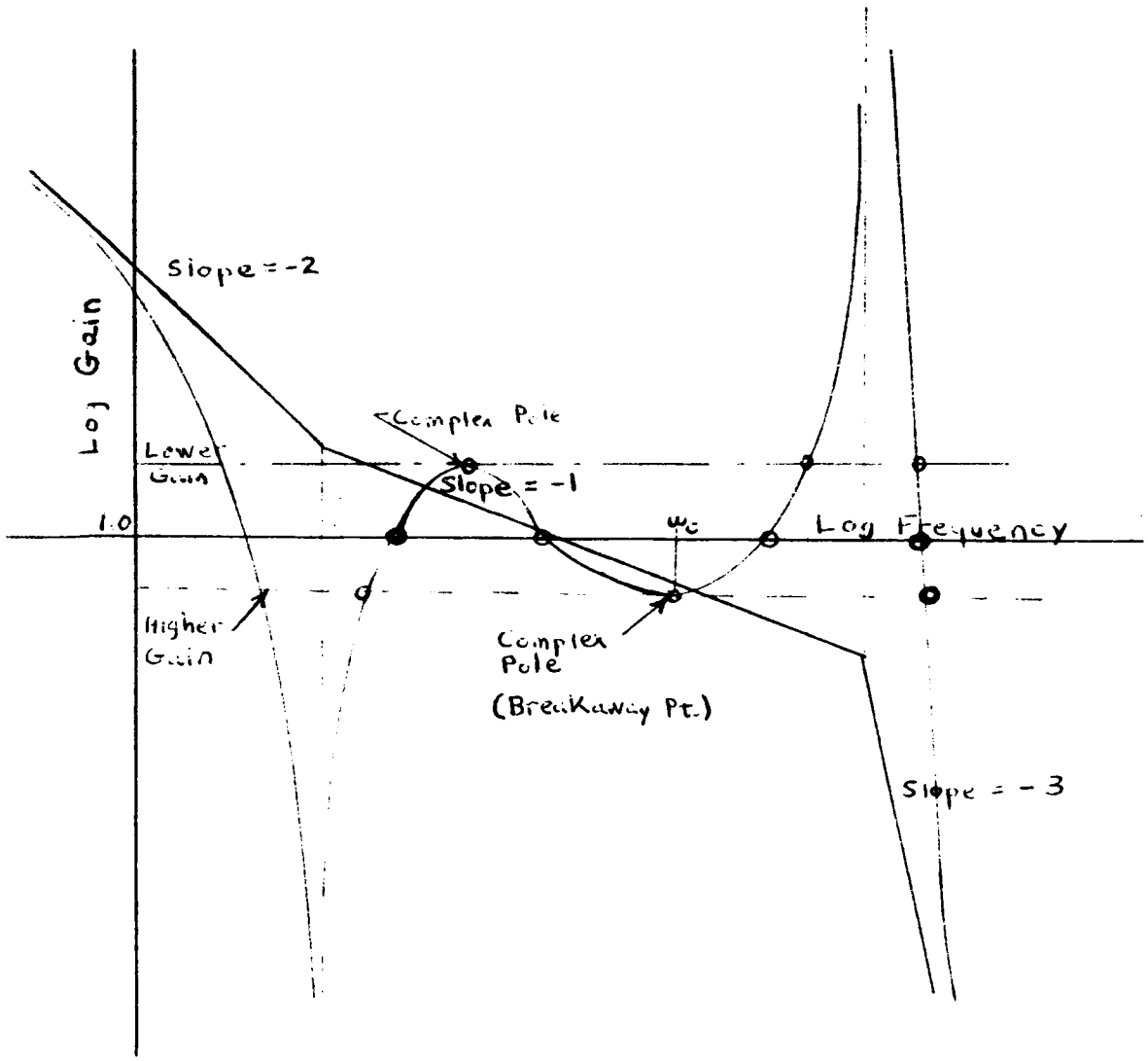

FIGURE VI-10. Asymptotic Characteristics of Phase Locked Loop.

b. Code Synchronization

The outer loop which supplies the local reference pseudo-random code must be aligned, code component by code component, with the incoming signal while bit locked by the inner loop but not phase locked over the period of the total code. Phase shifting the individual components of the codes is then accomplished with the aid of the correlator which controls the shifting.

3. Predicted Ranging Performance

An estimate of the time required to acquire the ranging code developed for the laser communications system assuming optimum detection in the laser receiver can be obtained as follows:

Let

T = Time for receiving one bit of information (one information bit)

L = Code length

p = Code correlation

k = Boltzmann's constant

t = Temperature (°K)

τ = Time required to acquire code

S = Signal power (watts)

χ = Signal to noise energy ratio

Then $$\tau = \frac{\log_2 L \cdot T \cdot L}{p^2}$$ where if $$\frac{ST}{(N/B)} = \chi$$

$$T = \frac{\chi (N/B)}{S}$$

$$T = \chi \frac{kt}{S} \text{ (sec)}$$

Total Acquisition Time $\tau_T = \sum_{i=1}^{n} \left(\frac{\log_2 L_i \cdot T_i \cdot L_i}{\rho^2} \right)$ (1-1)

Example - Ranging Code Acquisition Time from equation 1-1:

$$\tau \text{ (sec)} = \frac{(L)\ (\log_2 L)\ (kt)\ (\mathcal{X})}{S\ P^2} \qquad \text{(Using Fig. VI-11)}$$

Assumed:

$L = 31$

$t = 300^{\circ}$ K

$S = 10^{-11.7}$ watts = -87 dbm

$P = 3/8$

Desired error probability = 10^{-3}

* Digit Duration = 2×10^{-8} = 17 db increase over 1 usec for same error rate

$$\tau = \frac{(31)\ (4.96)\ (1.37 \times 10^{-23})\ (300)(3 + 17)^{*}\ (64)}{(10^{-11.7})\ (9)}$$

$$\tau = 9 \times 10^{-5.3}$$

$$\tau = 4.5 \times 10^{-5} \text{ sec}$$

$\therefore$ Using $\frac{4.5 \times 10^{-5}}{2 \times 10^{-8}} = 2.26 \times 10^{3}$ digits to acquire code component A (L = 31) with above assumptions

* Since the curves in Figure VI-11 are based on a digit period of 1 us (or 1 MB/sec) for 50 MB/sec we must ADD 17db to the abscissa coordinates which means 17 db more signal energy per information bit is required:

$$\left(\text{db} = 10 \log_{10} \frac{1 \times 10^{-6}}{2 \times 10^{-8}} \quad 10 \log_{10} (50) = 17 \right)$$

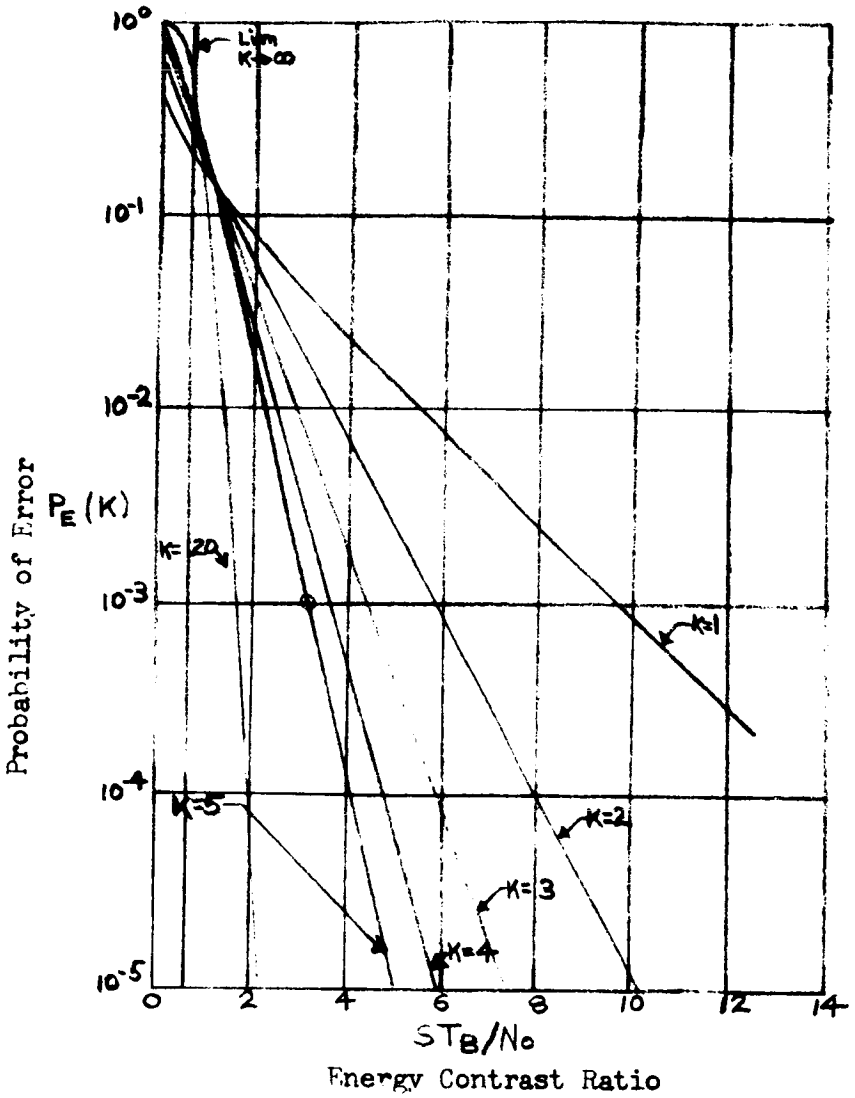

FIGURE VI-11

Probability of Error Versus Energy Contrast Ratio

A worse case estimate assuming a signal level of -100 dbm for acquiring the total code is given below:

L	$(\log_2 L)$	X(db)	T(sec)	TOTAL TIME /CODE COMPONENT τ (sec x 10^{-5})
11	3.46	23.0	94.5×10^{-8}	$3.46 \times 94.5\times10^{-8} \times 11\times \frac{64}{9} = 25.6$
31	4.96	20.4	83.8×10^{-8}	$4.96 \times 83.8\times10^{-8} \times 31\times \frac{64}{9} = 91.8$
79	6.31	19.7	81×10^{-8}	$6.31 \times 81\times10^{-8} \times 79\times \frac{64}{9} = 288$
97	6.6	19.7	81×10^{-8}	$6.6 \times 81\times10^{-8} \times 97\times \frac{64}{9} = 369$
103	6.69	19.6	80.6×10^{-8}	$6.69 \times 80.6\times10^{-8} \times 103\times \frac{64}{9} = 396$
127	6.99	19.5	80.1×10^{-8}	$6.99 \times 80.1\times10^{-8} \times 127\times \frac{64}{9} = 506$

$$\tau_{TOTAL} = 1.67\times10^{-2}\text{(sec)}$$

$$T = \frac{kt}{s} X$$

Assuming: $t = 300°K$

$s = 100 \text{ dbm} = 10^{-13} \text{watts}$

Error Probability = 10^{-3}

$$T = \frac{1.37\times10^{-23}\times300}{10^{-13}} \quad X = 1.37\times10^{-8}\times3 \; X$$

$$T = 4.11 \times 10^{-8} X$$

τ_{TOTAL} = total acquisition time for entire code using above assumption.

4. Communications Aspects of the System

Once the total ranging code has been acquired both in the spacecraft and the ground station and the range determined, the pseudo-random code generator of the spacecraft receiver may be used to key the T. V. Data over the spacecraft transmitter. A "secured" communications channel is therefore provided by the ranging system. The coded T. V. information is decoded at the ground station terminal, using as a reference the ground station receiver pseudo-random code generator, as mentioned previously. The method is entirely dependent on the ability of the ground terminal to track the incoming clock θ_3. This clock rate can be traced back to the ground station clock and includes the up-going doppler shift as well as the down link doppler shift. The net effect of the total doppler shift is then the sum of these two frequency shifts. The quality of the T. V. picture should not be adversely affected by the frequency shifts, since the T. V. data is digitized information, and will depend on the quantization levels when digitizing the information.

E. Implementation of Proposed System

1. Design of Sequence Generators With Specified Periods

The logical design of the component code generators is shown in Figures VI-12 through VI-19. In general, there are a number of ways to construct pseudo-random sequence generators with specified periods. For example, maximal length sequence generators, modified by the detection of certain code words to change the feedback sequence, thus changing the basic cyclic period, can be used. This method has successfully been used by JPL on the Mariner and Voyager Space Shot and it is the method used in this ranging system. Another technique is to construct a maximal sequence

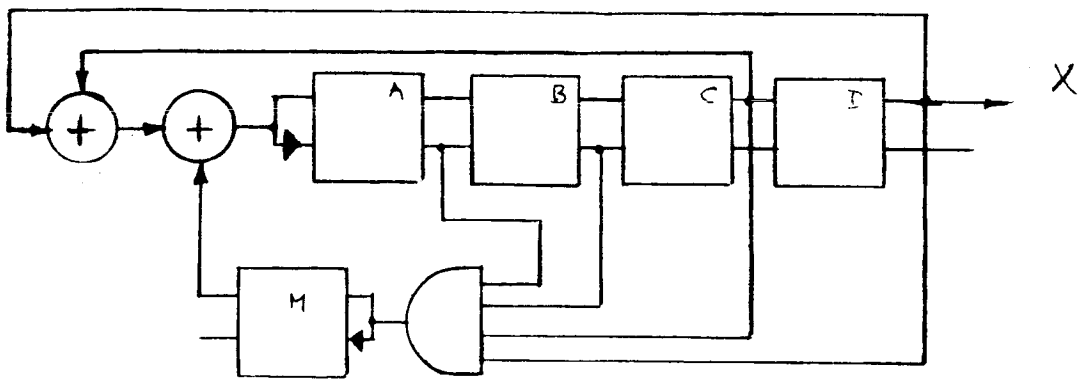

X Generator (Period = 11)
(Not shown with phase shift capability)

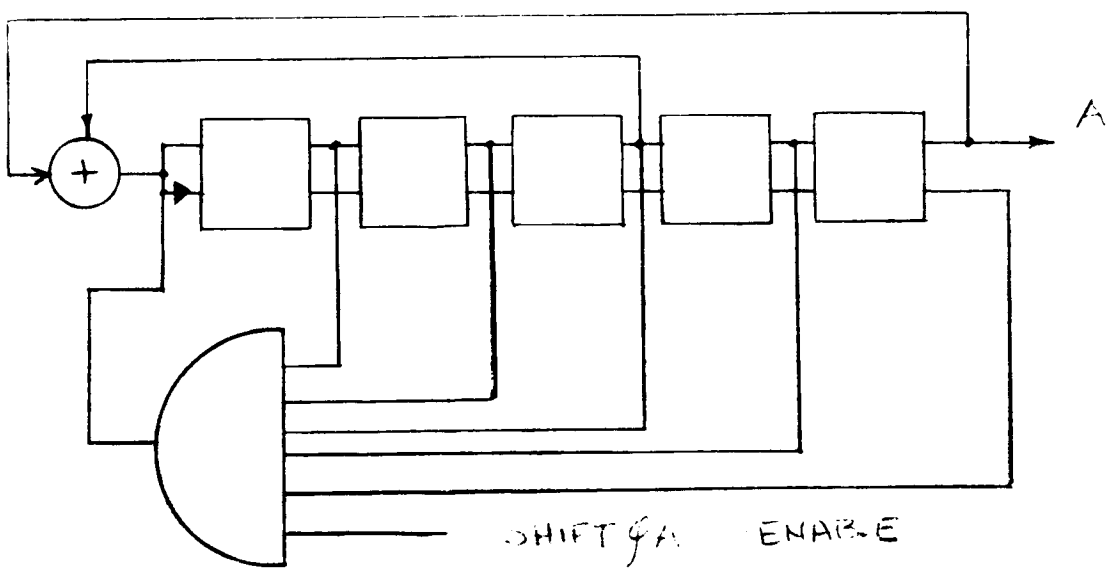

A Generator (Period = 31)

FIGURE VI-12

M^t	A^t	B^t	C^t	D^t
0	1	0	0	0
0	0	1	0	0
0	0	0	1	0
0	1	0	0	1
0	1	1	0	0
0	0	1	1	0
0	1	0	1	1
0	0	1	0	1
0	1	0	1	0
0	1	1	0	1
0	1	1	1	0
0	1	1	1	1
0	0	1	1	1
0	0	0	1	1
1	1	0	0	1
0	1	1	0	0
0	0	1	1	0
0	1	0	1	1
0	0	1	0	1
0	1	0	1	0
0	1	1	0	1
0	1	1	1	0
0	1	1	1	1
0	0	1	1	1
0	0	0	1	1
1	1	0	0	1

$$M^{t+1} = \bar{A}\,\bar{B}\,C\,D^t$$

$$P_{s_s} = 11$$

TRUTH TABLE FOR X GENERATOR

FIGURE VI-13

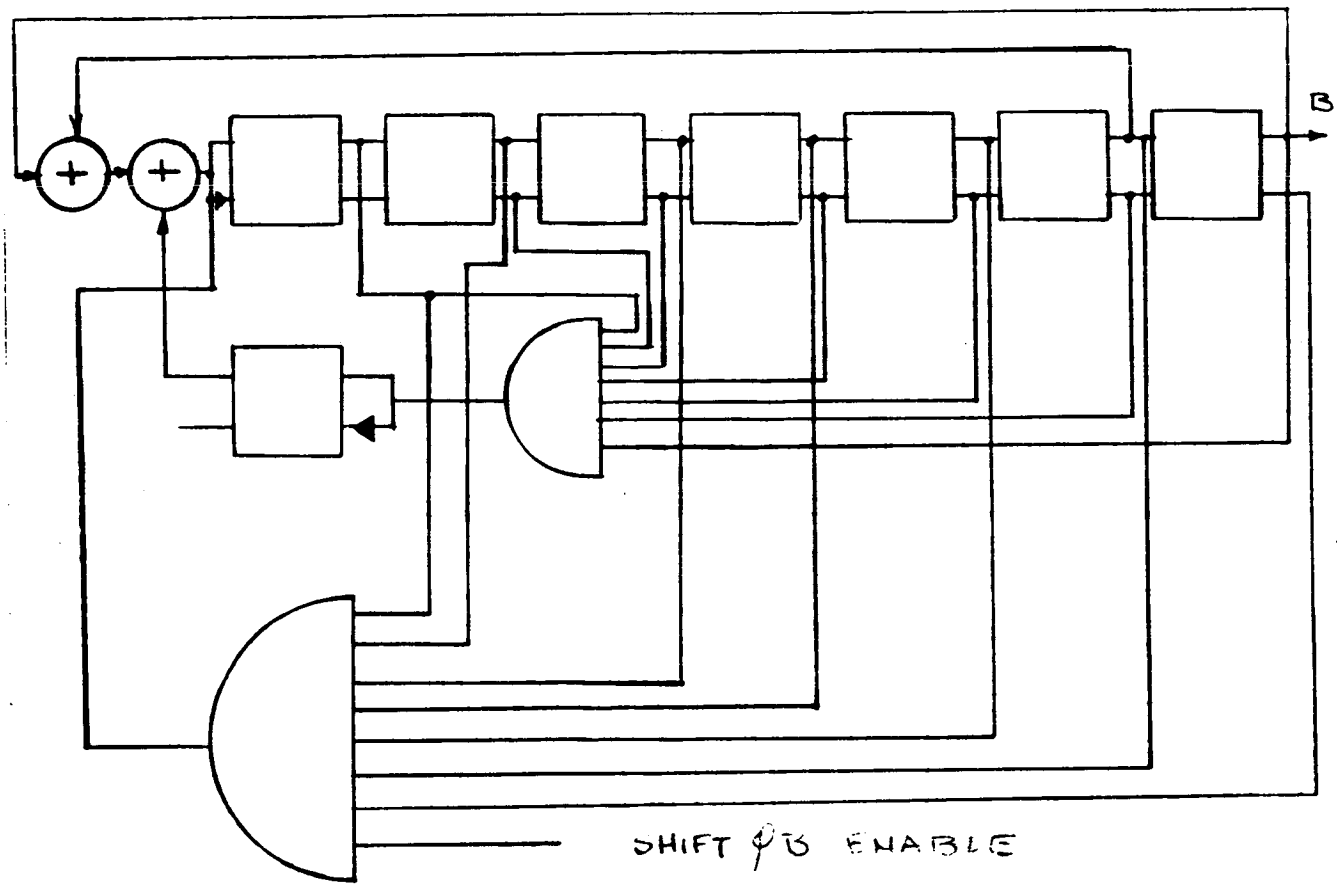

B Generator (Period = 79)

FIGURE VI-14

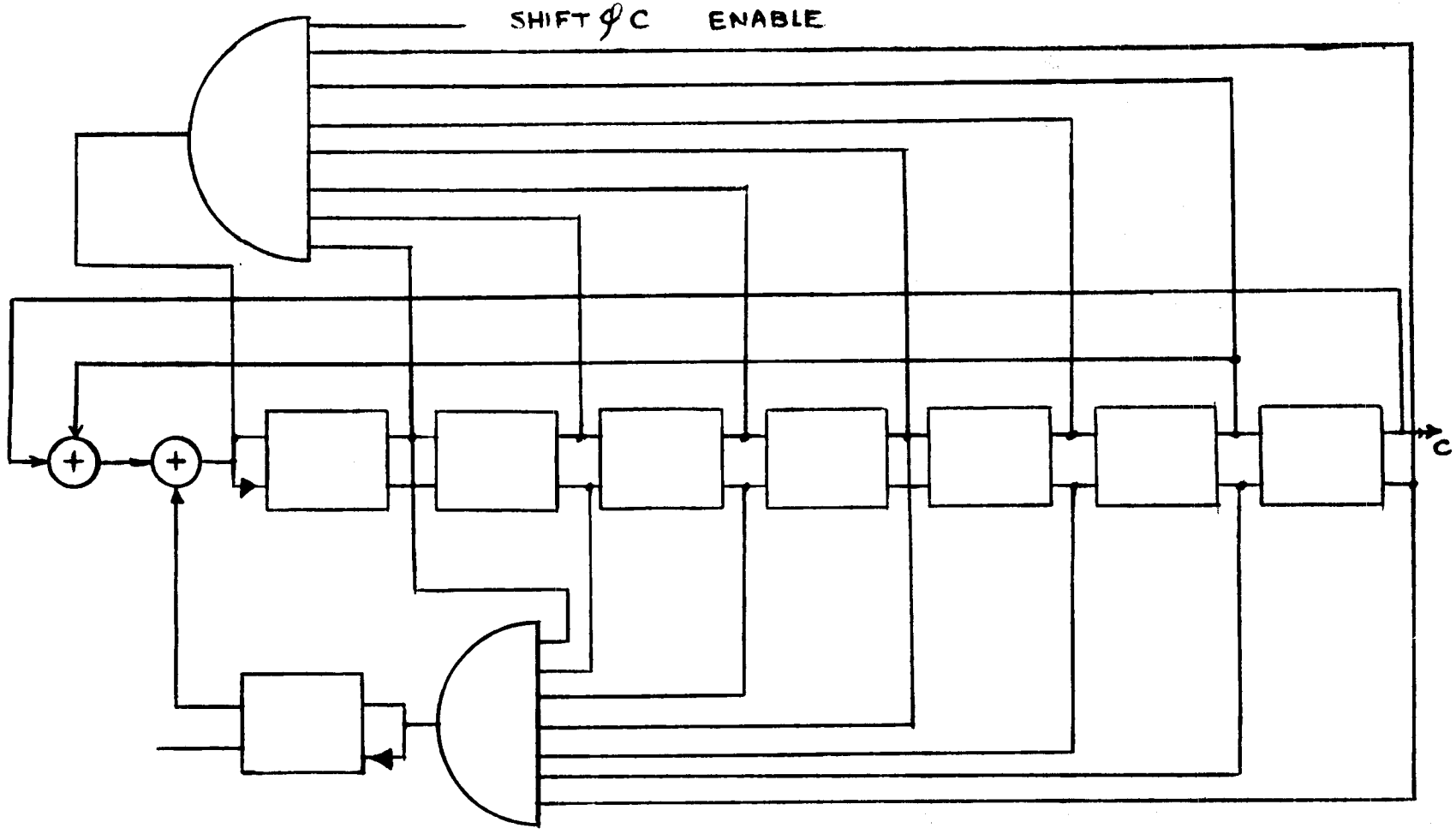

C Generator (Period = 97)

FIGURE VI-15

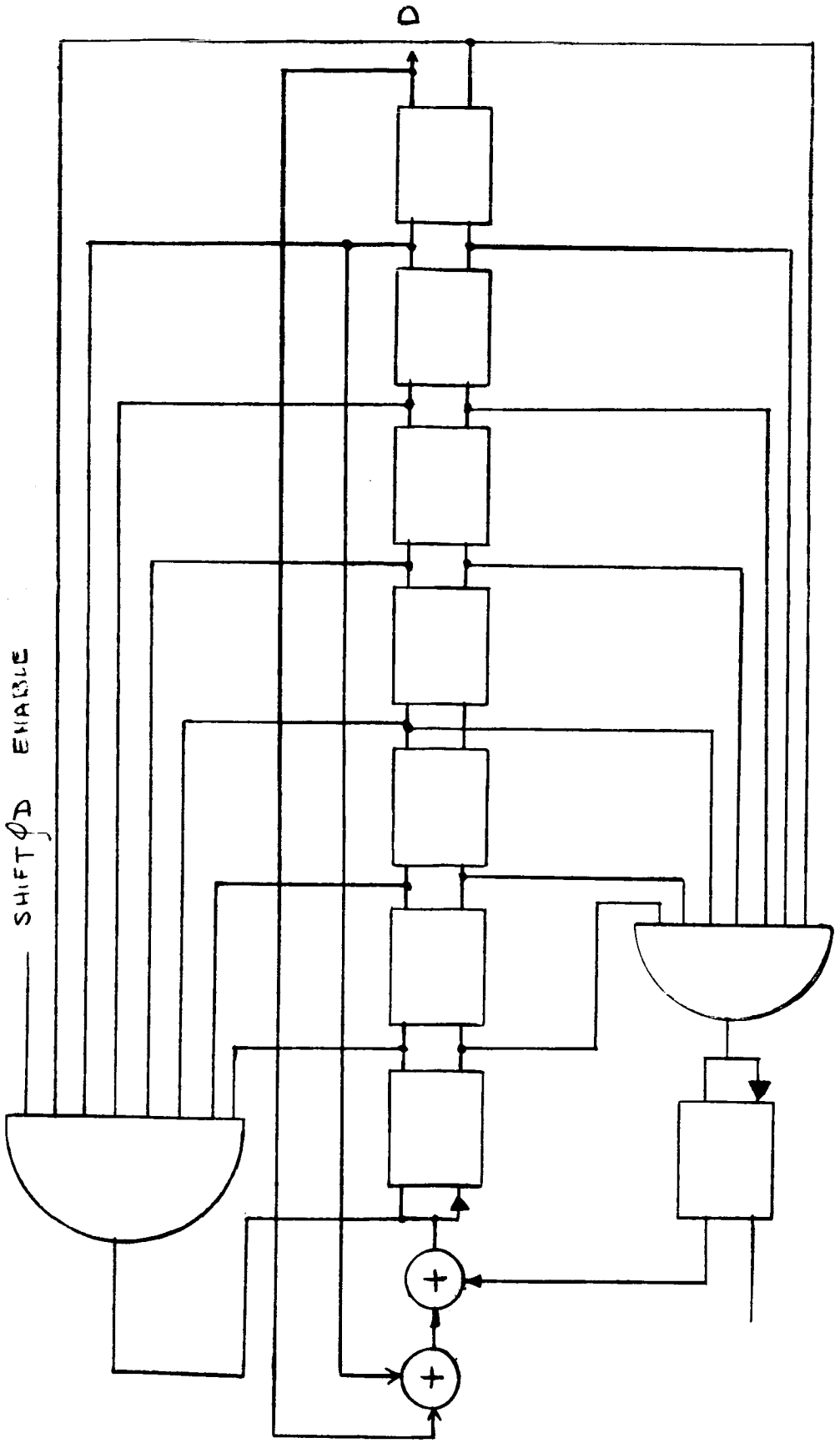

D Generator (Period = 103)

FIGURE VI-16

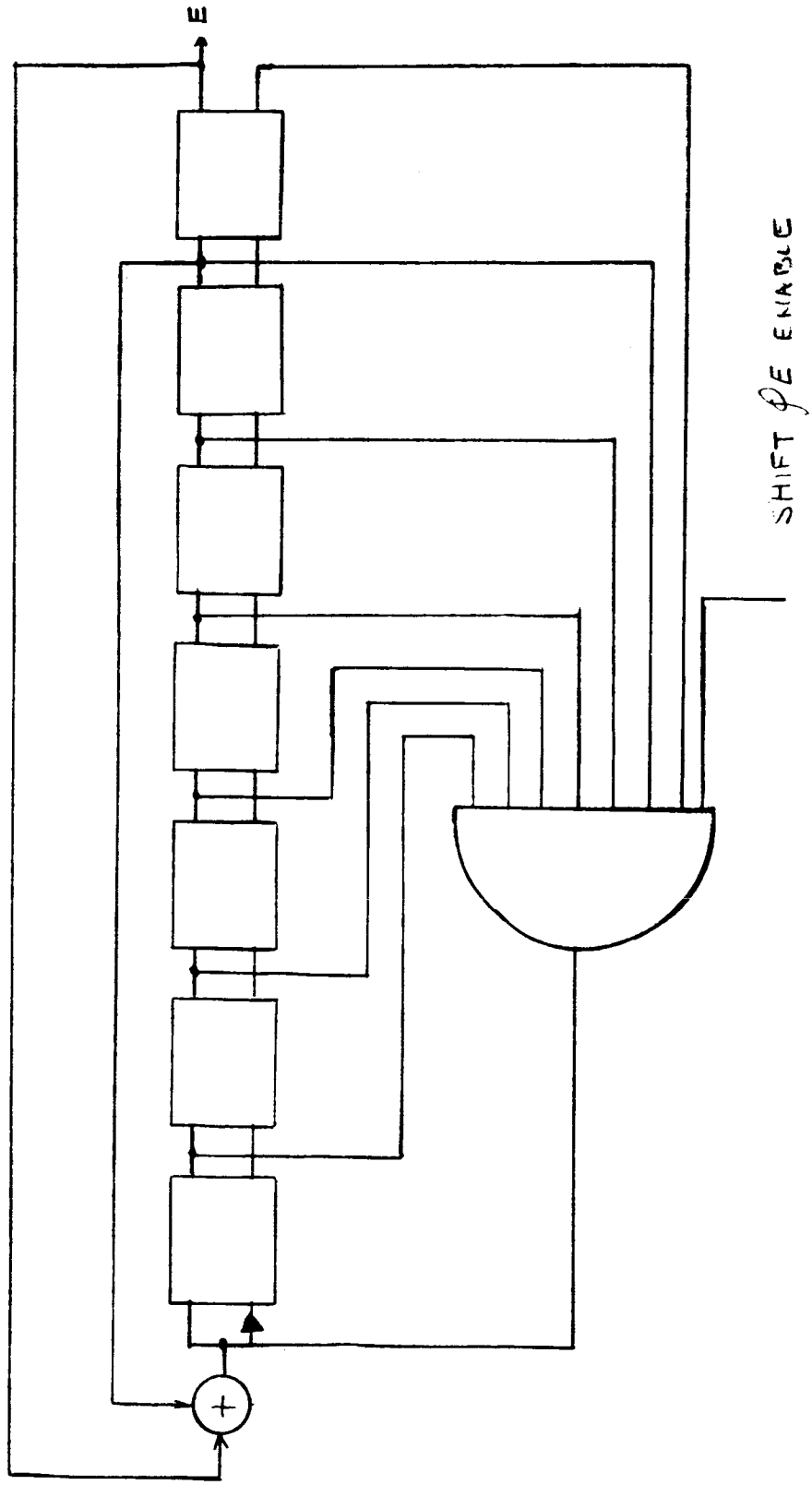

E Generator (Period = 127)

FIGURE VI-17

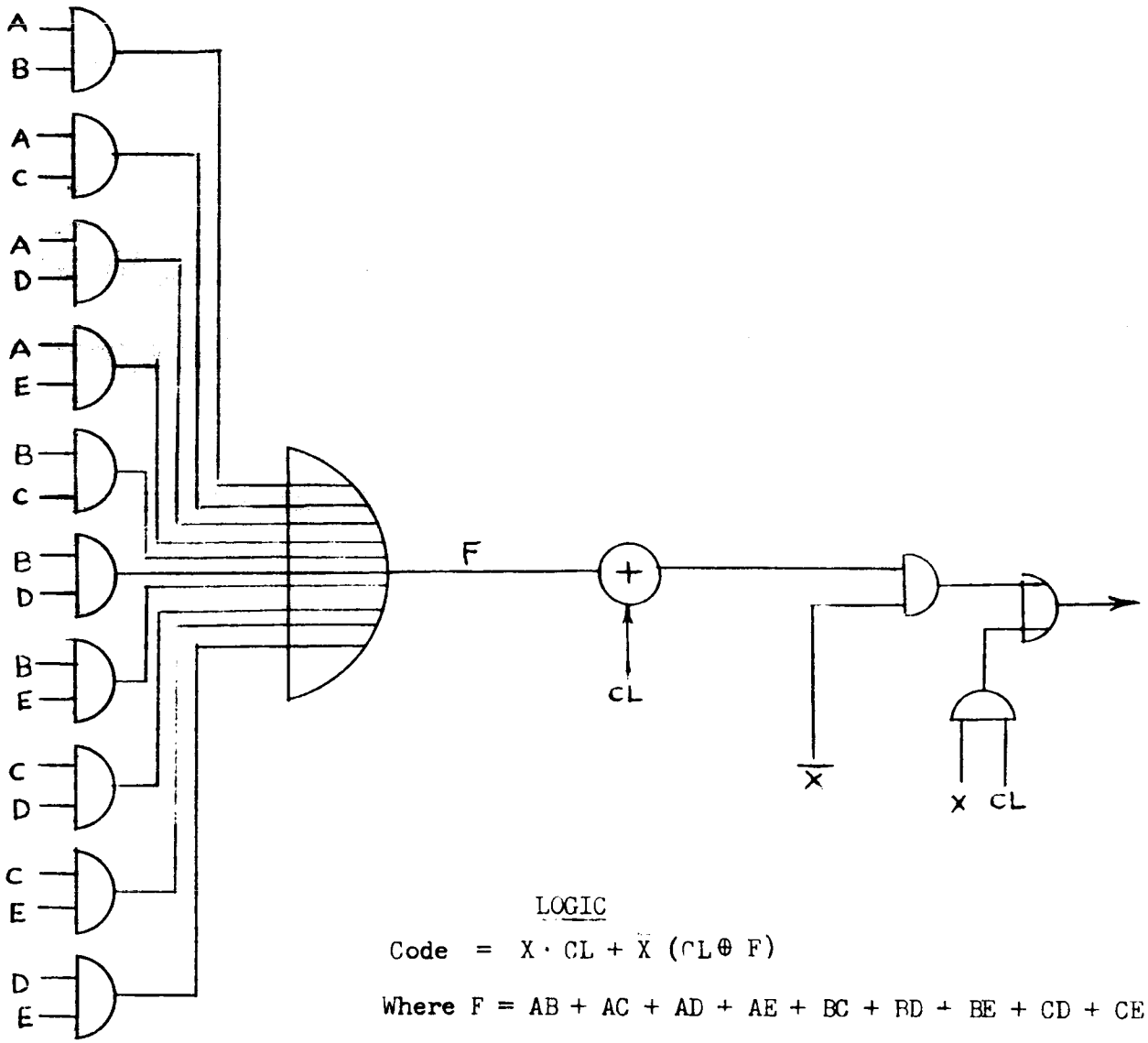

LOGIC

Code = $X \cdot CL + \bar{X} (CL \oplus F)$

Where F = AB + AC + AD + AE + BC + BD + BE + CD + CE + DE

$\cdot$ ≡ Logical "AND" Function
$+$ ≡ Logical "OR" Function
$\oplus$ ≡ Exclusive "OR" Function

FIGURE VI-18

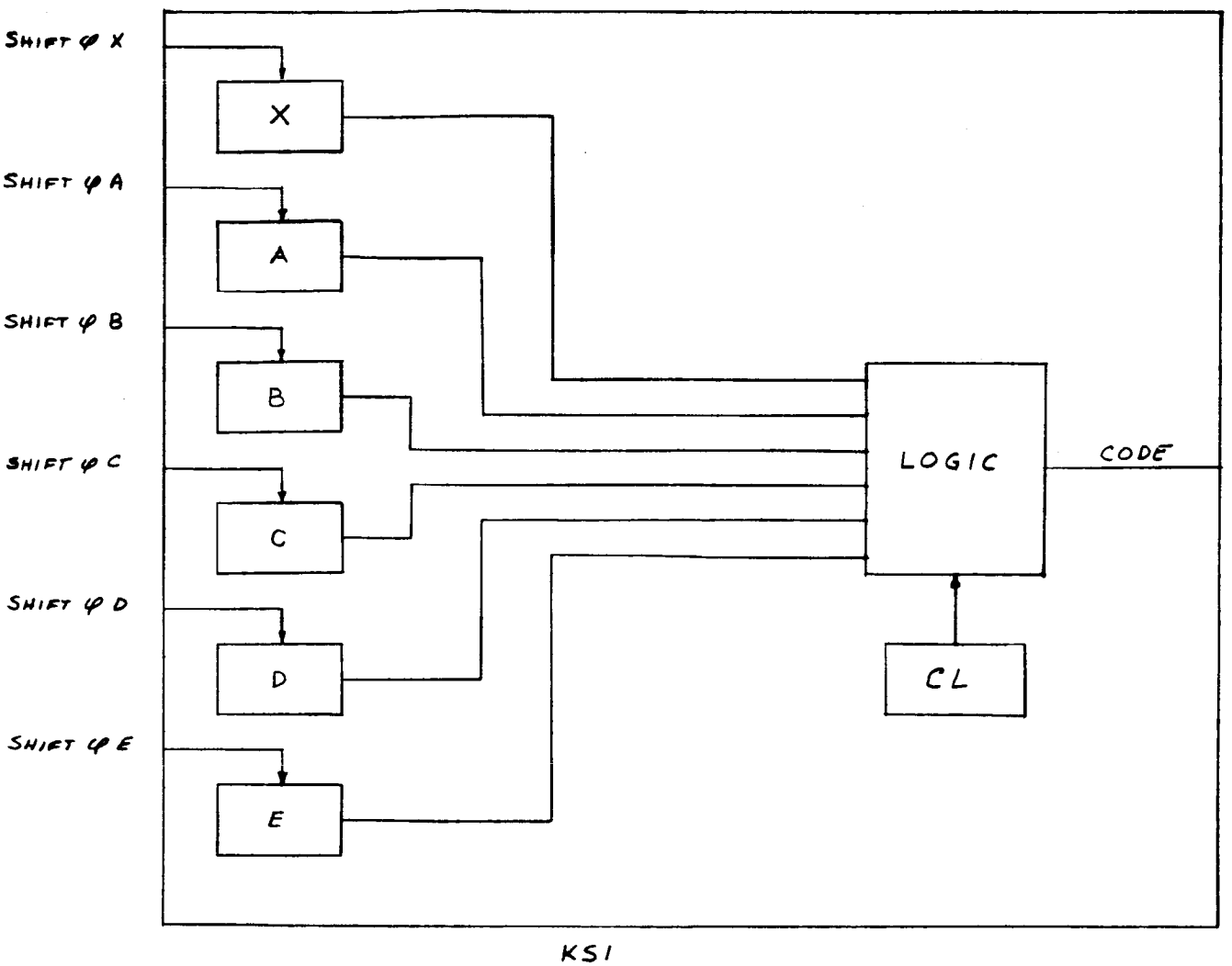

CODE	LENGTH
CL	2
X	11
B	79
C	97
D	103
E	127

FIGURE VI-19. KS1

Generator and simply count the desired number of digits, then reset the generator to its starting state. This technique has the obvious disadvantage of requiring excessive amounts of hardware. Still a third method is to use the ratio of relatively prime polynomials in a delay operator for specified periods. Unfortionally, not all period lengths can be realized by this method.

As shown in Figures VI-12 through VI-19, the indicated shift register connections will provide the corresponding cyclic period sequence lengths. To illustrate the operation, consider the X generator which is to provide a pseudo-random sequence with period 11. The truth table for this generator is shown in Figure VI-13. The generator continually shifts 0's until a 1 is placed in the A flip flop. The generator will initially go through 14 states until the state 0011 is present. When this state shows up it is detected and used to set the modifying flip flop M to the 1 state. The modifying flip flop causes the next state of the generator to B 1001. This becomes the starting state for the cyclic 11 digit period. Notice that in the 11 digit cyclic period there are 7 1's and 4 0's. Also notice that the states 1110, 1111, and 0111 are present in the cyclic 11 bit code. By decoding the 1110 state the next state of the generator may be made to be 0111 rather than 1111. One state in the cyclic sequence has been eliminated there by shifting the phase of the code 1 bit. If the states 1110, 1111, and 0111 were not used for phase shifting, the shifting would be on a probablistic basis, since it would not be known with certainty that a phase shift of

1 bit had been made. This could also adversely effect the period of component code being generated.

The method by which the indicated codes are combined is shown in Fig.VI-18. This follows a standard method for realizing non-linear codes described by Esterling[44] (pp 95). This non-linear combining of the individual code components will result in a code sequence of period 68363477446 bits with each code component of the total code having the capability of being shifted in phase.

The KS1 code generator with its code components and phase shifting controls is shown in Figure VI-19.

2. Compatability with Existing Deep Space Instrumentation Facility

A review of a number of reports[54, 55, 56] of the estimated capability of the Deep Space Instrumentation Facility for the APOLLO program indicate that Digitalized T.V. is not anticipated through 1970. For periods later than 1970 the use of Digitized T.V., although not specifically mentioned, should offer very interesting possibilities for Deep/Space Missions. Reference 55 states (pp 13) that "television is restricted to the FM channel only." The proposed digitized T.V. data link should not offer any conflicting compatability requirements with existing or planned equipment designs of the Deep Space instrumentation facility; it is simply another way of obtaining a real goal.

The ranging system technique for the laser communications system is quite similar to that used by the DSIF. The code is realized in a similar manner but component lengths are different.

It should be noted that a similar ranging systems was proposed and analyzed by R. B. Ward in the January 1967 Proceeding of the IEEE Professional Group of Communication Technology.[61] Mr. Ward's article contains results of laboratory testing of such a delay lock tracking systems when it is used for communications. The basic difference between his system, and the one presented here, is the number of ranging bits per information bit.

Section VII

REFERENCES

1. Final Report, "Advanced Study of Optical Communications from Deep Space", Westinghouse Electric Corporation, Contract NAS 9-3650, October 25, 1965.

2. First Interim Report, "Advanced Study on Optical Communications From Deep Space", Westinghouse Electric Corporation, Contract NAS 9-3650, December 7, 1964.

3. Second Interim Report, "Advanced Study on Optical Communications from Deep Space", Westinghouse Electric Corporation, Contract NAS 9-3650, March 8, 1965.

4. Third Interim Report, "Advanced Study on Optical Communications From Deep Space", Westinghouse Electric Corporation, Contract NAS 9-3650, August 15, 1965.

5. Modification Number 4, "Supplemental Agreement", Contract NAS 9-3650, August 12, 1966.

6. J. T. Bevans and A. D. LaVantine "Satellite Materials and Environmental Control System Investigation" Space Technology Labs., Inc., Los Angeles, California, AFBMD-TR-60-111, 1 January 30 June 1960, AF04 (647)-309.

7. Adli M. Bishay (Argonne National Lab., Ill.) "A Review of Some Gamma Radiation Effects on Glass (TID-17776) Oct. 1962, Contract W-31-109-eng- 38, 27 p. (VAC-7008).

8. E. A. Boettner and L. J. Miedler (University of Michigan, Ann Arbor) "Transmittance Changes in Glasses Induced by Ultraviolet Irradiation", J. Opt. Soc. Am. 51, 1310-11 (1961).

9. S. M. Brekhovskikh, "Color and Transparency Changes in Glasses under Action of CO-60 and Nuclear Reactor Radiation", Atomnaya Energie, Vol. 8, January 1960, pp 37-43.

10. M. Comstock and P. Ferrigno, "Effects of Radiation on Glass", Bibliography Brookhaven National Lab., Upton, New York, TID-17180, BNL-6513, 1962, AT(30-2)-GEN-16, 50 pp.

11. W. H. Cropper, "Radiation-Induced Coloration in Glass", Sandia Corp., SCR-79, Aug. 1959, Reprint available: ASTIA, AD 220599.

12. R. Fishcer, "Luminescence of Quartz and Quartz Glass Produced by Gamma Radiation", Silikat Tech., 11:453-4 (Oct. 1960).

13. G. Gigas, N. M. Ewbank, and D. E. Gruber, "Interim Report on the Appolo Window Materials Radiation Program", North American Aviation, Inc.,) Atomics International Canoga Park, Calif., IA-MEMO-9366, Feb. 1964, Interim Report, 142 pp.

14. J. Raymond Hensler, Norbert J. Kreidl, and Eberhardt Lell, "Irradiation Damage to Glass", Bausch and Lomb, Inc. TID-11034, Nov. 1960, AT(30-1)-1312, 46 pp.

15. E. E. Kerlin and E. T. Smith, "Measured Effects of the Various Combinations of Nuclear Radiation, Vacuum, and Cryotemperatures on Engineering Materials", General Dynamics/Fort Worth, Nuclear Aerospace Research Facility, Fort Worth, Texas, FXK, June 28, 1963, Quarterly Progress Report, March 1 - May 31, 1963, NAS8-2450, 77 pp.

16. Norbert J. Kreidl, Harold C. Hafner, Joseph R. Hensler, Robert A. Weidel, "Investigation of Ingrared Transmitting Materials", Bausch and Lomb Optical Company, WADC-TR-55-500, Part 3, October 1958, Jan. 1957 - Jan. 1958, AF33(616)2769, p 16.

17. Norbert J. Kreidl and J. Raymond Hensler, "Irradiation Damage to Glass", Bausch & Lomb Optical Co., Rochester, N. Y., NYO-2382, Nov. 1959, AT(30-1)1312.

18. T. M. Mike, B. L. Steierman, and Ed. F. Degering, Owen-Illinois, Toledo, Ohio, "Effects of Electron Bombardment on Properties of Various Glasses", Journal of the American Ceramic Society, Vol. 43, No. 8, 1 Aug. 1960, pp 405-407.

19. William S. Rothwell, "Radiation Shielding Window Glasses", Corning Glass Works, Research Lab., Corning, New York. 25 p.

20. P. S. Rudolph, Oak Ridge National Lab., Tenn., "The Irradiation of Glasses" Fusion, 9: 9-16 (Feb. 1962).

21. D. F. Heath, P. A. Sacher, "Effects of a Simulated "High Energy Space Environment on the Ultraviolet Transmittance of Optical Materials between 1050 Angstrom Units and 3000 Angstrom Units", NASA, Goddard Space Flight Center, Greenbelt, Maryland., Applied Optics, Vol. 5 June 1966, pp 937 - 943.

22. NASA, Marshall Space Flight Center, Huntsville, Ala., "Optical Properties of Satellite Materials - The Theory of Optical and Infrared Properties of Metals", Washington, NASA, Mar. 1963, 252 pp.

23. Army Signal Research and Development Lab., Fort Monmouth, N. J. "Effects of Irradiation on Quartz and Quartz Crystal Units Recorded Experiments" - A bibliography, R. Bechmann, May 26, 1958, 21 pp.

24. United Kingdom Atomic Energy Authority, Harwell, England, Research Group, "Radiation Resistant Glasses", J. V. Best, Nov. 1963 27 pp.

25. High Altitude Observatory, Boulder, Colorado, "A Bibliography on the Effects of Short-Wave and Particle Radiation on Glasses", Astro-geophysical Memorandum No. 164, L. Avery, 30 Jul. 1964, 9 pp.

26. Avco Corp., Tulsa, Okla., "Combined Space Environment, Effects on Typical Space Craft Window Materials", Final Report, June 1964 - June 1965, R. H. Jones July 1965 55 pp.

27. General Dynamics Corp., San Diego, Calif., John Jay Hopkins Lab. for Pure and Applied Science, "Radiation Effects on Lasers" Technical Report, July 1, 1965 - May 31, 1966, R. A. Cesena, 21 Sept. 1966, 77 pp.

28. Stanford Univ., Calif., Stanford Electronics Labs., "Radiation Effects in Optical Materials", W. E. Spicer, NASA, Washington 2nd Symp. on Protec. Against Radiations in Space 1965, pp. 123-129.

29. Air Force Systems Command, Wright-Patterson AFB, Ohio, Foreign Technology Division, "Effects of Gamma-Radiation on Certain Optical Properties of Synthetic Ruby", S. V. Starodubtsev, M. S. Yunusov, 25 June 1965, 6 pp.

30. Space Technology Labs., Inc., Redondo Beach, Calif., "Effects of Low Energy Protons and High Energy Electrons on Silicon", J. R. Carter, R. D. Dowing Washington, NASA, March 1966., pp 44.

31. Barnes Engineering Co., Stamford, Conn., "Nuclear Radiation Effects On Infrared Detectors and Optical Materials", R. DeWaard, Naval Ordnance Lab., Properties of Photodetectors 15 Feb. 1966 pp. 39-48.

32. NASA, Langley Research Center, Langley Research Center, Langley Station, Va., "Ionizing Particle Radiations Effects and Simulation Consideration", J. E. Duberg, W. C. Hulten in Va. Polytech. Inst. Proc. of the Conf. on the Role of Simulation in Space Technology, 50 p.

33. Office of Naval Research, London, England, "Conference on Optics in Space", E. H. Weinberg, 22 October, 1965, 55 pp. Conf. held at Southampton Univ., England, 27-29 Sept. 1965.

34. General Electric Co., Philadelphia, Pa., Missile and Space Division, "Nimbus Meteorological Satellite Integration and Testing Materials Report No. 2", July 1962, 107 p.

35. High Altitude Observatory, Boulder, Colo. "Proposed Irradiation Test of Sample Optical Materials", C. L. Ross, 30 Sept. 1965, 11 pp.

36. TRW Systems Group, Redondo Beach, Calif., "Investigation of Charged Particle Effects on Infrared Optical Materials, II Technical Report", 1 June 1965 - June 1, 1966, R. G. Downing, F. T. Snively, W. K. Van Atta, Wright Patterson AFB, Ohio, AF Mater. Lab., Aug 1966, 58 pp.

37. "High Data Rate Laser Communication System, Operating and Maintenance Manual", Hughes Aircraft Company, HAC Reference A 6395, Contract NAS 9-4266, July 1966.

38. R. B. Ward, "Application of Delay-Lock Radar Techniques to Deep Space Tasks", IEEE Transactions On Space Electronics And Telemetry Vol. Set-10 No. 2, June 1964, pp. 49-65.

39. J. J. Spilker, "Delay Lock Tracking of Binary Signals", IRE Transactions on Space Electronics and Telemetry, Vol. Set-9, March 1960, pp. 1-8

40. J. J. Spilker and D. T. Magill, "The Delay Lock Discriminator An Optimum Tracking Device", Proc. IRE, Vol. 49, Sept. 1961, pp. 1403-1416.

41. R. P. Mathison, "Tracking Techniques For Interplanetary Space-Craft", Proc. Nat'l Telemetering Conf., May 1962

42. R. Affe and E. Rechtin, "Design and Performance of Phase-Lock Circuits Capable of Near-Optimum Performance Over A Wide Range of Input Signal and Noise Levels", IRE Transactions on Information Theory, March 1955, pp. 66-76.

43. M. P. Ristenbatt, "Pseudo-Random Binary Coded Waveforms", Chapter 4 of R. S. Berkowitz, "Modern Radar Analysis Evaluation And System Design", J. Wiley, 1965

44. S. W. Golomb, L. D. Bauhert, M. F. Esterling, J. J. Stiffler and A. J. Viterbi, "Digital Communications With Space Applications", Prentice-Hall, 1964

45. W. J. Culver, and A. E. Fein, "A Markov-Chain Analysis of Steady State Behavior of Phase Lock Loops", Westinghouse Surface Division, Unpublished paper.

46. S. W. Golomb, J. R. Davey, I. S. Reed, H. L. Van Trees, and J. J. Stiffler, "Synchronization" IEEE Transactions On Communications Systems, December 1963 pp. 481-491

47. J. E. Levey, "Self Synchronizing Codes Derived From Binary Cyclic Codes" IEEE Transactions on Information Theory, Vol. IT-12, No. 3, July 1966 pp. 286-290.

48. G. B. Fitzpatrick, "Synthesis of Binary Ring Counters Of Given Periods" ACM Journal, July 1960, pp. 287-297.

49. J. P. Gordon, "Quantum Effects In Communications Systems", Proc. of IRE Sept., pp. 1898-1908

50. M. Ross, "Laser Receivers, Devices Techniques, Systems", John Wiley & Sons, 1966

51. Y. W. Lee, "Statistical Theory Of Communication", John Wiley & Sons, 1963

52. P. F. Panter, "Modulation, Noise and Spectral Analysis", McGraw-Hill, 1965

53. F. M. Riddle, R. P. Mathison, B. D. Martin, J. C. Springett and D. Bourke "JPL Contributions to the 1962 National Telemetering Conference", JPL Technical Memorandum No. 33-88, May 1962

54. E. Rectin, "Estimated 1963-1970 Capability of the Deep Space Instrumentation Facility for Apollo Project", Engineering Planning Document No. 29, Rev 1 2/1/62 JET Propulsion Laboratory

55. J. H. Painter, and G. Hondros, "Unified S-Band Telecommunication Techniques for Apollo", Vol. 1, Manned Space Craft Center, Houston, Texas, National Aeronautics and Space Administration.

56. P. Lindley, "Ranging Subsystem - Mark 1", Proc. Apollo Unified S-Band Technical Conference Goddard Space Flight Center, July 1965, National Aeronautics and Space Administration.

57. P. R. Westlake, "Digital Phase Control Techniques", IRE Transactions on Communications Systems Dec. 1960, pp. 237-246.

58. J. A. Develet, Jr., "An Analytic Approximation of Phase Lock Receiver Threshold" IEEE Transactions on Space Electronics And Telemetry, March 1963 pp. 9-12.

59. A. J. Viterbi, "Acquisition and Tracking Behavior of Phase Locked Loops" J.P.L. External Publication No. 673, July 1959

60. H. Van Trees, "Functional Techniques for the Analysis of the Nonlinear Behavior of Phase-Locked Loops", Proc. IEEE, Aug. 1964, pp. 894-911.

61. R. B. Ward, "Digital Communications on a Pseudonoise Tracking Link Using Sequence Inversion Modulation" IEEE Transactions on Communication Technology, Vol. COM-15, No. 1, Feb. 1967.

June 1, 1967

Errata for Final Report
NAS 9-3650

The following equations in Section IV of this report did not print legibly. They should read as follows:

Page	Equation No.	Equation
IV-6	1	$I = \frac{P \epsilon q}{hf}$
IV-7	2	$V = (\frac{\epsilon qGR}{hf})\ P$
IV-7	3	$\overline{i^2} = 2qIdf$
IV-8	4	$i^2 = 2qIG^2B$
IV-8	5	$S/N = \frac{I^2}{2qIB} = \frac{I}{2qB}$
IV-8	6	$S/N = \frac{P \epsilon}{2hfB}$
IV-8	7	$S/N = \frac{P}{2hfB}$
IV-10	8	$\overline{i_c^2} = 2qI_cG^2df$
IV-10	9	$\overline{i_d^2} = 2qI_dG^2df$
IV-10	10	$\overline{i_b^2} = 2qI_bG^2df$

Page	Equation No.	Equation
IV-11	11	$\overline{i_t^2} = \frac{4kTp(f)df}{R}$
IV-11	12	$\overline{i_t^2} = \frac{4kTdf}{R}$
IV-11	13	$\overline{i_s^2} = \frac{m^2 I_m^2 G^2}{2} = \frac{m^2 I_c^2 G^2}{2}$
IV-13	14	$\overline{v^2} = \frac{m^2 I_c^2 G^2 R^2}{2}$
IV-13	15	$\overline{V_t^2} = \int_o^\infty \frac{4kT}{R} \left\|Z\right\|^2 df$
IV-15	16	$\overline{V_t^2} = \frac{kT}{C}$
IV-15	17	$\frac{4kT}{R} \cdot R^2 \cdot B = \frac{kT}{C}$ Whence $B = \frac{1}{4RC}$
IV-15	18	$\overline{v^2} = \frac{qG^2R}{2C}(I_C + I_d + I_b)$
IV-16	19	$\overline{v^2} = \frac{kT}{C} + \frac{qG^2R}{2C}(I_C + I_d + I_b)$
IV-16	20	$S/N = \frac{\frac{m^2 I_c^2 G^2 R^2}{2}}{\frac{kT}{C} + \frac{qG^2R}{2C}(I_C + I_d + I_b)}$

Page	Equation No.	Equation
IV-16	21	$S/N = \dfrac{\frac{m^2 I_C{}^2 G^2 R}{2}}{4\ kT\ B + 2qG^2RB(I_C+I_d+I_b)}$
IV-17	22	$B = \frac{\pi}{2} \cdot \Delta f$
IV-17	23	$N_t/N_s = \dfrac{2\ kT}{qG^2R(I_C+I_d+I_b)}$
IV-17	24	$N_t/N_s \cong \dfrac{2\ kT}{qG^2RI_d}$
IV-18	25	$N_t/N_s \cong \dfrac{8kTBC}{qG^2I_d}$
IV-19	27	$S/N = \dfrac{m^2 I_C{}^2}{4qB(I_C+I_d+I_b)}$
IV-19	28	$S/N \cong \dfrac{m^2 I_C}{4qB\ (1 + \frac{I_d}{I_C})}$
IV-24	29	$S/N = \dfrac{I_m{}^2/2}{2qB(I_C+I_d+I_b)}$

Page	Equation No.	Equation
IV-24	30	$S/N = \dfrac{I^2}{\pi^2 qB\,(I/2 + I_d + I_b)}$
IV-24	31	$S/N = \dfrac{2I}{\pi^2 qB\,(1 + 2\frac{I_d}{I})}$
IV-39	32	$H = H_o B_o\,(\frac{d_o}{d})^2$
IV-41	33	$P = NA_s \Omega B_o$ watts
IV-42	34	$H = \dfrac{NA_s B_o}{d^2}$ watts/cm^2
IV-50	Line Preceeding Equation 36	$1 - \Delta = \dfrac{D}{D + \alpha F} = 1 - \dfrac{\alpha F}{D} + (\dfrac{\alpha F}{D})^2 - (\dfrac{\alpha F}{D})^3 + \ldots$
IV-50	36	$\Delta \cong \dfrac{\alpha f}{D}$
IV-52	38	$\dfrac{1}{d_4} + \dfrac{1}{d_1} = \dfrac{1}{f_m}$
IV-52	39	$\dfrac{1}{d_2} - \dfrac{1}{d_3} = \dfrac{1}{f_L}$
IV-60	40	$I_1 = \dfrac{k E_1^2}{2}$

Page	Equation No.	Equation
IV-60	41	$E_1 = \sqrt{\frac{2 I_1}{k}}$

Also; Figure IV-1 should be Figure IV-5.
Figure IV-5 should be Figure IV-1.